University of Hohenheim
Faculty of Agricultural Sciences
Institute of Soil Science and Land Evaluation
Biogeophysics

Turbulent exchange of energy, water and carbon between crop canopies and the atmosphere: An evaluation of multi-year, multi-site eddy covariance data

Dissertation

Ravshan Abdurazakovich Eshonkulov

Born in Karshi, Uzbekistan

2019

This thesis was accepted as a doctoral thesis (Dissertation) in fulfillment of the regulations to acquire the degree “Doktor der Agrarwissenschaften” (Dr.sc.agr. in Agricultural Sciences) by the Faculty of Agricultural Sciences at University of Hohenheim on 11.03.2019.

Date of oral examination: 21.03.2019

Examination Committee

Supervisor and Referee	Prof. Dr.Thilo Streck
Co-Referee:	PD Dr. Hans-Dieter Wizemann
Additional examiner:	Prof. Dr. Andreas Fangmeier
Head of the Committee:	Prof. Dr. Markus Rodehutscord

Self-publishing:	Ravshan Abdurazakovich Eshonkulov
Source of supply:	Institute of Soil Science and Land Evaluation University of Hohenheim 70593 Stuttgart

Table of contents

Summary

The increase of anthropogenic CO_2 emissions and other greenhouse gases has raised concern about climate change. Climate change has manifold impacts on yield and yield quality, crop rotations, carbon and nitrogen cycling, water regime and agricultural production systems. To understand its consequences on environmental systems, measuring the matter and energy exchange at the land surface provides data to help validate and inform a wide range of process models. Such flux measurements at the land-surface provide an opportunity to test simulations of processes in the soil-plant-atmosphere continuum. Currently, such measurements are mainly based on the eddy covariance (EC) method, for the quality of which the energy balance closure (EBC) is a problem. The EBC significantly influences the calibration and validity of land-surface models, especially in regard to the energy and water balance at the Earth's surface. The EBC quantifies the deviation between turbulent fluxes and available energy. It is crucial to obtain high-quality EC measurements to determine the reasons for the EBC.

The research aims of this dissertation were: 1) to clarify the role of minor storage and flux terms in the energy balance, 2) to determine the possible reasons for the energy imbalance using a long-term dataset (2010-2017) from agricultural croplands, and 3) to investigate the effects of region, site, year and crop type on carbon fluxes and budgets.

In the first study (Chapter 2) the contribution of minor storage terms to the EBC were investigated. I also determined the contribution of ground heat fluxes calculated by different methods. A harmonic analysis method was used to calculate ground heat fluxes from measurements of heat flux plates and soil temperature sensors. Soil heat storage and enthalpy change in the plant canopy were determined at different locations within the EC footprint. Considering minor storage terms improved the energy balance closure on average by 5.0 % in 2015 and by 6.8 % in 2016. The greatest energy balance closure improvement occurred in May of both study years. The dominant fraction of minor energy storage was energy uptake and release through photosynthesis and respiration. Additionally, the energy fluxes related to soil temperature change were also observed. The ground heat flux calculated by harmonic analysis from soil heat flux plates narrowed the EBC by 3 % compared to the calorimetric method. The results indicated that the typical correction approach to achieve energy balance closure, i.e. the Bowen-ratio method, overestimated the turbulent fluxes.

The second study (Chapter 3) investigated the effects of crop type, site characteristics, wind directions, atmospheric conditions and footprint on the EBC. The long-term evaluation of EC measurements showed

that, with the EC method, 25 % of the available energy could not be detected. Decreasing the flux footprint area increases the chance of a more homogeneous area. Homogeneity plays an important role in achieving a better energy balance closure. The synthesis of long-term EC data indicated that the sonic anemometer is very sensitive to orientation, not allowing accurate measurements from all wind directions. Discarding the measurements from wind directions 0° and 90° at EC4 improved the EBC from 80 to 84 %.

In the third study, presented in Chapter 4, a long-term and multi-site experiment was evaluated to clarify the effects of site, year and region on the CO_2 fluxes and budgets in agroecosystems. The net ecosystem exchange of CO_2 fluxes – measured on six sites during eight years – was comprehensively examined. Winter rapeseed had the lowest CO_2 uptake, cropping of silage maize resulted in the highest C losses. The management of harvest residues was the most effective means of controlling the C budgets. Comparing the CO_2 fluxes processed with the recently developed ogive optimization method versus the conventional calculation showed that eliminating low-frequency contributions had a considerable effect. On average, the ogive optimization method delivered 6.9 % higher net ecosystem exchange rates than the conventional method.

This dissertation provides new insights into how to obtain better measurements of matter and energy fluxes from EC measurements by a) considering storage terms otherwise neglected, b) using harmonic analysis for calculating ground heat fluxes, c) discarding fluxes from behind the anemometer and d) applying the ogive optimization method.

Zusammenfassung

Der Anstieg der anthropogenen, klimawandelverursachenden Emissionen von Kohlenstoffdioxid und anderer Treibhausgase löst Besorgnis aus. Der Klimawandel hat vielfältige Auswirkungen auf Ertrag und Ertragsqualität, Fruchtfolgen, Kohlenstoff- und Stickstoffkreislauf, Wasserregime und insgesamt das landwirtschaftliche Produktionssystem. Um die Auswirkungen auf Umweltsysteme zu verstehen, werden zur Optimierung und Validierung von Prozessmodellen Messungen des Stoff- und Energieaustauschs an der Landoberfläche durchgeführt. Dies ermöglicht es, Prozesse im Boden-Pflanze-Atmosphäre-Kontinuum detaillierter zu simulieren. Gegenwärtig basieren solche Messungen hauptsächlich auf der Eddy-Kovarianz-Methode (EC), im Rahmen derer die nicht vollumfängliche Energiebilanzschließung (EBC) ein methodisches Problem darstellt. Die EBC beeinflusst signifikant die Kalibrierung und Validierung von Landoberflächenmodellen, insbesondere hinsichtlich der Wasser- und Energiebilanz. Die EBC quantifiziert die Abweichung zwischen turbulenten Flüssen und verfügbarer Energie. Qualitativ hochwertige EC-Messungen sind wichtig, um die Gründe für die nicht vollständige EBC zu bestimmen.

Die Forschungsziele waren: 1) Klärung der Rolle von geringfügigen Speicher- und Flusstermen zur Verbesserung der Energiebilanzschließung, 2) Ermittlung der möglichen Gründe für die nicht vollständig gegebene EBC anhand eines Langzeitdatensatzes (2010-2017) von landwirtschaftlichen Nutzflächen, und 3) Untersuchung der Auswirkungen von Region, Standort, Jahr und Fruchtart auf Kohlenstoffflüsse und -bilanzen.

In der ersten Studie (Kapitel 2) wurde der Beitrag von geringfügigen Speichertermen zur EBC untersucht. Dabei wurde der Beitrag des Bodenwärmeflusses ermittelt, welcher mit verschiedenen Methoden berechnet wurde. Die Harmonische Analyse wurde verwendet, um den Bodenwärmefluss aus Messungen von Wärmeflussplatten und Bodentemperatursensoren zu berechnen. Die Wärmespeicherung des Bodens und die Enthalpieänderung im Pflanzenbestand wurden an verschiedenen Stellen innerhalb des EC-Fußabdrucks ermittelt. Unter Berücksichtigung der geringfügigen Speicherterme verbesserte sich die Schließung der Energiebilanz im Jahr 2015 um durchschnittlich 5,0 % und 2016 um 6,8 %. Die größte Verbesserung der Energiebilanzschließung trat im Mai beider Untersuchungsjahre auf. Der dominierende Anteil der geringfügigen Speicherterme war die Energieaufnahme und -freisetzung durch Photosynthese und Atmung. Zusätzlich wurden die Energieflüsse, die mit der Veränderung der Bodentemperatur zusammenhängen, untersucht. Der durch die harmonische Analyse berechnete Bodenwärmefluss erhöht die EBC um 3 % im Vergleich zur kalorimetrischen Methode. Die Ergebnisse

zeigen, dass der typische Korrekturansatz für die Schließung der Energiebilanz, das Bowen-Verhältnis-Verfahren, die turbulenten Flüsse überschätzte.

In der zweiten Studie (Kapitel 3) wurden die Auswirkungen von Fruchtart, Standorteigenschaften, Windrichtung, sonstigen atmosphärischen Bedingungen und des EC-Messbereichs auf die EBC untersucht. Die Langzeitauswertung zeigte, dass mit der EC-Methode 25% der verfügbaren Energie nicht erfasst werden konnten. Durch die Verringerung des EC-Messbereichs wird die Wahrscheinlichkeit einer homogeneren Fläche erhöht. Diese Homogenität spielt eine wichtige Rolle für die Erreichung einer besseren Energiebilanzschließung. Die Synthese von Langzeit-EC-Daten zeigte, dass auch die Orientierung des Ultraschallanemometers das Messergebnis stark beeinflusst. Durch Ausklammern der Messungen aus den Windrichtungen zwischen 0° und 90° bei EC4 verbesserte sich beispielsweise die EBC von 80 auf 84 %.

In der dritten Studie, die in Kapitel 4 vorgestellt wird, wurde eine Langzeit- und Multi-Site-Untersuchung durchgeführt, um die Auswirkungen von Standort, Jahr und Region auf die CO_2-Flüsse und Budgets in Agrarökosystemen zu analysieren. Der Netto-Ökosystemaustausch von CO_2-Flüssen, gemessen an sechs Standorten während acht Jahren, wurde umfassend untersucht. Es zeigte sich, dass Winterraps die geringste CO_2-Aufnahme aufweist und Silomais die höchsten C-Verluste verursacht. Das Management der Ernterückstände war das wirksamste Instrument zur Steuerung der Kohlenstoffbilanz. Ein Vergleich der CO_2-Flüsse, die mit der kürzlich entwickelten Ogive-Optimierungsmethode verarbeitet wurden, zeigte im Vergleich zur herkömmlichen Berechnung, dass die Eliminierung von Niedrigfrequenzflüssen eine beträchtliche Wirkung hatte. Im Durchschnitt lieferte die Ogive-Optimierung 6.9 % höhere Netto-Ökosystem-Austauschraten als die konventionelle Methode.

Diese Dissertation liefert neue Erkenntnisse darüber, wie man bessere Stoff- und Energieflussmessungen an der Landoberfläche erzielen kann: a) durch Berücksichtigung von vernachlässigten Speichertermen, b) durch Verwendung der Harmonischen Analyse zur Berechnung des Bodenwärmestroms, c) durch Ausschluss von Flüssen, die aus dem rückwärtigen Bereich des Anemometers stammen, und d) durch Anwendung der Ogive-Optimierungsmethode.

Chapter 1

1. General introduction

1.1. Measurement of matter and energy exchange in the soil-crop-atmosphere system

Matter and energy exchange in soil-crop systems is a complex and fundamental interaction of biophysical elements, crucial to life on the planet (Campbell and Norman, 1998; Heymsfield et al., 2017; Monteith and Unsworth, 2013). The cycling and transformation of elements depends on the physical and chemical system properties and environmental conditions. These processes are controlled by the sun, which is the main source of energy. In the Earth's layer known as the atmospheric or planetary boundary layer (ABL or PBL), which comprises the lowest 100 to 3000 m of the atmosphere (Stull, 1988). Measuring matter and energy fluxes at the Earth's surface is important to understand many processes, including the consequences of global climate change.

Today, global climate change is one of the most serious problems affecting the world. The consequences of global climate change are visible in increasingly severe weather conditions, which are expected to be more frequent in the future. The main factor behind climate change is linked to increasing anthropogenic greenhouse gas (GHG) emissions such as carbon dioxide (CO_2), methane (CH_4) and nitrous oxide (N_2O) (IPCC, 2014), leading to an associated increase in their concentrations in the atmosphere. The carbon dioxide from agriculture, forestry and other land use related activities is estimated to contribute 24% to anthropogenic climate change (IPCC, 2014). However, the GHG contribution of the agricultural sector is still not sufficiently studied and requires further quantification (FAO, 2014).

In particular, it is crucial to find solutions for sustainable development in agriculture with regard to the contribution of CO_2 from the agricultural sector to global climate change. During the last two decades, carbon sequestration in the agricultural sector has been discussed as an important contribution to overall carbon sequestration. The positive side effect is an increase of organic matter in soil. Nonetheless, the dynamics of carbon flux from agricultural ecosystems remain elusive (Inoue et al., 2004; Poyda et al., 2016). This calls for a better understanding of the matter and energy exchange processes in the boundary layer, in particular at the ground surface. This is an important step in assessing the impact of global climate change on a regional scale. A cornerstone is the continuous development of measurement instruments for surface exchange. For instance, high precision, fast-response gas analyzers and three-

dimensional sonic anemometers enable conducting measurements with a time resolution of 10-20 Hz on both short and long time scales.

Several methods are available for measuring energy fluxes at the land surface in the soil-plant-atmosphere continuum. The most commonly adopted micrometeorological methods can be divided into the following categories: eddy covariance (EC), flux-gradient, accumulation, and mass balance based methods (Burba, 2013; Foken, 2008a; Meyers and Baldocchi, 2005; Monteith and Unsworth, 2013). Among them, the EC method depends on fast-response instrumentation enabling the measurement of trace gases at a high-frequency resolution. Currently, no single sensor can measure all variables of interest. As a result, a multitude of different sensors, mounted and installed on so-called EC towers, are being used in micrometeorological measurements (Baldocchi, 2014).

Accurate measurement of water and heat fluxes is essential to inform the modelling of processes in the soil-plant-atmosphere continuum (Ezzahar et al., 2012; Gan and Gao, 2015; Ingwersen et al., 2018, 2015, 2011; Michiles and Gielow, 2008; Santanello et al., 2013). Long-term data are crucial for validating and improving regional and global climate models (Gu et al., 2007; Ingwersen et al., 2018; Wizemann et al., 2014).

1.2. Using the eddy covariance method in croplands

The EC method can yield long-term data sets of measured energy fluxes from agricultural landscapes. This improves the study of relationships within soil-crop-atmosphere systems. Since its early development and first applications stages, the EC method has come a long way. Today it has become a de facto standard in a wide range of scientific disciplines despite the mathematical complexity and other requirements in setting up and processing raw datasets (Burba, 2013; Burba and Anderson, 2007). Post-processing of raw data from EC requires several corrections to ensure that the determined fluxes correctly or at least closely represent the true fluxes (Arya, 2001; Aubinet et al., 2000; Foken, 2008a; Mauder et al., 2013; Nordbo et al., 2012). An important advantage of EC is the possibility to measure the fluxes between the (vegetated) ground surface and the atmosphere from short-term to long-term, and on spatial scales from hundreds to thousands of square meters (Kidston et al., 2010).

Processing the data of EC measurements is not a straightforward task. Accordingly, the software packages developed for EC flux calculations have found extended application around the world. The most prominent examples are: EdiRe (University of Edinburg, Edinburg, Scotland, UK), ECPack (Wageningen University and Research, Wageningen, The Netherlands), EddyUH (University of

Helsinki, Helsinki, Finland), EC processor (University of Toledo, Ohio, USA), TK3.1 (University of Bayreuth, Bavaria, Germany), EddyPro® (LiCOR Inc., Lincoln, NE, USA), and EddySoft® (Campbell Scientific, Inc., Logan, UT, USA). All these software packages are being successfully applied to process raw EC data.

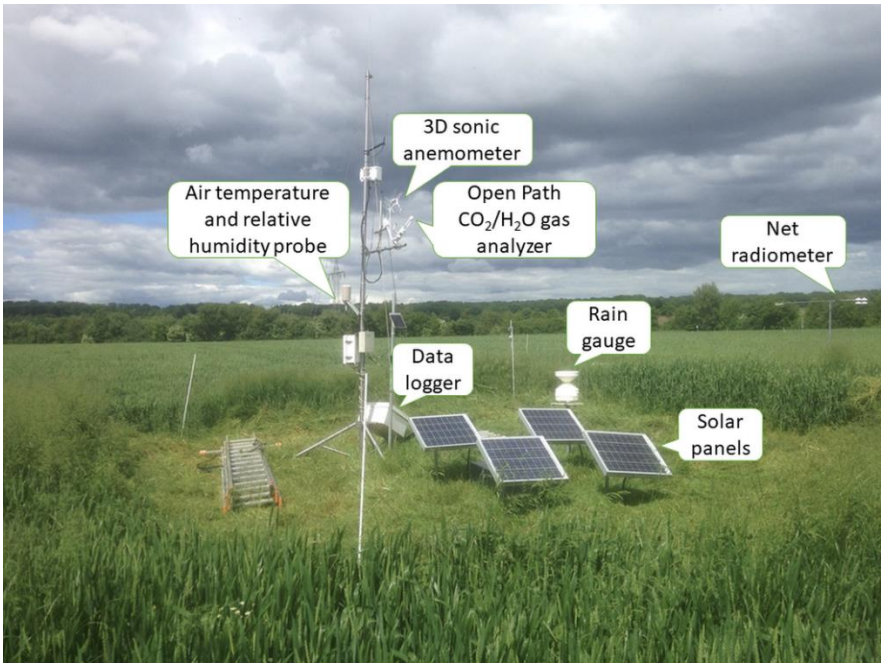

Fig. 1.1. Eddy covariance station with mounted fast-response, high-precision instruments over cropland (Kraichgau region)

The EC method enables the determination of fluxes of sensible heat (*H*), latent heat (*LE*) and trace gases such as carbon dioxide (CO_2) and methane (CH_4). This is facilitated by high-precision and fast-response gas analyzers and sonic anemometers. Currently, EC measurement campaigns are being conducted globally at several hundred sites in order to analyze the impacts and feedbacks of climate change on a regional scale (Baldocchi, 2014; Mauder et al., 2013). This helps to better understand and accurately represent complex feedback processes among climate and soil-crop systems. This approach is also crucial for obtaining better climate simulations and weather forecasting (Santanello et al., 2013, 2011; Wizemann et al., 2014). Numerous long-term observation networks are currently in operation in different parts of the world such as TERENO (Terrestrial Environmental Observatories) and ICOS (Integrated Carbon Observation System) in Europe, NEON (National Ecosystem Observatory Network) or AmeriFlux in the USA, AsiaFlux in Asia, and FLUXNET − the biggest global network, which operates more than 140 sites (Baldocchi et al., 2001). The EC method is also being used in various ecosystems

such as forests (Moderow et al., 2009), agricultural landscapes (Imukova et al., 2016; Masseroni et al., 2014; Wizemann et al., 2014), Fig.1.1)), aquatic habitats (Mammarella et al., 2015; Nordbo et al., 2011; Shao et al., 2015), and peatlands (Poyda et al., 2016; Weber et al., 2018, van den Berg et al., 2016).

1.3. Energy balance closure

Following the first law of thermodynamics, the input and output energy at the land surface must be equal (Arya, 2001). An important quality assessor of EC measurements is the obtained energy balance closure (EBC). The EBC is also important to assess land surface modelling accuracy (Ingwersen et al., 2015, 2011). Unfortunately, most studies have thus far failed to close the energy balance, a persistent problem and one of the unresolved problems regarding EC measurements (Foken, 2008b; Foken et al., 2010, 2006; Pardo et al., 2015; Sánchez et al., 2010). Leuning et al. (2012), however, postulated that solving the EBC is feasible by considering data processing errors and by accurately measuring all neglected energy storage terms. EC measurements show that in many cases either the turbulent fluxes ($LE+H$) are underestimated or the available energy (R_n-G) is overestimated (Foken, 2008b; Imukova et al., 2016; Ingwersen et al., 2015; Kidston et al., 2010; Oncley et al., 2007; Wilson et al., 2002; Wizemann et al., 2014). Energy balance closures are assessed with three typical methods: ordinary linear regression (OLR) of turbulent fluxes ($LE+H$) and available energy (R_n-G), energy balance ratio (EBR), and residual energy, where $Res=R_n-LE-H-G$ (Imukova et al., 2016; Oke, 1987; Ping et al., 2011; Wilson et al., 2002).

The components of comprehensive energy balance at the level surface can be derived into groups: (a) major fluxes and (b) minor fluxes and storage terms (Oncley et al., 2007). Major fluxes include net radiation (R_n) as well as latent (LE), sensible (H) and ground heat (G). Minor storage terms comprise the enthalpy change in the plant canopy (S_c), the air enthalpy change (S_a), the energy consumption and release by photosynthesis and respiration (S_p), and the atmospheric moisture change (S_q).

There are a number of reasons, most occurring concurrently, for the often perceived EBC problem. These include (1) neglected minor storage terms, (2) inaccurate calculation of ground heat flux, (3) inadequate turbulent mixing, (4) landscape-scale heterogeneity, (5) loss of high or low frequencies.

One important cause of the energy balance gap is that minor storage and flux terms are typically neglected (Eshonkulov et al., 2019). Also, estimating these terms inaccurately leads to an energy imbalance (Leuning et al., 2012). Due to their small contribution compared to other energy fluxes, the minor storage terms have often been omitted (Jones and Rotenberg, 2001; Teh, 2006). However, taking into account additional energy storage in various ecosystems (such as in forests) contributes considerably to EBC

(Blanken et al., 1997; Haverd et al., 2007; Lamaud et al., 2001; Lindroth et al., 2010; Michiles and Gielow, 2008; Moderow et al., 2009; Oliphant et al., 2004). Considering minor storage terms at a subalpine meadow site in northwest China (Wang and Zhang, 2011), maize and soybean fields (Meyers and Hollinger, 2004; Varmaghani et al., 2016), and a grassland site (Jacobs et al., 2008) showed a positive effect on EBC. In a maize field in the Po Valley, Italy, Masseroni et al. (2014) showed that the 20 % energy imbalance was mainly linked to minor storage terms. Similarly, an 8.5 % - 10 % improvement in EBC was achieved by considering minor storage terms in a study on irrigated sugarcane (Anderson and Wang, 2014).

The role of measured ground and soil heat flux on EBC and the associated measurement methods and techniques have been explained by Sauer and Horton (2005). The ground heat flux can be determined more accurately by considering the stored energy between installed soil heat flux plates at EC towers and the ground surface (Massman, 1992; Mayocchi and Bristow, 1995). This approach is termed the calorimetric method and has become a widely used standard.

Soil heat storage determined at a single point is commonly not representative for the entire footprint of the EC measurements. Measurements of soil heat storage at different points of a field in the Jornada Experimental Range in southern New Mexico (USA) showed discrepancies ranging from 50 to 100 W m^{-2} (Kustas et al., 2000). The spatial and temporal variability of soil heat storage was attributed to variability in soil physical properties and shading from vegetation. Another method to determine the ground heat fluxes is the Fourier transformation approach, which was developed based on harmonic analysis of soil temperature at one depth (An et al., 2015; Heusinkveld et al., 2004; Horton and Wierenga, 1983; Li et al., 2014; Ping et al., 2011; Zuo et al., 2011). A few studies have compared the de facto standard method to account for *G*, the calorimetric method, to the alternative harmonic analysis method (Heusinkveld et al., 2004; Jacobs et al., 2008). The latter can be used in conditions with homogeneous soil (Horton and Wierenga, 1983). In a measurement campaign in a desert (Israel), the harmonic analysis yielded ground heat fluxes that were considered more realistic than those obtained with the calorimetric method (Heusinkveld et al., 2004). At a grassland site (Netherlands), the EBC improved from 81 to 90 % when the calorimetric method was replaced by the harmonic analysis in calculating ground heat flux (Jacobs et al., 2008). Similar improvements were obtained for a natural grassland (China), with an EBC increase from 76 to 82 % (Zuo et al., 2011).

Besides ground heat fluxes, the atmospheric conditions also greatly impact the EBC, in most cases linked to an underestimation of turbulent fluxes. Insufficient turbulent mixing conditions are one of the causes for underestimating turbulent fluxes. Such conditions usually occur at night, resulting in poor EBC (Chen

and Li, 2012; Franssen et al., 2010; Masseroni et al., 2014; Wilson et al., 2002; Zeri and Sá, 2010). This indicates that EBC is highly sensitive to the turbulence of the atmosphere (Anderson and Wang, 2014; Du et al., 2014). Low wind speeds and low friction velocity are also partly responsible for the energy imbalance (Saigusa et al., 2002). Usually, low wind speeds hinder well-developed turbulent mixing conditions in the atmosphere, resulting in unreliable EC measurements. Typically, friction velocity, u*, is used as an indicator for poorly developed turbulence conditions. Numerous studies have analyzed the effect of u* on EBC. For instance, a better EBC (90 %) was observed when u* increased to 0.80 m s^{-1} at a boreal forest site in Finland (Sánchez et al., 2010). Some authors reported that the best EBC at different u* is connected with site turbulence-closure characteristics.

The heterogeneity/homogeneity of the source of the flux area, in particular the flux footprint of the measurements, is crucial in evaluating EBC. (Hui and Xuefa, 2015; Kljun et al., 2015; Schmid, 2002). The flux footprint depends on many factors such as measurement height, prevailing wind direction, atmospheric turbulence conditions and surface roughness. This is because the measurement area is not always homogeneous or does not satisfy the requirements of EC measurements. (Arriga et al., 2017; Finnigan, 2004; Kljun et al., 2002; Kormann and Meixner, 2001; Lee, 2003; Neftel et al., 2008). The relationship between the EBC and footprint area is poorly studied (Stoy et al., 2013). Some authors such as Stoy et al. (2013) and Xu et al. (2017) found that landscape heterogeneity significantly affected EBC. With increasing landscape heterogeneity, the EBR decreased at an oasis-desert area in China (Xu et al., 2017). The EBC difference between a homogeneous evergreen broadleaf forest (EBC – 94 %) and a heterogeneous deciduous forest (EBC – 70 %) led Stoy et al. (2013) to conclude that the higher EBC imbalance is caused by landscape heterogeneity. Therefore, every measurement site has particular characteristics that must be considered in measuring and calculating EBC (Masseroni et al., 2014; Reed et al., 2018; Varmaghani et al., 2016).

1.4. Carbon fluxes and budgets

Cropland plays a prominent role in the global carbon (C) cycle. It has a potential for GHG mitigation (Smith et al., 2008) and, under good agricultural practice, can help maintain stable SOC contents over the long-term (Körschens et al., 2014). Previous studies, however, after initiating CO_2 measurements with the EC methods, propose that cropland is a C source to the atmosphere when all relevant C fluxes of agroecosystems are taken into account (Ceschia et al., 2010). Past analyses show continuously ongoing SOC losses from croplands (Poyda et al., 2016; Smith et al., 2005). Optimizing agricultural management can help to mitigate greenhouse gas emissions from croplands and enhance C sequestration or reduce the

depletion of SOC stocks. This involves cover crops (Poeplau et al., 2011), nutrient supply, conservation tillage (Ceschia et al., 2010; Reicosky and Allmaras, 2003) and crop residue management (Lal, 2004). Nonetheless, understanding the inter-annual variability of C exchange, its budget and climatic dependence requires long-term measurements (Moors et al., 2010; Schmidt et al., 2012). Long-term measurements of CO_2 with the EC method, i.e. the quantification of net ecosystem exchange (NEE) and net biome productivity (NBP), are important in evaluating the potential of carbon fluxes and budgets of agroecosystems (Poyda et al., 2017, 2016; Schmidt et al., 2012). Moreover, long-term experiments and observation of C fluxes of croplands are essential to validate robust agroecosystem models (Klosterhalfen et al., 2017).

Recently, the seasonal and inter-annual variability of long-term cropland NEE has been investigated (Guo et al., 2013; Kutsch et al., 2010; Moors et al., 2010; Schmidt et al., 2012). The results indicate that the seasonal and annual NEE shows a net CO_2 uptake under intensive crop rotations. Even though C fluxes are measured with the EC method, the results have potential shortcomings. The EC method cannot capture all relevant fluxes in high/low frequencies, leading to an underestimation of turbulent fluxes and NEE (Kidston et al., 2010; Wilson et al., 2002). Liu et al. (2006), however, demonstrated that the lack in EBC does not considerably affect the quantification of CO_2 fluxes. Moreover, they concluded that mis-quantifications of CO_2 fluxes are associated with local atmospheric conditions. This calls for studying this problem more comprehensively. Loss of turbulent fluxes in the high and low frequency ranges is considered as a possible factor behind this energy imbalance. Wolf and Laca (2007) attempted to determine the turbulent fluxes in high-frequency signals in the shortgrass steppe region of Kazakhstan. They concluded that, in high frequencies, the sensible heat flux (H) was mainly underestimated. To determine uncaptured low-frequency fluxes, Leuning et al. (2012) proposed to use different averaging intervals instead of the standard 30-min interval to investigate if they contribute to the EBC. However, extending the averaging interval to more than 30 min makes it difficult to maintain a steady-state condition. Such extensions do not obey the Reynolds' averaging rules. Therefore, another method – namely block ensemble average – has been proposed because it maintains steady-state conditions (Charuchittipan et al., 2014; Sun et al., 2006). Unfortunately, the block ensemble average fail also did not achieve a closed energy balance.

Extending the averaging time in EC measurements in different ecosystems showed differing results (Charuchittipan et al., 2014; Chen and Li, 2012; Foken et al., 2010; Kidston et al., 2010; Masseroni et al., 2014; Sun et al., 2006). For forests, the recommendation is to use averaging intervals of 60-min or longer (Sun et al., 2006). Agreement has been reached about using 30-min averaging intervals: they are

thought to capture all the relevant fluxes from and to cropland (Charuchittipan et al., 2014; Sun et al., 2006). The extent to which captured low-frequency fluxes can improve the EBC is an ongoing debate (Kidston et al., 2010). The ogive analysis has been proposed to find adequate averaging intervals (Desjardins et al., 1989; Mauder and Foken, 2006). This analysis involves the cumulative summation of the co-spectrum of fluxes starting from highest to lower frequencies. Moreover, the most adequate averaging interval is mainly related to site characteristics (Kidston et al., 2010; Sun et al., 2006). Due to the chaotic behavior of turbulent fluxes, the averaging interval could be different for all time points (Mammarella et al., 2015) and should be optimized. In principle, the analysis is not commonly applied because it drastically increases the complexity of data processing.

A new ogive optimization method was recently proposed by Sievers et al. (2015). It enables separating low-frequency influences from vertical turbulent fluxes in order to isolate the local exchange processes of interest. The conventional method usually does not consider separate low-frequency fluxes. In comparison to the standard 30-min averaging interval, the ogive optimization showed that the average relative differences in fluxes (*H, LE* and CO_2) were in the range of 23-98 %. This implies that the conventional data processing method cannot capture all relevant fluxes, leading to an underestimation of turbulent and CO_2 fluxes. Kidston et al. (2010) and Wilson et al. (2002) highlighted that the fraction of underestimated turbulent fluxes and CO_2 is within a similar range. The ogive optimization method has been used only in arctic regions (Sievers et al., 2015) and at tundra sites (Pirk et al., 2017). At the Abisko site (Sweden), the data processing of CO_2 with the standard 30-min showed that the CO_2 flux was 310 mmol m^{-2} d^{-1}. In contrast, the ogive optimization method yielded up to 385 mmol m^{-2} d^{-1} (Sievers et al., 2015). The relative change was -19.5 %. This indicates that applying the ogive optimization method in data processing can help to quantify more precisely the carbon flux and soil organic carbon (SOC) loss in cropland.

1.5. Research aims

The research aims were: 1) to assess the contribution of minor storage and flux terms in improving the energy balance closure, 2) to study the causes of the energy imbalance in EC measurements in agricultural croplands, and 3) to investigate the effects of different regions, sites, years and crops on carbon fluxes and budgets. Pursuing these research aims was based on the analysis of a long-term dataset (2010-2017).

The work has been organized into three main parts:

In the first study, the effect of quantifying minor storage and flux terms to improve the EBC of EC measurements was assessed for two winter wheat crop stands during two consecutive years during the main vegetation period. The difference of soil heat storage close to the EC stations and within the footprint was investigated. The ground heat flux calculated with harmonic analysis was compared with the standard calorimetric method (Chapter 2).

In the second study, the EBC for 6 measurement sites in 2 regions over 8 years was evaluated and its dependency on different atmospheric stability parameters examined. For this, the effects that crop, yield, year, and site characteristics had on EBC were investigated. Additionally, the relationships between the footprint area and the EBC were identified (Chapter 3).

In the third study, EC measurements of CO_2 exchange over different croplands under different climatic conditions were used to investigate the effects of region, year, site and crops to the carbon fluxes and budgets. An attempt was made to identify the potential environmental, meteorological and agricultural drivers that promote SOC gains and losses (Chapter 4).

References

An, K., Wang, W., Zhao, Y., Huang, W., Chen, L., Zhang, Z., Wang, Q., Li, W., 2015. Estimation from soil temperature of soil thermal diffusivity and heat flux in sub-surface layers. Boundary-Layer Meteorol. 158, 473–488. https://doi.org/10.1007/s10546-015-0096-7

Anderson, R.G., Wang, D., 2014. Energy budget closure observed in paired eddy covariance towers with increased and continuous daily turbulence. Agric. For. Meteorol. 184, 204–209. https://doi.org/10.1016/j.agrformet.2013.09.012

Arriga, N., Rannik, Ü., Aubinet, M., Carrara, A., Vesala, T., Papale, D., 2017. Experimental validation of footprint models for eddy covariance CO_2 flux measurements above grassland by means of natural and artificial tracers. Agric. For. Meteorol. 242, 75–84. https://doi.org/10.1016/J.AGRFORMET.2017.04.006

Arya, S.P., 2001. Introduction to Micrometeorology, 2nd ed. Academic Press, San Diego, San Franscisko, New York, Boston, London, Sydney, Tokyo.

Aubinet, M., Grelle, A., Ibrom, A., Rannik, Ü., Moncrieff, J., Foken, T., Kowalski, A.S., Martin, P.H., Berbigier, P., Bernhofer, C., Clement, R., Elbers, J., Granier, A., Grünwald, T., Morgenstern, K., Pilegaard, K., Rebmann, C., Snijders, W., Valentini, R., Vesala, T., 2000. Estimates of the Annual Net Carbon and Water Exchange of Forests: The EUROFLUX Methodology. Adv. Ecol. Res. 30, 113–175. https://doi.org/10.1016/S0065-2504(08)60018-5

Baldocchi, D., 2014. Measuring fluxes of trace gases and energy between ecosystems and the atmosphere - the state and future of the eddy covariance method. Glob. Chang. Biol. 20, 3600–3609. https://doi.org/10.1111/gcb.12649

Baldocchi, D.D., Falge, E., Gu, L., Olson, R., Hollinger, D., Running, S., Anthoni, P., Bernhofer, C., Davis, K., Evans, R., Fuentes, J., Goldstein, A., Katul, G., Law, B., Lee, X., Malhi, Y., Meyers, T.,

Munger, W., Oechel, W., Paw, K.T.U., Pilegaard, K., Schmid, H.P., Valentini, R., Verma, S., Vesala, T., Wilson, K., Wofsy, S., 2001. FLUXNET : A new tool to study the temporal and spatial variability of ecosystem-scale carbon dioxide, water vapor, and energy flux densities. Bull. Am. Meteorol. Soc. 82, 2415–2434. https://doi.org/10.1175/1520-0477(2001)082<2415:FANTTS>2.3.CO;2

Blanken, P.D., Black, T. a., Yang, P.C., Neumann, H.H., Nesic, Z., Staebler, R., den Hartog, G., Novak, M.D., Lee, X., 1997. Energy balance and canopy conductance of a boreal aspen forest: Partitioning overstory and understory components. J. Geophys. Res. 102, 28915. https://doi.org/10.1029/97JD00193

Burba, G., 2013. Eddy covariance method for scientific, industrial, agricultural and regulatory applications. https://doi.org/10.1016/j.infsof.2008.09.005

Burba, G., Anderson, D., 2007. Introduction to the eddy covariance method: General guidelines and conventional workflow. LI-COR Biosciences, Lincoln, USA, 1-141. https://doi.org/10.13140/RG.2.1.3723.5683

Campbell, G.S., Norman, J.M., 1998. An introduction to environmental biophysics, 2nd ed. ed. Springer, New York Berlin Heidelberg.

Ceschia, E., Béziat, P., Dejoux, J.F., Aubinet, M., Bernhofer, C., Bodson, B., Buchmann, N., Carrara, A., Cellier, P., Di Tommasi, P., Elbers, J.A., Eugster, W., Grünwald, T., Jacobs, C.M.J., Jans, W.W.P., Jones, M., Kutsch, W., Lanigan, G., Magliulo, E., Marloie, O., Moors, E.J., Moureaux, C., Olioso, A., Osborne, B., Sanz, M.J., Saunders, M., Smith, P., Soegaard, H., Wattenbach, M., 2010. Management effects on net ecosystem carbon and GHG budgets at European crop sites. Agric. Ecosyst. Environ. 139, 363–383. https://doi.org/10.1016/J.AGEE.2010.09.020

Charuchittipan, D., Babel, W., Mauder, M., Leps, J.P., Foken, T., 2014. Extension of the averaging time in eddy-covariance measurements and its effect on the energy balance closure. Boundary-Layer Meteorol. 152, 303–327. https://doi.org/10.1007/s10546-014-9922-6

Chen, Y.-Y., Li, M.-H., 2012. Determining adequate averaging periods and reference coordinates for eddy covariance measurements of surface heat and water vapor fluxes over mountainous terrain. Terr. Atmos. Ocean. Sci. 23, 685. https://doi.org/10.3319/TAO.2012.05.02.01(Hy)

Desjardins, R.L., Macpherson, J.I., Schuepp, P.H., Karanja, F., 1989. An evaluation of aircraftfFlux measurements of CO_2, water vapor and sensible heat. Boundary-Layer Meteorol. 55–69.

Du, Q., Liu, H.Z., Feng, J.W., Wang, L., 2014. Effects of different gap filling methods and land surface energy balance closure on annual net ecosystem exchange in a semiarid area of China. Sci. China Earth Sci. 57, 1340–1351. https://doi.org/10.1007/s11430-013-4756-5

Eshonkulov, R., Poyda, A., Ingwersen, J., Pulatov, A., Streck, T., 2019. Improving the energy balance closure over a winter wheat field by accounting for minor storage terms. Agric. For. Meteorol. 264, 283–296. https://doi.org/10.1016/J.AGRFORMET.2018.10.012.

Ezzahar, J., Er-Raki, S., Marah, H., Khabba, S., Amenzou, N., Chehbouni, G., 2012. Coupling Soil-Vegetation-Atmosphere Transfer Model with Energy Balance Model for estimating energy and water vapor fluxes over an olive orchard in semi-arid region. Glob. Chang. 1, 1–9. https://doi.org/10.4081/gm.2012.e1

FAO, 2014. Agriculture, Forestry and other land use emissions by sources and removals by sinks. Rome.

Finnigan, J., 2004. The footprint concept in complex terrain. Agric. For. Meteorol. 127, 117–129.

https://doi.org/10.1016/j.agrformet.2004.07.008

Foken, T., 2008a. Micrometeorology. Springer-Verlag Berlin Heidelberg. 1st ed., 308 pp.

Foken, T., 2008b. The energy balance closure problem: An overview. Ecol. Appl. 18, 1351–1367. https://doi.org/10.1890/06-0922.1

Foken, T., Mauder, M., Liebethal, C., Wimmer, F., Beyrich, F., Leps, J.P., Raasch, S., DeBruin, H.A.R., Meijninger, W.M.L., Bange, J., 2010. Energy balance closure for the LITFASS-2003 experiment. Theor. Appl. Climatol. 101, 149–160. https://doi.org/10.1007/s00704-009-0216-8

Foken, T., Wimmer, F., Mauder, M., Thomas, C., Liebethal, C., 2006. Some aspects of the energy balance closure problem. Atmos. Chem. Phys. Discuss. 6, 3381–3402. https://doi.org/10.5194/acpd-6-3381-2006

Franssen, H.J.H., Stöckli, R., Lehner, I., Rotenberg, E., Seneviratne, S.I., 2010. Energy balance closure of eddy-covariance data: A multisite analysis for European FLUXNET stations. Agric. For. Meteorol. 150, 1553–1567. https://doi.org/10.1016/j.agrformet.2010.08.005

Gan, G., Gao, Y., 2015. Estimating time series of land surface energy fluxes using optimized two source energy balance schemes: Model formulation, calibration, and validation. Agric. For. Meteorol. 208, 62–75. https://doi.org/10.1016/j.agrformet.2015.04.007

Gu, L., Meyers, T., Pallardy, S.G., Hanson, P.J., Yang, B., Heuer, M., Hosman, K.P., Liu, Q., Riggs, J.S., Sluss, D., 2007. Influence of biomass heat and biochemical energy storages on the land surface fluxes and radiative temperature. J. Geophys. Res. Atmos. 112, 1–11. https://doi.org/10.1029/2006JD007425

Guo, Q., Li, W.W., Liu, D.D., Wu, W., Liu, Y., Wen, X.X., Liao, Y.C., 2013. Seasonal characteristics of CO_2 fluxes in a rain-fed wheat field ecosystem at the Loess Plateau. Spanish J. Agric. Res. 11, 980–988. https://doi.org/10.5424/sjar/2013114-4373

Haverd, V., Cuntz, M., Leuning, R., Keith, H., 2007. Air and biomass heat storage fluxes in a forest canopy: Calculation within a soil vegetation atmosphere transfer model. Agric. For. Meteorol. 147, 125–139. https://doi.org/10.1016/j.agrformet.2007.07.006

Heusinkveld, B.G., Jacobs, A.F.G., Holtslag, A.A.M., Berkowicz, S.M., 2004. Surface energy balance closure in an arid region: Role of soil heat flux. Agric. For. Meteorol. 122, 21–37. https://doi.org/10.1016/j.agrformet.2003.09.005

Heymsfield, S.B., Bourgeois, B., Thomas, D.M., 2017. Assessment of human energy exchange: historical overview. Eur. J. Clin. Nutr. 71, 294–300. https://doi.org/10.1038/ejcn.2016.221

Horton, R., Wierenga, P.J., 1983. Estimating the soil heat flux from observations of soil temperature near the surface. Soil Sci. Soc. Am. J. 47, 14–20. https://doi.org/10.2136/sssaj1983.03615995004700010003x

Hui, Z., Xuefa, W., 2015. Flux footprint climatology estimated by three analytical models over a subtropical coniferous plantation in southeast China. J. Meteorol. Res. J. Meteor. Res 29, 654–666. https://doi.org/10.1007/s13351-014-4090-7

Imukova, K., Ingwersen, J., Hevart, M., Streck, T., 2016. Energy balance closure on a winter wheat stand: comparing the eddy covariance technique with the soil water balance method. Biogeosciences 13, 63–75. https://doi.org/10.5194/bg-13-63-2016

Ingwersen, J., Högy, P., Wizemann, H.D., Warrach-Sagi, K., Streck, T., 2018. Coupling the land surface model Noah-MP with the generic crop growth model Gecros: Model description, calibration and

validation. Agric. For. Meteorol. 262, 322–339. https://doi.org/10.1016/J.AGRFORMET.2018.06.023

Ingwersen, J., Imukova, K., Högy, P., Streck, T., 2015. On the use of the post-closure methods uncertainty band to evaluate the performance of land surface models against eddy covariance flux data. Biogeosciences 12, 2311–2326. https://doi.org/10.5194/bg-12-2311-2015

Ingwersen, J., Steffens, K., Högy, P., Warrach-Sagi, K., Zhunusbayeva, D., Poltoradnev, M., Gäbler, R., Wizemann, H.D., Fangmeier, A., Wulfmeyer, V., Streck, T., 2011. Comparison of Noah simulations with eddy covariance and soil water measurements at a winter wheat stand. Agric. For. Meteorol. 151, 345–355. https://doi.org/10.1016/j.agrformet.2010.11.010

Inoue, Y., Olioso, A., Choi, W., 2004. Dynamic change of CO_2 flux over bare soil field and its relationship with remotely sensed surface temperature. Int. J. Remote Sens. 25, 1881–1892. https://doi.org/10.1080/0143116031000102449

IPCC, 2014. Climate Change 2014 Mitigation of Climate Change Working Group III Contribution to the Fifth Assessment Report of the Intergovernmental Panel on Climate Change. New York.

Jacobs, A.F.G., Heusinkveld, B.G., Holtslag, A.A.M., 2008. Towards closing the surface energy budget of a mid-latitude grassland. Boundary-Layer Meteorol. 126, 125–136. https://doi.org/10.1007/s10546-007-9209-2

Jones, H.G., Rotenberg, E., 2001. Energy, radiation and temperature regulation in plants. Encycl. Life Sci. 1–7. https://doi.org/10.1002/9780470015902.a0003199.pub2

Kidston, J., Brümmer, C., Black, T.A., Morgenstern, K., Nesic, Z., McCaughey, J.H., Barr, A.G., 2010. Energy balance closure using eddy covariance above two different land surfaces and Implications for CO_2 flux measurements. Boundary-Layer Meteorol. 136, 193–218. https://doi.org/10.1007/s10546-010-9507-y

Kljun, N., Calanca, P., Rotach, M.W., Schmid, H.P., 2015. A simple two-dimensional parameterisation for Flux Footprint Prediction (FFP). Geosci. Model Dev 8, 3695–3713. https://doi.org/10.5194/gmd-8-3695-2015

Kljun, N., Rotach, M.W., Schmid, H.P., 2002. A three-dimensional backward lagrangian footprint. Boundary-Layer Meteorol 103, 205–226.

Klosterhalfen, A., Herbst, M., Weihermüller, L., Graf, A., Schmidt, M., Stadler, A., Schneider, K., Subke, J.-A., Huisman, J.A., Vereecken, H., 2017. Multi-site calibration and validation of a net ecosystem carbon exchange model for croplands. Ecol. Modell. 363, 137–156. https://doi.org/10.1016/J.ECOLMODEL.2017.07.028

Kormann, R., Meixner, F.X., 2001. An analytical footprint model for non-neutral stratification. Boundary-Layer Meteorol. 99, 207–224. https://doi.org/10.1023/A:1018991015119

Körschens, M., Albert, E., Baumecker, M., Ellmer, F., Grunert, M., Hoffmann, S., Kismanyoky, T., Kubat, J., Kunzova, E., Marx, M., Rogasik, J., Rinklebe, J., Rühlmann, J., Schilli, C., Schröter, H., Schroetter, S., Schweizer, K., Toth, Z., Zimmer, J., Zorn, W., 2014. Humus and climate change - results of 15 long-term experiments. Arch. Agron. Soil Sci. 60, 1485–1517. https://doi.org/10.1080/03650340.2014.892204

Kustas, W.P., Prueger, J.H., Hatfield, J.L., Ramalingam, K., Hipps, L.E., 2000. Variability in soil heat flux from a mesquite dune site. Agric. For. Meteorol. 103, 249–264. https://doi.org/10.1016/S0168-1923(00)00131-3

Kutsch, W.L., Aubinet, M., Buchmann, N., Smith, P., Osborne, B., Eugster, W., Wattenbach, M., Schrumpf, M., Schulze, E.D., Tomelleri, E., Ceschia, E., Bernhofer, C., Béziat, P., Carrara, A., Di Tommasi, P., Grunwald, T., Jones, M., Magliulo, V., Marloie, O., Moureaux, C., Olioso, A., Sanz, M.J., Saunders, M., Søgaard, H., Ziegler, W., 2010. The net biome production of full crop rotations in Europe. Agric. Ecosyst. Environ. 139, 336–345. https://doi.org/10.1016/j.agee.2010.07.016

Lal, R., 2004. Soil carbon sequestration to mitigate climate change. Geoderma 123, 1–22. https://doi.org/10.1016/J.GEODERMA.2004.01.032

Lamaud, E., Ogée, J., Brunet, Y., Berbigier, P., 2001. Validation of eddy flux measurements above the understorey of a pine forest. Agric. For. Meteorol. 106, 187–203. https://doi.org/https://doi.org/10.1016/S0168-1923(00)00215-X

Lee, X., 2003. Fetch and footprint of turbulent fluxes over vegetative stands with elevated sources. Boundary-Layer Meteorol. 107, 561–579. https://doi.org/10.1023/A:1022819907480

Leuning, R., van Gorsel, E., Massman, W.J., Isaac, P.R., 2012. Reflections on the surface energy imbalance problem. Agric. For. Meteorol. 156, 65–74. https://doi.org/10.1016/j.agrformet.2011.12.002

Li, N., Jia, L., Zheng, C., 2014. Evaluation of the harmonic-analysis method for surface soil heat flux estimation: a case study in Heihe River Basin, in: Proc. SPIE 9260, Land Surface Remote Sensing II, 926043 (8 November 2014). p. 926043. https://doi.org/10.1117/12.2069270

Lindroth, A., Mölder, M., Lagergren, F., 2010. Heat storage in forest biomass improves energy balance closure. Biogeosciences 7, 301–313. https://doi.org/10.5194/bg-7-301-2010

Liu, H., Randerson, J.T., Lindfors, J., Massman, W.J., Foken, T., 2006. Consequences of incomplete surface energy balance closure for CO_2 fluxes from open-path CO_2/H_2O infrared gas analysers. Boundary-Layer Meteorol. 120, 65–85. https://doi.org/10.1007/s10546-005-9047-z

Mammarella, I., Nordbo, A., Rannik, Ü., Haapanala, S., Levula, J., Laakso, H., Ojala, A., Peltola, O., Heiskanen, J., Pumpanen, J., Vesala, T., 2015. Carbon dioxide and energy fluxes over a small boreal lake in Southern Finland. J. Geophys. Res. Biogeosciences 120, 1296–1314. https://doi.org/10.1002/2014JG002873

Masseroni, D., Corbari, C., Mancini, M., 2014. Limitations and improvements of the energy balance closure with reference to experimental data measured over a maize field. Atmosfera 27, 335–352. https://doi.org/10.1016/S0187-6236(14)70033-5

Massman, W.J., 1992. Correcting errors associated with soil heat flux measurements and estimating soil thermal properties from soil temperature and heat flux plate data. Agric. For. Meteorol. 59, 249.

Mauder, M., Cuntz, M., Drüe, C., Graf, A., Rebmann, C., Schmid, H.P., Schmidt, M., Steinbrecher, R., 2013. A strategy for quality and uncertainty assessment of long-term eddy-covariance measurements. Agric. For. Meteorol. 169, 122–135. https://doi.org/10.1016/j.agrformet.2012.09.006

Mauder, M., Foken, T., 2006. Impact of post-field data processing on eddy covariance flux estimates and energy balance closure. Meteorol. Zeitschrift 15, 597–609. https://doi.org/10.1127/0941-2948/2006/0167

Mayocchi, C.L., Bristow, K.L., 1995. Soil surface heat flux: some general questions on measurements 75, 43–50.

Meyers, T.P., Baldocchi, D.D., 2005. Current Micrometeorological Flux Methodologies with

Applications in Agriculture. Publ. Agencies Staff U.S. Dep. Commersee.

Meyers, T.P., Hollinger, S.E., 2004. An assessment of storage terms in the surface energy balance of maize and soybean. Agric. For. Meteorol. 125, 105–115. https://doi.org/10.1016/j.agrformet.2004.03.001

Michiles, A.A. dos S., Gielow, R., 2008. Above-ground thermal energy storage rates, trunk heat fluxes and surface energy balance in a central Amazonian rainforest. Agric. For. Meteorol. 148, 917–930. https://doi.org/10.1016/j.agrformet.2008.01.001

Moderow, U., Aubinet, M., Feigenwinter, C., Kolle, O., Lindroth, A., Mölder, M., Montagnani, L., Rebmann, C., Bernhofer, C., 2009. Available energy and energy balance closure at four coniferous forest sites across Europe. Theor. Appl. Climatol. 98, 397–412. https://doi.org/10.1007/s00704-009-0175-0

Monteith, J.L., Unsworth, M.H., 2013. Principles of Environmental Physics, 4th ed. Elsevier, Amsterdam, Boston, Heidelberg, London, New York, Oxford, Paris, San Diego, San Fransisco, Singapore, Sydney, Tokyo.

Moors, E.J., Jacobs, C., Jans, W., Supit, I., Kutsch, W.L., Bernhofer, C., Béziat, P., Buchmann, N., Carrara, A., Ceschia, E., Elbers, J., Eugster, W., Kruijt, B., Loubet, B., Magliulo, E., Moureaux, C., Olioso, A., Saunders, M., Soegaard, H., 2010. Variability in carbon exchange of European croplands. Agric. Ecosyst. Environ. 139, 325–335. https://doi.org/10.1016/j.agee.2010.04.013

Neftel, A., Spirig, C., Ammann, C., 2008. Application and test of a simple tool for operational footprint evaluations. Environ. Pollut. 152, 644–652. https://doi.org/10.1016/J.ENVPOL.2007.06.062

Nordbo, A., Järvi, L., Vesala, T., 2012. Revised eddy covariance flux calculation methodologies – effect on urban energy balance. Tellus B 64, 1–20. https://doi.org/10.3402/tellusb.v64i0.18184

Nordbo, A., Launiainen, S., Mammarella, I., Leppäranta, M., Huotari, J., Ojala, A., Vesala, T., 2011. Long-term energy flux measurements and energy balance over a small boreal lake using eddy covariance technique. J. Geophys. Res. Atmos. 116, 1–17. https://doi.org/10.1029/2010JD014542

Oke, T.R., 1987. Boundary layer climates. Routledge, London. Psychology Press, 435 pp.

Oliphant, a. J., Grimmond, C.S.B., Zutter, H.N., Schmid, H.P., Su, H.-B., Scott, S.L., Offerle, B., Randolph, J.C., Ehman, J., 2004. Heat storage and energy balance fluxes for a temperate deciduous forest. Agric. For. Meteorol. 126, 185–201. https://doi.org/10.1016/j.agrformet.2004.07.003

Oncley, S.P., Foken, T., Vogt, R., Kohsiek, W., DeBruin, H.A.R., Bernhofer, C., Christen, A., van Gorsel, E., Grantz, D., Feigenwinter, C., Lehner, I., Liebethal, C., Liu, H., Mauder, M., Pitacco, A., Ribeiro, L., Weidinger, T., 2007. The energy balance experiment EBEX-2000. Part I: overview and energy balance. Boundary-Layer Meteorol. 123, 1–28. https://doi.org/10.1007/s10546-007-9161-1

Pardo, N., Sánchez, M.L., Pérez, I.A., Garcií, M.A., 2015. Energy balance and partitioning over a rotating rapeseed crop. Agric. Water Manag. 161, 31–40. https://doi.org/10.1016/j.agwat.2015.07.015

Ping, Y., Qiang, Z., Shengjie, N., Hua, C., Xiyu, W., 2011. Effects of the soil heat flux estimates on surface energy balance closure over a semi-arid grassland. Acta Meteorol. Sin. 25, 774–782. https://doi.org/10.1007/s13351-011-0608-4

Pirk, N., Sievers, J., Mertes, J., Parmentier, F.-J.W., Mastepanov, M., Christensen, T.R., 2017. Spatial variability of CO_2 uptake in polygonal tundra: assessing low-frequency disturbances in eddy covariance flux estimates. Biogeosciences 14, 3157–3169. https://doi.org/10.5194/bg-14-3157-2017

Poeplau, C., Don, A., Vesterdal, L., Leifeld, J., Van Wesemael, B., Schumacher, J., Gensior, A., 2011. Temporal dynamics of soil organic carbon after land-use change in the temperate zone - carbon response functions as a model approach. Glob. Chang. Biol. 17, 2415–2427. https://doi.org/10.1111/j.1365-2486.2011.02408.x

Poyda, A., Reinsch, T., Kluß, C., Loges, R., Taube, F., 2016. Greenhouse gas emissions from fen soils used for forage production in northern Germany. Biogeosciences 13, 5221–5244. https://doi.org/10.5194/bg-13-5221-2016

Poyda, A., Reinsch, T., Skinner, R.H., Kluß, C., Loges, R., Taube, F., 2017. Comparing chamber and eddy covariance based net ecosystem CO_2 exchange of fen soils. J. Plant Nutr. Soil Sci. 1–15. https://doi.org/10.1002/jpln.201600447

Reed, D.E., Frank, J.M., Ewers, B.E., Desai, A.R., 2018. Time dependency of eddy covariance site energy balance. Agric. For. Meteorol. 249, 467–478. https://doi.org/10.1016/J.AGRFORMET.2017.08.008

Reicosky, D.C., Allmaras, R.R., 2003. Advances in tillage research in north American cropping systems. J. Crop Prod. 8, 75–125. https://doi.org/10.1300/J144v08n01_05

Saigusa, N., Yamamoto, S., Murayama, S., Kondo, H., Nishimura, N., 2002. Gross primary production and net ecosystem exchange of a cool-temperate deciduous forest estimated by the eddy covariance method, Agricultural and Forest Meteorology.

Sánchez, J.M., Caselles, V., Rubio, E.M., 2010. Analysis of the energy balance closure over a FLUXNET boreal forest in Finland. Hydrol. Earth Syst. Sci. 14, 1487–1497. https://doi.org/10.5194/hess-14-1487-2010

Santanello, J.A., Peters-Lidard, C.D., Kennedy, A., Kumar, S. V., Jr., J.A.S., Peters-Lidard, C.D., Kennedy, A., Kumar, S. V., 2013. Diagnosing the nature of land–atmosphere coupling: A case study of dry/wet extremes in the U.S. southern Great Plains. J. Hydrometeorol. 14, 3–24. https://doi.org/10.1175/JHM-D-12-023.1

Santanello, J.A., Peters-Lidard, C.D., Kumar, S. V., Jr., J.A.S., Peters-Lidard, C.D., Kumar, S. V., 2011. Diagnosing the sensitivity of local land–atmosphere coupling via the soil moisture–boundary layer Interaction. J. Hydrometeorol. 12, 766–786. https://doi.org/10.1175/JHM-D-10-05014.1

Sauer, T.J., Horton, R., 2005. Soil Heat Flux. Agron. J. 99, 304. https://doi.org/10.2134/agronj2005.0038s

Schmid, H.P., 2002. Footprint modeling for vegetation atmosphere exchange studies: A review and perspective. Agric. For. Meteorol. 113, 159–183. https://doi.org/10.1016/S0168-1923(02)00107-7

Schmidt, M., Reichenau, T.G., Fiener, P., Schneider, K., 2012. The carbon budget of a winter wheat field: An eddy covariance analysis of seasonal and inter-annual variability. Agric. For. Meteorol. 165, 114–126. https://doi.org/10.1016/j.agrformet.2012.05.012

Shao, C., Chen, J., Stepien, C.A., Chu, H., Ouyang, Z., Bridgeman, T.B., Czajkowski, K.P., Becker, R.H., John, R., 2015. Diurnal to annual changes in latent, sensible heat, and CO2 fluxes over a Laurentian Great Lake: A case study in western Lake Erie. J. Geophys. Res. Biogeosciences 120, 1587–1604. https://doi.org/10.1002/2015JG003025

Sievers, J., Papakyriakou, T., Larsen, S.E., Jammet, M.M., Rysgaard, S., Sejr, M.K., Sørensen, L.L., 2015. Estimating surface fluxes using eddy covariance and numerical ogive optimization. Atmos. Chem. Phys. 15, 2081–2103. https://doi.org/10.5194/acp-15-2081-2015

Smith, J.O., Smith, P., Wattenbach, M., Zaehle, S., Hiederer, R., Jones, R.J. a, Montanarella, L., Rounsevell, M.D. a, Reginster, I., Ewert, F., 2005. Projected changes in mineral soil carbon of European croplands and grasslands, 1990–2080. Glob. Chang. Biol. 11, 2141–2152. https://doi.org/10.1111/j.1365-2486.2005.01075.x

Smith, P., Martino, D., Cai, Z., Gwary, D., Janzen, H., Kumar, P., McCarl, B., Ogle, S., O'Mara, F., Rice, C., Scholes, B., Sirotenko, O., Howden, M., McAllister, T., Pan, G., Romanenkov, V., Schneider, U., Towprayoon, S., Wattenbach, M., Smith, J., 2008. Greenhouse gas mitigation in agriculture. Philos. Trans. R. Soc. Lond. B. Biol. Sci. 363, 789–813. https://doi.org/10.1098/rstb.2007.2184

Stoy, P.C., Mauder, M., Foken, T., Marcolla, B., Boegh, E., Ibrom, A., Arain, M.A., Arneth, A., Aurela, M., Bernhofer, C., Cescatti, A., Dellwik, E., Duce, P., Gianelle, D., van Gorsel, E., Kiely, G., Knohl, A., Margolis, H., Mccaughey, H., Merbold, L., Montagnani, L., Papale, D., Reichstein, M., Saunders, M., Serrano-Ortiz, P., Sottocornola, M., Spano, D., Vaccari, F., Varlagin, A., 2013. A data-driven analysis of energy balance closure across FLUXNET research sites: The role of landscape scale heterogeneity. Agric. For. Meteorol. 171–172, 137–152. https://doi.org/10.1016/j.agrformet.2012.11.004

Stull, B.R., 1988. An introduction to boundary layer meteorology. Kluwer Acd.Publ., Dordrecht, Boston, London, 670 pp.

Sun, X.-M., Zhu, Z.-L., Wen, X.-F., Yuan, G.-F., Yu, G.-R., 2006. The impact of averaging period on eddy fluxes observed at ChinaFLUX sites. Agric. For. Meteorol. 137, 188–193. https://doi.org/10.1016/J.AGRFORMET.2006.02.012

Teh, C.B.S., 2006. Introduction to mathematical modeling of crop growth : how the equations are derived and assembled into a computer model. Brown Walker Press, Boca Raton.

Varmaghani, A., Eichinger, W.E., Prueger, J.H., 2016. A diagnostic approach towards the causes of energy balance closure problem. Open J. Mod. Hydrol. 101–114.

Wang, R., Zhang, Q., 2011. An assessment of storage terms in the surface energy balance of a subalpine meadow in northwest China. Adv. Atmos. Sci. 28, 691–698. https://doi.org/10.1007/s00376-010-9152-x

Weber, T.K.D., Gerling, L., Reineke, D., Weber, S., Durner, W., Iden, S.C., 2018. Robust inverse modeling of growing season net ecosystem exchange in a mountainous peatland: influence of distributional assumptions on estimated parameters and total carbon fluxes. J. Adv. Model. Earth Syst. 10, 1319–1336. https://doi.org/10.1029/2017MS001044

Wilson, K., Goldstein, A., Falge, E., Aubinet, M., Baldocchi, D., Berbigier, P., Bernhofer, C., Ceulemans, R., Dolman, H., Field, C., Grelle, A., Ibrom, A., Law, B.., Kowalski, A., Meyers, T., Moncrieff, J., Monson, R., Oechel, W., Tenhunen, J., Valentini, R., Verma, S., 2002. Energy balance closure at FLUXNET sites. Agric. For. Meteorol. 113, 223–243. https://doi.org/10.1016/S0168-1923(02)00109-0

Wizemann, H.D., Ingwersen, J., Högy, P., Warrach-Sagi, K., Streck, T., Wulfmeyer, V., 2014. Three year observations of water vapor and energy fluxes over agricultural crops in two regional climates of southwest Germany. Meteorol. Zeitschrift 24, 39–59. https://doi.org/10.1127/metz/2014/0618

Wolf, A., Laca, E.A., 2007. Cospectral analysis of high frequency signal loss in eddy covariance measurements. Atmos. Chem. Phys. Discuss. 7, 13151–13173.

Xu, Z., Liu, S., Shi, W., Wang, J., 2017. Assessment of the energy balance closure under advective

conditions and its impact using remote sensing data. Am. Meteorol. Soc. 127–140. https://doi.org/10.1175/JAMC-D-16-0096.1

Zeri, M., Sá, L.D.A., 2010. The impact of data gaps and quality control filtering on the balances of energy and carbon for a southwest Amazon forest. Agric. For. Meteorol. 150, 1543–1552. https://doi.org/10.1016/j.agrformet.2010.08.004

Zuo, J., Wang, J., Huang, J., Li, W., Wang, G., Ren, H., 2011. Estimation of ground heat flux and its impact on the surface energy budget for a semi-arid grassland 3, 41–50. https://doi.org/10.3724/SP.J.1226.2011.00041

Chapter 2

Paper A

2. Improving the energy balance closure over a winter wheat field by accounting for minor storage terms[1]

Ravshan Eshonkulov[a], Arne Poyda[a], Joachim Ingwersen[a], Alim Pulatov[b] and Thilo Streck[a]

[a]Institute of Soil Science and Land Evaluation, Biogeophysics, Hohenheim University, 70593 Stuttgart, Germany

[b]EcoGIS center, Tashkent Institute of Irrigation and Agricultural Mechanization Engineers, 100000 Tashkent, Uzbekistan.

Keywords: minor storage terms, soil heat storage, ground heat flux, eddy covariance, winter wheat

Abstract

Turbulent fluxes at the land surface measured by the Eddy Covariance (EC) technique are typically considerably less than the difference between net radiation and ground heat flux. This is known as the energy balance closure (EBC) problem. It is crucial for validating land surface models as it provokes substantial uncertainty to the magnitude and partitioning of energy fluxes. The gap in the energy balance calls for searching for additional energy terms in the soil-plant-atmosphere system. To evaluate the contribution of these minor storage terms to the measured EBC, we conducted an experimental study to evaluate the contribution of these minor storage terms to measured EBC in the Kraichgau region in southwest Germany over two consecutive growing seasons (2015 and 2016). The measured and calculated minor storage terms comprised the enthalpy change in the plant canopy (S_c), the air enthalpy change (S_a), the energy consumption and release by photosynthesis and respiration (S_p), and the atmospheric moisture change (S_q). Furthermore, the soil heat storage (S_g) was determined at different locations within the EC footprint and compared to the single point measurements of S_g at the EC station. Calorimetric and harmonic analysis were performed to compute ground heat flux. S_p had the strongest effect in improving EBC due to the high net CO_2 uptake during the productive phase of plant growth. In

[1] The publication of Chapter 2 is done with the consent of the Elsevier B.V. The original publication was in: Journal of Agricultural and Forest Meteorology, Volume 264, Pages 283-296. It can be found under the following link: https://doi.org/10.1016/j.agrformet.2018.10.012

2015, all minor storage terms together increased EBC by 5.0 % on average, with a maximum value of 7.4 % in May, while the improvement in 2016 was 6.8 % on average and 8.4 % in May. Ground heat flux computed with the harmonic analysis based on plate data narrowed the EBC by 3 % more than the calorimetric method. In summary, a better EBC can be achieved by considering minor storage terms and applying a harmonic analysis to ground heat flux data. Regarding future research, we recommend to focus on year-round measurements of energy terms because energy stored during the growing season might be lost from the system during the rest of the year. Nonetheless, the significant contribution of minor energy terms to EBC indicates that turbulent energy fluxes are most likely overestimated when all the missing energy is assumed to be turbulent − the typical approach when fluxes are corrected by the Bowen ratio post-closure method for instance.

2.1. Introduction

The eddy covariance technique is a widespread micrometeorological method to assess the turbulent exchange of water, energy or trace gases between the land surface and the atmosphere. Today, the EC method is applied by a broad community of scientists including meteorologists, agronomists, biologists, hydrologists, geographers and environmentalists. The development of open software packages such as TK3.1 (Mauder et al., 2013) or EddyPro® (LI-COR Inc., 2012) has made processing and evaluating the EC data more practical. Nevertheless, applying the EC method to study energy fluxes at the land surface is associated with certain deficiencies. According to the first law of thermodynamics, incoming and outgoing energy at the land surface must be balanced. However, the turbulent fluxes from EC measurements are in general systematically smaller than the measured available energy at the land surface. This energy balance gap is a comprehensive and ongoing problem in micrometeorological research (Foken, 2008; Leuning et al., 2012).

Generally, the surface energy balance can be calculated from the sum of the turbulent fluxes of sensible heat (H) and latent heat (LE), the minor storage terms (S_p, S_c, S_a, and S_q) and the available energy, described by the difference of net radiation (R_n) and ground heat flux (G) (Jacobs et al., 2008):

$$H + LE + S_a + S_q + S_p + S_c = R_\mathrm{n} - G \tag{2.1}$$

Here, S_a (W m^{-2}) is the air enthalpy change, S_q (W m^{-2}) is the atmospheric moisture change, S_p (W m^{-2}) is the energy consumption and release by photosynthesis and respiration, and S_c (W m^{-2}) is the enthalpy change in the plant canopy. All fluxes are in W m^{-2}. Note: in standard EC studies, the storage terms on the left hand side are usually neglected.

The energy imbalance may in principle be attributed to the underestimation of turbulent fluxes or the overestimation of available energy. Typical values of EBC, defined as $(H + LE)/(R_n - G)$, range from 70 to 90 % for most (agro-) ecosystems (Barr et al., 2006; Foken et al., 2010; Leuning et al., 2012; Oncley et al., 2007; Poyda et al., 2017; Twine et al., 2000). Many studies have been conducted to identify potential reasons for the surface energy imbalance problem. Important reasons have been attributed to instrumental errors of the EC measurements (Foken, 2008; Kidston et al., 2010), neglected energy storage terms in soil, air and vegetation (Jacobs et al., 2008; Meyers and Hollinger, 2004) or problems with radiation measurements (Kohsiek et al., 2007). Other major explanations for the EBC gap include loss of low-frequency contributions during data processing because of inadequate temporal averaging periods, mesoscale fluxes that cannot be captured by a single EC tower (Foken et al., 2010), as well as complex terrain and surface heterogeneity (Guo et al., 2009).

While the above factors have been frequently discussed and investigated as factors behind the EBC problem (Foken et al., 2010; Oncley et al., 2007; Stoy et al., 2013; Twine et al., 2000; Wilson et al., 2002), a more recent explanation involves neglected energy storage terms in the soil-plant-atmosphere system that are not measured directly by typical EC instrumentations (Leuning et al., 2012; Varmaghani et al., 2016). These minor storage terms are usually omitted because they are difficult to measure and believed to be small. One of the initial attempts to assess the impact of these terms on the EBC in maize and soybean fields is that by Meyers and Hollinger (2004). The minor storage terms typically include air enthalpy change, atmospheric moisture change, energy consumption by photosynthesis and release by respiration, heat storage in plant biomass and dew water heat storage (Jacobs et al., 2008). Previous studies on agricultural fields showed that the energy stored by CO_2 uptake and the heat storage in plant biomass were the quantities best suited to improve EBC (Masseroni et al., 2014; Meyers and Hollinger, 2004). The energy exchange by photosynthesis and respiration is directly measurable by the EC as a conversion of the net ecosystem exchange (NEE) of CO_2 (Leuning et al., 2012).

In forest ecosystems, considering additional storage terms (biomass, air and soil heat storages) improved the EBC from 86 to 95 % (Lindroth et al., 2010). An improvement from 90 % to 100 % was reported by measuring heat storage in canopy air and biomass and heat stored due to photosynthetic activity in European coniferous forest sites (Moderow et al., 2009). Michiles and Gielow (2008) and Zeri and Sá (2010) also improved the EBC by accounting for minor heat storage terms. Most studies have been conducted in forest ecosystems, with little attention given to agricultural ecosystems.

The energy balance closure of EC measurements is also associated with scale dependency (Masseroni et al., 2014), which makes it important to consider the source area of turbulent fluxes (footprint) during the observation period (Kormann and Meixner, 2001; Lee, 2003). The footprint depends on wind speed and direction, surface roughness, measurement height, atmospheric stability and boundary layer height (Kljun et al., 2015; Masseroni et al., 2014; Sánchez et al., 2010). A few researchers studied the relationship between the EBC and the footprint. Masseroni et al. (2014) reported that the EBC declined with increasing footprint while Stoy et al. (2013) found no statistical relationship between the footprint and the EBC across FLUXNET research sites.

A fundamental component for more accurately quantifying the energy balance at the land surface is the ground heat flux (Gao et al., 2010; Jacobs et al., 2008; Núñez et al., 2010; Ochsner et al., 2007; Zuo et al., 2011). For growing crops, it accounts on an hourly basis for 1 - 10 % of net radiation (Ochsner et al., 2007), underlining that its omission would lead to substantial errors in the EBC (Heusinkveld et al., 2004; Ochsner et al., 2007). Sauer et al. (2007) presented a comprehensive review of the ground heat flux and its role for EBC. They also emphasized the significance of the spatial variation in soil heat storages under in-field conditions. However, the source area of the ground heat flux is generally much smaller than the footprint of *H* and *LE* adding a substantial uncertainty to the quantification of EBC. Moreover, the heat storage in soil is a major component of the ground heat flux and it plays an important role in estimating the surface EBC (Ping et al., 2011; Yuan et al., 2014) The ground heat flux at soil surface is underestimated if it is measured some centimeters below the soil surface. To obtain the 'true' ground heat flux at the soil surface one has to add the storage changes between the soil surface and the measurement point of the soil heat flux. Calculating the soil heat storage requires measuring soil water content, soil temperature, and bulk density (Ochsner et al., 2007; Yuan et al., 2014). In recent years, an increasing number of studies has been devoted to the contribution of the soil heat storage to EBC (Liu et al., 2017; Masseroni et al., 2014; Meyers and Hollinger, 2004; Wang and Zhang, 2011).

During the last three decades, it has become popular to calculate the ground heat flux by harmonic analysis (Heusinkveld et al., 2004; Horton and Wierenga, 1983; Li et al., 2014; Protic et al., 2012, Zuo et al., 2011). This analysis enables calculating the ground heat flux from measurements in deeper soil depths, but is restricted to homogeneous soils. Moreover, the EBC based on harmonic analysis was higher than EBC calculated with ground heat fluxes derived by the calorimetric method (Heusinkveld et al., 2004; Jacobs et al., 2008). This is because the former considers a complex interplay of high and low frequencies of ground heat flux and temperature in the calculation process (Heusinkveld et al., 2004).

Jacobs et al. (2008) found that, compared to the calorimetric method, harmonic analysis of ground heat flux increased EBC of a grassland site from 81 to 90 %.

This present study aims at reducing the EBC gap by assessing the contribution of minor energy storage terms. Further objectives were: (i) to check how assessing the minor storage terms within the EC footprint contributed to EBC, (ii) to investigate how single point measurements of the soil heat storage close to EC stations compare to measurements over the entire EC footprint and, (iii) to compare ground heat fluxes calculated by calorimetric and harmonic analysis.

2.2. Materials and methods

2.2.1. Site characteristics

The study was carried out on fields of the farm "Katharinentalerhof" (48.92 °N, 8.70 °E, 320 m a.s.l.) in Kraichgau (Fig. 2.1). The Kraichgau is one of the warmest regions of Germany. During the period 1981 – 2010, mean annual temperature was 9.4 °C and mean annual precipitation sum was 889 mm (German Weather Service, meteorological station Pforzheim-Ispringen). The dominant wind direction is southwest. Three eddy covariance (EC) stations were installed on neighboring fields in 2009 (Fig. 2.1). The observations of this study were conducted on the field surrounding EC1 in 2015 and on the field of EC3 in 2016. The distances from which 95 % of measured fluxes were observed (footprint) on EC1 were 81, 175, 113 and 187 m to the north, east, south and west, respectively. The respective distances for EC3 were 97, 222, 93 and 146 m (north, east, south, west) (Imukova et al., 2016; Fig. 2.1.) Crop rotation includes winter wheat, winter rapeseed, and energy maize following a winter cover crop. Winter wheat is the dominating crop, grown at least every second year on each field. Consequently, the investigated crop of this study was winter wheat in both years (cultivars *Sokal* in 2015 and *Estivus, Pamier and Ferrum* in 2016). Field sizes of EC1 and EC3 were 14.9 and 15.8 ha, respectively. The fields are managed by a local farmer and tillage is conducted as ploughing or grubbing. While the field of EC1 is surrounded by hedges along the north and west borders, the field of EC3 is surrounded by trees on all sides. During the main growing period the mean leaf area index (LAI) was 3.9 m^2 m^{-2} at EC1 and 3.0 m^2 m^{-2} at EC3 in 2015 and 2016, respectively.

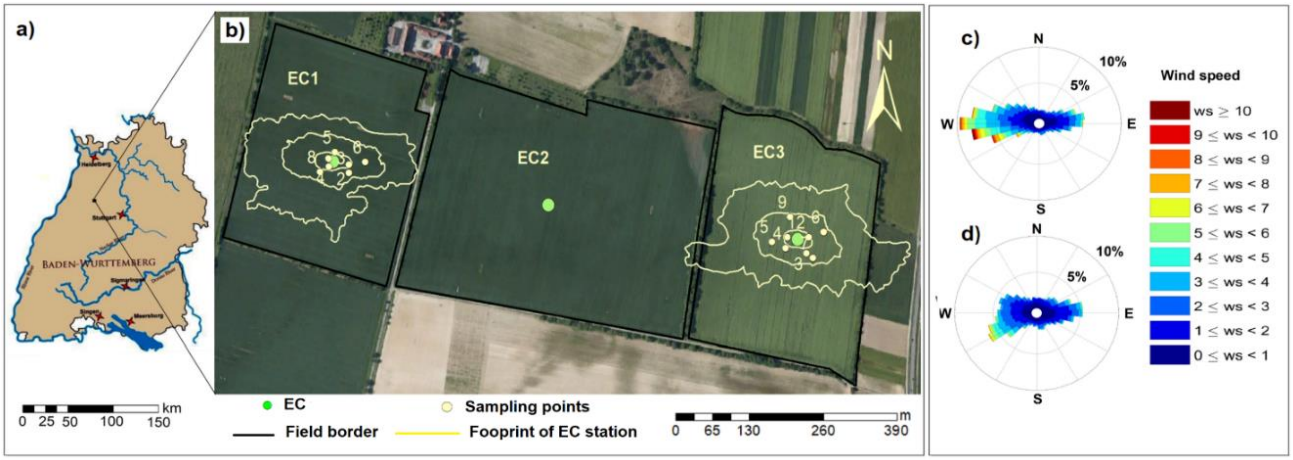

Fig. 2.1. a) Geographical overview of the study area, b) study sites with the position of the eddy covariance (EC) station and their footprints. The lines indicate (from inside to outside) the source areas that contribute on average 50, 80, and 95 % to the measured turbulent fluxes. The yellow points show the position of soil heat storage measurements (Image source: Google Earth scene from 16 June 2013), and c) and d) rose diagrams of wind speed and direction at EC1 and EC3, respectively.

The soil type of both fields is Stagnic Luvisol (IUSS Working Group WRB, 2014) which developed from loess sediments with a thickness of several meters. Topsoil properties are given in Table 2.1, reflecting homogeneous soil conditions. The underlying bedrock is shell limestone. Further information can be found in Ingwersen et al. (2011), Wizemann et al. (2014) and Imukova et al. (2015, 2016).

Table 2.1. Topsoil properties of the fields EC1 and EC3.

Depth (m)	Bulk density[a] (g cm^{-3})	Texture[b] S/U/C* (% by weight)	Organic matter content[b] (% by weight)	Carbonate content[b] (% by weight)	pH[b] (0.01 M $CaCl_2$)
			EC1		
0−0.1	1.39				
0.1−0.2	1.40	2.5/79.4/18.2	1.75	1.50	6.9
0.2−0.3	1.39				
			EC3		
0−0.1	1.46				
0.1−0.2	1.50	1.8/81.1/17.1	1.64	1.46	6.4
0.2−0.3	1.51				

*Fraction of sand (S), silt (U), clay (C).
[a] Mean value of two sampling campaigns during the vegetation periods 2015 (EC1) and 2016 (EC3) at 6 locations per station.
[b] Values obtained from a soil profile close to the EC station in 2009.

2.2.2. Eddy covariance measurements

The turbulent fluxes were measured using the EC technique according to the state of the art. All stations were equipped with an LI-7500 open path infrared CO_2/H_2O analyzer (LI-COR Biosciences, Lincoln, NE, USA) and a CSAT3 3-D sonic anemometer (Campbell Scientific Inc., Logan, UT, USA). At sites

EC1 and EC3, the sonic anemometers and the gas analyzers were mounted at a height of 2.94 and 2.68 m. The distance between the two instruments was 0.205 and 0.265 m, respectively. The CSAT orientation was 180 ° against north at both sites and the values were 52 and 29 ° for the LI-7500 at EC1 and EC3, respectively. Data were collected with 10 Hz and averaged over 30-min intervals. Incoming and outgoing long- and shortwave radiation was measured using a 4-component radiometer (NR01, Hukseflux Thermal Sensors, Delft, the Netherlands). The radiometers were placed next to the EC stations in the wheat, roughly 2 m above ground. Air temperature and humidity were measured at a height of 2 m at each EC station using a temperature and relative humidity probe (HMP45C, Vaisala Inc, Helsinki, Finland). Soil temperature probes (107 Thermistor probe (±0.2 °C), Campbell Scientific Inc., Logan, UT, UK) were installed at soil depths of 0.02, 0.06, 0.15, 0.30 and 0.45 m. For measuring the ground heat flux near the EC stations, three heat flux plates (HFP01, Hukseflux Thermal sensors, Delft, Netherlands) were buried in a depth of 0.08 m. Frequency-domain reflectometry (FDR) sensors (CS616, Campbell Scientific Inc., Logan, UT, USA) were used to continuously measure the soil volumetric water content at 0.05, 0.15, 0.30, 0.45 and 0.75 m depth. A 0.2 mm tipping bucket (ARG 100, Environmental measurements Ltd., North Shields, UK) was used to measure precipitation.

2.2.2.1. Data processing and filtering

The software TK3.1 (Mauder and Foken, 2011) was used to process the EC data and to compute the fluxes of latent heat (LE), sensible heat (*H*) and net ecosystem exchange (NEE) of CO_2. Using the quality flags of Mauder and Foken (2011) provided by TK3.1, the high (flags 1−3) and moderate quality data (flags 4−6) were used for further evaluation. Poor quality data (flags 7−9) were eliminated from the dataset. In the next step, spikes were identified in the remaining dataset using a median filter. For this purpose, three-day medians were calculated from absolute values of the fluxes. Each flux value exceeding six times the median flux of the previous three days was regarded as a spike and removed from the dataset. This was done in order to eliminate unphysically fluxes which remained in the dataset after excluding data labelled with flags 7 – 9. The same procedure was performed for all EC fluxes such as NEE, *LE*, and *H* for both growing seasons. The computation time interval for all recorded data was 30 min. After this filtering procedure, data availability ranged between 61 and 73 % depending on the observed period (Table 2.3). Mean data availability was 66 % from which 65 and 35 % were daytime and nighttime data, respectively, when a global radiation threshold of 20 W m^{-2} was used to distinguish between daytime and nighttime.

2.2.2.2. Energy balance closure from EC measurements

The EBC at the land surface derived from the EC measurements can be estimated by ordinary linear regression (OLR) of turbulent fluxes (*LE*+*H*) against the available energy. The latter is taken as the difference between net radiation (R_n) and ground heat flux (G). The outcome of OLR represents a perfect EBC if the slope equals 1 with an intercept of 0 (Tol et al., 2015; Wilson et al., 2002).

2.2.3. Minor storage terms of the energy balance

2.2.3.1. Measurement and calculation of air enthalpy change, atmospheric moisture change and CO_2 flux related energy exchange

The energy stored or released due to changes in air temperature was calculated by the following equation:

$$S_a = p_a \cdot C_a \cdot \frac{\Delta T_a}{\Delta t} \cdot L_{EC} \quad (2.2)$$

where p_a (kg m^{-3}) is the atmospheric moisture density, C_a (J kg^{-1} K^{-1}) is the specific heat capacity of moist air, ΔT_a (K) is the air temperature change, L_{EC} (m) is the distance between gas analyzer and upper end of the canopy and Δt (s) is the time averaging interval. Atmospheric moisture density, calculated based on the air temperature and on atmospheric pressure, ranged from 1.15 to 1.27 kg m^{-3}. For the parameter C_a, the standard value is 1004 J kg^{-1} K^{-1}.

For calculating the change in the energy storage as fluctuations in humidity, the following equation was applied:

$$S_q = \frac{p_a \cdot L_v \cdot \Delta q}{\Delta t} \cdot L_{EC} \quad (2.3)$$

where L_v (J kg^{-1}) is the latent heat for vaporization (2400 MJ kg^{-1}) and Δq (kg kg^{-1}) is the change in specific humidity of the atmosphere.

The energy stored or released by CO_2 exchange between the soil-plant-system and the atmosphere was calculated according to Leuning et al. (2012):

$$S_p = -a_p \cdot \overline{FCO_2} \quad (2.4)$$

where α_p is a photosynthetic energy conversion factor (0.469 J μmol^{-1}) and $\overline{FCO_2}$ is the CO_2 flux (μmol m^{-2} s^{-1}) measured at the EC station, generally referred to as net ecosystem exchange (NEE) of CO_2. The approach was initially established by Blanken et al. (1997) for forest ecosystems and was later used in several studies also for agricultural ecosystems (Masseroni et al., 2014; Meyers and Hollinger, 2004; Varmaghani et al., 2016).

2.2.3.2. Canopy heat storage

From 16 June 2015, the temperature in the plant canopy was measured by universal temperature loggers (UTL1, GEOTEST Ltd., Bern, Switzerland). The loggers were attached to plastic sticks in the canopy at three different positions (top, middle, and bottom) at eight locations within the field footprint. At installation time, the average plant height of the canopy was approximately 0.80 – 0.95 m. Each temperature logger was glued into two funnels with diameters of 0.12 m (inner funnel) and 0.16 m (outer funnel). The funnels protected the loggers from direct solar radiation and precipitation (Hubbart, 2011). To enable the exchange of air below and above the funnels, the inner funnel was provided with four small holes with 0.02 m in diameter.

In 2016, temperature measurements in the plant canopy began on 27 April. Temperature loggers were installed at nine sites within the field footprint. Only one sensor was installed in the middle of the canopy because the data of the first year indicated that this temperature is representative for the average canopy temperature (Fig. 2.2). Regarding the growing of wheat, the measurement height was adjusted regularly.

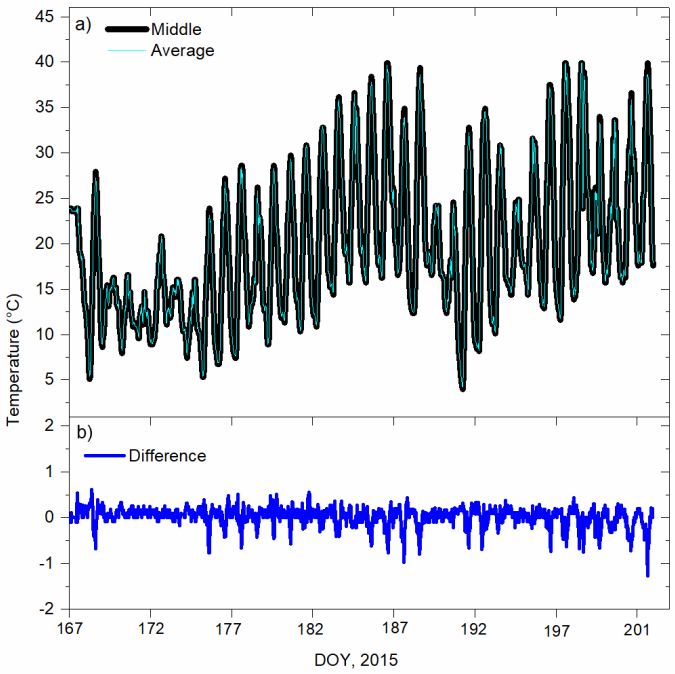

Fig. 2.2. Comparison of canopy temperature measured in the mid-level of the canopy and the average temperature of three different installation heights (a) as well as the temporal development of the difference (b).

The development of plant water content over the growing season was determined by biweekly plant samplings. Four plant samples were taken randomly from 50 m around the EC stations and were instantly

conserved in plastic bags to prevent water loss and transported to a lab within 1 h. In the lab, wet samples were weighed to determine the fresh mass and dried at 60 °C in the oven for roughly 48 h. From wet and dry masses, we calculated the water content of the fresh plant samples. Plant water content and dry biomass values were linearly interpolated between the sampling days.

The change of energy that is stored in the plant canopy in a time interval was calculated as follows:

$$S_c = \frac{\Delta T_c (m_w \cdot C_w + m_{om} \cdot C_{om})}{\Delta t} \quad (2.5)$$

where ΔT_c (K) is the change of the average canopy temperature determined by the three loggers, m_w (kg m^{-2}) is the mass of plant water per unit ground area, m_{om} (kg m^{-2}) is the mass of plant organic matter per unit ground area, C_w (J kg^{-1} K^{-1}) is the specific heat capacity of water, C_{om} (J kg^{-1} K^{-1}) is the specific heat capacity of organic matter and Δt (s) is the time averaging interval (taken as 30 min). Specific heat capacities of water (C_w) and organic matter of biomass (C_{om}) were considered as 4190 J kg^{-1} K^{-1} and 1920 J kg^{-1} K^{-1}, respectively (Atzema, 1993; Jacobs et al., 2008).

2.2.3.3. Measurement of soil heat storage within the EC footprint

The average footprints of the study sites were determined in a previous study (Imukova et al., 2016) using the Lagrangian stochastic model (Göckede et al., 2006). Universal temperature loggers (UTL1 (± 0.1 °C), GEOTEST Ltd., Bern, Switzerland) were used to determine the soil heat storage within the EC footprints of both fields. At six positions UTL1 were installed in 0.02, 0.06, 0.10 and 0.14 m depth in 2015 and in 0.02 and 0.06 m depth in 2016. Measurement periods were from 7 May to 8 June (DOY 127−159) in 2015 and from 26 April to 26 July in 2016 (DOY 117−208). Data obtained from loggers were used to calculate the change of soil heat storage within the soil layer of 0−0.08 m. The data were transferred from the loggers to the manufacturer software BoxCarPro 4.3 (GEOTEST Ltd, Bern, Switzerland) for subsequent data processing.

The soil heat storage was calculated by:

$$S_g = \frac{C_v \cdot \Delta T_s \cdot L_s}{\triangle t} \quad (2.6)$$

where C_v (J m^{-3} K) is the volumetric heat capacity of the soil, ΔT_s (K) is the measured change in soil temperature, L_s (0.08 m) is the thickness of the soil layer above the sensors and Δt (s) is the time interval. As C_v depends on soil moisture, SM1 soil moisture probes (Adcon Telemetry, Vienna, Austria) were installed close to the temperature loggers. The SM1 probes were calibrated against data from regular soil

moisture samplings. The volumetric heat capacity of the soil was calculated using the de Vries (1963) equation:

$$C_v = (\theta + 0.46 \cdot (1 - \emptyset - X_0) + 0.60 \cdot X_0) \cdot W_{hc} \quad (2.7)$$

where θ is the volumetric water content ($m^3\ m^{-3}$), $\emptyset$ is the soil porosity, X_0 is the volumetric fraction of soil organic carbon (0.016 for site EC1 and 0.015 for site EC3) and W_{hc} is the volumetric heat capacity of water ($4190 \cdot 10^3$ J m^{-3} K^{-1}) . Soil porosity was computed from the bulk density of the soil by:

$$\emptyset = 1 - \frac{p_s}{p_r} \quad (2.8)$$

where p_s (kg m^{-3}) is the soil bulk density (Table 2.1) and p_r (kg m^{-3}) is the density of solid matter in the soil (~2650 kg m^{-3}).

According to the two different periods of temperature measurements in soil and canopy in 2015, the results are mainly presented for the periods DOY 127−159 and DOY 168−202.

2.2.4. Calorimetric and harmonic analysis of ground heat flux

The calorimetric method for calculating ground heat flux is widely used in micrometeorological and soil system research (Evett et al., 2012; Zuo et al., 2011). The method is based on temporal changes in soil temperature and the heat storage as a function of soil moisture content (Eq. 7). The ground heat flux derived from measurements with soil heat flux plates and the calculation of the soil heat storage can be expressed by:

$$G_c = G_{0.08} + S_g \quad (2.9)$$

Here, G_c (W m^{-2}) is the ground heat flux estimated by the calorimetric method, $G_{0.08}$ (W m^{-2}) is the average of the soil heat flux recorded by three heat flux plates in 0.08 m soil depth, and S_g (W m^{-2}) denotes the soil heat storage in the soil layer above the plates.

Ground heat flux was additionally calculated by harmonic analysis from temperature measurements at 0.02 and 0.06 m, or measured soil heat flux at 0.08 m. The precondition for harmonic analysis is soil homogeneity, which can be assumed for the top soil of the study sites because of regular tillage measures. Applying harmonic analysis to measured temperature and soil heat flux data has been described in detail elsewhere (An et al., 2015; Heusinkveld et al., 2004; Wizemann et al., unpublished results; Zuo et al., 2011). The input variables used were the depth of temperature sensors in soil, the damping depth, the

thermal diffusivity of the soil and the number of observation days. The damping depth was determined using soil temperature data from the upper layers on clear-sky days. For each layer the amplitude of soil temperature was determined from two consecutive days. The damping depth was calculated as the inverse slope of the amplitude vs. depth semi logarithmic regression line. The mean value of monthly calculated damping depths was used for the whole vegetation period because it is relatively constant for volumetric water contents > 10 % (Wizemann et al., unpublished results.). As a quality criterion for calculating damping depths, only regressions with a coefficient of determination (R^2) > 0.98 were accepted. All calculations were performed with the free R software (R Core Team, 2014). In 2015, the average damping depths over the EC footprint and close to the station EC1 were 0.11 and 0.12 m, and thermal diffusivities were 0.00170 and 0.00193 $m^2\,h^{-1}$, respectively. For site EC3 in 2016, the average damping depth was 0.10 m for both the whole EC footprint and close to the station, while the average thermal diffusivity was 0.00145 and 0.00131 $m^2\ h^{-1}$, respectively. The harmonic analysis was applied to soil heat flux measurements at the EC stations (G_{hp}) as well as to temperature measurements at the EC station (G_{ht}) and over the EC footprint (G_{hf}). Note that the ground heat flux over the EC footprint (G_{hf}) is not given for the second period in 2015 due to non-availability of soil temperature measurements.

2.3. Results

2.3.1. Weather conditions during the observation periods

The main meteorological variables in the two growing seasons evaluated during the field experiment are shown in Fig. 2.3. In 2015, the mean air temperature was 14.7 °C. The daily maximum and minimum air temperatures were 27.7 and 2.4 °C, respectively (Fig.2.3a). The accumulated rainfall over the period was 241 mm (Fig. 2.3b). The daily mean values of global radiation and relative humidity were 235 W m^{-2} (Fig. 2.3c) and 67 % (Fig. 2.3d), respectively. Furthermore, Fig. 2.3e indicates minimum and maximum values of 0.9 and 6.0 m s^{-1} for daily horizontal wind speed.

In the second period (2016), the daily mean air temperature varied between 3.0 and 25.9 °C, averaging 14.1 °C (Fig. 2.3f). The seasonal rainfall (Fig. 2.3g) cumulated to 389 mm. Mean values of global radiation and relative humidity were 211 W m^{-2} and 73.9 %, respectively (Fig. 2.3h,i). Wind speed ranged between 0.9 and 3.4 m s^{-1} (Fig. 2.3k).

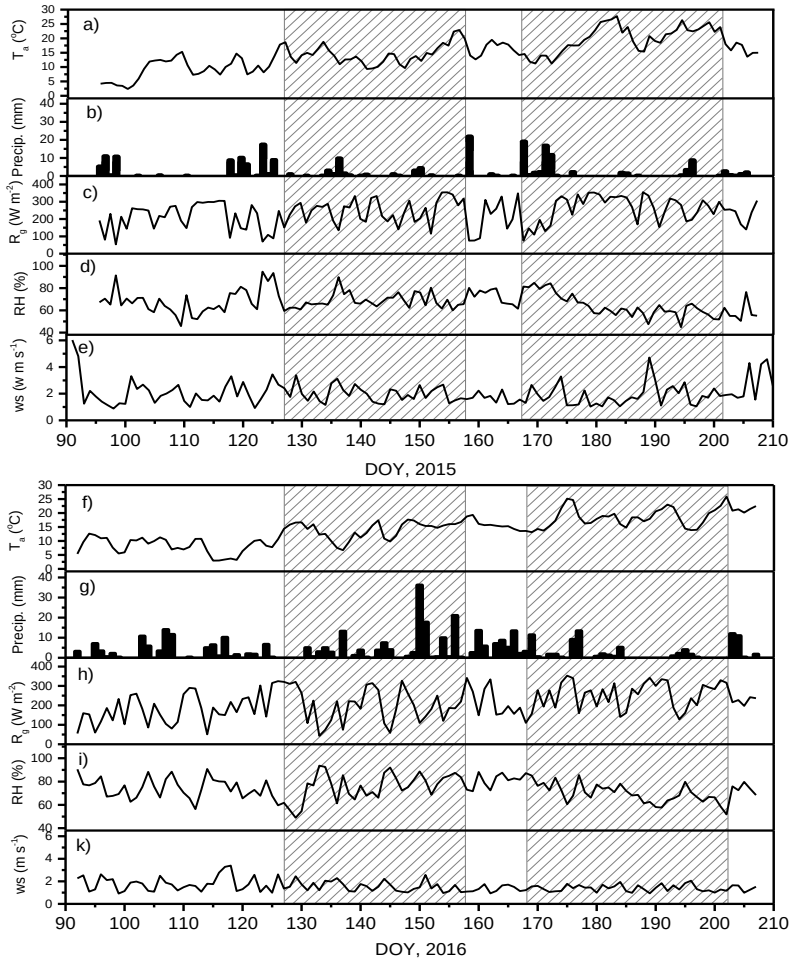

Fig. 2.2. Time series of mean daily air temperature (T_a), daily precipitation, mean daily global radiation (R_g), mean daily relative humidity (RH) and mean daily wind speed over the two observation periods in 2015 (a, b, c, d, e) and 2016 (f, g, h, i, k). Hatched zones indicate the two main measurement periods (DOY 127 – 159 and DOY 168 – 202).

2.3.2. Energy balance closure

From those time steps where all four components of the energy balance were available, mean values (Table 2.2) and mean diurnal courses (Fig. 2.4) were calculated. During all periods, the largest fraction of net radiation was converted into latent heat. While *LE* was rather stable throughout the vegetation periods, *H* increased from the first to the second period in both years. During three of the four periods, the residual energy was higher than the sensible heat flux and it was higher than the ground heat flux during all four periods. Furthermore, the mean residual energy was more than doubled at EC1 in 2015 compared to EC3 in 2016.

Table 2.2. Mean fluxes of the partitioned energy balance components for sites EC1 and EC3.

Flux	EC1 (2015)		EC3 (2016)	
	DOY 127−159	DOY 168−202	DOY 127−159	DOY 168−202
	W m^{-2}		W m^{-2}	
R_n	180.5	196.0	162.4	187.1
LE	107.0	111.6	114.4	119.5
H	6.0	19.3	5.8	31.1
G	10.5	13.5	13.8	12.4
Residual	57.0	51.5	28.4	24.1

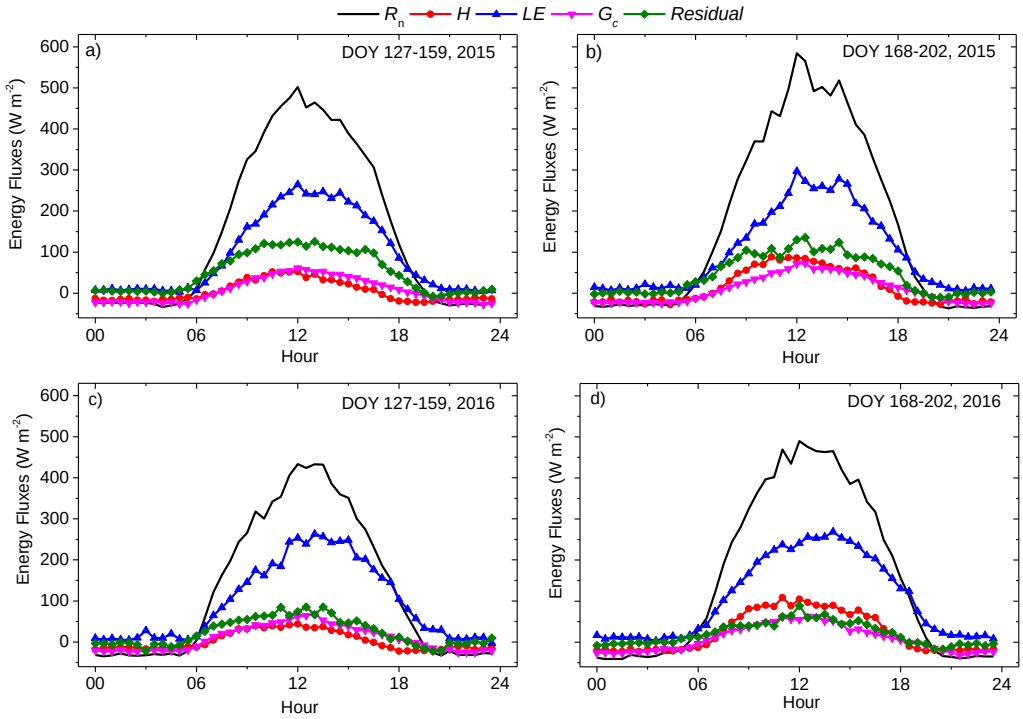

Fig. 2.3. Mean diurnal courses of net radiation (R_n), sensible heat (H), latent heat (LE) and ground heat flux (G_c) from winter wheat stands in the two observation periods in 2015 (a, b) and 2016 (c, d).

The energy balance closure varied with month at both sites (Table 2.3). While in 2015 (EC1), the highest EBC was observed in July, in 2016 (EC3) the highest closure was obtained in June. At both sites, the EBC was higher during the second observation period. However, irrespective of the particular month or period, the energy imbalance was systematically lower over the winter wheat grown at EC3 in 2016.

Table 2.3. Energy balance closure and energy residuals over winter wheat at EC1 and EC3.

Station (Year)	EC1 (2015)							EC3 (2016)						
Periods	April	May	June	July*	DOY 127–159	DOY 168–202	Whole season	April	May	June	July**	DOY 127–159	DOY 168–202	Whole season
EBC, %	67.5	69.6	69.3	76.4	70.0	73.8	70.8	73.6	76.1	83.3	79.8	78.3	82.9	79.9
Average residual, W m^{-2}	51.6	47.8	58.1	47.4	57.0	51.5	51.5	29.2	28.7	26.7	25.4	28.4	24.1	27.6
Number of available data points after flux filtering	890 (62%)	972 (65%)	1000 (69%)	685 (68%)	1118 (73%)	1108 (68%)	3546 (66%)	877 (61%)	1016 (68%)	938 (65%)	793 (69%)	1043 (68%)	1194 (73%)	3624 (66%)

* July 1–21; ** July 1–24

2.3.3. Minor flux and storage terms

Mean diurnal cycles of minor storage terms are presented in Fig. 2.5. The smallest storage terms were air enthalpy change (S_a) and atmospheric moisture change (S_q), which reached values between 1.8 and −1.9 W m^{-2}. The largest term was S_p with a maximum mean daily value of 28.4 W m^{-2} during the first period (DOY 127−159) in 2015 and a minimum of 8.7 W m^{-2} during DOY 168–202 in 2016. Canopy enthalpy change ranged between a daily mean of −8.8 W m^{-2} (DOY 168–202 in 2015) and 9.5 W m^{-2} (DOY 127–159 in 2016) and was rather similar in both years.

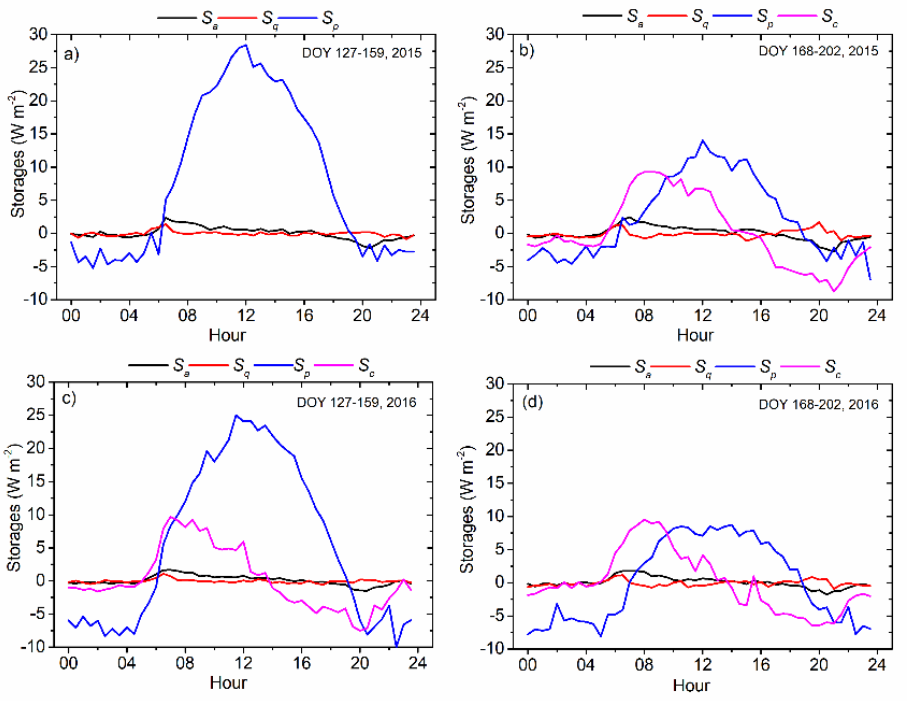

Fig. 2.4. Mean diurnal cycles of minor flux and storage terms from winter wheat stands: S_a: air enthalpy change, S_q: atmospheric moisture change, S_p: energy consumption and release by photosynthesis and respiration, S_c: enthalpy change in the plant canopy.

As expected, adding the minor storage terms (S_a+S_q+S_p+S_c) to the turbulent fluxes (LE+H) narrowed the EBC of all evaluated periods as indicated by the slope of linear regression when plotted against the available energy (Fig. 2.6). This effect was greatest during DOY 127−159 in 2016 (absolute improvement by 9 %) (Fig. 2.6e, f), lowest during DOY 168–202 of the same year (absolute improvement by 4 %) (Fig. 2.6g, h).

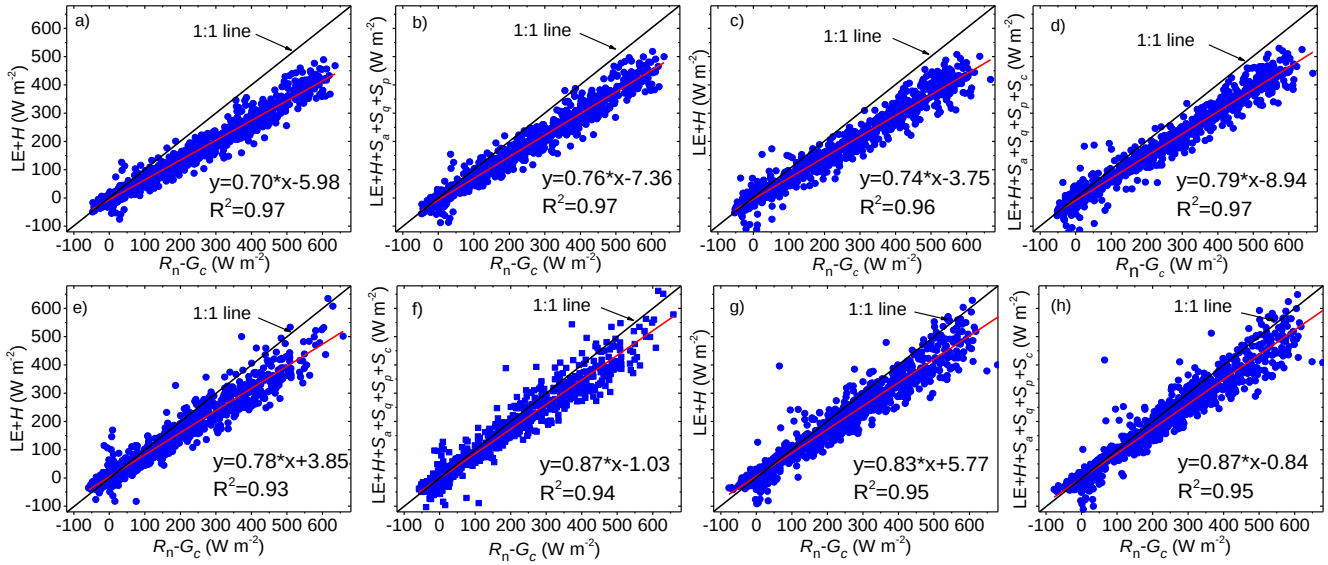

Fig. 2.5. Scatterplots of half-hourly available energy ($R_n - G_c$) versus measured turbulent energy fluxes and minor flux and storage terms (S_a: air enthalpy change, S_q: atmospheric moisture change, S_p: energy consumption and release by photosynthesis and respiration, S_c: enthalpy change in the plant canopy). G_c is the ground heat flux as the sum of flux plate measurements in 0.08 m depth and the soil heat storage above the plates determined by the calorimetric method. Upper panels: DOY 127–159 (a, b) and DOY 168–202 (c, d) in 2015; Lower panels: DOY 127–159 (e, f) and DOY 168–202 (g, h) in 2016.

In the two growing seasons of winter wheat, S_p showed the highest positive effect on EBC. This effect peaked in May and declined over June and July in both years (Table 2.4). The S_c, which was measured only over three of four periods, showed the second strongest effect on EBC improvement, but no clear temporal trend was apparent for this S_c effect. While a slight improvement in EBC was observed for S_a, the inclusion of S_q into the energy balance did not improve EBC at all.

Table 2.4. Change in energy balance closure by accounting for minor storage terms for different periods and years. Figures show the absolute improvement in percentage of available energy.

Station (year)	EC1 (2015)							EC3 (2016)						
Periods	April	May	June	July*	DOY 127–159	DOY 168–202	Whole season	April	May	June	July**	DOY 127–159	DOY 168–202	Whole season
							%							
S_a	0.4	0.3	0.2	0.2	0.2	0.2	0.3	0.3	0.2	0.2	0.2	0.2	0.2	0.2
S_q	0.0	0.0	0.0	0.0	0.0	−0.1	0.0	0.0	0.0	0.0	−0.1	0.0	0.0	0.0
S_p	5.0	7.1	4.6	2.1	6.2	2.9	4.7	6.7	6.8	4.9	1.9	6.8	3.0	5.1
S_c	–	–	–	1.7	–	1.7	–	–	1.4	1.8	1.2	1.7	1.3	1.5
Total	5.4	7.4	4.8	4.0	6.4	4.7	5.0	7.0	8.4	6.9	3.2	8.7	4.5	6.8

Note: S_a - air enthalpy change, S_q - atmospheric moisture change, S_p - energy consumption and release by photosynthesis and respiration, S_c - enthalpy change in the plant canopy. * July 1–21; ** July 1–24

2.3.4. Comparison of soil heat storage at different spatial resolution

During DOY 127−159 in 2015, the mean value of soil heat storage for both the single point measurement at the EC station and the multiple measurements over the EC footprint was close to zero (0.13 W m^{-2}). However, the range within the footprint (between -46.5 and 60.0 W m^{-2}) was higher compared to the measurement at the EC station (between -40.5 and 49.0 W m^{-2}) (Fig. 2.7a, b).

In 2016, the mean soil heat storage was similar in both observed periods and for both spatial resolutions, with 0.47 W m^{-2} during DOY 127–159 and 0.48 and 0.43 W m^{-2} for the footprint and the EC station during DOY 168–202, respectively. Maxima and minima, however, were lower at the EC station (89 W m^{-2} and −77 W m^{-2}) compared to the entire EC footprint (108 W m^{-2} and −64 W m^{-2}) during both periods. The highest discrepancies in soil heat storage between the two spatial resolutions occurred sporadically during noon. The maximum difference was 37.7 W m^{-2} in 2015, whereas in 2016 the maximum value increased to 59.1 W m^{-2} during DOY 127–159 (Fig. 2.7c, f, i).

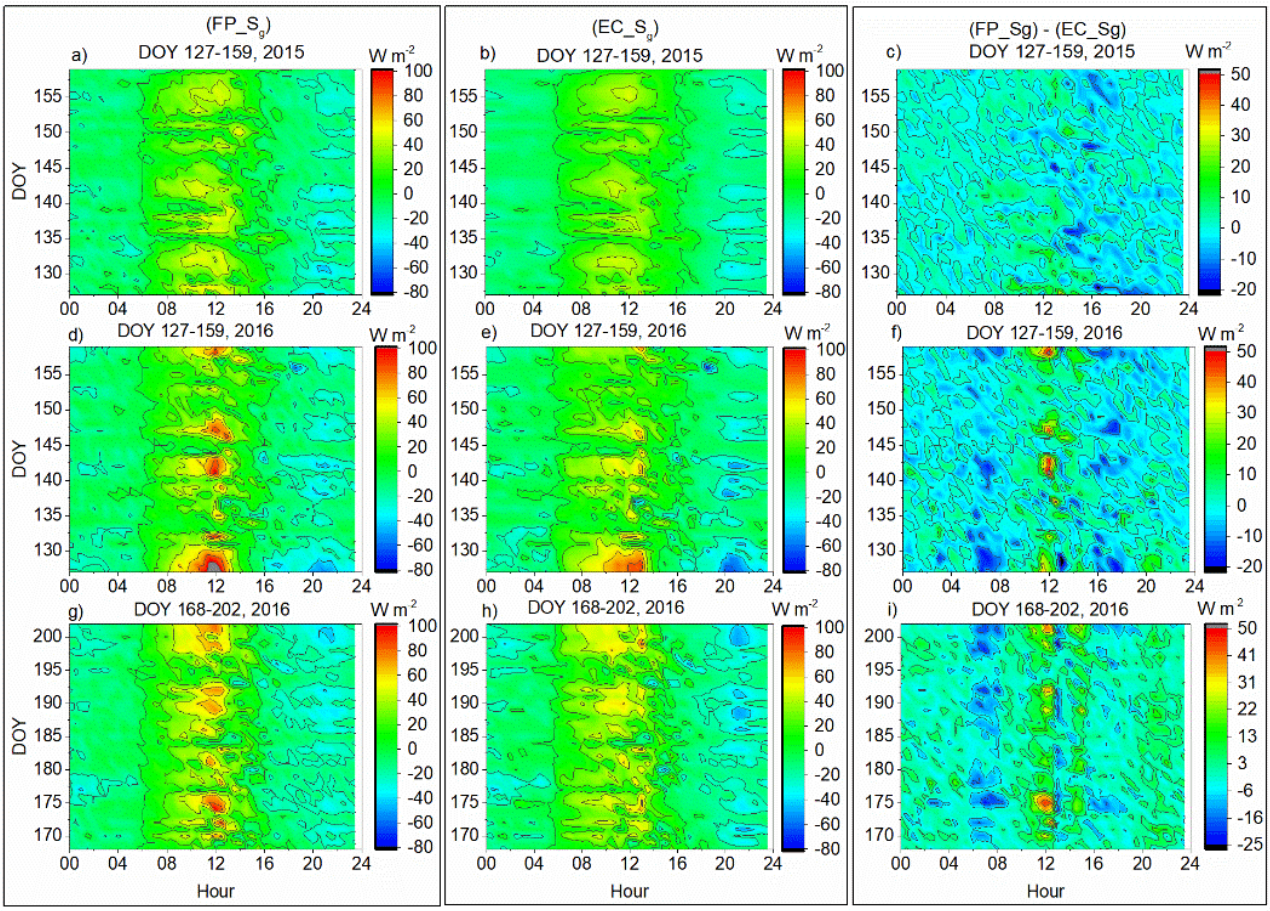

Fig. 2.7. Comparison of soil heat storage (S_g) changes in the upper 0.08 m soil layer averaged over all measurements within the eddy covariance (EC) footprint (FP_S_g, left panel) and the one determined in the vicinity of the EC station (EC_S_g, middle panel) as well as the difference between both ((FP_S_g) – (EC_S_g), right panel) in different periods and years. Upper panels (a, b, c): DOY 127–159 in 2015 at EC1; middle panels (d, e, f): DOY 127–159 in 2016 at EC3; lower panels (g, h, i): DOY 168–202 in 2016 at EC3.

The spatial variability of the ground heat storage over the EC footprint was much higher and variable over time in 2015 compared to 2016 (Fig. 2.8). The daily mean coefficient of variation (CV) ranged between 1.1 and 336 % in 2015 with the highest value observed on DOY 127 (Fig. 2.8a). Moreover, a high spatial variability was observed on DOY 141, 143 and 144 with a CV of 147, 204 and 206 %, respectively. In contrast, the CV of S_g over the EC footprint ranged only between 1.0 and 12.2 % during DOY 127 – 159 and between 0.6 and 10.7 % during DOY 168 – 202 of 2016, respectively (Fig. 2.8b, c).

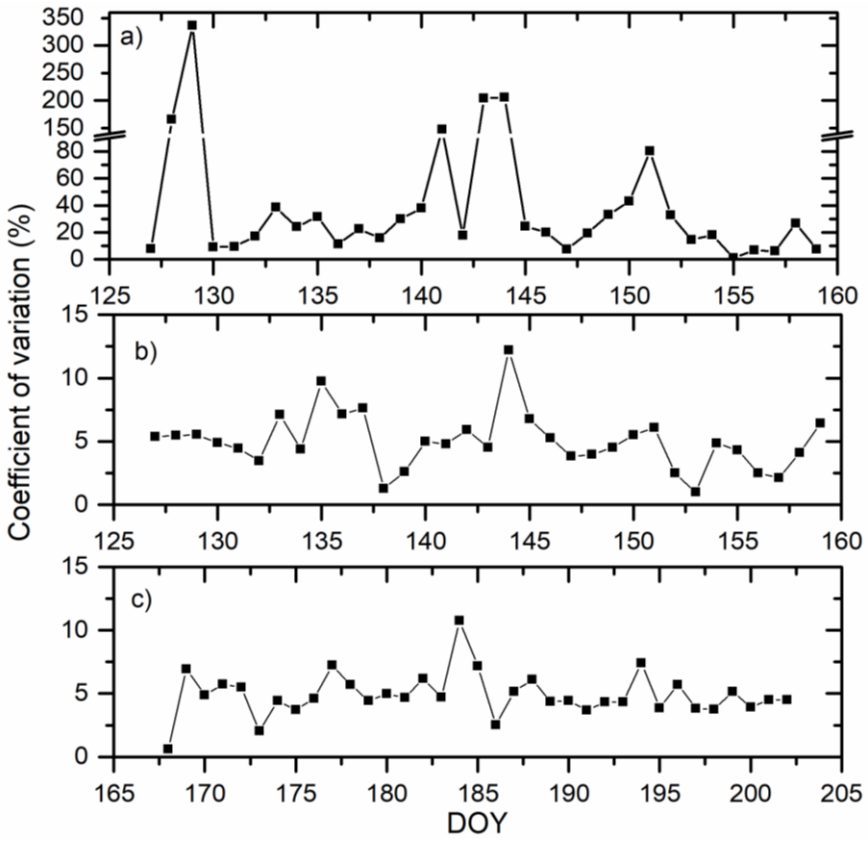

Fig. 2.8. Daily mean coefficient of variation of ground heat flux measured at six locations in the eddy covariance footprint during the different study periods. a) DOY 127–159 in 2015, b) DOY 127–159 in 2016, c) DOY 168–202 in 2016.

2.3.5. Ground heat fluxes from calorimetric and harmonic analyses

Figure 2.9 shows the mean diurnal cycles of ground heat fluxes estimated by harmonic analysis of the soil temperature at the EC station (G_{ht}), in the EC field footprint (G_{hf}), and of the heat flux measured by plates at the EC station (G_{hp}), as well as from the calorimetric analysis of soil heat storage added to the heat fluxes obtained from the plates at the EC station (G_c).

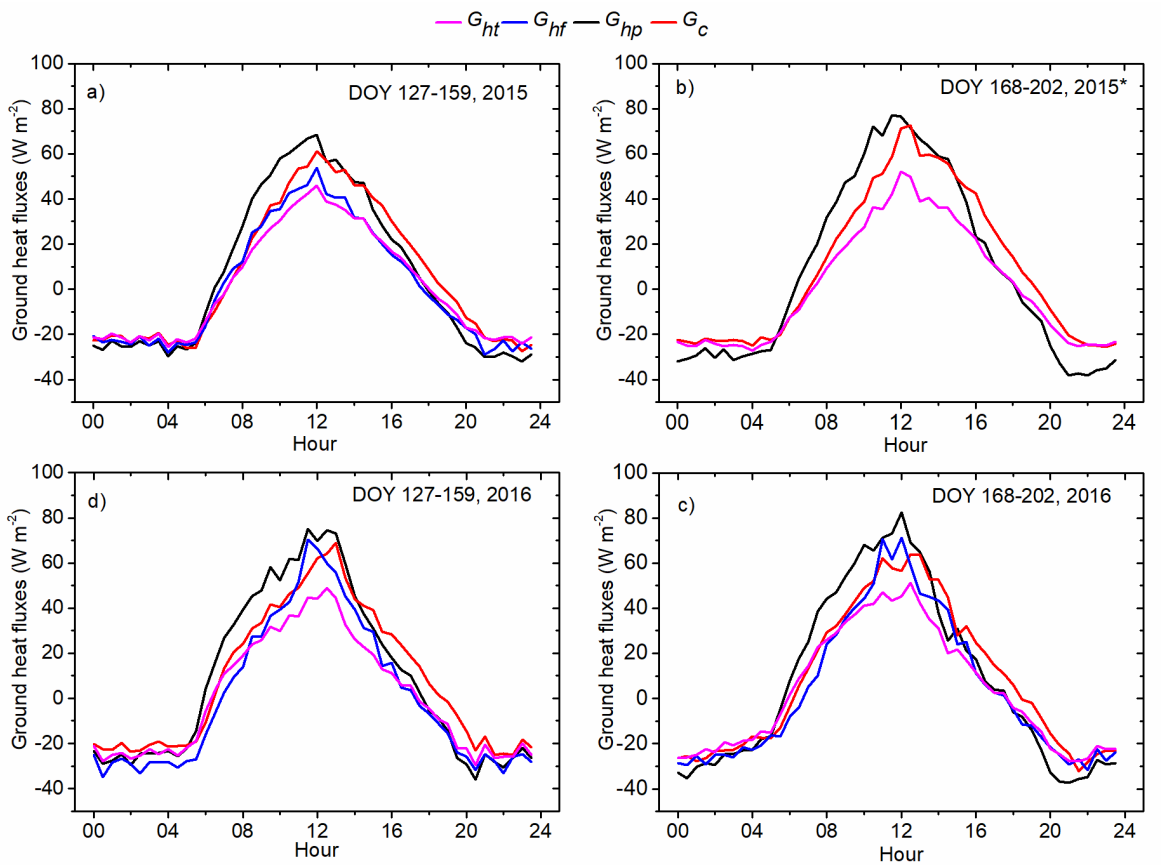

Fig. 2.9. Mean diurnal cycles of ground heat fluxes (G_{ht}, G_{hf}, G_{hp}, G_c) determined by four different methods. G_{ht}: harmonic analysis of soil temperatures measured at the EC station; G_{hf}: harmonic analysis of soil temperatures measured within the EC footprint; G_{hp}: harmonic analysis of ground heat fluxes measured by heat flux plates at the EC station; G_c: calorimetric calculation of soil heat storage added to the ground heat flux measurements at the EC station. *In 2015, no soil temperature was measured within the EC footprint during the second period, i.e. no estimates for G_{hf} could be obtained.

The comparison of ground heat fluxes by harmonic analysis from heat flux plate measurements (G_{hp}) and by the standard calorimetric method (G_c) revealed that G_{hp} was systematically higher during the morning hours and until midday, while G_c was higher in the afternoon and at night. Furthermore, G_{hp} had the greatest amplitudes in all observed periods. The harmonic analyses of the soil temperature data (G_{ht}, G_{hf}) revealed comparatively damped amplitudes, which became particularly apparent in the ground heat flux at the EC station (G_{ht}).

A further comparison of ground heat fluxes calculated by the two methods (G_{hp}, G_c) is presented in Fig. 2.10. From early morning until noon, the harmonic analysis produced systematically higher ground heat fluxes. In contrast, from late afternoon until midnight the harmonic analysis tended to yield lower values.

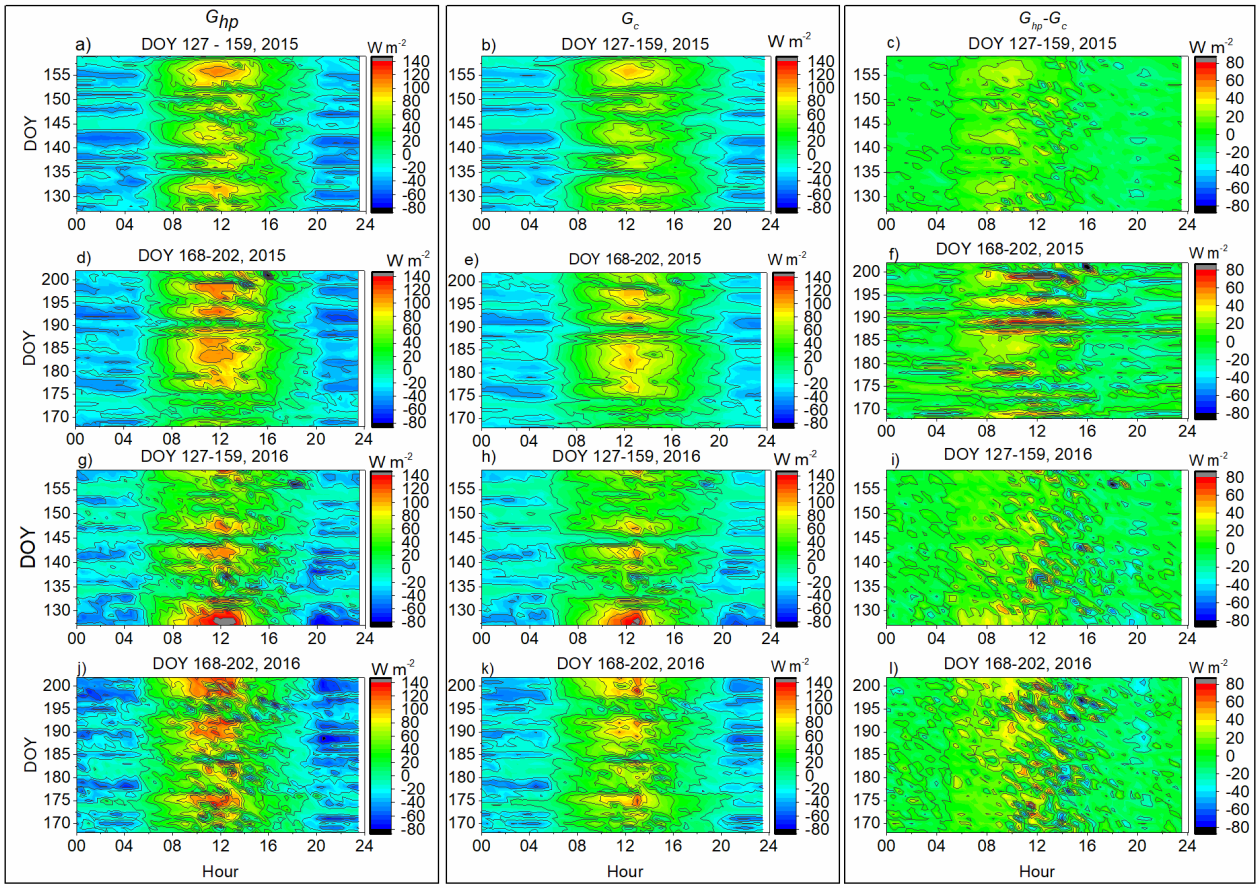

Fig. 2.10. Comparison of ground heat fluxes at the eddy covariance (EC) station based on harmonic analyses of heat flux plate measurements in 0.08 m soil depth (G_{hp}, left panel) and the calorimetrically calculated soil heat storage added to the plate measurements (G_c, middle panel) as well as the difference between the two methods ($G_{hp} - G_c$, right panel) during different periods and years. Measurements in 2015 and 2016 were conducted at EC1 and EC3, respectively.

The effect of the method of determining the ground heat flux on EBC was examined by regressing $LE + H$ on $R_n - G_x$ (Table 2.5). Compared to the standard method (G_c), EBC increased in three of the four investigated periods when ground heat flux was calculated by harmonic analysis from heat flux plate measurements (G_{hp}). With roughly 3 %, the best result was attained in the first period of 2016 (DOY 127−159). With G_{ht}, however, EBC decreased in all periods. The same was true with G_{hf} but the reduction in EBC was lower compared to G_{ht}. In summary, the method of calculating ground heat flux accounted for up to 5 % difference in EBC (Table 2.5).

Table 2.5. Energy balance closure with ground heat fluxes calculated by different methods (for abbreviations of differently calculated ground heat flux see caption of Fig. 2.9).

DOY	Station (year)	EC1 (2015)				EC3 (2016)			
		$LE+H$ vs R_n-G_{ht}	$LE+H$ vs R_n-G_{hf}	$LE+H$ vs R_n-G_{hp}	$LE+H$ vs R_n-G_c	$LE+H$ vs R_n-G_{ht}	$LE+H$ vs R_n-G_{hf}	$LE+H$ vs R_n-G_{hp}	$LE+H$ vs R_n-G_c
127 – 159	Slope	0.68	0.69	0.72	0.70	0.76	0.79	0.81	0.78
	Intercept	−6.66	−8.55	−9.63	−5.98	0.23	−4.09	−0.28	3.85
168 – 202	Slope	0.72	−	0.74	0.74	0.81	0.84	0.85	0.83
	Intercept	−4.83	−	−4.65	−3.75	5.14	0.92	1.66	5.56

2.4. Discussion

2.4.1. Evaluation of the surface EBC

The measured energy balances during two consecutive growing periods of winter wheat reached monthly EBCs of 67.5 to 83.3 % (Table 2.3). Our results are therefore in the range of findings from previous studies on cropland (Foken et al., 2010; Imukova et al., 2016; Ingwersen et al., 2011, 2015; Masseroni et al., 2014; Meyers and Hollinger, 2004; Oncley et al., 2007; Wilson et al., 2002; Wizemann et al., 2014). Highest energy balance closures for the two studied growing periods were obtained in July 2015 (76.4 %) and June 2016 (83.3 %).

The average residuals of the energy balances in 2015 and 2016 were 51.5 and 27.6 W m^{-2}, respectively, which is in line with results given by Foken (2008), Michiles and Gielow (2008) and Varmaghani et al. (2016). The high contribution of latent heat to the turbulent energy fluxes during the observation periods was due to intensive plant development and high soil moisture contents. However, energy partitioning changed in the ripening phase of the wheat. Sensible heat flux substantially increased due to decreasing transpiration (Aouade et al., 2016; Ingwersen et al., 2011; Masseroni et al., 2014). During these periods (DOY 168 – 202), the EBC was higher compared to the first study periods in both years (DOY 127 – 159). Potential reasons for these findings might be that the agricultural fields became more homogeneous during later crop development stages (Stoy et al., 2013), the field footprint decreased with increasing plant height (Masseroni et al., 2014) and a stronger development of heat induced turbulent fluxes (Franssen et al., 2010).

The EBC at EC3 in 2016 (79.9 %) was substantially higher than the EBC at EC1 in 2015 (70.8 %). Consistent to the present study, Imukova et al. (2016) found a higher EBC at EC3 in 2012 (71 %) compared to EC1 in 2013 (60 %) although in their study the closure was lower at both sites. As discussed

by Imukova et al. (2016), a possible reason for the higher EBC gap at EC1 could be a hilly forested area 500 m south of the field. It may have caused the formation of mesoscalic eddies from which most of the signal is missed by the EC method. Therefore, during periods with southern to southwestern winds this situation might have affected the EBC negatively on EC1. However, only few situations with southwestern winds were recorded in 2015 (Fig. 2.1). The EC method cannot fully capture the transit of large eddies, which are mainly caused by landscape heterogeneity (Foken, 2008; Foken et al., 2010, 2006). Heterogeneity of research areas has often been regarded as a main reason for measured EBC gaps (Foken, 2008; Foken et al., 2006; Stoy et al., 2013). Spectral analysis can be used to investigate uncaptured turbulent fluxes and to determine appropriate time averaging intervals in heterogeneous landscapes. In several studies it has been demonstrated that energy residuals tend to decrease with an increasing averaging period as result of more captured low frequencies (Kidston et al., 2010; Masseroni et al., 2014; Mauder and Foken, 2006; Sánchez et al., 2010). However, the effect of an extended time averaging interval depends on site characteristics with often greater impacts over tall vegetation such as forests (Charuchittipan et al., 2014; Sun et al., 2006). Moreover, Sievers et al. (2015) argued that low frequencies should be excluded from a dataset when EC fluxes are related to a specific field or activity. As this is mostly the case when measurements are conducted on agricultural fields as in the present study, a higher EBC by consideration of low frequencies might even be undesirable as these signals are nor related to the field of interest.

An additional possible reason for the energy imbalance at our sites is the underestimation of turbulent fluxes caused by insufficient turbulent mixing. The stability parameter was obtained as measurement height (z) divided by the Monin-Obukhov length (L) and a threshold of $z/L = 0.01$ was chosen above which the respective time intervals were regarded to represent stable atmospheric conditions. Both study years showed stable atmospheric conditions for 46 % of the available data. Also, no differences in friction velocity could be observed between EC1 and EC3. Thus, insufficient turbulent mixing might play an important role for the observed energy balance gaps at the studied sites although it can be excluded as a potential reason for differences in EBC between the two sites. Sánchez et al. (2010) obtained a 13 % improvement of EBC at a boreal forest when fluxes with friction velocities below 0.25 m s^{-1} were discarded. Considering the discussion above, further experimental investigations by other methods are needed for thorough estimation of the turbulent flux components and a comparison with the EC measurement. These methods may involve the use of manual (Poyda et al., 2017) or automatic chambers (Pumpanen et al., 2004; Wang et al., 2013), aerodynamic methods (Prueger and Kustas, 2005), eddy accumulation, lysimeter measurements (Castellví and Snyder, 2010; Ding et al., 2010; Gebler et al.,

2015) sap flow measurements (Nunn et al., 2014; Williams et al., 2004), the soil water balance method (Imukova et al., 2016) or others.

2.4.2. Effect of minor storage terms on EBC

The contribution of S_p to the surface energy balance was the highest among the tested storage terms, with 7.1 and 6.8 % during the intensive growing period (May) of 2015 and 2016, respectively. During the ripening phase of winter wheat (July), S_p showed a lower contribution to EBC with 2.1 and 1.9 % in 2015 and 2016, respectively. In our study, S_p was higher than in other studies (Jacobs et al., 2008; Masseroni et al., 2014; Meyers and Hollinger, 2004). Jacobs et al. (2008), for instance, reported that S_p contributed a maximum of 3 % to EBC at a grassland site. This was during the intensive growing period in May. The maximum value reported by Wang and Zhang (2011) – 0.6 % for a subalpine meadow in July and August was substantially lower. The contribution of S_p to EBC was considerably higher than that of other minor energy storage terms. Note that our analysis applies to the vegetation period on intensively cropped wheat fields with very high photosynthetic rates. Thus, for the non-growing season and measurements in less productive ecosystems, the impact of S_p on EBC is probably much lower, perhaps in the range of the studies mentioned above. Nonetheless, the high energy release related to nocturnal respiration rates reduce EBC at night, particularly during periods of enhanced plant growth. In ecosystems acting as net sources of CO_2, such as drained peatlands (Poyda et al., 2017, 2016), the consideration of S_p in the energy balance would even increase the imbalance. According to Schmidt et al. (2012) and Guo et al. (2013) the annual budgets of CO_2 measured by EC over winter wheat fields corresponded to an energy storage change of 0.33 and 0.49 W m^{-2}, respectively. From our results, it is highly advisable to include S_p into the calculation of surface energy balances due to its potentially high contribution (Wilson et al., 2002). As CO_2 fluxes are generally measured at EC stations, its consideration needs no further instrumentation and can simply be converted to the related energy flux.

The second highest contribution to EBC among the minor storage terms was the canopy heat storage (S_c) with a maximum improvement of 1.8 % in June 2016 (Table 2.4). This term improved the EBC by 1.0 % on a subalpine meadow in China (Wang and Zhang, 2011) and by 0.5 % on a grassland in the Netherlands (Jacobs et al., 2008). In our study, the mean water content of the winter wheat canopy was 3.6 kg m^{-2}, whereas it was 3.0 kg m^{-2} in the study of Wang and Zhang (2011) and 1.7 kg m^{-2} in the study of Jacobs et al. (2008), which explains the different magnitudes of S_c. The diurnal cycle of heat storage in the canopy (Fig. 2.5) indicates that the absorption of energy by the winter wheat plants is greatest in

the early morning after sunrise and decreases subsequently until the plants start to cool down, indicated by a negative S_c, from the early afternoon. Daily variations of the energy storage terms in the soil and the canopy were reported for the understorey of a pine forest by Lamaud et al. (2001), and for maize fields by Masseroni et al. (2014) and Xu et al. (2017). Their results indicate that canopy heat storage played a significant role among the total minor storages especially during the transition period around sunrise. Furthermore, Meyers and Hollinger (2004) confirmed that the high water contents in plant biomass caused an increase in the amount of energy stored within the canopy during the main growing season. In the maturity phase of winter wheat, S_c distinctly decreased due to lower plant water content.

The air enthalpy change (S_a) reduced the energy balance gap on average by 0.24 %. These results are comparable with those of Wang and Zhang (2011). They found that S_a improved the surface energy balance closure by 0.14 % in July on a subalpine meadow. Furthermore, Jacobs et al. (2008) reported that the air enthalpy change increased the surface EBC during May from 93.6 to 95.6 % over a grassland in the Netherlands. A possible reason for the different contributions of the air enthalpy change to the EBC might be differences in temperature variations between sites and seasons (Michiles and Gielow, 2008; Silberstein et al., 2001). The magnitude of heat storage in the air depends on above-canopy air temperature variations. For longer study periods it becomes more likely that positive and negative contributions of S_a to the EBC level off as it is the case when the results of Jacobs et al. (2008) are compared with those from our study.

The energy related to atmospheric moisture change (S_q) is stored in water vapor between the measurement height and the canopy. Its contribution to the surface EBC was negligible in our study, supporting the findings of Wang and Zhang (2011) where the contribution of S_q to the EBC was close to zero. With 0.5 %, this figure was slightly higher for a grassland in the Netherlands during May (Jacobs et al., 2008), possibly because the oceanic and more windy weather conditions induced larger variations in humidity compared to southwest Germany. The diurnal pattern of S_q showed a positive storage around sunrise and sunset and declined sharply after about two hours, resulting in a balanced energy exchange which was zero on average as also reported by Zeri and Sá (2010). Therefore, a positive contribution of S_q to EBC can be observed only during periods of net accumulation of water vapor above the canopy.

In summary, accounting for S_p and S_c had the greatest effects on EBC while S_a and S_q were negligible on our study sites. In total, minor storage terms improved the EBC between 4.5 % (DOY 168−202 in 2016) and 8.7 % (DOY 127−159 in 2016). These numbers are in line with those found in previous studies. For a maize field in Italy from 21 May – 7 September 2012, Masseroni et al. (2014) improved EBC by 5 %

(from 75 to 80 %). For a grassland site in the Netherlands (May and August), Jacobs et al. (2008) improved EBC by 6.1 % by accounting for minor storage terms. Accordingly, the contribution of minor storage terms to the surface EBC from EC measurements depends on canopy type as well as biomass and plant moisture conditions of the field.

2.4.3. The effects of soil heat storage and ground heat fluxes on surface EBC

The soil heat storage (S_g) measured within the EC footprint was compared to single point measurements at the EC station. The different spatial resolutions affected the amount of estimated S_g, with potential impacts on EBC evaluation. In general, the amplitude of S_g was greater when measured within the footprint. Thus, during the daytime a higher EBC could be achieved by determining S_g in the footprint and not only at the EC station. Our measurements showed large differences in the spatial variability of S_g between the two years and sites. Jansen et al. (2011) concluded that the spatial variability in soil heat storage is connected to differences in soil structure. We assume that the spatial variability of soil moisture and plant cover over the field footprint contributed to the variability of the soil heat storage as reported elsewhere (Agam et al., 2012; Colaizzi et al., 2016; Kustas et al., 2000). Interestingly, the absolute differences between the two observed spatial resolutions were smaller in 2015, while the coefficient of variation (CV) was extremely high on some days. A very high CV occurred mainly during the transition periods in the morning and evening with S_g values close to zero. For example, at single locations the soil might have already heated up while S_g was around zero at other locations. The absolute differences between the locations was, however, rather small during these periods. These results suggest that the course of S_g during the transition periods was more uniform in 2016 while the amplitude differed more between the spatial resolutions compared to 2015. Spatial variability implies an additional uncertainty in EBC estimation depending on the spatial reference. This supports the idea that a small spatial resolution for the observation of soil heat storage, as generally conducted in EC measurements, might not be representative for the surface energy balance of the entire field footprint.

Ground heat fluxes calculated from plate data by harmonic analysis showed a noticeably higher contribution (2−3 %) to EBC than that from the calorimetric method in three of four investigated periods. A similar result was obtained by Jacobs et al. (2008) at a low-altitude grassland site: the harmonic analysis showed a higher contribution to EBC. Furthermore, our study showed that it is possible to determine ground heat fluxes without using heat flux plates. Nonetheless, in such cases it is advisable to use soil temperature measurements for harmonic analysis that were taken within the EC footprint at

multiple locations. A single point measurement at the EC station runs the risk of under- or overestimating ground heat flux because the extent to which the point measurement is representative for the spatially heterogeneous EC footprint is uncertain.

2.5. Conclusions

To achieve a better EBC at cropland sites, we recommend to account for the energy consumption and release by photosynthesis and respiration, S_p, as well as the enthalpy change in the plant canopy, S_c. Harmonic analysis based on plate data yielded higher ground heat fluxes than the calorimetric method. Because of the spatial variability of soil, plants and radiation, single-site measurements of the ground heat flux may not be fully representative for the EC footprint. The largest improvement of EBC, from 83 to 89 %, was achieved by considering minor storage terms ($S_a + S_q + S_p + S_c$) and the ground heat flux calculated with harmonic analysis based on heat flux plate data. However, a minimum of 11 % of the available energy still remained uncovered. We conclude that minor flux and storage terms contribute substantially to explaining the energy balance gap, although accounting for them cannot fully close that gap. Our findings indicate that commonly applied EBC correction schemes which suppose 100 % of the energy balance gap as turbulent energy are likely to overestimate turbulent fluxes. We therefore recommend to consider minor energy terms and to calculate ground heat flux by harmonic analysis from plate measurements when the energy balance of EC measurements is evaluated.

Acknowledgements

The authors gratefully acknowledge the financial support received from the German Research Foundation (DFG) in the frame of the Research unit (RU) 1695 “Structure and function of agricultural landscapes under global climate change – Processes and projections on a regional scale”. We would also like to sincerely thank the Erasmus Mundus grant “TIMUR − Training of Individuals through Mobility from Uzbek Republic to EU (referenced as GA NO 213−2723/001−001−EM Action 2)”. Furthermore, we are greatly thankful to Dr. Hans-Dieter Wizemann for helping calculate the harmonic analysis and to the technical staff Benedikt Pretcher for support during the fieldwork. Moreover, we also thank the farmers Mr. Bosch senior (†) and Mr. Bosch junior for their cooperation.

References

Agam, N., Kustas, W.P., Evett, S.R., Colaizzi, P.D., Cosh, M.H., McKee, L.G., 2012. Soil heat flux variability influenced by row direction in irrigated cotton. Adv. Water Resour. 50, 31–40.

https://doi.org/10.1016/j.advwatres.2012.07.017

An, K., Wang, W., Zhao, Y., Huang, W., Chen, L., Zhang, Z., Wang, Q., Li, W., 2015. Estimation from soil temperature of soil thermal diffusivity and heat flux in sub-surface layers. Boundary-Layer Meteorol. 158, 473–488. https://doi.org/10.1007/s10546-015-0096-7

Aouade, G., Ezzahar, J., Amenzou, N., Er-Raki, S., Benkaddour, A., Khabba, S., Jarlan, L., 2016. Combining stable isotopes, eddy covariance system and meteorological measurements for partitioning evapotranspiration, of winter wheat, into soil evaporation and plant transpiration in a semi-arid region. Agric. Water Manag. 177, 181–192. https://doi.org/10.1016/j.agwat.2016.07.021

Atzema, A.J., 1993. The effect of the weather on the drying rate of cut diploid and tetraploid perennial ryegrass (Lolium perenne L.) and diploid hybrid ryegrass (Lolium perenne x L. multiflorum). Grass Forage Sci. 48, 362–368. https://doi.org/10.1111/j.1365-2494.1993.tb01870.x

Barr, A.G., Morgenstern, K., Black, T.A., McCaughey, J.H., Nesic, Z., 2006. Surface energy balance closure by the eddy-covariance method above three boreal forest stands and implications for the measurement of the CO_2 flux. Agric. For. Meteorol. 140, 322–337. https://doi.org/10.1016/j.agrformet.2006.08.007

Blanken, P.D., Black, T. a., Yang, P.C., Neumann, H.H., Nesic, Z., Staebler, R., den Hartog, G., Novak, M.D., Lee, X., 1997. Energy balance and canopy conductance of a boreal aspen forest: Partitioning overstory and understory components. J. Geophys. Res. 102, 28915. https://doi.org/10.1029/97JD00193

Castellví, F., Snyder, R.L., 2010. A comparison between latent heat fluxes over grass using a weighing lysimeter and surface renewal analysis. J. Hydrol. 381, 213–220. https://doi.org/10.1016/j.jhydrol.2009.11.043

Charuchittipan, D., Babel, W., Mauder, M., Leps, J.P., Foken, T., 2014. Extension of the averaging time in eddy-covariance measurements and its effect on the energy balance closure. Boundary-Layer Meteorol. 152, 303–327. https://doi.org/10.1007/s10546-014-9922-6

Colaizzi, P.D., Evett, S.R., Agam, N., Schwartz, R.C., Kustas, W.P., Cosh, M.H., Mckee, L., 2016. Soil heat flux calculation for sunlit and shaded surfaces under row crops: 2. Model test. Agric. For. Meteorol. 216, 129–140. https://doi.org/10.1016/j.agrformet.2015.10.009

De Vries, D.A.V.W.W.R., 1963. Thermal properties of soils. In: Van Wijk, WR. (Ed.) Physics of plant environment, North-Holland Publ. Co., Amsterdam. North-Holland Publ. Co., Amsterdam. https://doi.org/10.1002/qj.49709038628

Ding, R., Kang, S., Li, F., Zhang, Y., Tong, L., Sun, Q., 2010. Evaluating eddy covariance method by large-scale weighing lysimeter in a maize field of northwest China. Agric. Water Manag. 98, 87–95. https://doi.org/10.1016/j.agwat.2010.08.001

Evett, S.R., Agam, N., Kustas, W.P., Colaizzi, P.D., Schwartz, R.C., 2012. Soil profile method for soil thermal diffusivity, conductivity and heat flux: Comparison to soil heat flux plates. Adv. Water Resour. 50, 41–54. https://doi.org/10.1016/j.advwatres.2012.04.012

Foken, T., 2008. The energy balance closure problem: An overview. Ecol. Appl. 18, 1351–1367. https://doi.org/10.1890/06-0922.1

Foken, T., Mauder, M., Liebethal, C., Wimmer, F., Beyrich, F., Leps, J.P., Raasch, S., DeBruin, H.A.R., Meijninger, W.M.L., Bange, J., 2010. Energy balance closure for the LITFASS-2003 experiment. Theor. Appl. Climatol. 101, 149–160. https://doi.org/10.1007/s00704-009-0216-8

Foken, T., Wimmer, F., Mauder, M., Thomas, C., Liebethal, C., 2006. Some aspects of the energy balance closure problem. Atmos. Chem. Phys. Discuss. 6, 3381–3402. https://doi.org/10.5194/acpd-6-3381-2006

Franssen, H.J.H., Stöckli, R., Lehner, I., Rotenberg, E., Seneviratne, S.I., 2010. Energy balance closure of eddy-covariance data: A multisite analysis for European FLUXNET stations. Agric. For. Meteorol. 150, 1553–1567. https://doi.org/10.1016/j.agrformet.2010.08.005

Gao, Z., Horton, R., Liu, H.P., 2010. Impact of wave phase difference between soil surface heat flux and soil surface temperature on soil surface energy balance closure. J. Geophys. Res. 115, 1–10. https://doi.org/10.1029/2009JD013278

Gebler, S., Franssen, H.H., Pütz, T., Post, H., Schmidt, M., Vereecken, H., 2015. Actual evapotranspiration and precipitation measured by lysimeters: a comparison with eddy covariance and tipping bucket. Hydrol. Earth Syst. Sci 2145–2161. https://doi.org/10.5194/hess-19-2145-2015

Göckede, M., Markkanen, T., Hasager, C.B., Foken, T., 2006. Update of a footprint-based approach for the characterisation of complex measurement sites. Boundary-Layer Meteorol. 118, 635–655. https://doi.org/10.1007/s10546-005-6435-3

Guo, Q., Li, W.W., Liu, D.D., Wu, W., Liu, Y., Wen, X.X., Liao, Y.C., 2013. Seasonal characteristics of CO_2 fluxes in a rain-fed wheat field ecosystem at the Loess Plateau. Spanish J. Agric. Res. 11, 980–988. https://doi.org/10.5424/sjar/2013114-4373

Guo, X.F., Cai, X.H., Kang, L., Zhu, T., Zhang, H.S., 2009. Effects of vegetative heterogeneity and patch-scale harvest on energy balance closure and flux measurements. Theor. Appl. Climatol. 96, 281–290. https://doi.org/10.1007/s00704-008-0031-7

Heusinkveld, B.G., Jacobs, A.F.G., Holtslag, A.A.M., Berkowicz, S.M., 2004. Surface energy balance closure in an arid region: Role of soil heat flux. Agric. For. Meteorol. 122, 21–37. https://doi.org/10.1016/j.agrformet.2003.09.005

Horton, R., Wierenga, P.J., 1983. Estimating the soil heat flux from observations of soil temperature near the surface. Soil Sci. Soc. Am. J. 47, 14–20. https://doi.org/10.2136/sssaj1983.03615995004700010003x

Hubbart, J.A., 2011. An inexpensive alternative solar radiation shield for ambient air temperature micro-sensors. J. Nat. Environ. Sci. 2, 9–14.

Imukova, K., Ingwersen, J., Hevart, M., Streck, T., 2016. Energy balance closure on a winter wheat stand: comparing the eddy covariance technique with the soil water balance method. Biogeosciences 13, 63–75. https://doi.org/10.5194/bg-13-63-2016

Imukova, K., Ingwersen, J., Streck, T., 2015. Determining the spatial and temporal dynamics of the green vegetation fraction of croplands using high-resolution RapidEye satellite images. Agric. For. Meteorol. 206, 113–123. https://doi.org/10.1016/j.agrformet.2015.03.003

Ingwersen, J., Imukova, K., Högy, P., Streck, T., 2015. On the use of the post-closure methods uncertainty band to evaluate the performance of land surface models against eddy covariance flux data. Biogeosciences 12, 2311–2326. https://doi.org/10.5194/bg-12-2311-2015

Ingwersen, J., Steffens, K., Högy, P., Warrach-Sagi, K., Zhunusbayeva, D., Poltoradnev, M., Gäbler, R., Wizemann, H.D., Fangmeier, A., Wulfmeyer, V., Streck, T., 2011. Comparison of Noah simulations with eddy covariance and soil water measurements at a winter wheat stand. Agric. For. Meteorol. 151, 345–355. https://doi.org/10.1016/j.agrformet.2010.11.010

IUSS Working Group WRB, 2014. World reference base for soil resources 2014. International soil classification system for naming soils and creating legends for soil maps, World Soil Resources Reports No. 106. FAO, Rome, Italy. https://doi.org/10.1017/S0014479706394902

Jacobs, A.F.G., Heusinkveld, B.G., Holtslag, A.A.M., 2008. Towards closing the surface energy budget of a mid-latitude grassland. Boundary-Layer Meteorol. 126, 125–136. https://doi.org/10.1007/s10546-007-9209-2

Jansen, J., Stive, P.M., Giesen, N., Tyler, S., 2011. Estimating soil heat flux using distributed temperature sensing, in: Proceedings of Symposium J-H01 Held during IUGG2011 in Melbourne, Australia, July 2011. pp. 140–144.

Kidston, J., Brümmer, C., Black, T.A., Morgenstern, K., Nesic, Z., McCaughey, J.H., Barr, A.G., 2010. Energy balance closure using eddy covariance above two different land surfaces and Implications for CO_2 flux measurements. Boundary-Layer Meteorol. 136, 193–218. https://doi.org/10.1007/s10546-010-9507-y

Kljun, N., Calanca, P., Rotach, M.W., Schmid, H.P., 2015. A simple two-dimensional parameterisation for Flux Footprint Prediction (FFP). Geosci. Model Dev 8, 3695–3713. https://doi.org/10.5194/gmd-8-3695-2015

Kohsiek, W., Liebethal, C., Foken, T., Vogt, R., Oncley, S.P., Bernhofer, C., Debruin, H.A.R., 2007. The Energy Balance Experiment EBEX-2000. Part III: Behaviour and quality of the radiation measurements. Boundary-Layer Meteorol. 123, 55–75. https://doi.org/10.1007/s10546-006-9135-8

Kormann, R., Meixner, F.X., 2001. An analytical footprint model for non-neutral stratification. Boundary-Layer Meteorol. 99, 207–224. https://doi.org/10.1023/A:1018991015119

Kustas, W.P., Prueger, J.H., Hatfield, J.L., Ramalingam, K., Hipps, L.E., 2000. Variability in soil heat flux from a mesquite dune site. Agric. For. Meteorol. 103, 249–264. https://doi.org/10.1016/S0168-1923(00)00131-3

Lamaud, E., Ogée, J., Brunet, Y., Berbigier, P., 2001. Validation of eddy flux measurements above the understorey of a pine forest. Agric. For. Meteorol. 106, 187–203. https://doi.org/https://doi.org/10.1016/S0168-1923(00)00215-X

Lee, X., 2003. Fetch and footprint of turbulent fluxes over vegetative stands with elevated sources. Boundary-Layer Meteorol. 107, 561–579. https://doi.org/10.1023/A:1022819907480

Leuning, R., van Gorsel, E., Massman, W.J., Isaac, P.R., 2012. Reflections on the surface energy imbalance problem. Agric. For. Meteorol. 156, 65–74. https://doi.org/10.1016/j.agrformet.2011.12.002

LI-COR Inc., 2012. EddyPro Software. Instruction manual. LI-COR Biosciences.

Li, N., Jia, L., Zheng, C., 2014. Evaluation of the harmonic-analysis method for surface soil heat flux estimation: a case study in Heihe River Basin, in: Proc. SPIE 9260, Land Surface Remote Sensing II, 926043 (8 November 2014). p. 926043. https://doi.org/10.1117/12.2069270

Lindroth, A., Mölder, M., Lagergren, F., 2010. Heat storage in forest biomass improves energy balance closure. Biogeosciences 7, 301–313. https://doi.org/10.5194/bg-7-301-2010

Liu, X., Yang, S., Xu, J., Zhang, J., Liu, J., 2017. Effects of soil heat storage and phase shift correction on energy balance closure of paddy fields. Atmósfera 30, 39–52. https://doi.org/10.20937/ATM.2017.30.01.04

Masseroni, D., Corbari, C., Mancini, M., 2014. Limitations and improvements of the energy balance

closure with reference to experimental data measured over a maize field. Atmosfera 27, 335–352. https://doi.org/10.1016/S0187-6236(14)70033-5

Mauder, M., Cuntz, M., Drüe, C., Graf, A., Rebmann, C., Schmid, H.P., Schmidt, M., Steinbrecher, R., 2013. A strategy for quality and uncertainty assessment of long-term eddy-covariance measurements. Agric. For. Meteorol. 169, 122–135. https://doi.org/10.1016/j.agrformet.2012.09.006

Mauder, M., Foken, T., 2011. Documentation and instruction manual of the eddy-covariance software package TK3. Arbeitsergebnisse, Nr. 46, Universität Bayreuth, Abt. Mikrometeorologie, Bayreuth.

Mauder, M., Foken, T., 2006. Impact of post-field data processing on eddy covariance flux estimates and energy balance closure. Meteorol. Zeitschrift 15, 597–609. https://doi.org/10.1127/0941-2948/2006/0167

Meyers, T.P., Hollinger, S.E., 2004. An assessment of storage terms in the surface energy balance of maize and soybean. Agric. For. Meteorol. 125, 105–115. https://doi.org/10.1016/j.agrformet.2004.03.001

Michiles, A.A. dos S., Gielow, R., 2008. Above-ground thermal energy storage rates, trunk heat fluxes and surface energy balance in a central Amazonian rainforest. Agric. For. Meteorol. 148, 917–930. https://doi.org/10.1016/j.agrformet.2008.01.001

Moderow, U., Aubinet, M., Feigenwinter, C., Kolle, O., Lindroth, A., Mölder, M., Montagnani, L., Rebmann, C., Bernhofer, C., 2009. Available energy and energy balance closure at four coniferous forest sites across Europe. Theor. Appl. Climatol. 98, 397–412. https://doi.org/10.1007/s00704-009-0175-0

Núñez, C., Varas, E., Meza, F., 2010. Modelling soil heat flux. Theor. Appl. Climatol. 100, 251–260. https://doi.org/10.1007/s00704-009-0185-y

Nunn, A.J., Cieslik, S., Metzger, U., Wieser, G., Matyssek, R., 2014. Combining sap flow and eddy covariance approaches to derive stomatal and non-stomatal O3 fluxes in a forest stand. Environ. Pollut. 158, 2014–2022. https://doi.org/10.1016/j.envpol.2009.11.034

Ochsner, T.E., Sauer, T.J., Horton, R., 2007. Soil heat storage measurements in energy balance studies. Agron. J. 99, 311–319. https://doi.org/10.2134/agronj2005.0103S

Oncley, S.P., Foken, T., Vogt, R., Kohsiek, W., DeBruin, H.A.R., Bernhofer, C., Christen, A., van Gorsel, E., Grantz, D., Feigenwinter, C., Lehner, I., Liebethal, C., Liu, H., Mauder, M., Pitacco, A., Ribeiro, L., Weidinger, T., 2007. The energy balance experiment EBEX-2000. Part I: overview and energy balance. Boundary-Layer Meteorol. 123, 1–28. https://doi.org/10.1007/s10546-007-9161-1

Ping, Y., Qiang, Z., Shengjie, N., Hua, C., Xiyu, W., 2011. Effects of the soil heat flux estimates on surface energy balance closure over a semi-arid grassland. Acta Meteorol. Sin. 25, 774–782. https://doi.org/10.1007/s13351-011-0608-4

Poyda, A., Reinsch, T., Kluß, C., Loges, R., Taube, F., 2016. Greenhouse gas emissions from fen soils used for forage production in northern Germany. Biogeosciences 13, 5221–5244. https://doi.org/10.5194/bg-13-5221-2016

Poyda, A., Reinsch, T., Skinner, R.H., Kluß, C., Loges, R., Taube, F., 2017. Comparing chamber and eddy covariance based net ecosystem CO_2 exchange of fen soils. J. Plant Nutr. Soil Sci. 1–15. https://doi.org/10.1002/jpln.201600447

Protic, M., Stankovic, M., Mitic, D., Todorovic, B., 2012. Application of fractional calculus in ground

heat flux estimation. Therm. Sci. 16, 373–384. https://doi.org/10.2298/TSCI110131075P

Prueger, J., Kustas, W., 2005. Aerodynamic Methods for Estimating Turbulent Fluxes. Publ. from USDA-ARS / UNL Fac.

Pumpanen, J., Kolari, P., Ilvesniemi, H., Minkkinen, K., Vesala, T., Niinistö, S., Lohila, A., Larmola, T., Morero, M., Pihlatie, M., Janssens, I., Curiel, J., Grünzweig, J.M., Reth, S., Subke, J., Savage, K., Kutsch, W., Østreng, G., Ziegler, W., Anthoni, P., Lindroth, A., Hari, P., 2004. Comparison of different chamber techniques for measuring soil CO_2 efflux 123, 159–176. https://doi.org/10.1016/j.agrformet.2003.12.001

R Core Team, 2014. A language and environment for statistical computing. R foundation for statistical computing, Vienna, Austria.

Sánchez, J.M., Caselles, V., Rubio, E.M., 2010. Analysis of the energy balance closure over a FLUXNET boreal forest in Finland. Hydrol. Earth Syst. Sci. 14, 1487–1497. https://doi.org/10.5194/hess-14-1487-2010

Sauer, T.J., Horton, R., 2005. Soil Heat Flux. Agron. J. 99, 304. https://doi.org/10.2134/agronj2005.0038s

Schmidt, M., Reichenau, T.G., Fiener, P., Schneider, K., 2012. The carbon budget of a winter wheat field: An eddy covariance analysis of seasonal and inter-annual variability. Agric. For. Meteorol. 165, 114–126. https://doi.org/10.1016/j.agrformet.2012.05.012

Silberstein, R., Held, A., Hatton, T., Viney, N., Sivapalan, M., 2001. Energy balance of a natural jarrah (Eucalyptus marginata) forest in Western Australia: measurements during the spring and summer. Agric. For. Meteorol. 109, 79–104.

Stoy, P.C., Mauder, M., Foken, T., Marcolla, B., Boegh, E., Ibrom, A., Arain, M.A., Arneth, A., Aurela, M., Bernhofer, C., Cescatti, A., Dellwik, E., Duce, P., Gianelle, D., van Gorsel, E., Kiely, G., Knohl, A., Margolis, H., Mccaughey, H., Merbold, L., Montagnani, L., Papale, D., Reichstein, M., Saunders, M., Serrano-Ortiz, P., Sottocornola, M., Spano, D., Vaccari, F., Varlagin, A., 2013. A data-driven analysis of energy balance closure across FLUXNET research sites: The role of landscape scale heterogeneity. Agric. For. Meteorol. 171–172, 137–152. https://doi.org/10.1016/j.agrformet.2012.11.004

Tol, C. Van Der, Timmermans, W., Corbari, C., Carrara, A., Timmermans, J., Su, Z., 2015. An analysis of turbulent heat fluxes and the energy balance during the REFLEX campaign. Acta Geophys. 63, 1516–1539. https://doi.org/10.1515/acgeo-2015-0061

Twine, T.E., Kustas, W.P., Norman, J.M., Cook, D.R., Houser, P.R., Meyers, T.P., Prueger, J.H., Starks, P.J., Wesely, M.L., 2000. Correcting eddy-covariance flux underestimates over a grassland. Agric. For. Meteorol. 103, 279–300. https://doi.org/10.1016/S0168-1923(00)00123-4

Varmaghani, A., Eichinger, W.E., Prueger, J.H., 2016. A diagnostic approach towards the causes of energy balance closure problem. Open J. Mod. Hydrol. 101–114.

Wang, K., Liu, C., Zheng, X., Pihlatie, M., Li, B., Haapanala, S., Vesala, T., Liu, H., Wang, Y., Liu, G., Hu, F., 2013. Comparison between eddy covariance and automatic chamber techniques for measuring net ecosystem exchange of carbon dioxide in cotton and wheat fields 6865–6877. https://doi.org/10.5194/bg-10-6865-2013

Wang, R., Zhang, Q., 2011. An assessment of storage terms in the surface energy balance of a subalpine meadow in Northwest China. Adv. Atmos. Sci. 28, 691–698. https://doi.org/10.1007/s00376-010-

9152-x

Williams, D.G., Cable, W., Hultine, K., Hoedjes, J.C.B., Yepez, E.A., Simonneaux, V., Er-Raki, S., Boulet, G., Bruin, H.A.R. De, Chehbouni, A., 2004. Evapotranspiration components determined by stable isotope, sap flow and eddy covariance techniques. Agric. For. Meteorol. 125, 241–258. https://doi.org/10.1016/j.agrformet.2004.04.008

Wilson, K., Goldstein, A., Falge, E., Aubinet, M., Baldocchi, D., Berbigier, P., Bernhofer, C., Ceulemans, R., Dolman, H., Field, C., Grelle, A., Ibrom, A., Law, B.., Kowalski, A., Meyers, T., Moncrieff, J., Monson, R., Oechel, W., Tenhunen, J., Valentini, R., Verma, S., 2002. Energy balance closure at FLUXNET sites. Agric. For. Meteorol. 113, 223–243. https://doi.org/10.1016/S0168-1923(02)00109-0

Wizemann, H.D., Gwinner, A., Wulfmeyer, V., Streck, T., 2017. Quantification of ground heat flux by harmonic analysis with high temporal resolution over six years.

Wizemann, H.D., Ingwersen, J., Högy, P., Warrach-Sagi, K., Streck, T., Wulfmeyer, V., 2014. Three year observations of water vapor and energy fluxes over agricultural crops in two regional climates of Southwest Germany. Meteorol. Zeitschrift 24, 39–59. https://doi.org/10.1127/metz/2014/0618

Xu, Z., Liu, S., Shi, W., Wang, J., 2017. Assessment of the energy balance closure under advective conditions and Its impact using remote sensing data. Am. Meteorol. Soc. 127–140. https://doi.org/10.1175/JAMC-D-16-0096.1

Yuan, L.I., Shu, W., Bicheng, C., 2014. Comparative study on methods for computing soil heat storage and energy balance in arid and semi-arid areas 28, 308–322. https://doi.org/10.1007/s13351-014-3043-5.1.

Zeri, M., Sá, L.D.A., 2010. The impact of data gaps and quality control filtering on the balances of energy and carbon for a Southwest Amazon forest. Agric. For. Meteorol. 150, 1543–1552. https://doi.org/10.1016/j.agrformet.2010.08.004

Zuo, J., Wang, J., Huang, J., Li, W., Wang, G., Ren, H., 2011. Estimation of ground heat flux and its impact on the surface energy budget for a semi-arid grassland 3, 41–50. https://doi.org/10.3724/SP.J.1226.2011.00041

Chapter 3

Paper B

3. Evaluating multi-year, multi-site data on the energy balance closure of eddy-covariance flux measurements at cropland sites in southwestern Germany[2]

Ravshan Eshonkulov[1,3], Arne Poyda[1], Joachim Ingwersen[1], Hans-Dieter Wizemann[2], Tobias KD Weber[1], Pascal Kremer[1], Petra Högy[4], Alim Pulatov[5] and Thilo Streck[1]

[1]Institute of Soil Science and Land Evaluation, Biogeophysics, Hohenheim University, Emil-Wolff Str. 27, 70593 Stuttgart, Germany
[2]Institute of Physics and Meteorology, Physics and Meteorology, Hohenheim University, GarbenStr. 30, 70593 Stuttgart, Germany
[3]Environmental Protection and Ecology, Karshi Engineering Economic Institute, Mustakillik Avenue 225, 180100 Karshi, Uzbekistan
[4]Institute of Landscape and Plant Ecology, Plant Ecology and Ecotoxicology, Hohenheim University, August-von-Hartmann-Str. 3, 70593, Stuttgart, Germany
[5]EcoGIS center, Tashkent Institute of Irrigation and Agricultural Mechanization Engineers, Kary Niyoziy Str.39, 100000 Tashkent, Uzbekistan

Abstract

The energy balance of eddy covariance (EC) measurements is typically not closed resulting in one of the main challenges in evaluating and interpreting EC flux data. Energy balance closure (EBC) is crucial for validating and improving regional and global climate models. To investigate the nature of the gap in EBC for agro-ecosystems, we analysed EC measurements from two climatically contrasting regions (Kraichgau (KR) and Swabian Jura (SJ)) in southwest Germany. Data were taken at six fully equipped EC sites from 2010 to 2017. The gap in EBC was quantified by ordinary linear regression, relating the energy balance ratio (EBR) calculated as the quotient of turbulent fluxes and available energy, to the residual energy term. In order to examine potential reasons for differences in EBC, we compared the

[2] The publication of Chapter 3 is done with the consent of the Copernicus Publications on behalf of the European Geosciences Union under the Creative Commons Attribution 4.0 License. The original publication was in: Journal of Biogeosciences, Volume 16, Pages 521-540. It can be found under the following link: https://doi.org/10.5194/bg-16-521-2019

EBC under varying environmental conditions and investigated a wide range of possible controls. Overall, the variation in EBC was found to be higher during winter than summer. Moreover, we determined that site had a statistically significant effect on EBC, but neither did crop nor region (KR vs SJ). The time-variable footprints of all EC stations were estimated based on data measured in 2015, complemented by micro-topographic analyses along the prevailing wind direction. The smallest mean annual energy balance gap was 17 % in KR and 13 % in SJ. Highest EBRs were mostly found for winds from the prevailing wind direction. The spread of EBR distinctly narrowed under unstable atmospheric conditions, strong buoyancy, and high friction velocities. Smaller footprint areas led to better EBC due to increasing homogeneity. Flow distortions caused by the back head of the anemometer, negatively affected EBC during corresponding wind conditions.

3.1. Introduction

Studying turbulent exchange at the land surface is important for assessing water cycling, plant growth, and carbon fluxes of ecosystems and for enhancing soil–crop, climate, and weather models. Currently, the best technique for determining these fluxes is the eddy-covariance (EC) method. It is considered the most direct and accurate measurement of turbulent fluxes in the soil–plant–atmosphere system (Baldocchi et al., 2001; Burba, 2013). In EC flux data, the measured available energy (incoming net radiation minus ground heat flux) is generally higher than the sum of turbulent exchange fluxes (latent and sensible heat). Accordingly, either the turbulent fluxes are incompletely captured or the measured available energy is positively biased. This gap in energy balance closure (EBC) is a long-standing problem in EC measurements and is one of the most frequently discussed concerns in micrometeorological research (Foken, 2008a).

Globally, a large number of research sites have been established to, inter alia, study reasons for the energy imbalance. This includes the FLUXNET network, with more than 500 EC towers around the world (Wilson et al., 2002), and the AmeriFlux network operating in North, Central, and South America (Peng et al., 2017). An example is an energy balance experiment, which was conducted to determine the reasons for the energy imbalance of EC measurements over irrigated cotton fields. The results showed that the net radiation differed by up to 10 W m^{-2} across a single field (Kohsiek et al., 2007). In a review of EBC, Foken (2008b) summarized the most important factors for the energy imbalance as related to measurement errors of the energy balance components, incorrect sensor configurations, influences of heterogeneous canopy height, unconsidered energy storage terms in the soil–plant–atmosphere system,

inadequate time averaging intervals, and long-wave eddies (mesoscale circulations; Foken, 2008b; Jacobs et al., 2008; Wilson et al., 2002). Additionally, the energy transport with near-surface secondary circulations (large eddies) cannot be measured with a single EC station (Cava et al., 2008; Foken, 2008b; Xu et al., 2017).

In parts, this may be rectified by altering the time averaging intervals. For example, Kidston et al. (2010) found that at a forest site, EBC peaked at 90 % when applying a 240 min averaging interval. At a boreal forest site, Sánchez et al. (2010) applied a range of different time averaging intervals and found that increasing the interval from the traditional 30 min to 1 day improved the EBC from 75 % to 100 %. However, this picture is inconclusive, since Oncley et al. (2007) found that increasing the time averaging interval up to 4 h at an irrigated cotton field did not result in a higher contribution of turbulent fluxes and that the contribution of low turbulent fluxes was less than 10 W m^{-2}. In most cases, the standard 30 min averaging period is proven to be the best compromise for simultaneously capturing most of the turbulent fluxes while fulfilling the precondition of stationarity (Charuchittipan et al., 2014; Masseroni et al., 2014; Sun et al., 2006).

The influence of site characteristics (e.g., vegetation type, canopy height, and terrain) on the EBC has been studied extensively. Wilson et al. (2002) reported no clear differences in EBC between flat and sloped terrain sites across 22 research sites. A comparison of two different agroecosystems in China, a degraded grassland and a maize cropland, showed similar EBC of about 80 % (Du et al., 2014). The comparison of a mature boreal jack pine forest and a jack pine clear-cut site by Kidston et al. (2010) revealed that depending on the surface characteristics, the loss of low frequencies can contribute significantly to the energy imbalance. Canopy height may impact EBC, although Wilson et al. (2002) found, in their study, that vegetation height did not control EBC. However, consideration of the stored energy in the soil–plant–atmosphere zone can noticeably improve EBC (Jacobs et al., 2008; Meyers and Hollinger, 2004; Zeri and Sá, 2010). Meyers and Hollinger (2004) compared the energy stored or released by CO_2 exchange and crop enthalpy change and showed that in their study maize stored more energy than soybean crops. Additionally, Eshonkulov et al. (2019) reported that mean EBC improved from 78 % to 87 % when minor energy storage and flux terms were taken into account during the main vegetation period. Lastly, the mismatch of measurement scales is also considered to be a reason for the energy imbalance (Sánchez et al., 2010; Xu et al., 2017).

During the last decade, the identification of the contributing source area (footprint) and evaluation of the representativeness of the EC flux data for the field of interest has received increased interest (Göckede

et al., 2006; Kljun et al., 2004; Schmid, 2002). Knowledge about the footprint is important for clarifying whether the EC station measures local or nonlocal energy fluxes (Eugster and Merbold, 2015; Pirk et al., 2017). Currently, there are a variety of models in use for estimating footprint areas. While most analytical footprint models assume a homogeneous flux source area, footprint calculations for heterogeneous sites require greater computational effort and detailed information on surface characteristics (Mauder et al., 2013). Despite the existing methods and studies, Stoy et al. (2013) concluded that the relationship between the footprint and EBC in agricultural cropland has not been sufficiently studied.

Therefore, the presented study evaluates the energy balance at agricultural croplands. The analyses are based on EC measurements conducted from 2010 to 2017 at six fully equipped sites in two climatically different regions of southwestern Germany. We hypothesized that multi-year, multi-site observations will provide new insights into the nature of the energy imbalance of EC flux measurements. The objectives of this study are to evaluate if the crop type, site characteristics, wind direction, atmospheric conditions, and footprint area act as controls on the EBC.

3.2. Materials and methods

3.2.1. Site description

The study sites in the Kraichgau region (KR) were located at "Katharinentalerhof", characterized by mostly flat terrain, and are located approximately 4 km north of the city Pforzheim (48.92° N, 8.70° E). Three EC stations (EC1, EC2, and EC3) were installed at adjacent fields with the respective areas of 14.9, 23.6, and 15.8 ha (Fig. 3.1). The prevailing wind direction is west. A former landfill site is locatedapproximately 500 m to the south of the experimental fields whose maximum elevation is about 41 m above its surroundings. KR is one of the warmest regions in Germany, with a mean temperature and annual precipitation of 9.4 °C and 890 mm in 1981–2010 (meteorological station Pforzheim-Ispringen, German Weather Service, located about 3 km from the research sites). The soils of this region developed from deep loess layers overlying a shell limestone. Detailed information about meteorological and soil conditions can be found in Table 3.1 and in Imukova et al. (2016), Ingwersen et al. (2015), and Wizemann et al. (2014).

Table 3.1. Main characteristics of the investigated sites.

Region	Kraichgau			Swabian Jura		
Station name	EC1	EC2	EC3	EC4	EC5	EC6
Latitude (°)	48.928496N	48.927743N	48.927199N	48.527214N	48.529780N	48.546632N
Longitude (°)	8.702782E	8.708901E	8.715950E	9.769950E	9.773474E	9.774280E
Elevation (m)	319	320	319	682	681	690
Soil type, (WRB, 2014)	Stagnic Luvisol			Calcic Luvisol	Anthrosol	Rendzic Leptosol

Due to its higher elevation, the Swabian Jura region (SJ) is characterized by a colder and harsher climate compared to KR. The prevailing wind direction is southwest to west. Mean temperature and annual precipitation were 7.5 °C and 1042 mm in 1981–2010 (Meteorological station Merklingen, German Weather Service, about 2 km from the research sites). Information about meteorological and soil variables is given in Table 3.1. Accordingly, crops are generally sowed and harvested later than in KR. SJ is the largest contiguous karst landscape in Germany, with generally rather shallow soils. The study sites are located close to the town of Merklingen (Fig. 3.1). The areas of the three research fields at EC4, EC5, and EC6 were 8.7, 16.7, and 13.4 ha, respectively. While EC4 and EC5 were adjacent fields, EC6 was situated 1.5 km to the north (Fig. 3.1).

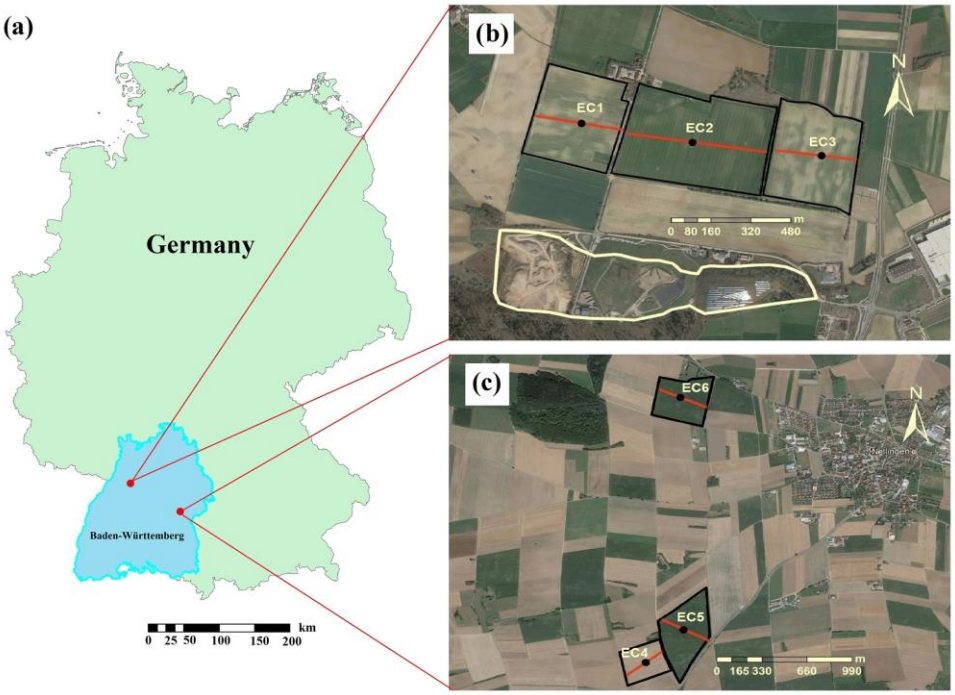

Fig. 3.1. (a) Geographical overview (a) and locations of the study sites and EC stations in Kraichgau (b) and Swabian Jura (c) (Google Earth; KR on 31.03.2017 and SJ on 26.08.2016). Red transect lines indicate positions of conducted micro-topographic measurements along the prevailing wind directions. The yellow line demarks the boundaries of a former landfill site (b).

The crop rotation in SJ was more diverse than in KR, and the most frequently grown crops were winter wheat and silage maize (Table 3.2). In 50 % of the years on-site in KR, winter wheat was cultivated; this value was only 25 % in SJ. KR showed a lower variety in cultivated crops to SJ, with three in KR and six in SJ. At all sites, farmers frequently grew cover crops between winter and summer crops. These were mainly mustard, phacelia, or multi-species mixtures.

Table 3.2. Crop grown at the six study sites from 2010 to 2017 (harvest year).

Region	Kraichgau			Swabian Jura		
	Sites			Sites		
Harvest year	EC1	EC2	EC3	EC4	EC5	EC6
2010	SM	WR	WW	WR	WW	SM
2011	WW	WW	SM	WW	SM	WW
2012	WR	SM	WW	SB	SM	WB
2013	WW	WW	WR	WR	WB	SM
2014	SM	SM	WW	WW	SP	WW
2015	WW	WW	SM	WW	SM	WB
2016	GM	WR	WW	SB	SM	SM
2017	WW	WW	WW	SM	WB	WB

WW-winter wheat, WR-winter rapeseed, SM-silage maize, GM-grain maize, SB-summer barley, WB-winter barley, SP-spelt.

3.2.2. Eddy covariance measurements

One EC station was installed at the center of each field site in spring 2009 (Ingwersen et al., 2011; Wizemann et al., 2014). All stations were equipped with a fast-response CO_2/H_2O open-path infrared gas analyzer (LI-7500; LI-COR Biosciences, Lincoln, NE, USA) and a three-axis ultrasonic anemometer (CSAT3; Campbell Scientific Inc., Logan, UT, USA). The raw data of the gas analyzer and sonic anemometer were recorded at 10 Hz and stored on a CR3000 data logger (Campbell Scientific Inc., Logan, UT, USA). In early 2009, the CSAT3 orientation at EC1 and EC3 was 230°, and at EC2, it was 255°. In late April 2010, the orientation was changed to 170° and varied over the subsequent years between 160 and 190°, ensuring that winds from the prevailing wind direction (west and east) enter the anemometer from the side. In SJ, the mean CSAT3 orientation was 220∘±15 from late March 2010 until the end of 2017. The gas analyzers were factory-calibrated biannually. Sensor heights were adjusted to account for increasing canopy heights, particularly during the vegetation periods of maize. This ensured that the distance between sensors and canopy was roughly 2–3 m. Maximal sensor heights in KR and SJ were 6.00 m at EC2 (2014) and 4.80 m at EC6 (2010), and the minimal sensor height was approximately 2 m in both regions. Each EC system was powered by two 12 V batteries (each 240 Ah) charged by four 20 W solar panels. To enable continuous EC measurements during winter, portable fuel cell systems

(Efoy Pro 800 Duo, FSC Energy AG, Brunnthal-Nord, Germany) were installed in autumn 2015: one at EC2 and one at EC6. At the others stations the LI-7500 was shut down during the winter, mostly from late November to mid-March.

Net radiation was measured using a four-component radiometer (NR01, Hukseflux Thermal Sensors, Delft, The Netherlands). The radiometers were placed above the cropped field area in close proximity to the EC stations. Air temperature and relative humidity were measured at a height of 2 m at each EC station using a temperature and relative humidity probe (HMP45C, Vaisala Inc, Helsinki, Finland). Soil temperature was measured at the depths of 0.02, 0.06, 0.15, 0.30, and 0.45 m (107 Thermistor probe, Campbell Scientific Inc., Logan, UT, UK). To measure the soil heat flux near the EC stations, three heat flux plates (HFP01, Hukseflux Thermal sensors, Delft, The Netherlands) were installed at a depth of 0.08 m. The soil volumetric water content at 0.05, 0.15, 0.30, 0.45, and 0.75 m depth was monitored with frequency-domain reflectometry sensors (CS616, Campbell Scientific Inc., Logan, UT, USA). In the shallow soil at EC6, however, soil variables could be measured only down to 0.3 m. Data from thermistor (0.02 and 0.06 m) and water content sensors (0.05 m) were used to calculate the soil heat storage between the soil heat flux plates and the ground surface (Eshonkulov et al., 2019; Wizemann et al., 2014). Precipitation was measured with a 0.2 mm tipping bucket rain gauge (ARG 100, Environmental Measurements Ltd., North Shields, UK), which was installed 1 m above ground. The rain gauges were recalibrated once per year.

3.2.3. Data processing and quality control

High-frequency raw data from 2010 to 2017 were processed with a 30 min averaging interval using the software package TK3.1 (Mauder et al., 2013). The following settings were used to compute latent and sensible heat flux: spike detection (Vickers and Mahrt, 1997), planar fit coordinate rotation (Wilczak et al., 2001), correction of spectral loss (Moore, 1986), sonic virtual temperature conversion into actual temperature (Schotanus et al., 1983), and correction for density fluctuations (Webb et al., 1980). Additionally, the raw data of 2015 were processed with the software Eddypro® (Version 6.2.1, LI-COR Inc., 2012) to obtain input parameters (Obukhov length, standard deviation of lateral velocity fluctuations after rotation, friction velocity, mean wind speed, and direction) for deriving flux source area (footprint). Data processing and correction in EddyPro® were conducted with the same settings as in TK 3.1. Both programs yield comparable results (Fratini and Mauder, 2014).

The nine flag system after Foken et al. (2004) was used as the quality criterion. For the evaluation, we used only data with quality flags 1–3, as suggested by Mauder and Foken (2011). Moderate (flags 4–6) and poor-quality (flags 7–9) data were discarded. In a second step, a median filter was applied for additional de-spiking of half-hourly fluxes. The filter removes all fluxes exceeding 5 times the median of the previous 3 days (Demyan et al., 2016). No gap-filling was performed in this study.

3.2.4. Energy balance closure of eddy covariance measurements

In the ideal case, the surface energy balance obeys the following equation:

$$R_n - G = \mathrm{LE} + H, \tag{3.1}$$

where R_n is the incoming net radiation, LE is the latent heat flux, H is the sensible heat flux (both positive upwards), and G is the ground heat flux (positive downwards). All components are expressed in W m^{-2}. Note that in Eq. (3.1) minor flux terms such as energy storage in the canopy or energy conversion by photosynthesis are neglected. All available filtered half-hourly flux data of the four terms in Eq. (3.1) were used to calculate the EBC. Three measures were used to evaluate the EBC. Firstly, we determined the slope and intercept from ordinary linear regression (OLR) of turbulent fluxes (H+LE) against available energy (R_n−G). In the ideal case of a fully closed energy balance, the slope and intercept of the linear regression are equal to 1 and zero, respectively (Ping et al., 2011; Wilson et al., 2002). In this study, we also considered the intercept (W m^{-2}) of the OLR in evaluating EBC, as suggested by Franssen et al. (2010).

Secondly, by the energy balance ratio (*EBR*) calculated as:

$$EBR = \frac{H+LE}{R_n-G}, \tag{3.2}$$

Thirdly, by comparing the energy balance residual (*Res*; W m^{-2}) given by:

$$Res = R_n - G - H - LE, \tag{3.3}$$

3.2.4. Atmospheric conditions

As a proxy for the role of shear and buoyancy in the production or consumption of turbulent kinetic energy, we used the friction velocity, u^* (m s^{-1}), and the kinematic virtual temperature flux, respectively. The latter is the covariance (w′T′v) between vertical wind speed (w) and virtual temperature (T_v). As the virtual temperature can be replaced by the sonic temperature (T_s) with negligible loss of accuracy (Kaimal

and Gaynor, 1991), we computed the virtual temperature flux from the covariance ($w'T'_s$) between w and T_s.

The relationship between atmospheric stability and the EBC was examined using the dimensionless atmospheric stability parameter ζ defined by Stull (1988):

$$\zeta = z_m/L, \tag{3.4}$$

where z_m (m) is the measurement height of the sonic anemometer and L (m) is the Obukhov length. The stability parameter expresses the relative roles of shear and buoyancy. Using ζ, the stability of the atmosphere can be divided into three classes (Franssen et al., 2010): stable ($\zeta \geq 0.1$), neutral ($-0.1 < \zeta < 0.1$), and unstable ($\zeta \leq -0.1$).

3.2.5. Footprint analyses and micro-topography

To determine the relationship between the contributing source area of turbulent fluxes and the EBC, we performed footprint analyses. We used the flux footprint prediction online tool of a simple two-dimensional parameterization (Kljun et al., 2015, http://geography.swansea.ac.uk/nkljun/ffp/www/, last access: 17 July 2018). The footprint parameterization uses the Lagrangian stochastic particle dispersion model (Kljun et al., 2002). As input parameters to the model, we used displacement height, z_d (m), mean wind speed (m s^{-1}), Obukhov length (m), standard deviation of horizontal wind speed (m s^{-1}), friction velocity, u^* (m s^{-1}), wind direction (°), and measurement height above the ground surface, z_m (m), which was calculated by

$$z_m = z_{receptor} - z_d, \tag{3.5}$$

where $z_{receptor}$ is the height of the sonic anemometer and the gas analyzer, and z_d is calculated by

$$z_d = 0.67 * z_{can}, \tag{3.6}$$

where z_{can} (m) is the time-variable canopy height because of crop growth. This was accounted for by biweekly measurements and was considered in TK3.1 for the respective 2-week periods. Data for footprint analyses were constrained to $u^* > 0.1$ m s^{-1} and $\zeta \geq -15.5$.

Additionally, the micro-topography of the EC sites was determined along a transect in the prevailing wind direction (Fig. 3.1). About every two meters, the elevation of the fields above mean sea level was measured with a differential global positioning system (Altus APS 3M, Septentrio, Belgium).

3.2.6. Statistical analyses

For the statistical analyses, we used all available data on energy fluxes from the onset of measurements (late March or early April) until harvest. In the case of maize, however, full data for the calculation of energy balances were generally available from May. Autocorrelation of the data was tested using the Durbin–Watson test (Faraway, 2014). Analysis of variance (ANOVA) was used to test for significant effects of region, site, year, and crops on EBC, for which linear mixed models were defined (Piepho et al., 2004). The data were assumed to be normally distributed but heteroscedastic due to the different years. We based these assumptions on graphical residual analyses. Generally, the factors of interest were defined as fixed, and interaction terms were considered. Remaining factors not included in the ANOVA were defined as random. Multiple contrast tests (Bretz et al., 2011) were performed to identify significant differences between the different factor levels. Unless indicated otherwise, the significance level was set to α=0.05. Calculations were done using the statistical software R (R Core Team, 2014) and packages multcomp for simultaneous tests of linear mixed models (Hothorn et al., 2017), nlme for fitting and comparing the models (Pinheiro et al., 2016), gplots for creating plots (Gregory et al., 2009), and gdata for importing input data from files formatted by Microsoft Excel files (Gregory et al., 2017).

3.3. Results

3.3.1. Meteorological and terrain conditions

3.3.1.1. Kraichgau

At the KR sites, the annual mean air temperature ranged between 8.4 °C in 2010 and 10.9 °C in 2014. The overall average was 9.8 °C (Fig. 3.2a), which is 0.4 °C higher than the 30-year climatological mean (1981–2010) measured at the meteorological station Pforzheim-Ispringen. The lowest and highest monthly mean temperature was −3.2 °C in February 2012 and 21.1 °C in July 2015. The mean annual precipitation was 796 mm, which is 93 mm lower than measured in Pforzheim-Ispringen. In 2013, the wettest year within the 8-year period, total precipitation amounted to 973 mm. The lowest annual precipitation (629 mm) was measured in 2015 (Fig. 3.2b).

Figure 3.3 shows the height transects along the prevailing wind direction. At the KR sites, the mean slopes along the transects were 0.4 %, <0.01 %, and 0.3 % at EC1, EC2, and EC3, respectively. The micro-relief of station EC1, located on a micro-bank, fluctuates more strongly than that of EC2. The immediate surroundings of EC2 are very homogeneous in elevation. Station EC3 was positioned in a

micro-depression. Overall, the three transects show that the KR fields can be regarded as flat, with EC2 being the flattest.

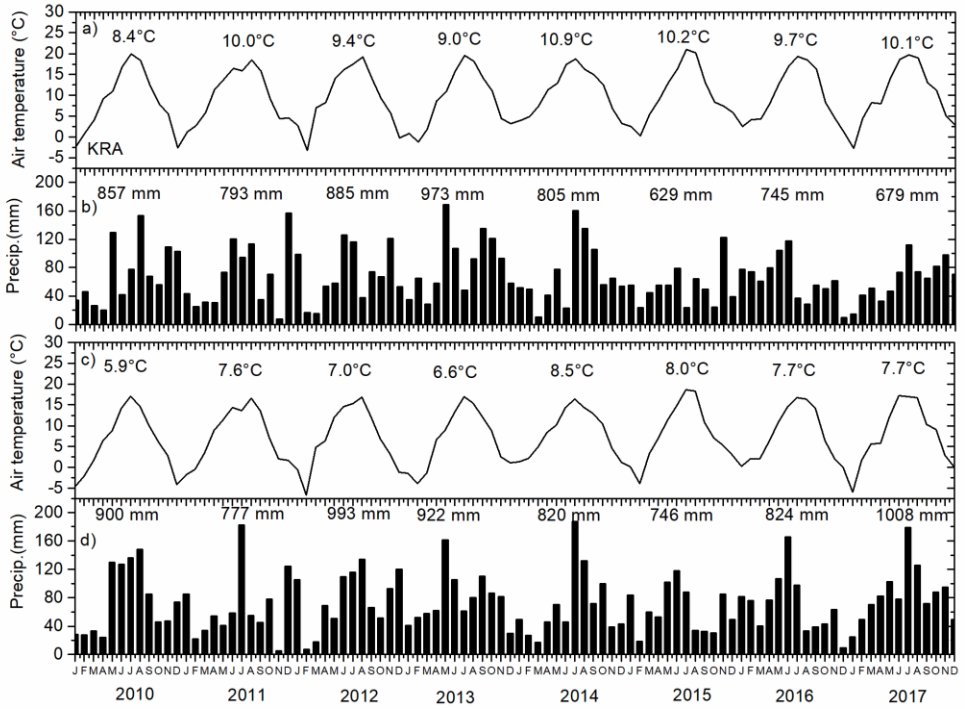

Fig. 3.2. Mean monthly air temperatures and precipitation sums at the Kraichgau site EC1 and Swabian Jura site EC4 from 2010 to 2017. Annual mean temperatures and precipitation sums are given on top of the lines or bars.

3.31.2. Swabian Jura

The mean temperature in SJ (7.4 °C) was 2.4 °C lower than in KR, varying from 5.9 °C in 2010 to 8.5 °C in 2015 (Fig. 3.2c). As in KR, the lowest and highest mean monthly temperatures were recorded in February 2012 (−6.6 °C) and July 2015 (18.6 °C). The mean annual precipitation was 874 mm. As in KR, 2015 was the year with the lowest precipitation. Highest total rainfall was measured in 2017, not in 2013 as in KR. November 2011 was the month with the lowest monthly cumulative precipitation (5 mm), and July 2014 was that with the highest (187 mm; Fig. 3.2d).

In SJ, only EC4 is relatively flat (Fig. 3.3). Its topography is comparable with that of EC1 in KR. The elevation along the transect at EC5 gently increases, with a mean slope of 0.6 % from SE to NW. Station EC5 itself is situated in a local micro-depression. The topography of station EC6 differs considerably from that of the other fields. The station is positioned on the top of a ridge. Whereas in NW direction

the terrain drops with a mean rate of 3.7 m per 100 m, in SE direction the terrain is nearly flat (slope=0.3 %).

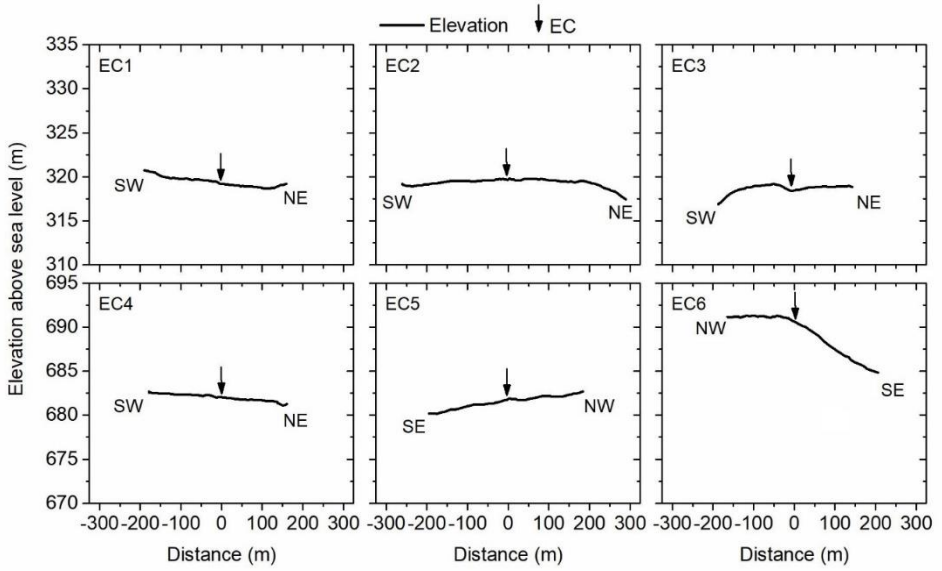

Fig. 3.3. Elevations at EC sites along the dominant wind directions (see Figs. 1 and 3). Arrows present positions of EC stations.

3.3.2. Energy partitioning at the land surface

The energy partitioning at the canopy surface of different crop stands is shown, by way of example, for the vegetation period of 2016 (Fig. 3.4). In that year, five different crops (winter rapeseed – WR, spring barley – SB, winter wheat – WW, silage maize – SM, and grain maize – GM) were grown at the EC sites. From April to June, most of the net radiation was transformed into latent heat at the crop stands, except for SM at EC5. The daytime Bowen ratio was lowest for WW and WR, with 0.14 and 0.13, respectively. Also GM, SB, and SM at EC6 led to daytime Bowen ratios distinctly below unity (about 0.21). Only silage maize at EC5 had a Bowen ratio of about unity, which indicates that the available energy was partitioned into latent and sensible heat in similar proportions. For the WW, SB, and WR sites and years, the ground and sensible heat fluxes were nearly the same and showed a similar diurnal course. At the maize stands, the ground heat flux tended to be higher than the sensible heat flux during the morning hours, while in the afternoon the order switched and more sensible heat than ground heat was formed. At all sites, the measured energy residual was similar to the sensible heat fluxes, ranging from 23 W m^{-2} at EC3 to 44 W m^{-2} at EC1. The daily net radiation was 149, 133, 134, 130, 138, and 164 W m^{-2} at EC1 to EC6, respectively. The mean daily LE ranged from 54 W m^{-2} at EC5 to 94 W m^{-2} at EC3.

For July to September, the strongest shift in energy partitioning occurred at the WR site. In the afternoon, the Bowen ratio was in the range of unity, and sometimes the half-hourly sensible heat flux was even higher than the latent heat flux. A similar shift was observed at the WW site, but it was weaker than at the WR site. At the GM, SM, and SB sites the largest difference compared with the period April to June was the ratio between the sensible and ground heat flux. From July to September the sensible heat was about twice the ground heat flux. The mean net radiation ranged from 125 W m^{-2} at EC5 to 176 W m^{-2} at EC2, and LE varied from 78 W m^{-2} at EC4 to 89 W m^{-2} at EC1. The residual energy for this period was 23, 28, 22, 24 and 16 W m^{-2} at the sites EC1, EC2, EC3, EC4, and EC6, respectively. Note that EC5 data are missing due to damage in the sonic anemometer and gas analyzer.

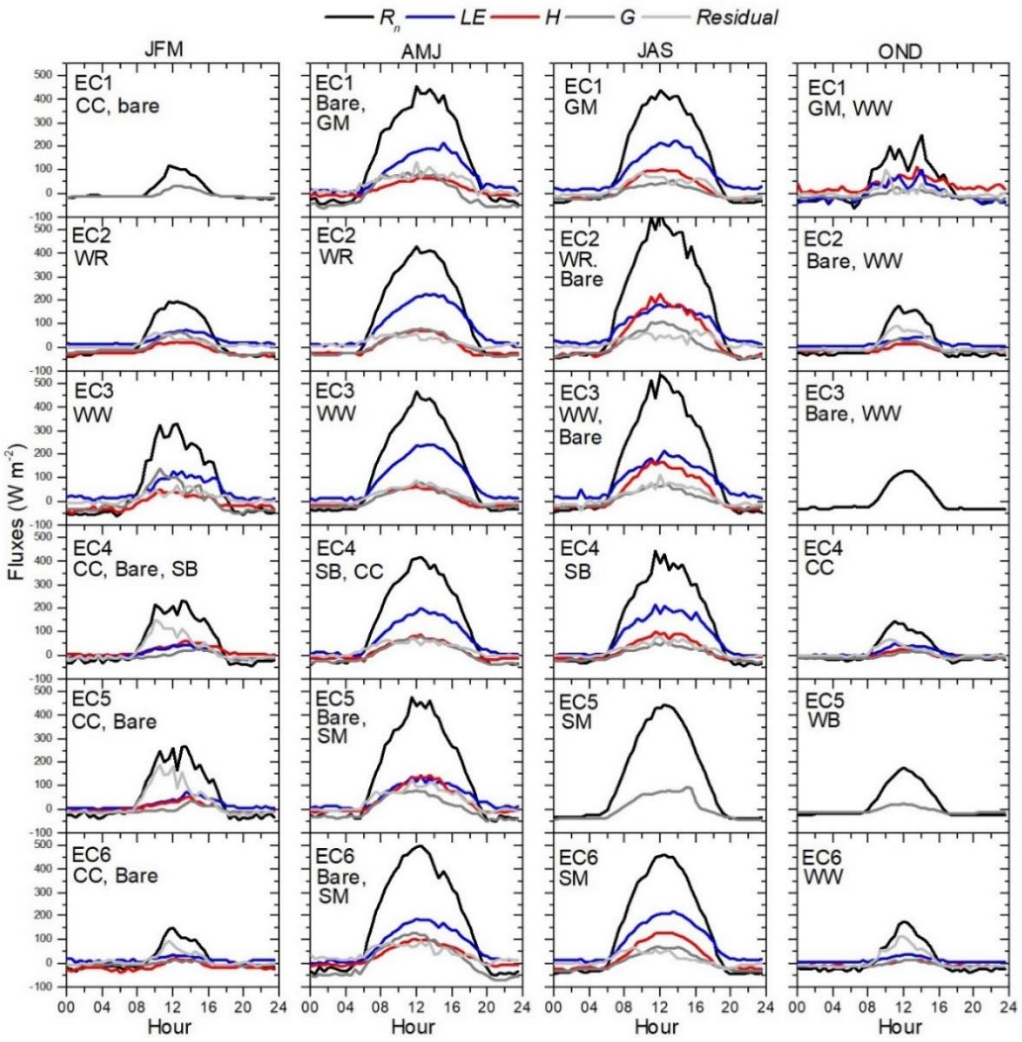

Fig. 3.4. Diurnal courses of energy balance components averaged over 3-month periods in Kraichgau (EC1, EC2, EC3) and Swabian Jura (EC4, EC5, EC6) in 2016. Insets denote the different crops grown in 2016; see main text for explanation. Because of energy shortage during winter at the EC1, EC3, EC4 and EC5 sites, the fluxes shown in the JFM and OND graphs were measured only in March and from 1 October to mid-November, respectively.

3.3.3. Energy balance closure

The mean EBR over the 48 years on-site was 0.75, corresponding to a mean energy residual of 41.6 W m^{-2} (Table 3.3). The mean annual EBR ranged between 0.62 at EC1 (WW in 2013) and 0.90 at EC4 (SM in 2017). The mean EBR over the six EC stations was highest in 2010 (EBR = 0.78) and lowest in 2013 (EBR = 0.71). Averaged over the period from 2010 to 2017, the best EBC was achieved at EC4 (EBR = 0.82), whereas the largest mean energy gap occurred at the neighboring station EC5. There, the mean residual was 49.0 W m^{-2}.

Figure 3.5 presents the course of monthly mean EBC determined by the OLR for all six stations averaged over the period 2010–2017. In general, the EC method performed best (EBC was highest) over the vegetation period from April to August. The highest EBC was usually found during July and August and distinctly declined over autumn and winter. At station EC6, the SJ station equipped with a fuel cell system, for example, the EBC declined to 42 % in January 2016 and 23 % in December 2017. A low EBC was usually associated with a larger variation (see winter months; Fig. 3.5).

3.3.4. What impacts the EBC?

3.3.4.1. Effect of region, station, year and crop

The statistical analyses showed that the EBC over the main vegetation period from early April until harvest did not differ between the two regions (Fig. 3.6a). The EBC was significantly higher at stations EC2 and EC4 ($p<0.001$; p – probability level) than at the other stations (Fig. 3.6b). The lowest spread in values was observed at station EC4. In 2013 and 2014, EBC was lower ($p<0.001$) than in the other 6 years (Fig. 3.6c). The crops had no significant effect on mean EBC (Fig. 3.6d). EBC over winter rapeseed showed the highest variation in comparison to the other four crops, varying between 57 % and 88 %.

Table 3.3. Annual mean energy balance closure (EBC, slope of linear regression) and energy balance ratio (EBR) at the eddy covariance stations EC1 to EC6 in Kraichgau and Swabian Jura during 2010 – 2017. Regressions are based on half-hourly data.

Region			Kraichgau			Swabian Jura			
			Sites			Sites			
Growing season, year	Parameter	Unit	EC1	EC2	EC3	EC4	EC5	EC6	Mean
2010	Slope		0.82	0.69	0.70	0.87	0.74	0.74	0.76
	Intercept	W m^{-2}	-2.09	-5.55	8.59	3.06	2.86	11.84	3.12
	R^2		0.91	0.85	0.84	0.94	0.86	0.90	0.88
	EBR		0.80	0.66	0.77	0.89	0.75	0.79	0.78
	Residual	W m^{-2}	23.5	62.7	30.8	22.8	45.7	43.5	38.2
2011	Slope		0.70	0.76	0.70	0.77	0.77	0.72	0.74
	Intercept	W m^{-2}	-4.95	-0.13	5.22	1.54	12.62	4.57	3.15
	R^2		0.95	0.94	0.86	0.92	0.88	0.94	0.92
	EBR		0.69	0.76	0.73	0.78	0.82	0.74	0.75
	Residual	W m^{-2}	54.8	32.1	55.4	52.4	43.0	63.7	50.2
2012	Slope		0.74	0.67	0.69	0.81	0.78	0.72	0.74
	Intercept	W m^{-2}	-3.14	7.48	4.17	3.65	6.48	2.00	3.44
	R^2		0.96	0.86	0.94	0.90	0.89	0.93	0.91
	EBR		0.73	0.69	0.71	0.84	0.82	0.74	0.76
	Residual	W m^{-2}	53.2	75.6	57.3	24.7	31.5	38.4	46.8
2013	Slope		0.66	0.71	0.70	0.79	0.67	0.72	0.71
	Intercept	W m^{-2}	-6.59	-0.26	4.40	4.17	-0.77	3.28	0.71
	R^2		0.95	0.96	0.95	0.92	0.94	0.93	0.94
	EBR		0.62	0.71	0.72	0.82	0.67	0.74	0.71
	Residual	W m^{-2}	59.8	42.1	53.9	32.5	52.8	46.4	48.0
2014	Slope		0.69	0.74	0.70	0.79	0.66	0.74	0.72
	Intercept	W m^{-2}	4.34	5.66	4.78	-2.69	0.50	0.46	2.18
	R^2		0.89	0.86	0.92	0.93	0.93	0.94	0.91
	EBR		0.71	0.77	0.73	0.78	0.66	0.75	0.73
	Residual	W m^{-2}	51.2	36.7	39.2	43.7	69.9	44.9	47.6
2015	Slope		0.71	0.81	0.77	0.81	0.73	0.76	0.77
	Intercept	W m^{-2}	-5.14	-5.65	8.13	-2.85	7.22	-4.99	-0.55
	R^2		0.96	0.94	0.92	0.94	0.87	0.94	0.93
	EBR		0.67	0.77	0.81	0.79	0.77	0.72	0.76
	Residual	W m^{-2}	46.4	29.1	34.4	30.4	42.9	36.9	36.7
2016	Slope		0.75	0.83	0.80	0.77	0.62	0.75	0.75
	Intercept	W m^{-2}	7.50	-5.99	3.39	-0.66	5.70	3.42	2.23
	R^2		0.89	0.92	0.94	0.92	0.84	0.88	0.90
	EBR		0.79	0.78	0.82	0.76	0.66	0.79	0.77
	Residual	W m^{-2}	40.8	23.3	33.3	28.8	47.9	22.3	32.7
2017	Slope		0.70	0.73	0.86	0.84	0.66	0.76	0.76
	Intercept	W m^{-2}	-6.41	-0.81	2.36	10.63	11.50	-0.67	2.77
	R^2		0.96	0.95	0.93	0.86	0.87	0.94	0.92
	EBR		0.66	0.73	0.87	0.90	0.72	0.75	0.77
	Residual	W m^{-2}	48.2	52.8	17.4	20.5	58.4	39.7	32.9
Mean	Slope		0.72	0.74	0.74	0.81	0.70	0.74	0.74
	Intercept	W m^{-2}	-2.06	-0.66	5.13	2.11	5.76	2.49	2.13
	R^2		0.93	0.91	0.91	0.92	0.89	0.93	0.91
	EBR		0.71	0.73	0.77	0.82	0.73	0.75	0.75
	Residual	W m^{-2}	42.7	44.3	39.9	32.0	49.0	42.0	41.6

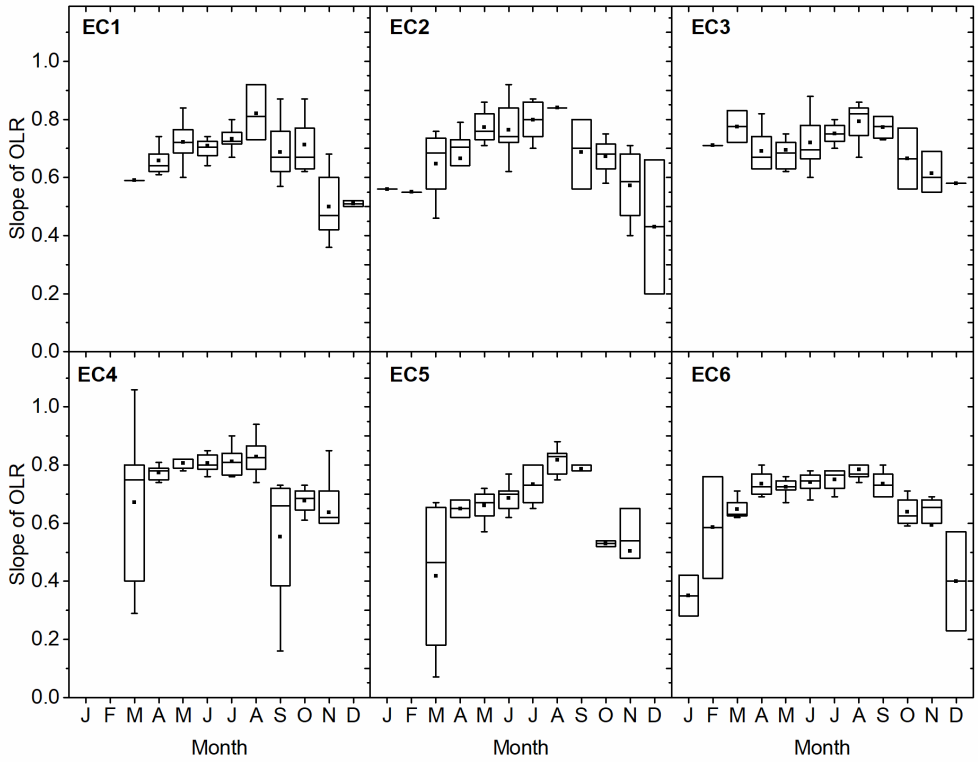

Fig. 3.5. Monthly aggregated energy balance closure (EBC) obtained by ordinary linear regression of turbulent fluxes (LE+*H*) against available energy (R_n−*G*) for all stations during 2010–2017.

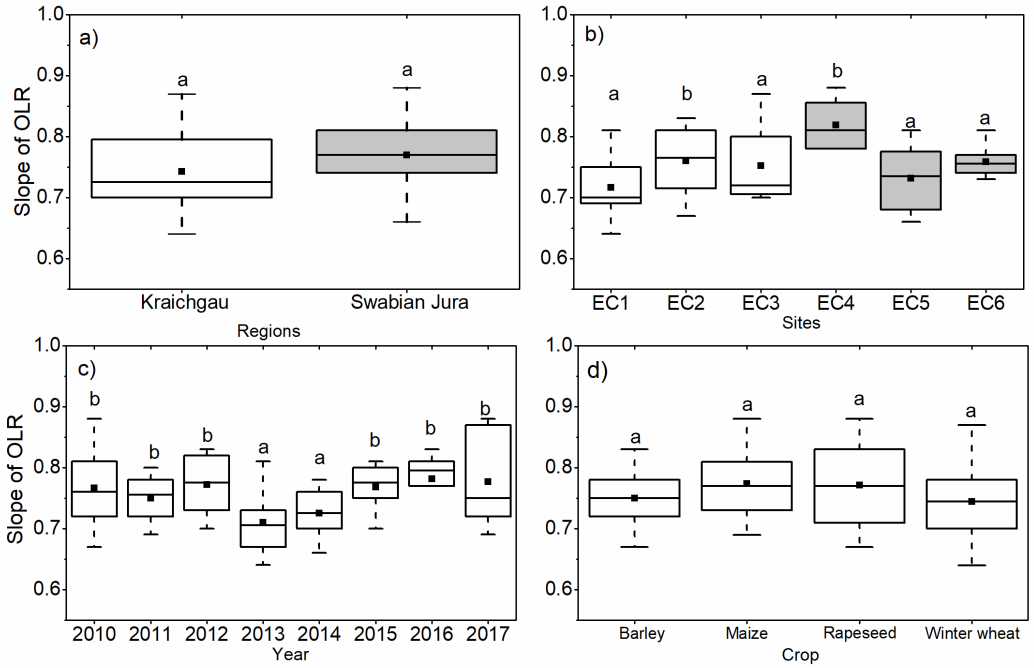

Fig. 3.6. Comparison of energy balance closure (EBC) measured by linear regression, grouped for the different regions, sites, years, and crops. Measurements were conducted from early spring until harvest. Different letters indicate significant (a – insignificant, b – significant) differences between the factor levels at α=0.05.

3.3.4.2. Effect of wind speed and direction

Typical for the midlatitudes, the KR sites' prevailing wind direction was from west to east. The fraction of WSW to WNW (240–300°) winds was 43.2 %, 36.8 % and 33.7 % at EC1, EC2, and EC3, respectively (Fig. 3.7). The highest wind speeds were also measured within these wind direction sectors. Wind blowing from north- and southward directions was rarely measured (<10 %). While at EC1 the wind speed averaged 2.9 m s^{-1}, at EC2 and EC3 the values were 2.4 and 1.9 m s^{-1}, respectively. Moreover, high wind speeds (>6 m s^{-1}) clearly decreased from the most westerly station (EC1) to the most easterly station (EC3). At EC1, EC2, and EC3, the share of these high wind speeds was 4.6 %, 3.3 %, and 0.2 %, respectively.

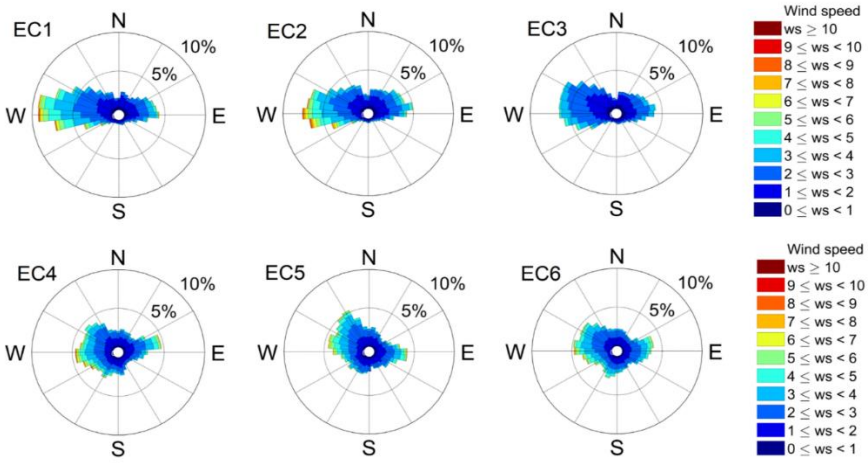

Fig. 3.7. Distribution of wind direction and wind speed (m s^{-1}) from 2010 to 2017 in Kraichgau (EC1 – EC3) and Swabian Jura (EC4 – EC6).

In SJ, the wind blew mostly from westerly or easterly directions (Fig. 3.7). The wind from the 240–300° sector was less than in KR, with shares of 14.4 %, 25.5 %, and 26.6 % at EC4, EC5, and EC6, respectively. At EC5, more wind was recorded from the NW sector (300–330°). Mean horizontal wind speeds at EC4, EC5, and EC6 were 2.44, 2.38, and 2.51 m s^{-1}, respectively. Wind speeds above 6 m s^{-1} made up 2.0 (EC4), 1.7 (EC5), and 1.3 % (EC6) of all measured wind speeds in SJ.

The distribution of the EBR as a function of wind direction is shown in Fig. 3.8. The EBR was averaged for 30° wind sectors over all available daytime data (global radiation >10 W m^{-2}). At the KR sites, the highest EBR was achieved when the wind blew from westerly directions, which is the prevailing wind direction. Wind from northern and southern directions was related to a lower EBR. Particularly wind from the south was associated with an EBR below 0.6 at all three stations. This phenomenon was most

pronounced at station EC1. Also at the SJ sites, the highest EBR usually coincided with wind from the prevailing direction. One exception is the high EBR at EC4 for the south–southeast sector. At EC4, for six out of the 12 wind sectors, EBR was above 0.8. In contrast, at EC5 and EC6, the EBR exceeded 0.8 in only three wind sectors. At all stations, the EBR was lowest (<0.6) for winds from the northeast (Fig. 3.9).

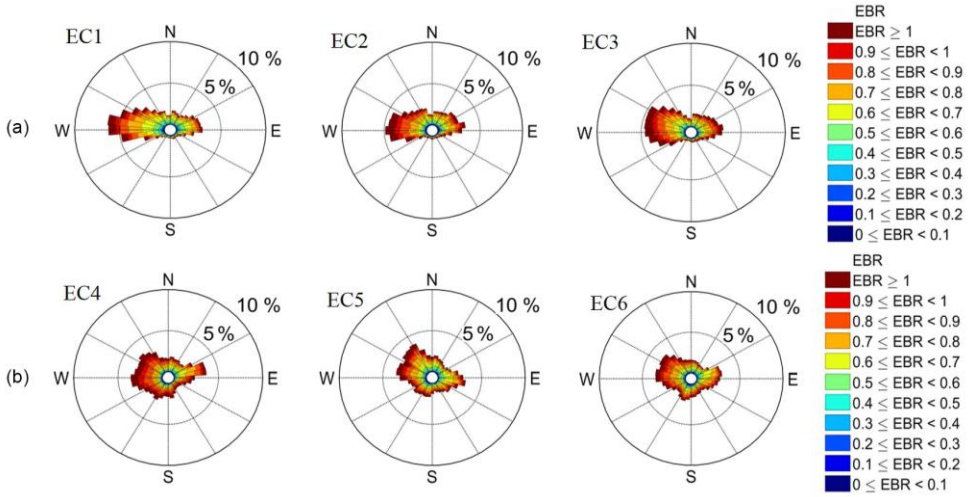

Fig. 3.8. Distribution of half-hourly energy balance ratios (EBR) in terms of wind direction at eddy-covariance (EC) stations during the 2010–2017 study period. Spike lengths in diagram show relative frequency of wind directions; color of legend shows EBR. This is shown for (a) Kraichgau and (b) Swabian Jura.

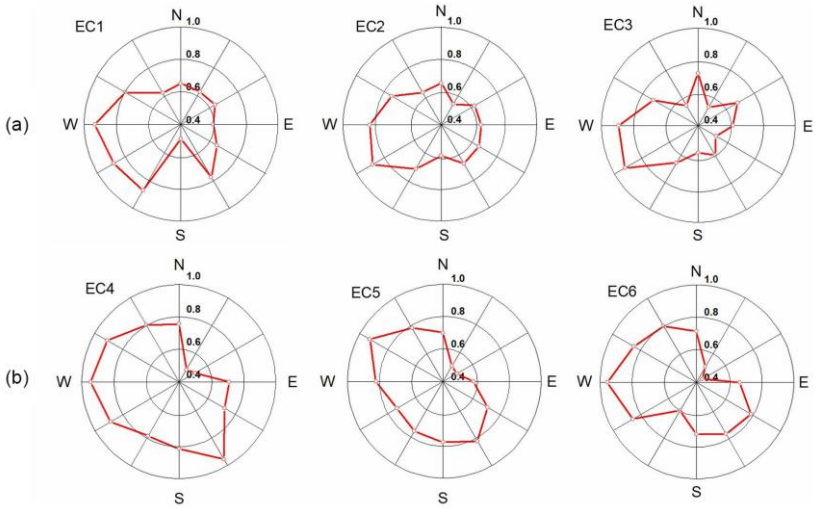

Fig. 3.9. Half-hourly energy balance ratio (EBR) averaged for 30° wind sectors at the six eddy-covariance (EC) stations during the 2010 to 2017 study period. This is shown for (a) Kraichgau and (b) Swabian Jura.

3.3.4.3. Effect of atmospheric conditions

This section evaluates the EBR as a function of buoyancy, shear and atmospheric stability. For this purpose, we plotted EBR against the kinematic virtual temperature flux ($w'T_v'$; proxy for buoyancy), friction velocity (u^*, proxy for shear) and the stability parameter ζ (Fig. 3.10). Again, only half-hourly daytime fluxes (R_s > 10 W m^{-2}) were evaluated. The plot EBR versus $w'T_v'$ shows a vast scatter at weak buoyancy. Here, the EBR ranges from plus four to minus four. The scatter decreases substantially as the modulus of $w'T_v'$ increases. Note that $w'T_v' < -0.15$ K m s^{-1} were measured only at stations EC2 and EC4.

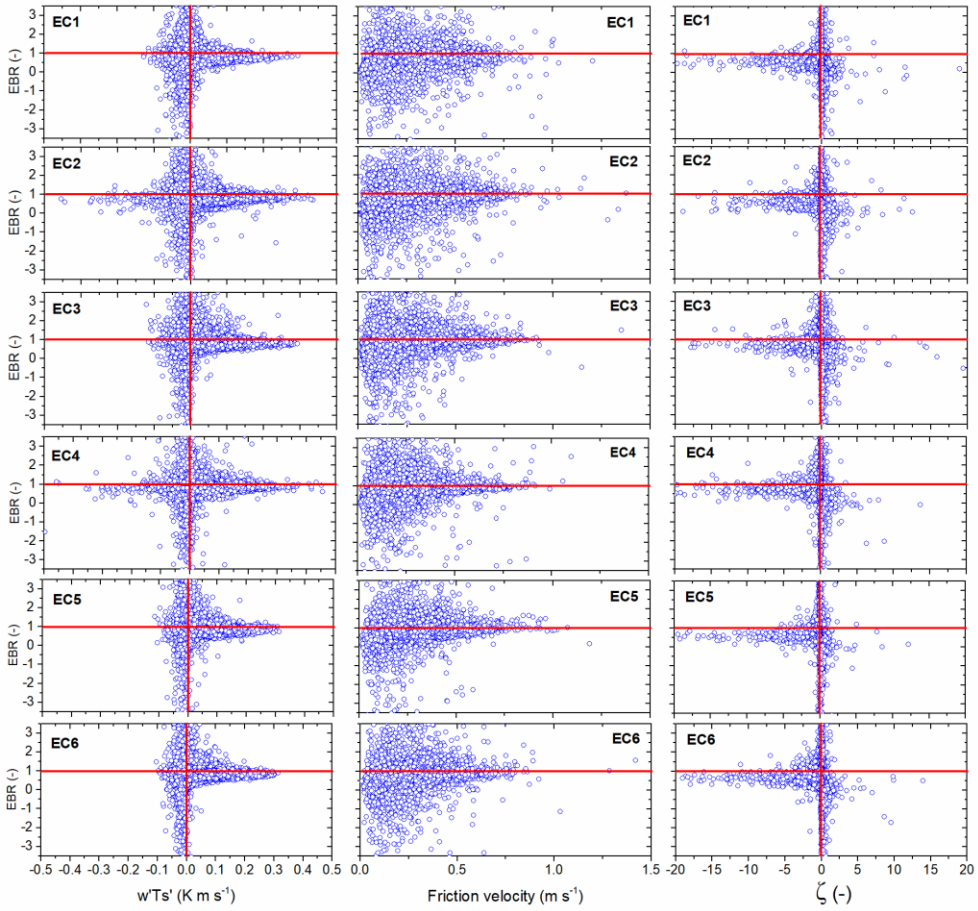

Fig. 3.10. The mean energy balance ratio (EBR) as a function of buoyancy flux ($w'T_s'$), friction velocity (u^*), and the stability parameter (ζ) during the 2010 to 2017 study period.

Plotting the EBR against friction velocity also reveals a large scatter, which narrows as friction velocity (shear) increases. The scatter, however, does not narrow as much as for increasing buoyancy. During neutral or stable atmospheric conditions, the EBR showed a large spread (Fig. 3.10). In contrast, this range distinctly declined when the stability parameter reached strongly negative values, indicative of

highly unstable conditions. An EBR above unity or below zero was rarely observed under these conditions.

Table 3.4. Energy balance closure (EBC) as indicated by the slope of linear regression of turbulent vs. available energy and energy balance ratio (EBR) under different atmospheric stability conditions. EBC and EBR are given as site-specific averages from 2010 to 2017. SD is standard deviation.

Region			Kraichgau			Swabian Jura		
			Sites			Sites		
Stability condition	Parameter	Unit	EC1	EC2	EC3	EC4	EC5	EC6
Unstable	Slope		0.69	0.74	0.70	0.79	0.68	0.74
	Intercept	W m^{-2}	-6.14	-9.12	9.58	0.21	1.18	-2.57
	R^2		0.87	0.85	0.83	0.87	0.84	0.8
	EBR		0.67	0.69	0.73	0.78	0.68	0.73
	SD (EBR)		0.32	0.34	0.37	0.28	0.32	0.27
	Residual	W m^{-2}	94.7	82.0	81.4	59.1	95.1	78.4
	SD (Residual)	W m^{-2}	62.3	61.5	67.3	54.4	68.2	58.3
	*N**		5478	4992	5926	7145	5755	8533
Neutral	Slope		0.73	0.79	0.75	0.82	0.75	0.77
	Intercept	W m^{-2}	-0.95	0.04	10.22	3.58	7.44	1.59
	R^2		0.90	0.88	0.87	0.89	0.85	0.89
	EBR		0.72	0.78	0.73	0.85	0.78	0.78
	SD (EBR)		0.63	0.67	0.64	0.83	0.70	0.65
	Residual	W m^{-2}	61.5	43.3	48.2	34.37	52.1	45.6
	SD (Residual)	W m^{-2}	59.1	60.0	62.2	50.6	64.4	52.8
	*N**		9957	10781	11180	11575	9563	12149
Stable	Slope		0.66	0.69	0.71	0.57	0.57	0.48
	Intercept	W m^{-2}	-3.25	-1.88	6.48	4.06	6.17	3.01
	R^2		0.86	0.82	0.86	0.61	0.68	0.52
	EBR		0.41	0.46	0.56	0.41	0.30	0.33
	SD (EBR)		1.34	0.67	1.56	1.48	1.44	1.51
	Residual	W m^{-2}	18.7	13.3	6.4	7.3	6.23	6.6
	SD (Residual)	W m^{-2}	31.5	29.0	34.5	29.2	36.2	28.9
	*N**		1292	1398	1642	1105	787	1075

* Number of data points

From the total dataset, only 7 % of daytime measurements were made under stable conditions, 34 % under unstable conditions, and 59 % under neutral conditions (Table 3.4). During unstable conditions, the EBC and EBR at all sites were slightly lower compared to neutral conditions. During neutral conditions, however, the standard deviation (SD) of EBR was about twice as high as under unstable conditions. During stable conditions, the EBC and EBR were systematically lower than at unstable and neutral conditions. At EC4, for example, the EBR was 0.78 and 0.85 under neutral and unstable conditions, respectively. Under stable conditions, the value declined to 0.41. Moreover, the huge spread in the EBR under stable conditions is underlined by its high SD, which is about 3 times the mean value.

3.3.4.4. Effect of footprint

Figure 11 shows exemplary footprints for sites EC3 and EC5 in 2015, illustrating the substantially different size of flux source areas determined for the different months. Both fields were cropped with maize. At EC3, EBC continuously increased from 68 % in June to 79 % in July and 90 % in August. In this period, as the maize plants got taller, the footprint area became continuously smaller. A similar relation between footprint area and EBC was observed at EC5: the larger the footprint, the lower the EBC. A linear regression between EBC and the 90 % footprint area of all data from 2015 confirmed this relation (not shown). Although R^2 was only 0.21, the slope of −1.25 % ha^{-1} (0.50 % ha^{-1}; standard error) per hectare was significantly different from zero. The intercept of the regression was 79 %.

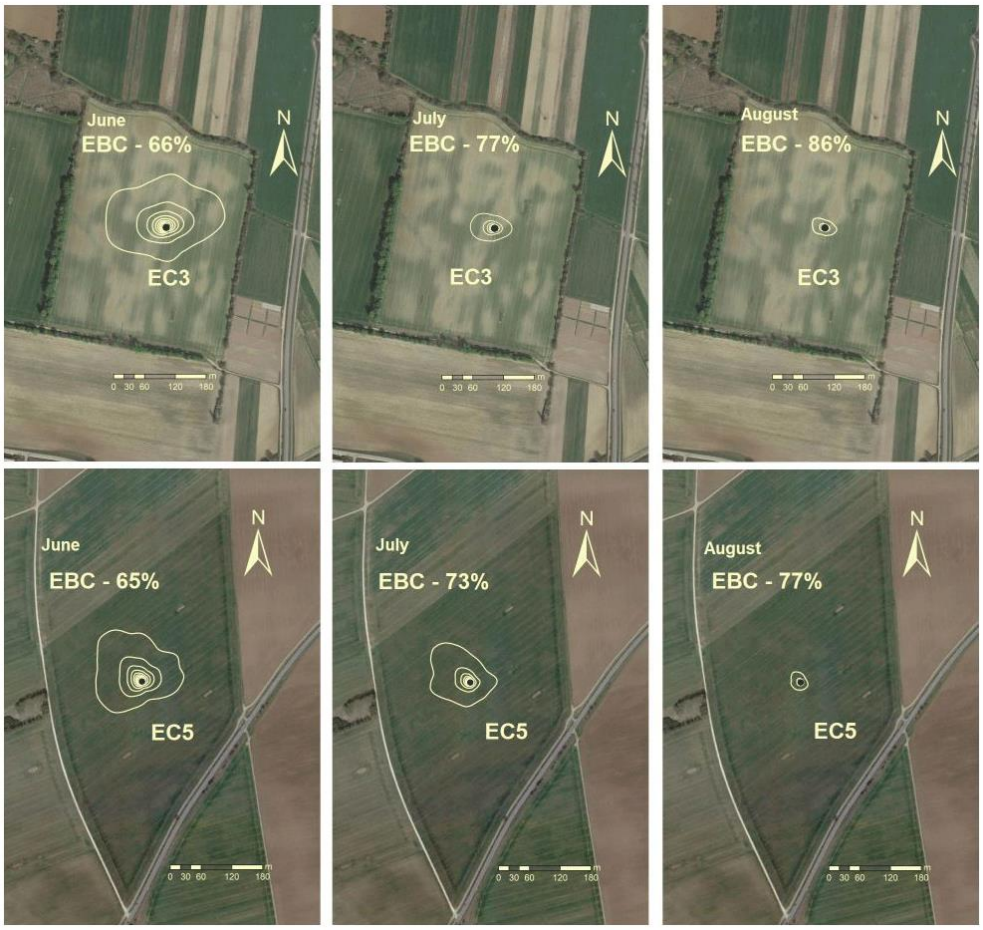

Fig. 3.11. Footprint area of EC3 and EC5 in selected months of 2015 and the corresponding energy balance closure (EBC). Black points represent positions of EC stations. Yellow lines indicate relative areal contributions to total flux in 10 % steps, where the outmost yellow line indicates the area from which 90 % of measured fluxes originated. The satellite image was taken from Google Earth (images from 31 March 2017 and 30 March 2014 for EC3 and EC5, respectively).

3.4. Discussion

3.4.1. EBC and energy balance components

From July to September, daily mean R_n varied between 125 and 176 W m^{-2}. Similar ranges of R_n were observed over maize in Livraga, Italy (Masseroni et al., 2014). The latent and sensible heat fluxes varied strongly over the observational period. In early-covering crops (winter rapeseed, winter wheat, winter barley), *LE* was about two to three times higher than *H* in the period AMJ (April-May-June), while in the period JAS (July-August-September) *LE* and *H* were in a similar range (Fig. 3.4, EC3-WW, EC4-SB). The period JAS is when ripening and harvest of cereals and winter rapeseed occurs, as well as post-harvest management such as tillage and seeding of cover crops or winter rapeseed. During AMJ, the patterns of *LE* and *H* at EC5 and EC6 differed, even though the maize was sown on similar days of the year (May 07 at EC5 and May 03 at EC6). This can be explained by the substantially higher leaf area index at EC6 (0.74±0.15) compared to EC5 (0.35 ±0.06), measured on June 22.

The mean EBR of the 48 site-years was 0.75 (Table 3.3). In comparison, Wilson et al. (2002) reported an EBR of 0.84, on average, for the 50 analyzed FLUXNET site-years, ranging from 0.34 to 1.69. In three agricultural and one industrial site in South Korea, the mean value varied between 0.46 and 0.83 (Kim et al., 2014). Majozi et al. (2017) found a mean EBR of 0.93 at a semi-arid savannah site in South Africa, over a period of 15 years.

The slopes of the OLR and EBR differed by a maximum of 5 %, which is consistent with previously published data. Such a small difference points at a high reliability of the presented EC measurements (Wilson et al., 2002). The highest annual EBC occurred at EC4 (87 % in 2010), the second highest at EC2 (83 % in 2016), the lowest at EC5 (62 % in 2016). The lowest EBC was observed mainly in the cold, non-growing season, which may be attributed to insufficient thermally and mechanically induced turbulence (Franssen et al., 2010) as well as to freezing (Varmaghani et al., 2016).

The incomplete EBC in our dataset has several potential explanations. One is related to the neglected minor storage terms (Eshonkulov et al., 2019; Masseroni et al., 2014; Meyers and Hollinger, 2004). Importantly, considering minor storage terms is not straightforward because they are not measured when conventional EC equipment is used. Only the energy fixed and released by photosynthesis and respiration can be directly derived from EC data because the net CO_2 flux is generally measured. Considering minor storage terms in calculating the EBC at a maize field improved the mean value from 87 to 91 % (Xu et al., 2017) and from 81 to 86 % (Masseroni et al., 2014). Eshonkulov et al. (2019) demonstrated that the

contribution of minor storage and flux terms over winter wheat in southwest Germany was largest during the main vegetation period in May. During this month the minor terms helped to close the energy balance by an additional 7−8 %.

3.4.2. The effect of meteorological conditions and surface-layer turbulent parameters

In both KR and SJ, the EBR was highest for winds blowing from the prevailing wind direction. These winds were associated with high wind speeds favoring well-developed turbulent conditions. This is consistent with other studies. Xin et al. (2018), for example, also found that winds with high speeds blowing from the prevailing direction yielded consistently higher EBC compared to other directions. Kim et al. (2014), for example, grouped EBR into two different categories, one with a lower EBR (<0.75) and one with a higher EBR (>0.75), and observed for their four research sites that the EBR was higher at high wind speed.

Figure 10 shows that the spread of the EBR distinctly narrowed at high friction velocities ($u* \geq 0.5$). Prior studies have noted the importance of u^* on the EBC. Anderson and Wang (2014) found that, under these conditions, EBC was closed on days with continuous turbulence. Results of the hourly daytime EBR and u^* showed a strong relationship at our sites (Fig. 3.10). This is consistent with other studies carried out in selected croplands such as irrigated sugarcane (Anderson and Wang, 2014), maize plantations (Masseroni et al., 2014), and rice fields (Kim et al., 2014). Sánchez et al. (2010) also reported that EBR was >0.90 when high friction velocities prevailed (>0.8 m s^{-1}) at a boreal forest site in Finland. Mauder et al. (2013) investigated EBC at the TERENO site in Lackenberg (Germany) and found that it was almost closed. They explain this result by the very good turbulent mixing and the high homogeneity at this site. This confirms that, at high u^*, the production of high-frequency fluxes is elevated (Fratini and Mauder, 2014).

At our study sites, neutral conditions dominated (~60 %), followed by unstable conditions (~34 %) and stable conditions (6 %; Table 3.4). Importantly, average EBR changed from 0.67 (±0.32) to 0.72 (±0.69) and 0.41 (±1.33) during unstable, neutral, and stable conditions, respectively (SD in brackets). Under stable conditions, the EBR was lowest and had the largest variation. Averaged over all EC stations, the slope of OLR under neutral conditions was slightly higher than under unstable conditions. This is also evident in the mean and variance of the calculated energy residuals. The average residuals under stable, neutral, and unstable conditions were 9.7 (±31.5), 47.5 (±58.2), and 81.5 (±62.0) W m^{-2}, respectively. The coefficient of variation was highest under stable conditions and decreased over neutral to unstable

conditions. This result differs from previous studies. Mauder et al. (2010) reported a residual energy close to zero for a cropland in Ontario, Canada, under stable conditions, peaking at 150 W m^{-2} under neutral conditions and decreasing to 100 W m^{-2} under unstable conditions.

The scatter of EBR versus buoyancy flux at EC2 and EC4, the two stations with the highest EBC, differed from those of the other stations (Fig. 3.10). At these two sites, strong negative buoyancy fluxes below −0.15 K m s^{-1} were recorded. This means that the atmosphere was not heated by the land surface but that the land surface was significantly heated by the atmosphere. Such a situation points to a stable boundary layer (SBL). Lan et al. (2018) report that they measured the highest buoyancy fluxes under a weak SBL with strong surface shear. They argue that the strong mechanical shear produced at the ground favors the development of turbulent eddies with larger scales that enhance vertical mixing of momentum and heat transporting the warm air aloft downward and the surface cold air upward. Moreover, the mechanical mixing weakens the magnitude of the mean temperature gradient and allows turbulent eddies with larger vertical scales to develop. Conversely, under a SBL, weak winds occur near the surface, and turbulent eddies are depressed and detached from the boundary leading to suppressed vertical mixing.

Several studies recommended considering secondary circulations to achieve a better EBC (Foken et al., 2010; Kidston et al., 2010; Mauder et al., 2010). Those studies postulate that heterogeneity-induced and buoyancy-driven quasi-stationary circulations are probably the dominant processes behind underestimated energy fluxes. The studies that suggested the use of an averaging period higher than 30 min usually refer to unstable conditions. These studies suggested that averaging periods of 2–4 h are often needed to statistically resolve the largest convective turbulent eddies or also non-stationary mesoscale motions that sometimes can modulate turbulent fluxes (Mahrt, 1998). Larger averaging improved short-term EBC during the diurnal hours in the Salentum peninsula of Apulia, Italy (Cava et al., 2008). In considering secondary circulations, different time averaging intervals can be used instead of the standard 30 min period. Although a 60 min interval might be suitable for capturing the major turbulent fluxes (Kilinc et al., 2012), in most cases the standard 30 min period is still sufficient (Kidston et al., 2010). The classical averaging period of 30 min can be a proper choice for unstable or neutral conditions. A shorter averaging period is suitable for capturing energy fluxes in very stable conditions (Sun et al., 2012; Vickers and Mahrt, 2006). Finding an optimum averaging period is a very complex and nearly impossible task. This is because atmospheric turbulence changes irregularly, and there is no clear-cut “switch” in time. Therefore, the averaging time could be modified during raw data processing. In practice, however, this is unlikely, because it drastically increases the complexity of data processing

(Lenschow et al., 1994). Moreover, the sources of secondary circulations are unclear, and they are most probably not well linked with the locally measured available energy. Accordingly, excluding secondary circulations in EC measurements can be locally meaningful. Recently, a new method, known as ogive optimization, was proposed by Sievers et al. (2015). The method enables the separation of low-frequency influences from vertical turbulent fluxes for isolating the local exchange processes of interest.

Although EC measurements contain uncaptured energy components, the flux data are used, among others, to evaluate models and interpret simulation results. In such studies, EC flux data are usually post-closed, i.e., the measured turbulent fluxes are adjusted so as to close the energy balance (Ingwersen et al., 2015). The standard approach is the Bowen-ratio post-closure method (Twine et al., 2000). It assumes that the missing energy has the same Bowen ratio as the measured turbulent fluxes. This approach, however, may introduce a systematic bias to simulated surface energy fluxes (Chen and Li, 2012). Analyses of the energy imbalance by Ingwersen et al. (2011) showed that soil water contents simulated by a land surface model agreed better with measurements when the residual was fully assigned to *H*. As discussed by Charuchittipan et al. (2014), secondary near-surface circulations attributed to low frequencies mainly transport sensible heat. Therefore, they proposed a new alternative energy balance correction method they termed the Buoyancy flux ratio. At very large Bowen ratios (>10), the Bowen-ratio post-closure and buoyancy flux correction methods yield similar results. At Bowen ratios ranging from 0.1 to 0.2, which are typical for croplands during the main growing period, the Buoyancy flux ratio method assigns most of the energy residual (>50 %) to the sensible heat flux. The Bowen-ratio method, in contrast, distributes most of it (>90 %) to latent heat. As long as the composition of the residual remains unknown, it is important to communicate the possible error in EC flux data, for example with the post-closure method uncertainty band (PUB; Ingwersen et al., 2015). Working with only one post-closure method may result in serious misinterpretations in model–data comparisons (Ingwersen et al., 2018).

3.4.3. The effect of the instrumental setup

At the SJ sites, we found a particularly low EBR in the wind sector 0–90°. The CSAT3 sensor was oriented mostly to 225° so that the sector 30–90° was located behind the anemometer head. To substantiate the idea that the anemometer negatively influences EC measurement quality, and taking the data from EC4 as an example, we recalculated EBR across all years, excluding the wind directions of the sector 0–90°. This increased the mean EBC in 2010–2017 by 4 percentage points, from 80 % to 84 %

(data not shown). Friebel et al. (2009) used a wind tunnel experiment to show that there is a 40° shadow zone behind the sonic anemometer where the measured wind speeds were reduced by up to 16 %. Within a shadow zone of about 20° behind the anemometer, the turbulent spectra were corrupted. Our findings indicate that under field conditions the shadow zone was even somewhat wider (about 60°). A practical solution for measuring reliable fluxes when winds blow from the back of the anemometer could be to operate an anemometer tandem: a first anemometer orientated in the prevailing wind direction and a second one in the opposite direction. Whether this setup could solve the problem requires further investigation.

3.4.4. Relationships between EBC and footprint

Accurate measurements of energy balance components are important to achieve a good EBC. In this context, one key requirement is that the EC station be located in a place that represents the fluxes from the area of interest (Burba and Anderson, 2010). According to those authors, the terrain must be horizontal and uniform. Three parameters are needed in footprint analysis: measurement height, surface roughness, and atmospheric stability. When turbulent fluxes originate from a horizontal and homogeneous surface, the footprint depends solely on the distance between the location of the measurement point and the emission element. We found a distinct tendency that the smaller the footprint, the higher the EBC. We give two explanations. First, the smaller the footprint, the higher the chance that the assumption of a homogeneous source area is fulfilled. Second, the smaller the footprint, the better the scale match between the measurement of available energy and turbulent fluxes. Alfieri and Blanken (2012) found that variations of surface energy fluxes over tens of meters ranged from 30 to 40 W m^{-2} using single-point (immobile) and mobile EC towers at a uniform site (Colorado, USA). They concluded that a single-point EC tower cannot capture all the relevant energy fluxes, because they vary spatially. Our results confirm that if the footprint is small, the EBC from EC measurements is better, which can be interpreted as a reduction in the variation of surface energy fluxes.

Many studies claimed that surface heterogeneity is a potential reason for the energy imbalance (Stoy et al., 2013; Xu et al., 2017). The latter authors reported that EBC decreased with increasing surface heterogeneity. The degree of heterogeneity was derived from high-resolution remote sensing images and land surface temperatures. To handle this effect, some authors recommend using direction-specific coefficients that indicate the degree of heterogeneity. For example, Panin et al. (1998) introduced a heterogeneity factor that comprises surface parameters such as roughness, radiation, and the thermal

humidity of the internal boundary layer. That factor can be used for data interpretation. Nonetheless, deploying heterogeneity factors still does not explain how the residual energy is composed. The lack of EBC at the KR sites might partly reflect katabatic advection (Heinesch et al., 2008; Kutsch et al., 2008), which results from stable atmospheric conditions and occurs especially in hillslope areas (Loescher et al., 2006; Mauder et al., 2010). Moreover, complex topography can induce advective fluxes (Feigenwinter et al., 2008; Rebmann et al., 2010). The former landfill site located about 500 m south of the fields in KR (Fig. 3.1) might have been responsible for advective fluxes, since its elevation is approximately 41 m higher than the study sites. Moreover, the topography could also affect EBC. The elevation transects show that the immediate terrain surrounding the stations EC3, EC5, and EC6 is not totally flat (Fig. 3.4). This is a well-known problem for micrometeorological field measurements (Wilczak et al., 2001). At EC1, EC2, and EC4, however, the terrain can be considered flat.

3.5. Conclusions

We evaluated the EBC of long-term EC measurements at six different cropland sites in two contrasting environmental regions in southwestern Germany. EBC depended on how well thermally and mechanically induced turbulence was developed. On average, 25 % of the available energy was not detected by our EC stations, with the lowest annual imbalances (energy residual) of 17 % in KR and 13 % in SJ. This range of EBC is common in cropland, and such recovery rates must be accepted in heterogeneous landscapes. We interpret the range of the highest mean annual EBC (83 % at KR, 87 % at SJ) as the upper detection limit of the EC method at our sites and settings. During winter months and under stable atmospheric conditions, EBC was problematic. EBC was negatively affected by (i) stable atmospheric conditions, (ii) non-horizontal or heterogeneous source area, (iii) larger obstacles in the landscape, i.e., the former landfill site that may have induced adjective flux components, and (iv) flow distortions of winds that first traveled past the back head of the anemometer, which reduces wind speed and corrupts the spectral characteristics of turbulence at specific wind directions. EBC was positively affected as the footprint area decreased, probably because this tends to decrease the heterogeneity of the source area and improves the match of available energy measured locally with the mean available energy in the footprint.

Acknowledgements.

This study was financially supported by the German Research Foundation (DFG) in the frame of the Research Unit (RU) 1695 “Structure and function of agricultural landscapes under global climate change – Processes and projections on a regional scale”. Part of the work was sponsored by an Erasmus Mundus grant “TIMUR – Training of Individuals through Mobility from Uzbek Republic to EU (referenced as GA NO 213-2723/001-001-EM Action 2)”. Additionally, this work received support from the funding by the Collaborative Research Centre 1253 CAMPOS (Project 7: Stochastic Modelling Framework), funded by the German Research Foundation (DFG, Grant Agreement SFB 1253/1 2017).
We thank Paul Stoy for handling the paper and one anonymous reviewer and Marcelo Zeri for helpful and constructive comments.

We would like to thank the following farmers: Hans Bosch Sr., Günter Bosch Jr., in KR (EC1, EC2, and EC3), and Hans-Gerhard Fink (EC4), Gerhard and Markus Hermann (EC5), and Reichart GbR (EC6) in SJ for the permission to conduct measurements in their fields. The authors would also like to thank the technical staff Benedikt Prechter, Felix Baur, Christian Schade, and Thomas Schreiber.

References

Alfieri, J. G. and Blanken, P. D.: How representative is a point? The spatial variability of surface energy fluxes across short distances in a sand-sagebrush ecosystem, J. Arid. Environ., 87, 42–49, https://doi.org/10.1016/j.jaridenv.2012.04.010, 2012.

Anderson, R. G. and Wang, D.: Energy budget closure observed in paired eddy covariance towers with increased and continuous daily turbulence, Agr. Forest Meteorol., 184, 204–209, https://doi.org/10.1016/j.agrformet.2013.09.012, 2014.

Baldocchi, D. D., Falge, E., Gu, L., Olson, R., Hollinger, D., Running, S., Anthoni, P., Bernhofer, C., Davis, K., Evans, R., Fuentes, J., Goldstein, A., Katul, G., Law, B., Lee, X., Malhi, Y., Meyers, T., Munger, W., Oechel, W., Paw, K. T. U., Pilegaard, K., Schmid, H. P., Valentini, R., Verma, S., Vesala, T., Wilson, K., and Wofsy, S.: FLUXNET: A new tool to study the temporal and spatial variability of ecosystem-scale carbon dioxide, water vapor, and energy flux densities, B. Am. Meteorol. Soc., 82, 2415–2434, https://doi.org/10.1175/1520-0477(2001)082<2415:FANTTS>2.3.CO;2, 2001.

Bretz, F., Hothorn, T., and Westfall, P.: Multiple Comparisons Using R, Chapman and Hall, CRC Press, London, 2011.

Burba, G.: Eddy covariance method for scientific, industrial, agricultural and regulatory applications, LI-COR Biosciences, 2013.

Burba, G. and Anderson, D.: A brief practical guide to eddy covariance flux measurements: Principles

and workflow examples for scientific and industrial applications, LI-COR Biosciences, Lincoln, Nebraska, USA, available at: http://www.ncbi.nlm.nih.gov/pubmed/18767616 (last access: 17 July 2018), 2010.

Cava, D., Contini, D., Donateo, A., and Martano, P.: Analysis of short-term closure of the surface energy balance above short vegetation, Agr. Forest Meteorol., 148, 82–93, https://doi.org/10.1016/j.agrformet.2007.09.003, 2008.

Charuchittipan, D., Babel, W., Mauder, M., Leps, J. P., and Foken, T.: Extension of the averaging time in eddy-covariance measurements and its effect on the energy balance closure, Bound.-Lay. Meteorol., 152, 303–327, https://doi.org/10.1007/s10546-014-9922-6, 2014.

Chen, Y.-Y. and Li, M.-H.: Determining adequate averaging periods and reference coordinates for eddy covariance measurements of surface heat and water vapor fluxes over mountainous terrain, Terr. Atmos. Ocean. Sci., 23, 685, https://doi.org/10.3319/TAO.2012.05.02.01(Hy), 2012.

Demyan, M. S., Ingwersen, J., Funkuin, Y. N., Ali, R. S., Mirzaeitalarposhti, R., Rasche, F., Poll, C., Müller, T., Streck, T., Kandeler, E., and Cadisch, G.: Partitioning of ecosystem respiration in winter wheat and silage maize-modeling seasonal temperature effects, Agr. Ecosyst. Environ., 224, 131–144, https://doi.org/10.1016/j.agee.2016.03.039, 2016.

Du, Q., Liu, H. Z., Feng, J. W., and Wang, L.: Effects of different gap filling methods and land surface energy balance closure on annual net ecosystem exchange in a semiarid area of China, Sci. China Earth Sci., 57, 1340–1351, https://doi.org/10.1007/s11430-013-4756-5, 2014.

Eshonkulov, R., Poyda, A., Ingwersen, J., Pulatov, A., and Streck, T.: Improving the energy balance closure over a winter wheat field by accounting for minor storage terms, Agr. Forest Meteorol., 264, 283–296, https://doi.org/10.1016/J.AGRFORMET.2018.10.012, 2019.

Eugster, W. and Merbold, L.: Eddy covariance for quantifying trace gas fluxes from soils, SOIL, 1, 187–205, https://doi.org/10.5194/soil-1-187-2015, 2015.

Faraway, J. J.: Linear models with R, CHAPMAN and HALL/CRC, Boca Raton London NewYork Washington, DC, 2014.

Feigenwinter, C., Bernhofer, C., Eichelmann, U., Heinesch, B., Hertel, M., Janous, D., Kolle, O., Lagergren, F., Lindroth, A., Minerbi, S., Moderow, U., Montagnani, L., Queck, R., Rebmann, C., Vestin, P., Yernaux, M., Zeri, M., Ziegler, W., and Aubinet, M.: Comparison of horizontal and vertical advective CO_2 fluxes at three forest sites, Agr. Forest Meteorol., 148, 12–24, https://doi.org/10.1016/j.agrformet.2007.08.013, 2008.

Foken, T.: Micrometeorology, 1st ed., Springer-Verlag Berlin Heidelberg, 2008.

Foken, T.: The energy balance closure problem: an overview, Ecol. Appl., 18, 1351–1367, https://doi.org/10.1890/06-0922.1, 2008b.

Foken, T., Göockede, M., Mauder, M., Mahrt, L., Amiro, B., and Munger, W.: Post-Field Data Quality Control, in Handbook of Micrometeorology, 181–208, Kluwer Academic Publishers, Dordrecht, 2004.

Foken, T., Mauder, M., Liebethal, C., Wimmer, F., Beyrich, F., Leps, J. P., Raasch, S., DeBruin, H. A. R., Meijninger, W. M. L., and Bange, J.: Energy balance closure for the LITFASS-2003 experiment, Theor. Appl. Climatol., 101, 149–160, https://doi.org/10.1007/s00704-009-0216-8, 2010.

Franssen, H. J. H., Stöckli, R., Lehner, I., Rotenberg, E., and Seneviratne, S. I.: Energy balance closure of eddy-covariance data: A multisite analysis for European FLUXNET stations, Agr. Forest

Meteorol., 150, 1553–1567, https://doi.org/10.1016/j.agrformet.2010.08.005, 2010.

Fratini, G. and Mauder, M.: Towards a consistent eddy-covariance processing: an intercomparison of EddyPro and TK3, Atmos. Meas. Tech., 7, 2273–2281, https://doi.org/10.5194/amt-7-2273-2014, 2014.

Friebel, H. C., Herrington, T. O., and Benilov, A. Y.: Evaluation of the flow distortion around the Campbell Scientific CSAT3 sonic anemometer relative to incident wind direction, J. Atmos. Ocean. Tech., 26, 582–592, https://doi.org/10.1175/2008JTECHO550.1, 2009.

Göckede, M., Markkanen, T., Hasager, C. B., and Foken, T.: Update of a footprint-based approach for the characterisation of complex measurement sites, Bound.-Lay. Meteorol., 118, 635–655, https://doi.org/10.1007/s10546-005-6435-3, 2006.

Gregory, R. W., Ben, B., Lodewijk, B., Robert, G., Wolfgang, H., Andy, L., Thomas, L., Martin, M., Arni, M., Steffen, M., Marc, S., and Bill, V.: gplots: Various R programming tools for plotting data, available at: https://cran.r-project.org/web/packages/gplots/index.html (last access: 17 July 2018), 2009.

Gregory, R. W., Bolker, B., Gorjanc, G., Grothendieck, G., Korosec, A., Lumley, T., MacQueen, D., Magnusson, A., and Rogers, J.: Package "gdata". Various R programming tools for data manipulation, available at: https://cran.r-project.org/web/packages/gdata/index.html (last access: 17 July 2018), 2017.

Heinesch, B., Yernaux, Y., and Aubinet, M.: Dependence of CO_2 advection patterns on wind direction on a gentle forested slope, Biogeosciences, 5, 657–668, https://doi.org/10.5194/bg-5-657-2008, 2008.

Hothorn, T., Bretz, F., and Westfall, P.: Simultaneous Inference in General Parametric Models, Biometrical J., 50, 346–363, 2017.

Imukova, K., Ingwersen, J., Hevart, M., and Streck, T.: Energy balance closure on a winter wheat stand: comparing the eddy covariance technique with the soil water balance method, Biogeosciences, 13, 63–75, https://doi.org/10.5194/bg-13-63-2016, 2016.

Ingwersen, J., Steffens, K., Högy, P., Warrach-Sagi, K., Zhunusbayeva, D., Poltoradnev, M., Gäbler, R., Wizemann, H. D., Fangmeier, A., Wulfmeyer, V., and Streck, T.: Comparison of Noah simulations with eddy covariance and soil water measurements at a winter wheat stand, Agr. Forest Meteorol., 151, 345–355, https://doi.org/10.1016/j.agrformet.2010.11.010, 2011.

Ingwersen, J., Imukova, K., Högy, P., and Streck, T.: On the use of the post-closure methods uncertainty band to evaluate the performance of land surface models against eddy covariance flux data, Biogeosciences, 12, 2311–2326, https://doi.org/10.5194/bg-12-2311-2015, 2015.

Ingwersen, J., Högy, P., Wizemann, H. D., Warrach-Sagi, K., and Streck, T.: Coupling the land surface model Noah-MP with the generic crop growth model Gecros: Model description, calibration and validation, Agr. Forest Meteorol., 262, 322–339, https://doi.org/10.1016/J.AGRFORMET.2018.06.023, 2018.

IUSS Working Group WRB: World reference base for soil resources 2014, International soil classification system for naming soils and creating legends for soil maps, FAO, Rome, Italy, 2014.

Jacobs, A. F. G., Heusinkveld, B. G., and Holtslag, A. A. M.: Towards closing the surface energy budget of a mid-latitude grassland, Bound.-Lay. Meteorol., 126, 125–136, https://doi.org/10.1007/s10546-007-9209-2, 2008.

Kaimal, J. C. and Gaynor, J. E.: Another look at sonic thermometry, Bound.-Lay. Meteorol., 56, 401–410, 1991.

Kidston, J., Brümmer, C., Black, T. A., Morgenstern, K., Nesic, Z., McCaughey, J. H., and Barr, A. G.: Energy balance closure using eddy covariance above two different land surfaces and Implications for CO_2 flux measurements, Bound.-Lay. Meteorol., 136, 193–218, https://doi.org/10.1007/s10546-010-9507-y, 2010.

Kilinc, M., Beringer, J., Hutley, L. B., Haverd, V., and Tapper, N.: An analysis of the surface energy budget above the world's tallest angiosperm forest, Agr. Forest Meteorol., 166–167, 23–31, https://doi.org/10.1016/J.AGRFORMET.2012.05.014, 2012.

Kim, S., Lee, Y.-H., Kim, K. R., and Park, Y.-S.: Analysis of surface energy balance closure over heterogeneous surfaces, Asia-Pacific, J. Atmos. Sci., 50, 1–13, https://doi.org/10.1007/s13143-014-0045-2, 2014.

Kljun, N., Rotach, M. W., and Schmid, H. P.: A three-dimensional backward lagrangian footprint, Bound.-Lay. Meteorol., 103, 205–226, 2002.

Kljun, N., Calanca, P., Rotach, M. W., and Schmid, H. P.: A simple parameterisation for flux footprint predictions, Bound.-Lay. Meteorol., 112, 503–523, https://doi.org/10.1023/B:BOUN.0000030653.71031.96, 2004.

Kljun, N., Calanca, P., Rotach, M. W., and Schmid, H. P.: A simple two-dimensional parameterisation for Flux Footprint Prediction (FFP), Geosci. Model Dev., 8, 3695–3713, https://doi.org/10.5194/gmd-8-3695-2015, 2015.

Kohsiek, W., Liebethal, C., Foken, T., Vogt, R., Oncley, S. P., Bernhofer, C., and Debruin, H. A. R.: The Energy Balance Experiment EBEX-2000. Part III: Behaviour and quality of the radiation measurements, Bound.-Lay. Meteorol., 123, 55–75, https://doi.org/10.1007/s10546-006-9135-8, 2007.

Kutsch, W. L., Kolle, O., Rebmann, C., Knohl, A., Ziegler, W., and Schulze, E. D.: Advection and resulting CO_2 exchange uncertainty in a tall forest in central Germany, Ecol. Appl., 18, 1391–1405, https://doi.org/10.1890/06-1301.1, 2008.

Lan, C., Liu, H., Li, D., Katul, G. G., and Finn, D.: Distinct turbulence structures in stably stratified boundary layers with weak and strong surface shear, J. Geophys. Res.-Atmos., 123, 7839–7854, https://doi.org/10.1029/2018JD028628, 2018.

Lenschow, D. H., Mann, J., Kristensen, L., Lenschow, D. H., Mann, J., and Kristensen, L.: How long is long enough when measuring fluxes and other turbulence statistics?, J. Atmos. Ocean. Tech., 11, 661–673, https://doi.org/10.1175/1520-0426(1994)011<0661:HLILEW>2.0.CO;2, 1994.

LI-COR Inc.: EddyPro Software. Instruction manual, LI-COR Biosciences, 2012.

Loescher, H. W., Law, B. E., Mahrt, L., Hollinger, D. Y., Campbell, J., and Wofsy, S. C.: Uncertainties in, and interpretation of, carbon flux estimates using the eddy covariance technique, J. Geophys. Res, 111, 21–90, https://doi.org/10.1029/2005JD006932, 2006.

Mahrt, L.: Flux sampling errors for aircraft and towers, J. Atmos. Ocean. Tech., 15, 416–429, https://doi.org/10.1175/1520-0426(1998)015<0416:FSEFAA>2.0.CO;2, 1998.

Majozi, N. P., Mannaerts, C. M., Ramoelo, A., Mathieu, R., Nickless, A., and Verhoef, W.: Analysing surface energy balance closure and partitioning over a semi-arid savanna FLUXNET site in Skukuza, Kruger National Park, South Africa, Hydrol. Earth Syst. Sci., 21, 3401–3415,

https://doi.org/10.5194/hess-21-3401-2017, 2017.

Masseroni, D., Corbari, C., and Mancini, M.: Limitations and improvements of the energy balance closure with reference to experimental data measured over a maize field, Atmosfera, 27, 335–352, https://doi.org/10.1016/S0187-6236(14)70033-5, 2014.

Mauder, M. and Foken, T.: Documentation and instruction manual of the eddy-covariance software package TK3, Arbeitsergebnisse, Nr. 46, Universität Bayreuth, Abt. Mikrometeorologie, Bayreuth, 2011.

Mauder, M., Desjardins, R. L., Pattey, E., and Worth, D.: An attempt to close the daytime surface energy balance using spatially-averaged flux measurements, Bound.-Lay. Meteorol., 136, 175–191, https://doi.org/10.1007/s10546-010-9497-9, 2010.

Mauder, M., Cuntz, M., Drüe, C., Graf, A., Rebmann, C., Schmid, H. P., Schmidt, M., and Steinbrecher, R.: A strategy for quality and uncertainty assessment of long-term eddy-covariance measurements, Agr. Forest Meteorol., 169, 122–135, https://doi.org/10.1016/j.agrformet.2012.09.006, 2013.

Meyers, T. P. and Hollinger, S. E.: An assessment of storage terms in the surface energy balance of maize and soybean, Agr. Forest Meteorol., 125, 105–115, https://doi.org/10.1016/j.agrformet.2004.03.001, 2004.

Moore, C. J.: Frequency response corrections for eddy correlation systems, Bound.-Lay. Meteorol., 37, 17–35, https://doi.org/10.1007/BF00122754, 1986.

Oncley, S. P., Foken, T., Vogt, R., Kohsiek, W., DeBruin, H. A. R., Bernhofer, C., Christen, A., van Gorsel, E., Grantz, D., Feigenwinter, C., Lehner, I., Liebethal, C., Liu, H., Mauder, M., Pitacco, A., Ribeiro, L., and Weidinger, T.: The energy balance experiment EBEX-2000. Part I: overview and energy balance, Bound.-Lay. Meteorol., 123, 1–28, https://doi.org/10.1007/s10546-007-9161-1, 2007.

Panin, G. N., Tetzlaff, G., and Raabe, A.: Inhomogeneity of the land surface and problems in the parameterization of surface fluxes in natural conditions, Theor. Appl. Climatol., 60, 163–178, https://doi.org/10.1007/s007040050041, 1998.

Peng, D., Zhang, X., Wu, C., Huang, W., Gonsamo, A., Huete, A. R., Didan, K., Tan, B., Liu, X., and Zhang, B.: Intercomparison and evaluation of spring phenology products using National Phenology Network and AmeriFlux observations in the contiguous United States, Agr. Forest Meteorol., 242, 33–46, https://doi.org/10.1016/J.AGRFORMET.2017.04.009, 2017.

Piepho, H. P., Buchse, A., and Richter, C.: A mixed modelling approach for randomized experiments with repeated measures, J. Agron. Crop Sci., 190, 230–247, https://doi.org/10.1111/j.1439-037X.2004.00097.x, 2004.

Ping, Y., Qiang, Z., Shengjie, N., Hua, C., and Xiyu, W.: Effects of the soil heat flux estimates on surface energy balance closure over a semi-arid grassland, Acta Meteorol. Sin., 25, 774–782, https://doi.org/10.1007/s13351-011-0608-4, 2011.

Pinheiro, J., Bates, D., DebRoy, S., Sarkar, D., and Team, R. C.: nlme: Linear and nonlinear mixed effects models, R package version 3.1-125, 2016.

Pirk, N., Sievers, J., Mertes, J., Parmentier, F.-J. W., Mastepanov, M., and Christensen, T. R.: Spatial variability of CO_2 uptake in polygonal tundra: assessing low-frequency disturbances in eddy covariance flux estimates, Biogeosciences, 14, 3157–3169, https://doi.org/10.5194/bg-14-3157-2017, 2017.

R Core Team: A language and environment for statistical computing. R foundation for statistical computing, Vienna, Austria, 2014.

Rebmann, C., Zeri, M., Lasslop, G., Mund, M., Kolle, O., Schulze, E., and Feigenwinter, C.: Treatment and assessment of the CO_2 exchange at a complex forest site in Thuringia, Germany, Agr. Forest Meteorol., 150, 684–691, https://doi.org/10.1016/j.agrformet.2009.11.001, 2010.

Sánchez, J. M., Caselles, V., and Rubio, E. M.: Analysis of the energy balance closure over a FLUXNET boreal forest in Finland, Hydrol. Earth Syst. Sci., 14, 1487–1497, https://doi.org/10.5194/hess-14-1487-2010, 2010.

Schmid, H. P.: Footprint modeling for vegetation atmosphere exchange studies: A review and perspective, Agr. Forest Meteorol., 113, 159–183, https://doi.org/10.1016/S0168-1923(02)00107-7, 2002.

Schotanus, P., Nieuwstadt, F. T. M., and De Bruin, H. A. R.: Temperature measurement with a sonic anemometer and its application to heat and moisture fluxes, Bound.-Lay. Meteorol., 26, 81–93, https://doi.org/10.1007/BF00164332, 1983.

Sievers, J., Papakyriakou, T., Larsen, S. E., Jammet, M. M., Rysgaard, S., Sejr, M. K., and Sørensen, L. L.: Estimating surface fluxes using eddy covariance and numerical ogive optimization, Atmos. Chem. Phys., 15, 2081–2103, https://doi.org/10.5194/acp-15-2081-2015, 2015.

Stoy, P. C., Mauder, M., Foken, T., Marcolla, B., Boegh, E., Ibrom, A., Arain, M. A., Arneth, A., Aurela, M., Bernhofer, C., Cescatti, A., Dellwik, E., Duce, P., Gianelle, D., van Gorsel, E., Kiely, G., Knohl, A., Margolis, H., Mccaughey, H., Merbold, L., Montagnani, L., Papale, D., Reichstein, M., Saunders, M., Serrano-Ortiz, P., Sottocornola, M., Spano, D., Vaccari, F., and Varlagin, A.: A data-driven analysis of energy balance closure across FLUXNET research sites: The role of landscape scale heterogeneity, Agr. Forest Meteorol., 171–172, 137–152, https://doi.org/10.1016/j.agrformet.2012.11.004, 2013.

Stull, B. R.: An introduction to boundary layer meteorology, Kluwer Acd.Publ., Dordrecht, Boston, London, 1988.

Sun, J., Mahrt, L., Banta, R. M., Pichugina, Y. L., Sun, J., Mahrt, L., Banta, R. M., and Pichugina, Y. L.: Turbulence regimes and turbulence intermittency in the stable boundary layer during CASES-99, J. Atmos. Sci., 69, 338–351, https://doi.org/10.1175/JAS-D-11-082.1, 2012.

Sun, X. M., Zhu, Z. L., Wen, X. F., Yuan, G. F., and Yu, G. R.: The impact of averaging period on eddy fluxes observed at ChinaFLUX sites, Agr. Forest Meteorol., 137, 188–193, https://doi.org/10.1016/j.agrformet.2006.02.012, 2006.

Twine, T. E., Kustas, W. P., Norman, J. M., Cook, D. R., Houser, P. R., Meyers, T. P., Prueger, J. H., Starks, P. J., and Wesel, M. L.: Correcting eddy-covariance flux understimates over a grassland, Agr. Forest Meteorol., 103, 229–317, 2000.

Varmaghani, A., Eichinger, W. E., and Prueger, J. H.: A diagnostic approach towards the causes of energy balance closure problem, Open J. Mod. Hydrol., 6, 101–114, 2016.

Vickers, D. and Mahrt, L.: Quality control and flux sampling problems for tower and aircraft data, J. Atmos. Ocean. Tech., 14, 512–526, https://doi.org/10.1175/1520-0426(1997)014<0512:QCAFSP>2.0.CO;2, 1997.

Vickers, D. and Mahrt, L.: A solution for flux contamination by mesoscale motions with very weak turbulence, Bound.-Lay. Meteorol., 118, 431–447, https://doi.org/10.1007/s10546-005-9003-y,

2006.

Webb, E. K., Pearman, G. I., and Leuning, R.: Correction of flux measurements for density effects due to heat and water vapour transfer, Q. J. Roy. Meteorol. Soc., 106, 85–100, https://doi.org/10.1002/qj.49710644707, 1980.

Wilczak, J. M., Oncley, S. P., and Stage, S. A.: Sonic anemometer tilt correction algorithms, Bound.-Lay. Meteorol., 99, 127–150, https://doi.org/10.1023/A:1018966204465, 2001.

Wilson, K., Goldstein, A., Falge, E., Aubinet, M., Baldocchi, D., Berbigier, P., Bernhofer, C., Ceulemans, R., Dolman, H., Field, C., Grelle, A., Ibrom, A., Law, B., Kowalski, A., Meyers, T., Moncrieff, J., Monson, R., Oechel, W., Tenhunen, J., Valentini, R., and Verma, S.: Energy balance closure at FLUXNET sites, Agr. Forest Meteorol., 113, 223–243, https://doi.org/10.1016/S0168-1923(02)00109-0, 2002.

Wizemann, H. D., Ingwersen, J., Högy, P., Warrach-Sagi, K., Streck, T., and Wulfmeyer, V.: Three year observations of water vapor and energy fluxes over agricultural crops in two regional climates of Southwest Germany, Meteorol. Z., 24, 39–59, https://doi.org/10.1127/metz/2014/0618, 2014.

Xin, Y.-F., Chen, F., Zhao, P., Barlage, M., Blanken, P., Chen, Y.-L., Chen, B., and Wang, Y.-J.: Surface energy balance closure at ten sites over the Tibetan plateau, Agr. Forest Meteorol., 259, 317–328, https://doi.org/10.1016/j.agrformet.2018.05.007, 2018.

Xu, Z., Liu, S., Shi, W., and Wang, J.: Assessment of the energy balance closure under advective conditions and Its impact using remote sensing data, Am. Meteorol. Soc., 56, 127–140, https://doi.org/10.1175/JAMC-D-16-0096.1, 2017.

Zeri, M. and Sá, L. D. A.: The impact of data gaps and quality control filtering on the balances of energy and carbon for a Southwest Amazon forest, Agr. Forest Meteorol., 150, 1543–1552, https://doi.org/10.1016/j.agrformet.2010.08.004, 2010.

Chapter 4

Paper C

4. Carbon fluxes and budgets of intensive crop rotations in two regional climates of southwest Germany[3]

Arne Poyda[a,1,*], Hans-Dieter Wizemann[b], Joachim Ingwersen[a], Ravshan Eshonkulov[a], Petra Högy[c], Michael S. Demyan[d,e,2], Pascal Kremer[a], Volker Wulfmeyer[b], Thilo Streck[a]

[a]Institute of Soil Science and Land Evaluation, Biogeophysics, Hohenheim University, Emil-Wolff-Str. 27, 70599 Stuttgart, Germany
[b]Institute of Physics and Meteorology, Hohenheim University, Garbenstr. 30, 70599 Stuttgart, Germany
[c]Institute of Landscape and Plant Ecology, Plant Ecology and Ecotoxicology, Hohenheim University, August-v.Hartmann-Str. 3, 70599 Stuttgart, Germany
[d]Institute of Agricultural Sciences in the Tropics, Plant Production in the Tropics and Subtropics (Hans-Ruthenberg-Institute), University of Hohenheim, Garbenstr. 13,70599 Stuttgart, Germany
[e]Institute of Crop Science, Fertilization and Soil Matter Dynamics, University of Hohenheim, Fruwirthstr. 20, 70599 Stuttgart, Germany

[1]Current affiliation: Institute of Crop Science and Plant Breeding, Grass and Forage Science/Organic Agriculture, Kiel University, Hermann-Rodewald-Str. 9, 24118 Kiel, Germany.

[2]Current affiliation: School of Environment and Natural Resources, The Ohio State University, 2021 Coffey Rd., Columbus, Ohio, U.S.A.

Keywords: eddy covariance, crop rotation, soil organic carbon, carbon removal

Abstract

The carbon (C) sequestration potential of croplands has recently become a subject of debate because it may contribute significantly to global climate change mitigation. By contrast, carbon dioxide (CO_2) emissions from German croplands have continuously increased over the past decades as a result of soil organic carbon (SOC) losses. Contrasting results, however, have been obtained on the C sink or source function of European croplands based on long-term experiments and rather recent eddy covariance (EC) measurements. Over a period of eight years (2010–2017), we measured the net ecosystem exchange

[3] The publication of Chapter 4 is done with the consent of the Elsevier B.V. The original publication was in: Journal of Agriculture, Ecosystems and Environment, Volume 276, Pages 31-46. It can be found under the following link: https://doi.org/10.1016/j.agee.2019.02.011

(NEE) of CO_2 on six intensively managed cropland sites in two climatically different regions of southwest Germany (Kraichgau (KR) and Swabian Jura (SJ)) using the EC technique. Additionally, we measured aboveground crop biomass at three development stages and estimated management-related C inputs and exports. The inter-annual on-site variability of cumulated annual NEE was large, and neither the region nor the different sites significantly affected NEE budgets. Winter rapeseed showed the lowest CO_2 uptake capacity among the observed crops, and the mean annual NEE in the years with winter rapeseed harvest was significantly lower compared to winter wheat, silage maize and winter barley. On average over 46 site-years, annual NEE showed a distinct CO_2 uptake of −2580 kg CO_2-C ha^{-1} yr^{-1}. Considering management-related C fluxes, the resulting net biome productivity (NBP) indicated a C source function of the study sites with mean annual losses of 1190 kg C ha^{-1} yr^{-1}. Due to high C removals after whole plant harvests, silage maize cropping resulted in significantly higher C losses of 4280 kg C ha^{-1} yr^{-1} compared to winter rapeseed, winter wheat and winter barley, with mean annual NBPs of 1430, −188 and −1340 kg C ha^{-1} yr^{-1}, respectively. Consequently, a higher share of exported C in annual NBP resulted in higher C losses. We conclude that the recently increased importance of silage maize in crop rotations destabilizes SOC stocks, threatening the efforts in enhancing soil C sequestration. This calls for further investigations on the C sequestration potentials of more diverse crop rotations including perennial phases.

4.1. Introduction

The land area covered by croplands plays a substantial role for the global carbon (C) cycle due to its large extent and highly dynamic nature with frequent disturbances of the soil-plant system. In Germany, 33% of the land area was covered by croplands in 2016, corresponding to 71 % of the total agriculturally utilized area (Destatis, 2017). Estimated CO_2 emissions from German croplands reported under the United Nations Framework Convention on Climate Change (UNFCCC) amounted to 14577 Gg in 2016, equivalent to 1.9 % of total German CO_2 emissions. These cropland CO_2 emissions have been steadily increasing, i.e. by 17.2 % since 1990 (UBA, 2018), underlining the potential of croplands for greenhouse gas (GHG) mitigation (Smith et al., 2008). A large proportion of the reported cropland CO_2 emissions is attributed to organic soils, whereas the rest is assigned to grasslands recently converted to croplands. Croplands under good agricultural practice are generally considered to show stable soil organic carbon (SOC) contents over the long-term (Körschens et al., 2014). In contrast, recent measurements from eddy covariance (EC) flux tower networks demonstrated that croplands act as C sources to the atmosphere

when all relevant C fluxes of the agroecosystem are considered (Ceschia et al., 2010, Prescher et al., 2010).

Measures proposed to mitigate C losses from croplands typically involve management practices such as cover crops (Poeplau and Don, 2015), nutrient supply, tillage (Eugster et al., 2010) or residue management (Lal, 2004). Moreover, a change in land use intensity is potentially promising to enhance C sequestration or reduce the depletion of SOC stocks under certain conditions. In low-productivity systems, agronomic measures that increase plant biomass can build up SOC stocks by allocating more C into the soil via roots and harvest residues (Smith et al., 2005). Under conditions unfavorable for intensive cropping, however, reducing land use intensity or even abandoning these areas (i.e. land use change) can be the most effective measure for reducing SOC losses (Smith et al., 1997).

Robust information on ecosystem functions with regard to C budgets and thus climatic impact can be gained only from long-term measurements. This is because the inter-annual variability of C exchange is large (Moors et al., 2010). Studying the full C budget of a cropland and assessing the net biome productivity (NBP) requires considering all relevant C fluxes in the system. Alternatively, the temporal development of SOC stocks has to be monitored over many years to decades with a consistent methodology (Smith et al., 2010). These types of observations are rare, although some valuable networks of long-term experiments exist (Smith et al., 2002). Robust agroecosystem models are essential to extrapolate C budgets of croplands to larger spatial scales (Klosterhalfen et al., 2017), underlining the importance of the aforementioned long-term experiments and observations. Moreover, accounting for spatial heterogeneity is essential for upscaling C fluxes in agricultural landscapes (Premke et al., 2016).

Several multi-year observations that used the EC method to study the net ecosystem exchange (NEE) of CO_2 over croplands are available (e.g., Kutsch et al., 2010). For typical crops grown on mineral soils in intensive crop rotations, the seasonal and annual NEE often shows a net CO_2 uptake. Accordingly, the gross primary production (GPP) from photosynthesis is higher than the respiration of the total ecosystem (R_{ECO}). Nonetheless, most of the fixed C is removed from these systems via harvest, often resulting in net C losses to the atmosphere (Ceschia et al., 2010, Loubet et al., 2011, Schmidt et al., 2012).

A well-known limitation of the EC method is the imbalance between measured turbulent energy fluxes and the available energy at the land surface (Foken, 2008). One potential reason for the energy balance gap is uncaptured low-frequency fluxes, also termed mesoscalic eddies, which can be analyzed by varying the averaging time for flux computation (Mauder and Foken, 2006). However, investigating the extent to which the energy gap also affects CO_2 fluxes and thus C budgets is challenging (Kidston et al.,

2010). Applying the ogive or cumulative flux analysis enables determination of a suitable averaging time (Foken and Wichura, 1996). Recently, an ogive optimization method was developed following the idea that low-frequency influences must be separated from vertical turbulent fluxes in order to isolate the local exchange processes of interest (Sievers et al., 2015). Using this new approach, Sievers et al. (2015) demonstrated that the relative differences between fluxes estimated by a common 30 min averaging interval and the ogive optimization can be very high (up to 98 %) when fluxes are rather low. Importantly, the method was applied to field sites without agricultural management: it remains uncertain how much low-frequency contributions might affect the CO_2 exchange of intensively managed croplands.

Typically, studies based on EC measurements are performed as single-field observations in a given region or environment (Osborne et al., 2010). This yields insights into temporal variability but leaves the spatial variability between different fields with the same management and site properties unexplored. Here, we present results from EC measurements of CO_2 exchange over eight years in two regions of southwest Germany with different pedoclimatic conditions. In each region, three EC stations measured the CO_2 fluxes over separate adjacent or nearby arable fields. The main objective of this study was to investigate whether systematic differences exist between the annual C budgets of sites in different pedoclimatic regions, between different sites within the regions and between the most frequently grown crops in intensively managed crop rotations. We hypothesize that the study sites represent C sources due to recent intensification and specialization processes of the respective arable production systems. The corresponding C losses are expected to be higher at sites with larger SOC stocks.

4.2. Material and methods

4.2.1. Study sites

The measurements were performed on a total of six sites in two different regions of the federal state Baden-Württemberg in southwest Germany. The two regions, Kraichgau (KR) and Swabian Jura (SJ), differ in their pedoclimatic conditions as a consequence of parent material and elevation. For detailed information on the two regions, see Wizemann et al. (2015).

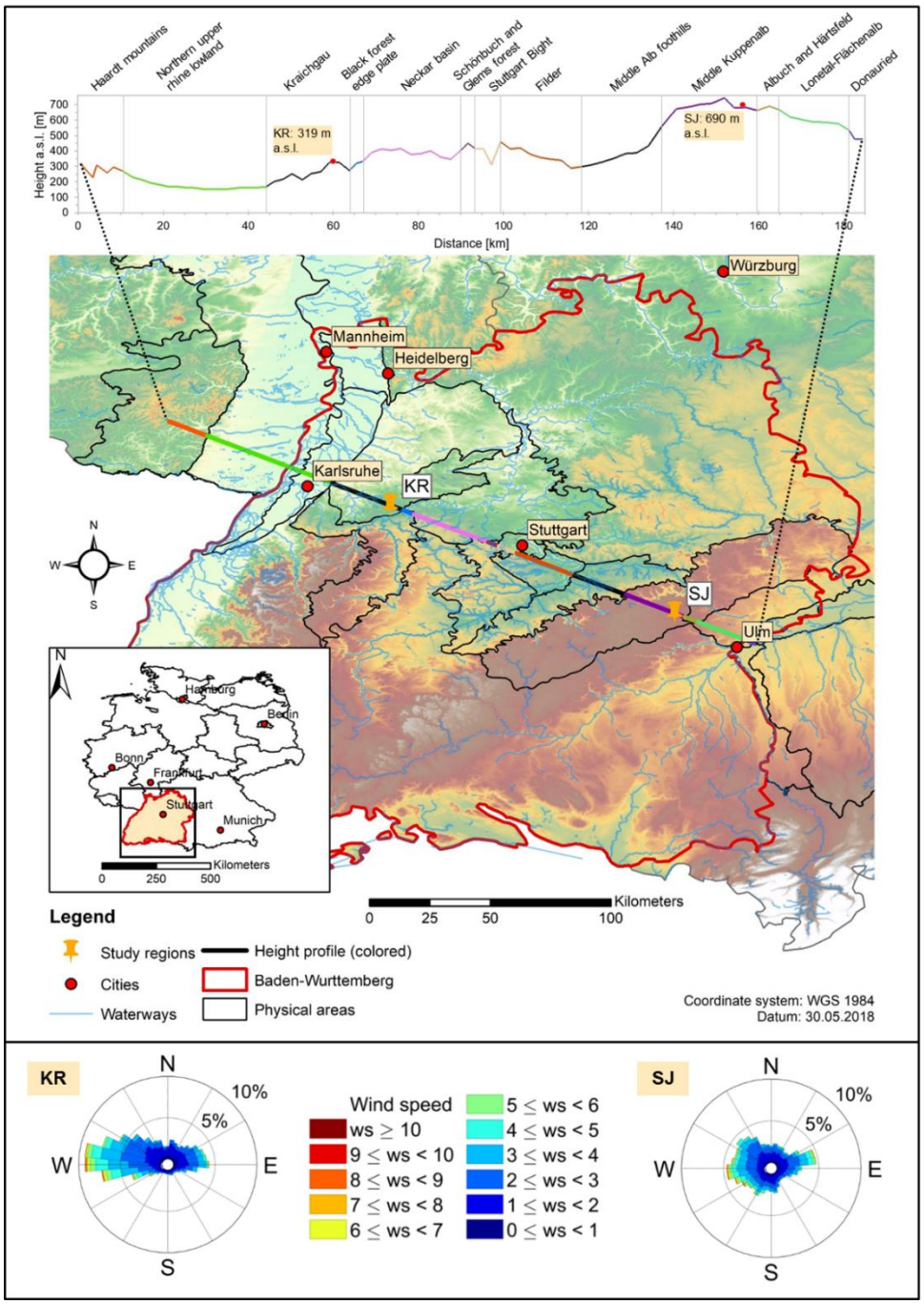

Fig. 4.1. Overview. Top: Height transect through the two study regions Kraichgau (KR) and Swabian Jura (SJ). Middle: Geographical overview of the two study regions. Bottom: Rose diagrams of wind direction and wind speed. Wind data are an average over eight years (2010 – 2017). Calculations based on data of eddy covariance stations EC1 and EC4 were used for KR and SJ, respectively.

In the KR region, the study sites were located close to the city of Pforzheim at 48.9 °N, 8.7 °E and 319 m above sea level (a.s.l.) (Fig. 4.1). Over the period 1981-2010, the mean annual temperature was 9.4 °C and the mean annual precipitation was 889 mm at the nearby weather station Pforzheim-Ispringen (48.9

°N, 8.7 °E, 333 m a.s.l.; German Weather Service, 2016). The soils for this study developed from deep Holocene silty loess layers (Table 4.1). They are typical for the KR region and have been classified as Stagnic Luvisols (WRB, 2015) due to periodically occurring stagnic water conditions, particularly in winter and spring. The underlying rock material is shell limestone (Ingwersen et al., 2011). According to the three installed EC stations, the sites were named EC1, EC2 and EC3, located on three adjacent arable fields aligned in west-east direction (Wizemann et al., 2015; Imukova et al., 2015). The fields are managed by a local farmer with regular applications of mainly mineral fertilizers and pesticides typical for conventional cropping systems on high yielding sites in Central Europe. During the 2010-2017 observation period, only three main crops were harvested on the three sites. Nitrogen (N) intensities were rather high, particularly in those years when organic fertilizers were applied additionally. No organic fertilizers were applied on EC3. The most frequent tillage procedure was moldboard ploughing (n = 17) followed by grubbing (n = 11) and disc harrowing (n = 6) (Table 4.2). The ploughing depth usually did not exceed 0.25 m.

The study sites in the SJ region were located at 48.5 °N, 9.8 °E and 690 m a.s.l. near the village Nellingen (Fig. 4.1). In this region, the climate is colder and wetter compared to KR, with a mean annual temperature and precipitation of 7.5 °C and 1042 mm, respectively, measured at the nearby weather station Merklingen during 1981-2010 at 48.5 °N, 9.8 °E and 685 m a.s.l. (German Weather Service, 2016). Of the three sites - named EC4, EC5 and EC6 - EC4 and EC5 were adjacent to each other, while EC6 was located about 1.5 km north (see Wizemann et al., 2015). Soils in SJ developed from Jurassic limestone and are typically shallow and much more heterogeneous with higher C stocks compared to KR (Table 4.1). Thus, the soil types differed between the three sites and were classified as Calcic Luvisol (EC4, solum thickness 0.45 m), Anthrosol (EC5, solum thickness > 0.9 m) and Rendzic Leptosol (EC6, solum thickness 0.2 m) according to WRB (2015). As in KR, field management can be classified as conventional and intensive cropping. On average, the N fertilization intensity was lower on EC4 and no organic fertilizers were applied except for the last season. As the farmer of field EC5 kept livestock, slurry was applied regularly. On EC6, organic fertilizers were applied mainly as biogas digestate with the highest fractions on total N input over all sites. Ploughing was carried out only in two years at EC5, whereas tillage was mainly restricted to harrowing at the shallower sites EC4 and EC6. Furthermore, the number of crop types grown was higher at the SJ than at the KR sites (Table 4.2).

Table 4.1. Top soil (0 – 30 cm) properties of the six study sites. EC1 – 3: Kraichgau, EC4 – 6: Swabian Jura. Ranges are standard deviations.

Site	Texture S/U/C[a] (% by mass)	Porosity (% by vol.)	Bulk density[b] (g cm^{-3})	C/N ratio[b] (1)	C stock[b] (Mg ha^{-1})	Carbonate (% by mass)	pH (0.01 M $CaCl_2$)
EC1	2.5/79.4/18.2	48.3	1.29 ± 0.12	9.1 ± 0.5	32.0 ± 4.2	1.50	6.9
EC2	2.6/79.5/17.9	49.8	1.24 ± 0.14	10.7 ± 1.6	32.6 ± 8.4	1.38	6.2
EC3	1.8/81.1/17.1	48.3	1.25 ± 0.14	9.0 ± 0.4	27.6 ± 2.8	1.46	6.4
EC4	7.6/54.2/38.2	50.0	1.30 ± 0.19	9.5 ± 0.3	67.8 ± 11.6	2.62	6.9
EC5	2.8/68.3/28.9	48.3	1.22 ± 0.12	9.7 ± 0.7	71.8 ± 7.6	2.95	6.4
EC6	3.6/49.8/46.6	56.0	1.24 ± 0.14	9.9 ± 0.2	80.9 ± 9.9	4.72	7.0

[a]Fractions of sand (S), silt (U) and clay (C).
[b]Samplings from 8 and 9 November 2017.
[c]Mean values of regular samplings between May 2009 and November 2017 as well as the mean annual change in carbon concentrations calculated by linear regression of the time series with n = 8 (EC3), n = 9 (EC1, EC2, EC4), and n = 10 (EC5, EC6). n.s. = not significant, * = significant with $0.01 < p < 0.05$

4.2.2. Eddy covariance measurements

4.2.2.1. Instrumentation

In 2009, the six EC stations were set up in the center of the fields, ensuring 130 m (EC4) to 300 m (EC2) fetch in the main wind direction (W, see Fig. 4.1). All stations were equipped with an LI-7500 open path CO_2/H_2O infrared gas analyzer (LI-COR Biosciences, Lincoln, NE, USA) and a CSAT3 3D-sonic anemometer (Campbell Scientific Inc., Logan, UT, USA), installed 2 – 3 m above the crop canopy and oriented in southern (KR) and south-western (SJ) direction. Data were collected with 10 Hz and stored on a CR3000 data logger (Campbell Scientific Inc., Logan, UT, USA). Global radiation (R_g) and net radiation were measured with a 4-component net radiometer (NR01, Hukseflux Thermal Sensors B.V., Delft, The Netherlands) that were installed about 1.5 m above the canopy. The soil heat flux at 8 cm soil depth was measured with three replicates of heat flux plates (HFP01, Hukseflux Thermal Sensors B.V., Delft, The Netherlands) at each EC station. The CR3000 data loggers were used to store the 30 min averages of radiation, soil heat flux, air temperature (T_a) and humidity in 2 m height (HMP45, Vaisala Inc., Helsinki, Finland; EC2 from September 2016 and EC1 from December 2016: HC2S3 Hygroclip2, Rotronic GmbH, Ettlingen, Germany) and precipitation (ARG100, EML, North Shields, UK). Additionally, CR1000 data loggers (Campbell Scientific Inc., Logan, UT, USA) stored the 30 min averages of soil temperature (107, Campbell Scientific Inc., Logan, UT, USA), volumetric soil water content (CS616, Campbell Scientific Inc., Logan, UT, USA) and soil matric potential (253, Campbell Scientific Inc., Logan, UT, USA). For each of these three soil variables, five sensors were installed in different depths depending on the variable and the solum thickness at the SJ sites. For more details, including measurement accuracies, refer to Wizemann et al. (2015).

Table 4.2. Crop rotation, management and yields at the six study sites during the period 2010 – 2017.

Site	Period	Crop[a]	N fertilization		Tillage[c]	Yield[d]
			Total (kg ha $^{-1}$)	Organic (percentage)[b]		(Mg ha^{-1} ± SD)
EC1 (14.9 ha)	2010	SM	273	27 (BD)	P	19.8 ± 2.4
	2010/2011	WW	170	/	P	10.2 ± 0.5
	2011/2012	WR	210	/	G	4.8 ± 0.4
	2012/2013	WW	179	/	DH, G	8.9 ± 0.9
	2013/2014	CC – SM	283	35 (CS)	G, P	23.2 ± 1.7
	2014/2015	WW	246	26 (CS)	P	9.4 ± 1.6
	2015/2016	CC – GM	213	/	DH, P	14.0 ± 1.6
	2016/2017	WW	183	/	P	8.2 ± 0.8
EC2 (23.6 ha)	2009/2010	WR	333	29 (BD)	G	4.4 ± 0.2
	2010/2011	WW	170	/	DH	9.4 ± 0.2
	2011/2012	CC – SM	272	27 (BD)	G, P	24.5 ± 1.4
	2012/2013	WW	180	/	P	7.9 ± 0.4
	2013/2014	CC – SM	210	/	DH, G, P	23.2 ± 1.2
	2014/2015	WW	246	26 (CS)	P	10.1 ± 0.9
	2015/2016	WR	173	/	DH, G	4.4 ± 1.0
	2016/2017	WW	183	/	P	9.5 ± 1.5
EC3 (15.8 ha)	2009/2010	WW	220	/	P	7.9 ± 0.9
	2010/2011	CC – SM	223	/	P, P	25.5 ± 1.8
	2011/2012	WW	203	/	P	9.9 ± 0.8
	2012/2013	WR	235	/	DH, G	7.2 ± 0.6
	2013/2014	WW	198	/	G	10.5 ± 1.1
	2014/2015	CC – SM	203	/	G, P	21.9 ± 2.1
	2015/2016	WW	202	/	G	6.9 ± 0.9
	2016/2017	WW	183	/	P	6.2 ± 1.3
EC4 (8.7 ha)	2009/2010	WR	205	/	DH, DH	2.8 ± 0.5
	2010/2011	WW	237	/	DH, DH	8.3 ± 1.9
	2011/2012	CC – SB	95	/	DH, G	8.9 ± 0.4
	2012/2013	WR	133	/	DH	1.8 ± 1.1
	2013/2014	WW	190	/	DH	10.4 ± 0.4
	2014/2015	WW	203	/	DH	9.9 ± 1.0
	2015/2016	CC – SB	80	/	DH	6.2 ± 0.7
	2016/2017	CC – SM	133	79 (CS)	DH	30.5 ± 11.8
EC5 (16.7 ha)	2009/2010	WW	245	14 (BD)	G, G	9.0 ± 1.2
	2010/2011	CC – SM	206	17 (CS)	G, DH	18.7 ± 1.6
	2012	SM	268	39 (CS)	DH	14.5 ± 1.7
	2012/2013	WB	227	25 (CS)	G	8.7 ± 0.3
	2013/2014	SP	170	35 (CS)	P, DH	6.6 ± 1.1
	2014/2015	CC – SM	192	16 (CS)	P, DH	17.3 ± 2.6
	2015/2016	CC – SM	151	/	DH, DH	21.8 ± 1.5
	2016/2017	WB	192	40 (CS)	DH	10.4 ± 2.1
EC6 (13.4 ha)	2009/2010	CC – SM	210	57 (BD)	DH, DH	14.8 ± 3.1
	2010/2011	WW	221	/	DH	9.5 ± 0.9
	2011/2012	WB	273	59 (BD)	DH	8.6 ± 1.3
	2012/2013	CC – SM	246	60 (BD, CS)	DH, DH	20.7 ± 3.5
	2013/2014	WW	229	/	DH	9.3 ± 2.1
	2014/2015	WB	150	48 (BD)	DH	8.4 ± 1.3
	2015/2016	CC – SM	203	56 (BD)	DH, DH	19.5 ± 4.2
	2016/2017	WW	198	45 (BD)	DH, CH	9.0 ± 0.7

[a]WW: Winter wheat, SM: Silage maize, WR: Winter rapeseed, WB: Winter barley, SB: Summer barley, CC: Cover crop, GM: Grain maize, SP: Spelt; [b] BD: biogas digestate, CS: cattle slurry; [c] P: ploughing, G: grubbing, DH: disc harrow, CH: circular harrow; [d]For cereals and grain maize, yields are reported as grain dry matter (DM) and for silage maize as total aboveground DM.

On five sites, the described instrumentation was operational during the observation period January 2010-October 2017. On 11 April 2017, however, the system on EC1 was changed. A new EC station equipped with an LI-7200RS enclosed path CO_2/H_2O gas analyzer (LI-COR Biosciences, Lincoln, NE, USA) and a HS-50 3D-sonic anemometer (Gill Instruments Ltd., Hampshire, UK) was installed. Long- and shortwave radiation was measured with a 4-component CNR4 net radiometer (Kipp and Zonen B.V., Delft, The Netherlands). Three self-calibrating heat flux plates (HFP01SC, Campbell Scientific Inc., Logan, UT, USA) were buried 8 cm below the soil surface. To measure soil volumetric water content as well as soil temperature, three HydraProbe II sensors (Stevens Water Monitoring Systems Inc., Portland, OR, USA) were installed at 5, 10 and 15 cm soil depth, respectively. Air temperature and humidity were measured by a HMP155 probe (Vaisala Inc., Helsinki, Finland) at this station. The soil and weather data were stored on an XLite 9210 data logger (Sutron Corporation, Sterling, VA, USA).

Power supply for all EC stations was ensured by two solar-power batteries with capacities of 12 V and 250 Ah each (Keckeisen Akkumulatoren e.K., Memmingen, Germany). The batteries were charged by four 20 W solar panels (SP20, Campbell Scientific Inc., Logan, UT, USA) at each station. During periods with low solar altitude, however, the power supply was generally insufficient to ensure the operation of the LI-7500. For this reason, no CO_2 fluxes were measured during winter time, mainly from late November until March. To assess the CO_2 exchange during winter time, direct methanol fuel cell systems with 45 W maximum power supply (Efoy Pro 800 Duo, FSC Energy AG, Brunnthal-Nord, Germany) were installed at EC2 and EC6 in autumn 2015. This enabled operating the CO_2/H_2O analyzers during the subsequent two winters at these sites.

4.2.2.2. Data processing and flux filtering

Turbulent fluxes were computed for 30-min intervals using the software package TK3.1 (Mauder et al., 2013). This program enabled spike detection (Vickers and Mahrt, 1997), planar fit coordinate rotation (Wilczak et al., 2001), correction of spectral loss (Moore, 1986), conversion of sonic temperature into actual temperature (Schotanus et al., 1983) as well as correction for density fluctuations and vertical mass transport (Webb et al., 1980). For quality classification of the calculated fluxes, the nine class flagging scheme after Foken et al. (2004) was used. To estimate the uncertainty of computed fluxes, the random error and the instrumental noise calculated by TK3.1 were summed up.

The processed 30-min fluxes were filtered by applying quality criteria that were chosen in order to remove unreliable data from the dataset on the one hand, but to provide sufficient data coverage for C budgeting on the other. The approach of Demyan et al. (2016), who used data from the same dataset for their respiration model, was modified accordingly. Here, we used data flagged with 1-6 as recommended for long-term observation programs. For additional despiking of half-hourly fluxes, we applied a median filter using the median of absolute fluxes of the previous four days; fluxes that were greater than 5-times this median were discarded from the dataset.

4.2.2.3. Gap filling and flux partitioning

The REddyProc (Wutzler et al., 2018) web application was used to derive complete datasets for NEE, R_{ECO} and GPP in order to calculate seasonal and annual budgets. This tool applies a friction velocity filter (Papale et al., 2006) to the pre-processed 30-min fluxes as a first step. The data gaps are then filled with the average values under similar meteorological conditions using look-up tables (LUT) (Reichstein et al., 2005). The considered meteorological variables are R_g, T_a and vapor pressure deficit (VPD). The initial time window of the LUT is 7 days, which is increased to 14 days if no similar conditions are found. In this step-wise approach depending on data availability, only similar conditions of R_g are used if no T_a and VPD data are available. If none of these requirements can be fulfilled, then the mean diurnal variation method according to Falge et al. (2001) with step-wise increased window-sizes is applied until the gap is filled. To evaluate the uncertainty of the gap-filling procedure, the web application creates artificial data gaps, fills the gaps using the described algorithm, and compares them with the measured fluxes.

The day-time based approach following Lasslop et al. (2010) was used to partition the net CO_2 exchange into photosynthesis and respiration. In this approach, the activation energy parameter (E_0) in the Lloyd and Taylor (1994) model is estimated from nighttime data, whereas the respiration at base temperature (r_b) and the parameters of the hyperbolic light-response curve (Falge et al., 2001) are estimated using daytime data. This approach also accounts for the limitation of GPP at high VPD. Therefore, the maximum CO_2 uptake rate of the canopy at light saturation (β) is replaced by an exponentially decreasing function at VPD > 10 hPa with a new parameter (k), describing the response of the maximum C uptake to VPD for time windows of four days. In contrast to the nighttime-based approach for flux partitioning (Reichstein et al., 2005), GPP and R_{ECO} derived from the daytime-based approach do not sum up to the gap-filled NEE value at each time step because they are not calculated from NEE.

4.2.2.4. Ogive optimization

To evaluate the contribution of low-frequency fluctuations on the EC measurements, the ogive optimization method of Sievers et al. (2015) was applied. We used the Ogive Optimization Toolbox (OOT, Version 1.0.5) coded in MATLAB® (Mathworks Inc., Boston, MA, USA). In OOT, an ensemble of usually 10,000 flux ogives is generated by perturbation of the flux averaging time and the running mean window. Both methods - adjusting the flux averaging time and subtracting a running mean from the observed signal - are established methods for filtering out low-frequency contributions while retaining the local turbulent contributions (Sakkai et al., 2001; Mcmillen, 1988). Based on the resulting ogive density ensemble, a theoretical generalized co-spectral distribution model is fitted, and the best fit is regarded as the most likely local turbulent flux. For a detailed description of the ogive optimization process, see Sievers et al. (2015).

2.3. Crop parameters

During the observation period, crop development was monitored at each site in intervals of roughly four and two weeks during the non-growing season and main growing season, respectively. On five permanent plots per site, canopy height and phenological development stage were determined with ten replicates. At the beginning of shoot development, at full flowering and at the time of maturity, aboveground biomass samples were taken at each plot. At intermediate harvests, the fresh weight of the biomass was measured in the lab, and after oven drying at 60 °C the dry matter (DM) content was determined. Samples taken at final harvest were separated into vegetative and generative organs (oven drying at 30 °C until constant weight) after weighing the total fresh matter. Dried samples were ball milled and analyzed for their total C and N contents with an elemental analyzer (Vario EL, Elementar Analysensysteme, Hanau, Germany) (Högy et al., 2009; 2010).

We calculated the growing degree days (GDD) as a function of time (*n*, days) following McMaster and Wilhelm (1997) in order to characterize the growing conditions for crops in the different years and regions:

$$\sum (((T_{max,i} + T_{min,i})/2) - T_{base}) \quad (4.1)$$

where $T_{max,i}$ (°C) and $T_{min,i}$ (°C) are the daily maximum and minimum temperature, respectively. T_{base} is the temperature from which crop growth takes place. As described in Wizemann et al. (2015), an upper threshold temperature, T_{ut}, was used, and temperatures < T_{base} were set to T_{base} and temperatures > T_{ut}

were set to T_{ut}. T_{base} and T_{ut} were 0 and 37 °C for winter wheat and 10 and 30 °C for silage maize, respectively.

4.2.4. Net biome productivity

To calculate NBP for particular periods and sites, C fluxes related to agricultural management were added to the measured CO_2 fluxes:

$$NBP = NEE + C_{in} + C_{ex} \quad (4.2)$$

where NEE is the gap-filled and cumulated CO_2 exchange for the respective period (kg CO_2-C ha^{-1}), C_{in} is the C input by organic fertilizers (kg C ha^{-1}) and C_{ex} is the C export via harvested biomass (kg C ha^{-1}). To estimate C_{in} and C_{ex}, information provided by the farmers, standard values and own analyses were combined. Farmers reported on the total amounts of organic fertilizers (slurry or biogas digestate) that were applied to each field in each year. To calculate C_{in}, we used well-documented standard values (TLL, 2012; LWKSH, 2013) for dry matter (DM) and C contents. To calculate C_{ex}, we used the documented yields from the farmers together with the proportions of harvest residues left on the fields. Total amounts of straw were calculated from the harvest index measured on the sampling plots at the time of harvest. If DM yields were not reported, as is generally the case for silage maize, yields were corrected for their DM contents. For this, we assumed typical values for valuable harvest products: 32 % DM for silage maize, 91 % DM for rapeseed and 86 % DM for cereal grains (winter wheat, winter and summer barley, winter spelt). Finally, the removed biomass (grains and straw) was multiplied with its measured C content to obtain C_{ex}. It was assumed little to no C left the field due to erosion.

4.2.5. Statistical analyses

The software R studio (R version 3.2.4) was used to evaluate the data. Statistical tests were based on the definition of linear mixed models (Laird and Ware, 1982; Verbeke and Molenberghs, 2000). The data were assumed to be normally distributed but heteroscedastic due to the different years. These assumptions and the identification of appropriate mixed models were based on graphical residual analyses. Analyses of variance (ANOVA) were performed to identify significant effects of the factors region, site and crop as well as their interactions on the annual values of NEE and NBP. The year as an integrative parameter for the variability caused by weather characteristics was treated as a random factor. Multiple contrast tests (Bretz et al., 2011), based on the comparison of means by Tukey tests, were conducted to identify significant differences between sites, regions and crops. The relationships between

cumulated GPP or NEE over particular periods and the corresponding GDD as well as ANPP were evaluated by ordinary linear regression analyses.

4.3. Results

4.3.1. Weather conditions

The two study regions differed distinctly in their weather characteristics during the 8-year study period (Fig. 4.2). In almost every month, the mean temperature at KR was higher than at SJ (Fig. 4.2a). Lowest annual mean temperatures were recorded in 2010 (8.5 °C in KR, 6.1 °C in SJ). The warmest year was 2014, with 10.9 °C in KR and 8.4 °C in SJ. The coldest month was February 2012, with -3.1 and -6.2 °C, whereas the warmest month was July 2015, with 21.2 and 18.7 °C in KR and SJ, respectively. The deviations of monthly mean temperatures from the long-term average (1981-2010) followed a very similar pattern in both regions (Fig. 4.2b). Concurrent with the lowest monthly mean temperatures, the most negative temperature anomalies were observed in February 2012 (-4.8 °C in KR, -5.6 °C in SJ). The most positive anomalies were also recorded in winter, with +4.2 and +3.5 °C in December 2015 for KR and SJ, respectively.

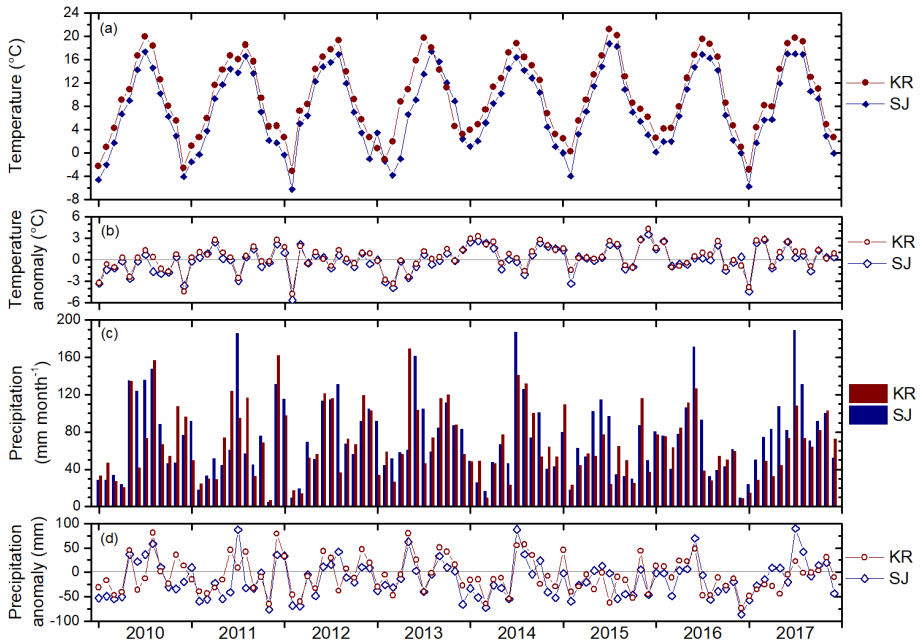

Fig. 4.2. Weather and climate. Monthly temperatures and precipitation over the period 2010 – 2017 in the two study regions Kraichgau (KR) and Swabian Jura (SJ). (a) Mean monthly temperature, (b) difference between the monthly mean temperatures and the climatological 30-yr means (1981 – 2010), (c) monthly precipitation, and (d) difference between the monthly precipitation and the climatological 30-yr (1981 – 2010) mean monthly precipitation.

In KR, the wettest year was 2013, with a total precipitation amount of 947 mm, whereas the highest precipitation in SJ was recorded in 2017 (1056 mm). In both regions, the lowest precipitation occurred in 2015 with 682 and 761 mm in KR and SJ, respectively. In KR, the highest monthly precipitation occurred in August 2010 (157 mm), December 2011 (162 mm) and May 2013 (169 mm). Highest monthly precipitation in KR was 186 mm in July 2011, 187 mm in July 2014 and 189 mm in July 2017 (Fig. 4.2c). Very dry months occurred mainly in autumn and winter, with lowest precipitation in November 2011 (7 and 5 mm in KR and SJ, respectively) and December 2016 (9 mm in both KR and SJ). Compared to the temperature anomalies, the temporal pattern of precipitation anomalies was less similar between the two regions (Fig. 4.2d). However, the above-mentioned months with highest and lowest precipitation also showed the highest deviations from the long-term mean monthly value. Anomalies ranged from -74 mm (December 2016) to +82 mm (August 2010) in KR and from -87 mm (December 2016) to +90 mm (July 2017) in SJ.

4.3.2. CO_2 measurements and budgeting

4.3.2.1. Variability of CO_2 exchange

Depending on the region, the time of year and the crop, the pattern of mean diurnal CO_2 exchange rates differed substantially (Fig. 4.3). As winter wheat was never seeded before October and harvested not later than August, there are no measurements over winter wheat in September. During this time, winter rapeseed seeded in August had already emerged, and distinctive CO_2 fixation rates up to monthly mean values of -1.73 (KR) and -1.05 kg CO_2-C ha^{-1} 30 min^{-1} (SJ) occurred in October. The CO_2 exchange of winter rapeseed and winter wheat in April revealed two regional differences between KR and SJ. Firstly, the diurnal patterns of the two crops were similar in KR, while in SJ the daytime NEE of winter wheat was substantially higher (i.e., more negative), with a 2-fold mean maximum net CO_2 uptake at midday compared to winter rapeseed. Secondly, maximum daytime NEE of both winter rapeseed and winter wheat were higher in KR than in SJ. Both crops reached their maximum mean monthly net CO_2 fixation rates in May, with -4.28 and -4.48 kg CO_2-C ha^{-1} 30 min^{-1} for winter rapeseed and -6.16 and -5.76 kg CO_2-C ha^{-1} 30 min^{-1} for winter wheat in KR and SJ, respectively. Thus, the CO_2 uptake capability was higher for winter wheat in KR, while the opposite held true for winter rapeseed. Also regarding the nighttime CO_2 release, regional differences were documented for winter rapeseed: the maximum monthly nighttime NEE was 1.63 in KR and 1.98 kg CO_2-C ha^{-1} 30 min^{-1} in SJ, both recorded in June. Also over winter wheat, the monthly peaks of CO_2 release occurred in June but were slightly higher in

KR (1.59) compared to SJ (1.36 kg CO_2-C ha^{-1} 30 min^{-1}). The mean diurnal courses in July reveal that the daytime CO_2 uptake of winter rapeseed and winter wheat decreased earlier in KR than SJ.

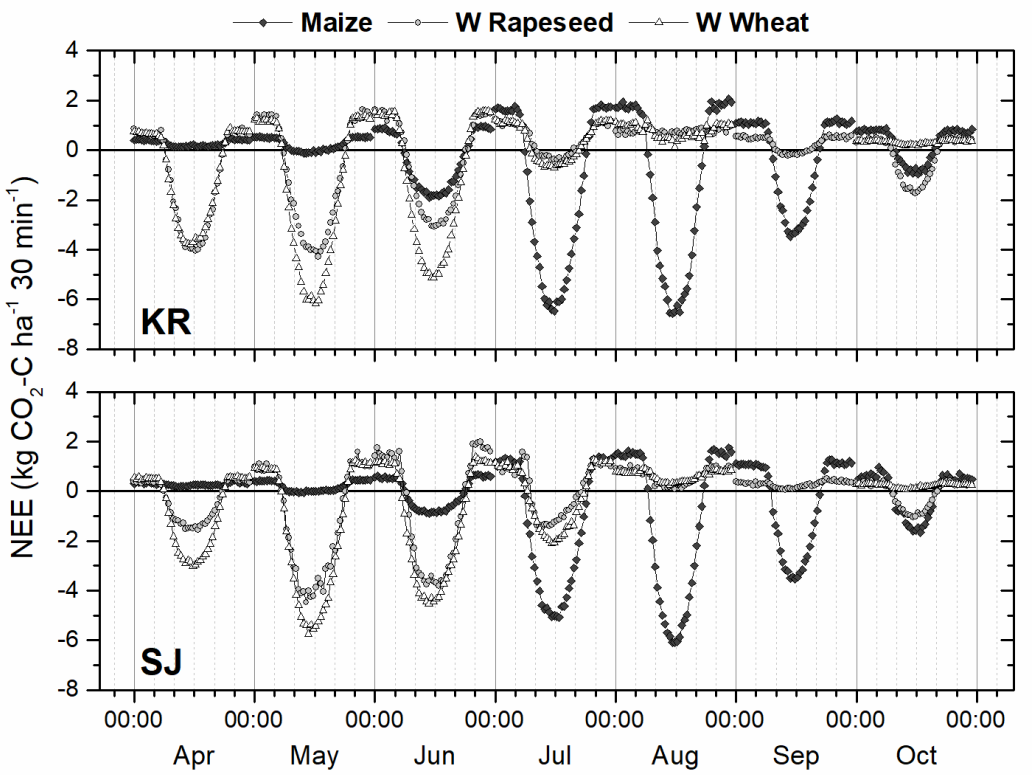

Fig. 4.3. NEE variability. Mean diurnal courses of net ecosystem exchange (NEE) on a monthly basis for the main growing season of maize, winter rapeseed and winter wheat in the two study regions Kraichgau (KR) and Swabian Jura (SJ). The number of site years that were averaged for maize, winter rapeseed and winter wheat were 7, 4 and 13 in KR and 8, 2 and 7 in SJ, respectively.

The annual pattern of CO_2 exchange measured over the maize canopies showed a 3-months shift compared with winter rapeseed and winter wheat (Fig. 4.3). As observed for the other two crops, the maize plants in KR showed higher maximum CO_2 fixation and respiration rates at the beginning of the productive phase (June). In SJ, these rates were higher at the end of the growth period (October). Maximum monthly mean fluxes for maize were recorded in August in both regions: -6.58 and 2.06 kg CO_2-C ha^{-1} 30 min^{-1} in KR and -6.09 and 1.76 kg CO_2-C ha^{-1} 30 min^{-1} in SJ.

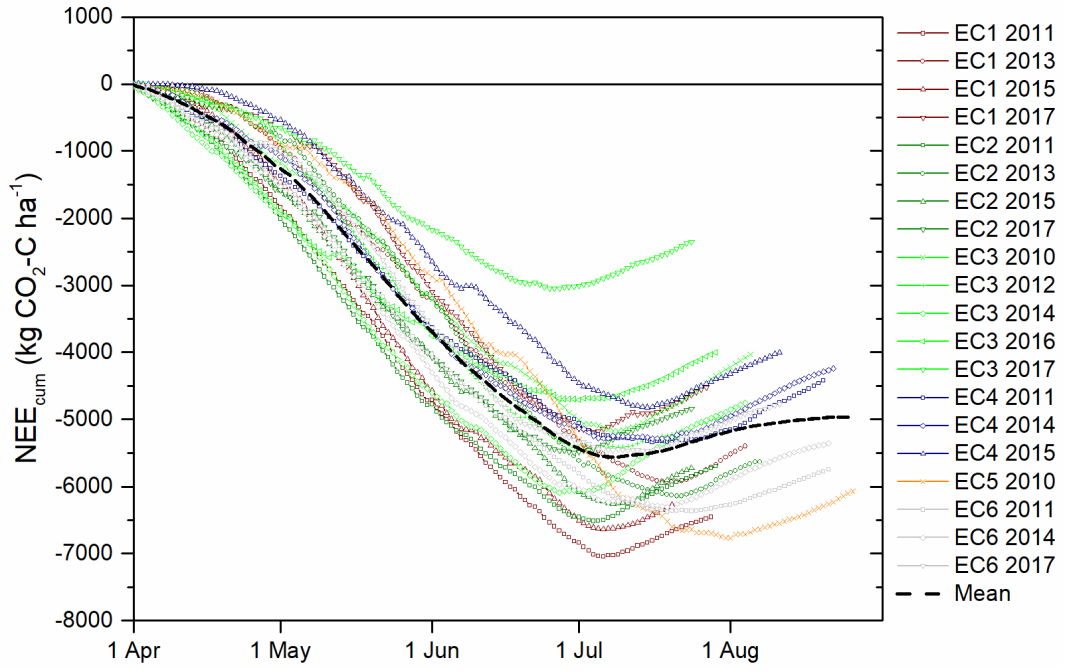

Fig. 4.4. Cumulative NEE. Variability of cumulative net ecosystem exchange (NEE) shown for the observed 20 site years of winter wheat from 1 April until harvest.

Beyond the crop-specific effects on CO_2 exchange patterns (Fig. 4.3), inter-site and inter-annual variability was large, as evident from the cumulative NEE from 1 April to harvest for the 20 site years of winter wheat cropping (Fig. 4.4). At the time of winter wheat harvest, the mean cumulative NEE was -4960 kg CO_2-C ha^{-1}. The lowest and highest uptakes were -2360 (EC3 2017) and -6460 kg CO_2-C ha^{-1} (EC1 2011), respectively. Over the first three months (April-June), the cumulative NEE (NEE_{cum}) steadily decreased. After reaching an inflexion point, NEE_{cum} increased until harvest. Thus, maximum net CO_2 uptake was between 369 (EC1 2015) and 1340 kg CO_2-C ha^{-1} (EC3 2014) higher compared to NEE_{cum} at the time of harvest. In SJ, winter wheat was harvested later than in KR throughout the study period. Earliest and latest harvest dates were 20 July (EC1 2015) and 7 August (EC2 2013) in KR and 11 August (EC4 2015/EC6 2017) and 26 August (EC5 2010) in SJ, respectively. Finally, the time span between maximum cumulative CO_2 uptake and the harvest date was on average six days longer in SJ (30 d) than in KR (24 d).

4.3.3. Annual carbon budgets

The single components of the site- and year-specific C budgets are summarized in Table 4.3. In general, C_{ex} was lower at winter rapeseed sites, while the whole-crop harvest of silage maize resulted in very high C removals. Due to the very similar crop rotations on the KR sites, mean annual C exports were also similar, whereas the differences on the SJ sites were more pronounced, particularly between EC4 and the other two sites. The annual budgets of NEE were extremely variable. This is underlined by the minimum and maximum NEE in KR, observed for the same site in two consecutive years (EC1 2011 and 2012). In SJ as well, annual NEE varied from strongly negative (EC6 2012) to positive (EC4 2016). Note that for those years in which winter wheat was cropped, annual NEE was distinctively negative in 18 out of 20 site years. Interestingly, the two successive winter wheat years 2016 and 2017 at EC3 showed net CO_2 losses of almost the same magnitude. As for NEE, the annual budgets of the net biome productivity (NBP) also showed a high variability, with similar ranges in both regions (-3290-7650 kg C ha^{-1} yr^{-1} in KR and -3970-7320 kg C ha^{-1} yr^{-1} in SJ). Averaged over the study period, all six sites were net C sources with comparable mean annual emissions of around 1000 kg C ha^{-1}. The exception is EC3 with mean annual losses of 2000 kg C ha^{-1}.

The ANOVA showed no significant effects of region, site or their interaction on the annual NEE or NBP. Consequently, no significant differences between the NEE and NBP of the two regions or any of the six sites were detected based on the comparison of means. Crop-specific effects were evaluated using a linear mixed model that considered the crop effect as fixed for both NEE and NBP. Only crops grown in more than two years were considered (silage maize, winter barley, winter rapeseed, winter wheat). The different sites were considered as random effect. The ANOVA confirmed a highly significant effect ($p \leq 0.001$) of crops on NEE and NBP. The model explained 53 % (NEE) and 65 % (NBP) of data variability. The annual NEE of winter rapeseed was significantly higher than that of winter barley and winter wheat. Moreover, the NEE of silage maize was lower than that of winter rapeseed, although the difference was not significant ($p = 0.08$). In contrast, the comparison of means revealed a significantly higher annual NBP of silage maize compared to the other three crops, with $p \leq 0.01$ for winter rapeseed and $p \leq 0.001$ for winter barley and winter wheat. The budgets of the other three crops did not differ significantly (Fig. 4.5).

Table 4.3. Annual carbon budgets of the six study sites. NEE: net ecosystem exchange of CO_2, C_{in}: carbon input by organic fertilizers, C_{ex}: carbon export via harvest, NBP: net biome productivity.

Site	Component	2010	2011	2012	2013	2014	2015	2016	2017[a]	Mean
						(kg C ha^{-1} yr^{-1})				
EC1	NEE	-2836	-6543	2398	-3730	-3940	-4216	-2087	-2974	-2991
	C_{in}	-756	0	0	-1120	0	-720	0	0	-324
	C_{ex}	5716	3254	2444	4622	7232	3010	3309	2739	4040
	NBP	**2123**	**-3289**	**4843**	**-228**	**3292**	**-1926**	**1222**	**-238**	**725**
EC2	NEE	523	-2303	/[b]	-4360	-3323	-3963	-1244	-2952	-2517
	C_{in}	0	0	-700	0	0	-720	0	0	-177
	C_{ex}	2042	3470	7726	2622	6892	3780	1716	3733	3998
	NBP	**2565**	**1167**	**/**	**-1737**	**3569**	**-903**	**472**	**782**	**845**
EC3	NEE	-2840	-326	-4324	-2132	-4297	-2048	1487	1429	-1631
	C_{in}	0	0	0	0	0	0	0	-280	-35
	C_{ex}	2768	7974	3024	2218	2958	6531	2335	2101	3739
	NBP	**-72**	**7648**	**-1300**	**86**	**-1339**	**4483**	**3822**	**3251**	**2072**
EC4	NEE	-784	-2477	-1856	-776	-2910	-2697	1081	-2942	-1670
	C_{in}	0	0	0	0	0	0	-280	-560	-105
	C_{ex}	1524	3228	3208	634	3163	2898	2121	6453	2904
	NBP	**740**	**751**	**1352**	**-142**	**252**	**200**	**2922**	**2951**	**1128**
EC5	NEE	-4906	-1191	-3395	-3226	-4323	-3981	/[b]	-4398	-3632
	C_{in}	-280	-400	-1200	-720	-1200	0	0	-1600	-675
	C_{ex}	3089	8915	7381	4046	3831	7007	7462	4693	5803
	NBP	**-2097**	**7324**	**2787**	**100**	**-1692**	**3015**	**/**	**-1305**	**1163**
EC6	NEE	-2723	-5156	-6290	-1666	-3996	-1140	-1056	-3229	-3157
	C_{in}	-840	-420	-1120	-1000	0	-1600	-616	-1240	-854
	C_{ex}	6063	3454	3438	8275	6502	2571	7783	3225	5164
	NBP	**2500**	**-2122**	**-3972**	**5609**	**2506**	**-169**	**6111**	**-1243**	**1152**

[a]No full annual budgets for NEE and NBP. End of datasets in 2017: EC1: 26 September, EC2: 24 October, EC3: 24 October, EC4-6: 3 November.

[b]No NEE measurement during most of the growing season. EC2 2012: Malfunction of the CSAT3; EC5 2016: CSAT3 and LI-7500 damaged due a tractor accident.

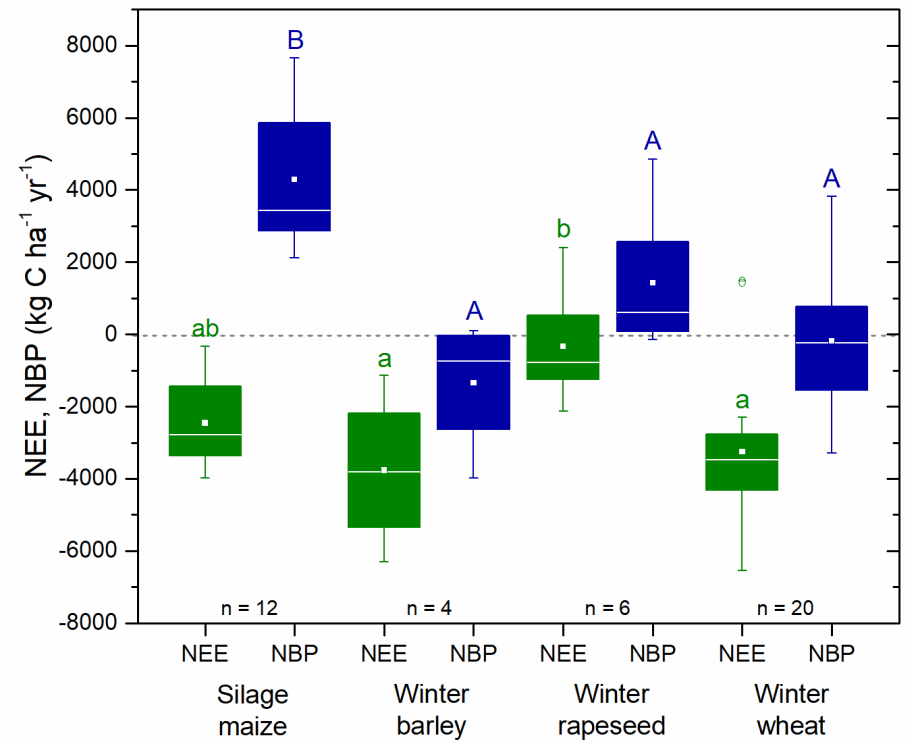

Fig. 4.5. Budgets. Annual budgets of net ecosystem exchange (NEE) and net biome productivity (NBP) for the harvest years (January – December) of the four most frequently grown crops on the six study sites. Different lowercase and capital letters indicate significant differences between the mean NEE and NBP of the different crops, respectively ($p \leq 0.05$).

4.3.4. Effect of low frequency contributions to CO_2 flux

Applying the ogive optimization method filtered out low-frequency contributions. For reasons of comparability, the OOT fluxes were computed for the same month (June 2015) at all sites and compared to the conventional 30 min-fluxes. Over this period, all sites showed a net uptake of CO_2 although the magnitudes differed depending on crop type. Additionally, months with net CO_2 release (when no crop was present) were selected (Fig. 4.6). The mean diurnal courses reveal that the OOT fluxes are less scattered and thus daily dynamics are more steady, particularly during nighttime. In most cases, the OOT daytime fluxes shifted towards slightly higher absolute values, irrespective of flux direction. In contrast, almost no effects were found for daytime fluxes in June 2015 at EC3 and EC5. Nevertheless, the mean monthly flux for June 2015 decreased at most sites except for EC3 (i.e., the net uptake of CO_2 increased). The relative change ranged from -32 % at EC5 to +2 % at EC3. For those months with net CO_2 release, the effect of eliminating low-frequencies was less systematic, but yielded a higher mean flux at four out of the six sites. The relative change of mean monthly NEE as a result of ogive optimization ranged from -3 % (EC3 and EC5) to +13 % (EC4).

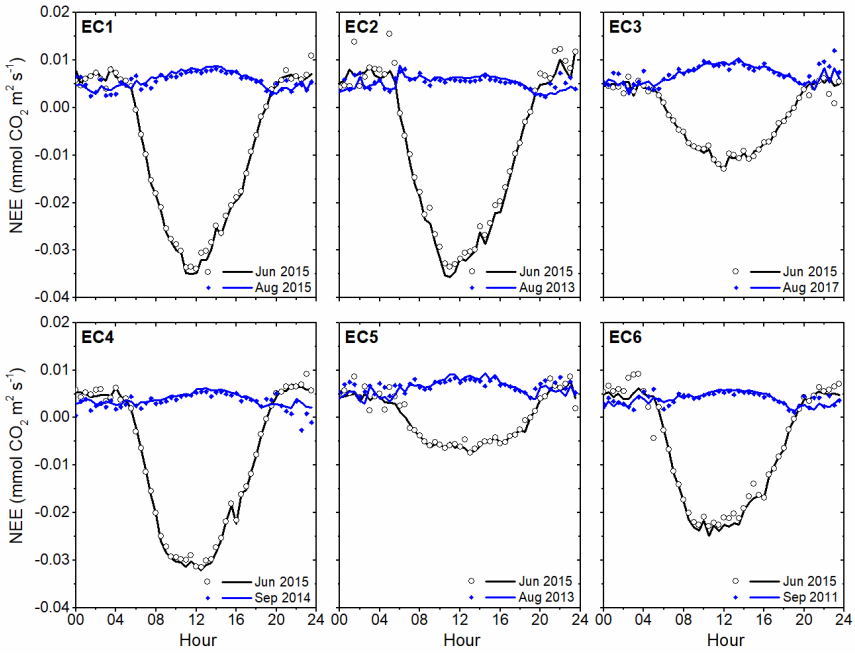

Fig. 4.6. Low-frequency contributions. Monthly mean diurnal courses of net ecosystem exchange (NEE) of fully developed canopies (black) and fallow periods (blue). NEE was computed based on the conventional 30 min averaging interval (symbols) and the ogive optimization method (OOM, lines). The OOM filters out low-frequency flux contributions.

4.3.5. Controlling factors of CO_2 exchange

No significant relationship was found between the GDD from 1 April until the harvest of winter wheat and the cumulative NEE or GPP of winter wheat for these periods (Fig. 4.7a, b). Moreover, no distinct differences between the GDD of the two regions were evident when accumulated until the day of harvest. Contrastingly, significant relationships were found when only April and May were considered, with a stronger relationship between GDD and GPP (Fig. 4.7c, d). A higher GDD in April/May was observed in KR compared to SJ, with mean values of 671 and 565 °C, respectively. Relationships between GDD and the CO_2 exchange were stronger in KR than in SJ (Table 4.4). Nonetheless, the coefficient of correlation between the GDD in April/May and the NEE was comparable for both regions, while a stronger relationship with GPP was found in KR, but a much weaker one in SJ.

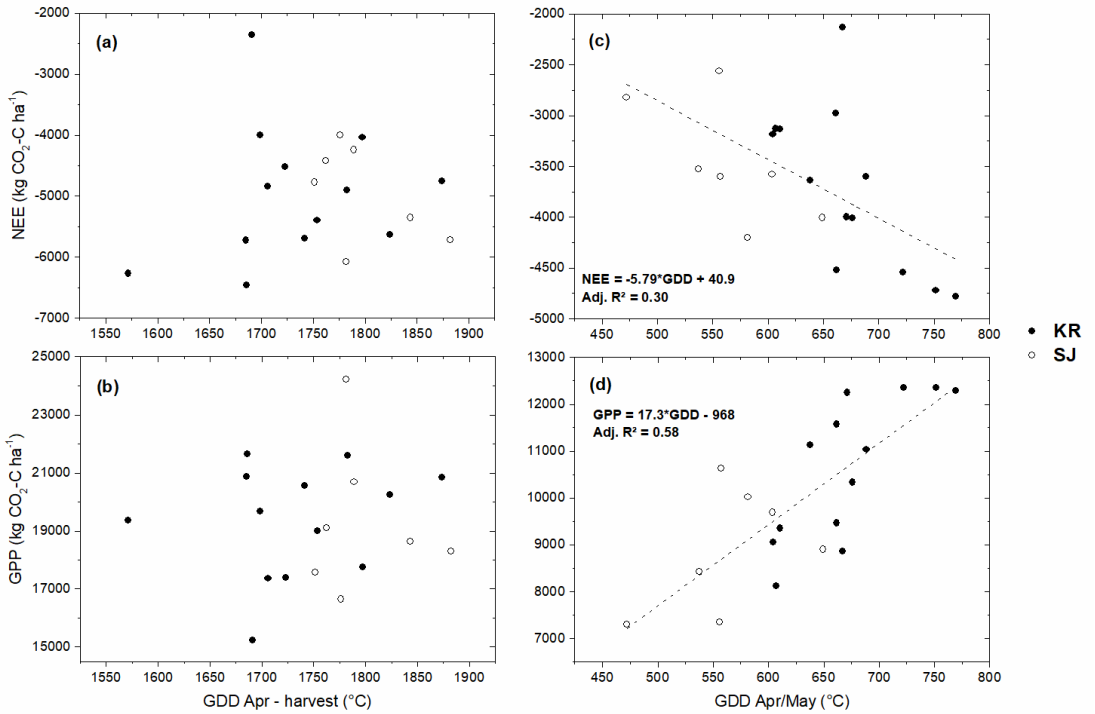

Fig. 4.7. Growing degree days. Correlation between net ecosystem exchange (NEE) and growing degree days (GDD), and gross primary productivity (GPP) and GDD measured in Kraichgau (KR, full circles) and Swabian Jura (SJ, open circles). The scatterplots are based on 20 site-years of winter wheat seasons. Panels (a) and (b) evaluate the period 1 April until harvest. Panels (c) and (d) evaluate the months April and May (main growing period).

Table 4.4. Linear regression of growing degree days (GDD) in April and May (°C) versus net ecosystem exchange (NEE) of CO_2 (kg CO_2-C ha^{-1}) and gross primary production (GPP, kg CO_2-C ha^{-1}) for the same period of the 20 site years with winter wheat cropping as well as the measured aboveground net primary production (ANPP, kg C ha^{-1}) versus NEE and GPP for all site years with sufficient data availability (46).

Linear regression	Kraichgau				Swabian Jura			
	Slope	Intercept	Pearson's r	Adj. R^2	Slope	Intercept	Pearson's r	Adj. R^2
NEE *vs.* GDD A/M	-10.5	3359	-0.69	0.42	-6.93	446	-0.65	0.30
GPP *vs.* GDD A/M	22.4	-4403	0.77	0.56	11.5	2413	0.49	0.09
NEE *vs.* ANPP	-0.51	-418	-0.81	0.65	-0.50	-530	-0.71	0.48
GPP *vs.* ANPP	1.86	3748	0.92	0.84	1.48	5175	0.63	0.37

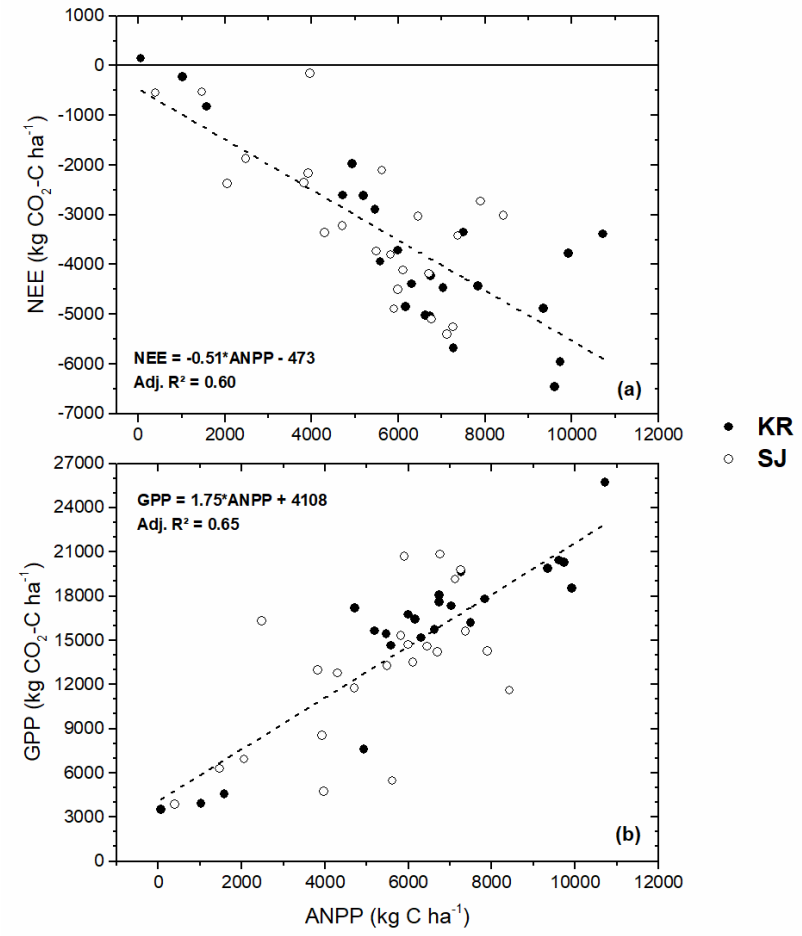

Fig. 4.8. Aboveground net primary production. Relationship between (a) the net ecosystem exchange (NEE) and aboveground net primary production (ANPP) and (b) gross primary productivity (GPP) and ANPP. Figures created based on all available site-years for Kraichgau (KR) and Swabian Jura (SJ).

To investigate the relationship between crop growth dynamics and CO_2 exchange, we related the observed C accumulation in aboveground biomass during a particular period to measured and gap-filled NEE and simulated GPP for the same period and all available site years (Fig. 4.8). As indicated by the slope of linear regression, the measured net CO_2-C exchange above the canopy was roughly 50 % of the aboveground net primary production (ANPP) of the crops (Fig. 4.8a). The coefficient of correlation (r) and the adjusted coefficient of determination (Adj. R^2) suggested a rather strong relationship. Separating the data for the two regions showed an even closer relationship in KR, but a weaker one in SJ, while the slope of linear regression remained almost constant (Table 4.4). The same result was obtained for GPP *vs*. ANPP, while the relationship was closer compared to NEE *vs*. ANPP in each case. For the whole dataset, the slope of linear regression indicated that an additional 75 % of photosynthetically fixed C was necessary to generate a certain amount of C in crop tissues (Fig. 4.8b). Regarding the individual regions,

the relationship was clearly closer in KR than in SJ; the slope of linear regression increased for the KR data, but decreased for SJ compared to the complete dataset. Both regressions for ANPP yielded a higher absolute intercept for SJ compared to KR (Table 4.4).

4.4. Discussion

4.4.1. Methodological aspects

Long-term experiments in German croplands showed no significant depletion of SOC under constant management (Körschens et al., 2014). In contrast, C budgets based on measuring the CO_2 exchange above the crop canopy over shorter periods (e.g., Kutsch et al., 2010; Prescher et al., 2010; Schmidt et al., 2012; Buysse et al., 2017) consistently revealed net C losses from agroecosystems. Although we observed slightly decreasing SOC concentrations in the top soils at four of our six study sites, the annual concentration change was not significantly different from zero (Table 4.1). At EC6, a significant increase in SOC concentration was observed. It has to be noted, however, that these measurements were based on three permanently installed plots at each study site. Due to the generally high spatial variability of SOC, the number of plots was probably not sufficient to represent this variability on the large study sites. Skinner and Dell (2014) demonstrated that C budget estimates based on EC and soil core measurements can differ substantially and comparing both methods is challenging. As EC is the state-of-the-art method for analyzing the spatially integrated ecosystem-scale C exchange, we will focus our discussion on the results obtained by EC.

Depending on site and weather conditions, winter-time CO_2 fluxes might contribute significantly to annual NEE (Buysse et al., 2017). Importantly, by generating two full-year datasets at sites EC2 and EC6, we were able to quantify the contribution of cumulated NEE during the period without measurements at the other four sites to the annual NEE budgets. Clearly, the proportion of NEE during a certain period on annual NEE becomes greater the more one component, GPP or R_{ECO}, dominates during that period. Our measurements demonstrated that winter-time CO_2 exchange can generally be regarded as being balanced. The exception is distinctively warm periods combined with the absence of assimilating vegetation cover and thus dominated by R_{ECO}.

The approach of filling missing winter measurements by using the parameterizations from Lasslop et al. (2010) for the periods before and after the gaps yielded in most cases equal or even smaller mean residuals compared to parameterizations based on winter data (Figs. S1 and S2). We argue that the residue analysis presented here demonstrated the validity and usability of this gap-filling approach, although the

periods without measurements should be kept as short as possible. The onset of the growing season was identified as being the determining period for the total annual CO_2 budget. This makes it important to obtain reliable measurements during this transition period (Poyda et al., 2017).

For selected periods, the ogive optimization method demonstrated that the contribution of low-frequency fluctuations explained part of the scatter often observed for fluxes averaged over 30 min, particularly at night (Fig. 4.6). As postulated by Sievers et al. (2015), relative differences between conventionally calculated and ogive-optimized fluxes tended to be higher when flux values were small. However, on a monthly basis, over- and underestimation of the ogive optimization method outbalanced each other. This led to negligible total effects, particularly during periods without CO_2 uptake. Importantly, the method eliminated implausible outliers from the dataset that might, in some cases, affect CO_2 budgets, such as for example in June 2015 at EC2 and in September 2014 at EC4. Finally, fluxes driven by low-frequency fluctuations can legitimately be disregarded when the aim of the research is to link fluxes to local site or management activities. Particularly under non-stationary conditions, the EC method systematically fails to capture both high and low frequencies at the same time (Kidston et al., 2010), further supporting the notion of neglecting low-frequency fluctuations.

As the state-of-the-art approach, we used the widely-accepted WPL correction for density effects due to water vapor and heat transfer on CO_2 fluxes (Webb et al., 1980). As this approach only accounts for density fluctuations of dry air, Liu (2005) raised concerns about the suitability of the WPL correction for ecosystems where water vapor significantly contributes to air density fluctuations. In agroecosystems with high transpiration rates of the crop canopy, latent heat fluxes are generally high, with Bowen ratios well below unity during the main growing season (Wizemann et al., 2015). By applying an alternative approach that accounts for density fluctuations in both dry air and water vapor, Liu (2005) obtained a 26 % larger C sink during the growing season at a spruce forest stand in Alaska. This resulted from higher CO_2 uptake during the day and lower respiration rates at night compared to the WPL correction. Although boreal spruce forests and temperate agroecosystems differ distinctly, water vapor density fluctuations are likely to have a substantial effect on measured fluxes at our study sites as well. Thus, the applied WPL correction might have underestimated the C sink or overestimated the C source activity at our sites. In the light of the debate on the validity of the different concepts (Kowalski, 2006; Liu, 2006), we applied the standard WPL correction to our dataset.

4.4.2. Characteristics of CO_2 exchange patterns

Although no systematic differences were recorded between the annual CO_2 budgets of the two study regions KR and SJ, the temporal dynamics over the course of the year differed distinctly due to different pedoclimatic conditions. The higher elevation in SJ was reflected in generally lower temperatures, and the growing season started 2-3 weeks later in the year. This was the case in each of the eight years, with the most pronounced shift in the period March-July 2013 (Fig. 4.2a). As the GDD in spring significantly affected photosynthetic activity (Fig. 4.7), the lower net CO_2 uptake (Fig. 4.3) most likely reflected the lower temperatures in SJ. When calculated for the period 1 April until final harvest, however, the GDD showed no significant differences between the regions, and no relationship with GPP or NEE was found. This can be explained by the later harvest in SJ. Thus, the later onset of the growing season in SJ is compensated by later harvest dates, reaching similar GDD as in KR.

While the mean diurnal course of NEE above winter wheat was similar in both regions in June, daily CO_2 uptake rates in July were much higher in SJ. This reflects the high summer temperatures in KR, accelerating ripening of the wheat plants (Dietiker et al., 2010), while the milder summers in SJ allow the crops to conduct photosynthesis and to accumulate biomass over a longer period. Thus, at our study sites, the theoretical approach of calculating GDD following McMaster and Wilhelm (1997) does not give a valid proxy for CO_2 uptake until maturity. This is because, firstly, no heat stress is considered and, secondly, photosynthesis is low during the ripening phase when assimilates are re-allocated to the storage organs (even though GDD might be very high during this period).

Multi-site studies have revealed that net C losses from arable fields tend to be higher at sites with high soil C contents (Kutsch et al., 2010). The results of our study did not confirm this (compare Tables 4.1 and 4.3): we observed no general trend towards higher soil respiration at the C-rich SJ sites. Note, however, that respiration measured by the EC method is the sum of heterotrophic and autotrophic respiration, making it difficult to separate the two processes. Higher nighttime CO_2 release could therefore reflect higher productivity and thus crop respiration rather than higher soil respiration. This is underlined by a very close relationship between the annual sums of GPP and R_{ECO} (slope = 1.03, r = 0.91), as was also shown in other studies (e.g., Gilmanov et al., 2013).

At the three KR sites, Demyan et al. (2016) used chamber respiration measurements on vegetated and bare fallow plots to separate the different components of R_{ECO} from EC measurements. They estimated that heterotrophic respiration accounted for an average 31 % of R_{ECO} under winter wheat. No such estimate was available for SJ. The relationship between the annual R_{ECO} and GPP, however, showed the

same strength for both regions (r = 0.89), while for SJ the linear regression showed a slightly larger slope (0.99 compared to 0.95 for KR) and a much lower intercept (53 compared to 2470 kg CO_2-C ha^{-1} yr^{-1} for KR). This indicates that the proportion of heterotrophic respiration from total R_{ECO} was lower at the SJ sites despite their higher SOC contents. Along the same line, Ali et al. (2018) reported that specific soil respiration (g^{-1} SOC) and potential enzyme activities were higher in KR *vs*. SJ soil samples. While microbial biomass significantly explained soil respiration in SJ, the SOC content was the most important factor in KR. These results suggest that the abiotic conditions for microbial growth limited SOC decomposition in SJ, while substrate availability limited it in KR. Thus, the colder and wetter climate in SJ presumably reduced soil microbial activity due to lower soil temperatures and temporarily high soil moisture contents.

The relationships between the ANPP and the NEE and GPP (Fig. 4.8) provided insights into the proportions of fixed C accumulated in aboveground crop biomass. The linear regression slopes revealed that the gross photosynthetic C uptake was on average 75 % higher, while the net C uptake was 50 % lower than the C accumulation in aboveground crop biomass over a given period. The intercept from GPP *vs*. ANPP illustrated that, on average, roughly 4100 kg CO_2-C ha^{-1} were fixed without any aboveground C enrichment. This was due to autotrophic respiration in the same magnitude or a pronounced belowground C allocation. Nonetheless, measurements with low ANPP were made during the ripening phase, and annual, highly cultured crops are mainly allocating assimilates to their generative organs at this stage, resulting in low fractions of belowground net primary production (fBNPP) (Loges et al., 2018; Pausch and Kuzyakov, 2018).

While the negative intercept of NEE *vs*. ANPP suggests that BNPP exceeded R_{ECO} during periods with no ANPP, this finding may reflect the variable dataset involving different crops and periods covered. Time series with ANPP close to zero were available only for winter wheat. The wheat-specific linear regression of NEE *vs*. ANPP showed an intercept of 622 kg CO_2-C ha^{-1}, supporting the aforementioned assumption that BNPP is also very low during these periods. Interestingly, the wheat-specific analysis of GPP also yielded in a different picture compared to the whole dataset. For winter wheat, each kg of C in ANPP was related to 2.2 kg C fixed by photosynthesis, indicating that the sum of autotrophic respiration and BNPP was more than twice the ANPP. This slope was only 1.55 for maize, illustrating the potentially higher C use efficiency (CUE) of C4 crops (Choudhury, 2001).

Beyond these crop-specific differences, regional characteristics were also observed (Table 4.4). The lower slope of GPP *vs*. ANPP at the SJ sites potentially reflects less root growth due to the low solum

thicknesses and a higher water availability in top soil layers compared to KR. Furthermore, lower autotrophic respiration due to lower temperatures in SJ likely contributed to the observed higher mean CUE (Choudhury, 2001). The much weaker relationship in SJ than in KR represented the higher variability in site and weather conditions as well as the crops grown there. More research is needed to provide more detailed insights into the plant functional traits of different crops, particularly under variable environmental conditions. These future efforts should combine highly resolved measurements of above- and belowground net primary production (NPP), ecosystem scale fluxes and flux partitioning as well as isotopic labeling (Riederer et al., 2015).

4.4.3. CO_2 and carbon budgets

4.4.3.1. NEE

Annual NEE showed a distinct variability and ranged from -6540 to 2400 kg CO_2-C ha^{-1} yr^{-1}. Interestingly, minimum and maximum NEE were observed in two consecutive years on the same site (EC1 2011 and 2012) cropped with winter wheat and winter rapeseed, respectively. Our results emphasize that the inter-annual variability of CO_2 fluxes clearly outweighed site-specific effects in these intensively managed crop rotations. The mean annual NEE from the six study sites and the eight-year observation period was -2580 kg CO_2-C ha^{-1} yr^{-1}, with a site-specific range between -1630 (EC3) and -3630 kg CO_2-C ha^{-1} yr^{-1} (EC5). This result corresponds well with the mean annual NEE of -2400 kg CO_2-C ha^{-1} yr^{-1} reported by Kutsch et al. (2010) for a four-year observation period on seven European crop sites with site-specific means between -1470 and -4610 kg CO_2-C ha^{-1} yr^{-1}. Schmidt et al. (2012) conducted EC measurements over a winter wheat field in western Germany and observed a constant NEE of -2700 kg CO_2-C ha^{-1} yr^{-1} during two consecutive years. This is very close to the mean annual NEE of -2920 kg CO_2-C ha^{-1} yr^{-1} for 13 winter wheat site-years on European croplands measured by Ceschia et al. (2010).

In the present study, the mean annual net CO_2 uptake from 20 site-years of winter wheat cropping was -3250 kg CO_2-C ha^{-1} yr^{-1}. The variability, however, was large, ranging from very high net uptakes to net losses in 2016 and 2017 on EC3. As these two years showed the overall lowest wheat yields, crop productivity seems to be the major factor controlling net CO_2 budgets on our study sites. This was underlined by the results of the statistical analysis, indicating no significant effects of region or site on NEE. Weather conditions, however, indirectly affected CO_2 exchange by determining the variability of crop growth. This effect, for example, was evident in the two winter barley years on EC6, showing a

high variability with NEE of -6290 kg CO_2-C ha^{-1} yr^{-1} in 2012 and -1140 kg CO_2-C ha^{-1} yr^{-1} in 2015. Crop rotational effects can be excluded in this case because the rotation was constant at EC6, with winter wheat preceding winter barley and cover crops being seeded after harvest. Thus, the weather conditions most likely explain this huge difference in annual NEE: 2015 was the driest and second warmest year of the observation period. This resulted in the highest annual R_{ECO} observed in SJ, while GPP was slightly reduced compared to 2012.

Beside these occasional strong inter-annual deviations for the same crops, the predominant crop effect on NEE was particularly pronounced for winter rapeseed, i.e. no significant differences were observed between the mean NEE of the other main crops (Fig. 4.5). Those years with winter rapeseed harvest were characterized by the lowest mean net CO_2 uptake (-336 kg CO_2-C ha^{-1} yr^{-1}), and two out of six years showed net CO_2 emissions. In contrast, Ceschia et al. (2010) reported a rather high net uptake of -3060 kg CO_2-C ha^{-1} yr^{-1} for a winter rapeseed year on a site in eastern Germany. On a cropland in France, Béziat et al. (2009) measured an NEE of -2860 kg CO_2-C ha^{-1} yr^{-1} over winter rapeseed; this was slightly lower than over winter wheat, but distinctly higher compared to maize. At our study sites, the monthly patterns of mean diurnal CO_2 exchange (Fig. 4.3) clearly indicated a lower CO_2 uptake capacity of winter rapeseed compared to winter wheat and silage maize in both regions, whereas the nocturnal CO_2 release was similar or higher. Our results support the findings of Moors et al. (2010), who emphasized that crop choice is the most important factor determining the magnitude of cropland CO_2 exchange.

In interpreting annual NEE, note that budgets were calculated for calendar years in order to compare periods of similar length. Thus, some of the variability likely reflects different conditions after harvest of the main crop (and in the case of summer crops, also before seeding). When NEE was cumulated from seeding until harvest, the relative variability decreased for the summer crops silage maize (from 46 to 29 %) and spring barley (from 379 to 12 %). In contrast, relative variability increased from 50 to 78 % for winter barley and from 57 to 67 % for winter wheat when NEE was calculated from seeding until harvest. The very high variability of winter rapeseed decreased from 432 to 155 % of mean NEE. These results illustrate the great importance of the non-growing season CO_2 exchange on annual NEE budgets. As the growing season is particularly short for summer cereals such as spring barley, the non-growing season strongly determines its annual C budgets (Prescher et al., 2010).

The higher variability in cropping period budgets of winter cereals might be a result of different seeding dates between the regions and years, combined with a variable pre-winter development of crops depending on weather conditions. As the growth rates of winter cereals are generally low in autumn,

R_{ECO} often dominates NEE (Béziat et al., 2009). For instance, mean gap-filled daily NEE in October was 7.7, 12.5 and -8.2 kg CO_2-C ha^{-1} d^{-1} for winter barley, winter wheat and winter rapeseed, respectively. This reflects the differences in seeding dates, with highest net emissions for the generally later seeded winter wheat. Accordingly, conditions controlling heterotrophic respiration can strongly impact NEE during these periods and therefore also the variability of C budgets. Mild temperatures during the non-growing season, in combination with moderate amounts of rainfall and readily available substrates from harvest residues, probably enhanced microbial activity in the soil and therefore increased non-growing season C losses (Ali et al., 2015.

4.4.3.2. NBP

In the present study, the mean annual NBP from 46 site-years was 1190 kg C ha^{-1} yr^{-1}, which was somewhat higher than the average 950 kg C ha^{-1} yr^{-1} observed by Kutsch et al. (2010) on seven European sites. With a standard deviation (SD) of 2690 kg C ha^{-1} yr^{-1}, the variability on our sites was large, and the cultivated crop was the most important factor explaining this variability. Statistical analysis of annual NBP, however, was limited by the huge differences in the number of available years for the different crops. Nonetheless, mean annual NBP showed distinct differences among the observed crops, from net C gains to high net C losses. For winter cereals, a negative to neutral mean annual NBP was observed: -1690 kg C ha^{-1} yr^{-1} for spelt (n = 1), -1340 ± 1860 kg C ha^{-1} yr^{-1} for winter barley (n = 4) and -190 ± 1860 kg C ha^{-1} yr^{-1} for winter wheat (n = 20). Winter rapeseed lost on average 1430 ± 1930 kg C ha^{-1} yr^{-1} (n = 6), while the late covering (summer) crops such as grain maize (n =1), spring barley (n = 2) and silage maize (n = 12) lost 1220, 2140 ± 1110 and 4280 ± 1920 kg C ha^{-1} yr^{-1}, respectively. In contrast, Kutsch et al. (2010) reported net C losses of 1780 kg C ha^{-1} yr^{-1} for winter wheat years, and during the two-year study of Schmidt et al. (2012) the NBP of wheat was even higher, with losses of 2460 and 2010 kg C ha^{-1} yr^{-1}. Sites with winter rapeseed lost slightly lower amounts of C (1090 kg C ha^{-1} yr^{-1}) in the study of Kutsch et al. (2010). Those authors reported almost exactly the same high C losses for silage maize years (4300 kg C ha^{-1} yr^{-1}).

While the NEE is affected by crop- and soil-specific CO_2 exchange patterns as well as weather-induced inter-annual variability, the variability of NBP is additionally controlled by management-related C fluxes. On our study sites, the share of C inputs in total NBP was relatively low (overall mean: 4.3 %) when absolute values of NBP components were summed up. Only in a single year (EC6 2015) was a share of 30 % reached due to very high organic fertilizer inputs. The NBP was mainly controlled by the

amount of C export via harvest, with NBP increasing as the ratio of exported to imported C ($C_{ex}/(NEE+C_{in})$) increased (Fig. 4.9). Sites acted as C sources when this ratio reached values greater 1. For the main crops observed, the ratio was 0.8 (winter barley), 0.9 (winter wheat), 1.3 (winter rapeseed) and 4.5 (silage maize).

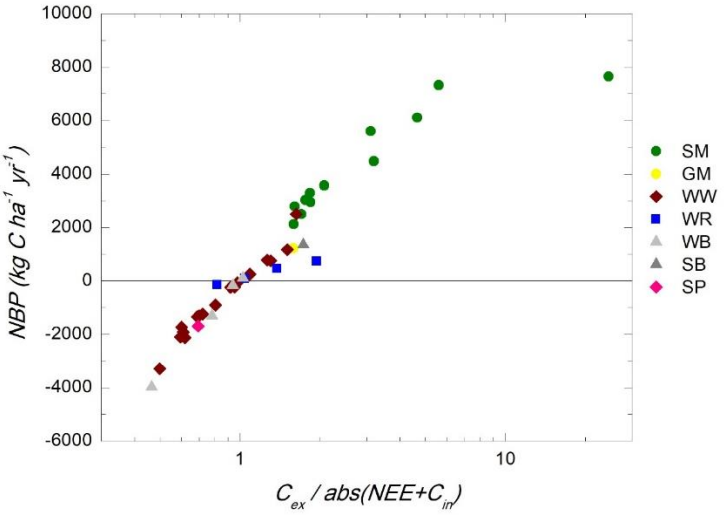

Fig. 4.9. Carbon export. Relationship between net biome productivity (NBP) and the ratio of exported carbon to carbon import as the absolute values of net ecosystem exchange (if negative) and organic fertilization. SM: Silage maize, GM: Grain maize, WW: Winter wheat, WR: Winter rapeseed, WB: Winter barley, SB: Summer barley, SP: Spelt. Share computed as percentage of exported carbon in NBP**.**

4.4.4 Management strategies to avoid carbon losses

Our findings of net C losses from croplands strongly challenge the '4 per mille goal' as the theoretical annual increase of global SOC stocks needed to compensate for CO_2 emissions from fossil fuels (Minasny et al., 2017). As stated above, the mean annual C loss of 1.19 t C ha^{-1} from our study sites was within the range of values reported in other studies on croplands in Germany or Europe. This significant C source function of croplands is alarming because it promotes global climate change. Another important concern is that diminishing SOC stocks threaten soil quality and thus agricultural production potential (Loveland and Webb, 2003).

Several management recommendations have been forwarded to mitigate C losses from agricultural soils or to enhance soil C sequestration (e.g., Lal, 2004; Smith et al., 2008). In their review, Stockmann et al. (2013) provided a potential C sequestration rate of 0.5-1.0 t C ha^{-1} yr^{-1} for conservation tillage. In non-tilled soils, soil organic matter (SOM) is stabilized due to intensive aggregation and the formation of persistent micro-within-macroaggregate fractions (Six and Paustian, 2014). At our SJ sites, however, the

lower tillage intensity did not result in lower net C losses compared to the regularly ploughed KR fields (Tables 4.2 and 4.3). The higher C stocks at the SJ sites more likely reflect the clay-rich soils and the cooler climate conditions compared to the KR (Poeplau et al., 2011). By evaluating studies on no-till management and its effects on soil C sequestration and crop productivity, Ogle et al. (2012) identified a threshold of 15 % decline in total (above- and belowground) C inputs in no-till versus conventional tillage. Below this threshold, no-till increased SOC stocks due to lower decomposition rates. Eugster et al. (2010) reported that short-term (7 days) respiration rates increased most strongly after late-season inverting moldboard ploughing among several management activities on European croplands. Despite the evidence of positive effects of reduced or no tillage agricultural practices, their potential for C sequestration and climate change mitigation has recently been challenged. This is mainly due to the relatively minor additional C accumulation (Powlson et al., 2014) as well as to the discontinuous application of no-till in practice and potentially elevated nitrous oxide (N_2O) emissions (VandenBygaart, 2015).

Cover crops are often linked to various environmental benefits. Besides positive effects on erosion control and nutrient use efficiencies (Valkama et al., 2015; Komainda et al., 2017), they probably enhance C sequestration because they are generally not removed from the field but incorporated into the soil (Poeplau and Don, 2015). Stockmann et al. (2013) specified a C sequestration potential of 0.2-0.5 t C ha^{-1} yr^{-1} by introducing cover crops in crop rotations. The ability of cover crops to accumulate sufficient biomass before winter, however, strongly depends on species and sowing date (Komainda et al., 2016). Own measurements of cover crop biomass at the end of the growing season indicated very variable plant development ranging from 0.6 (EC5 2015/16) to 5.5 t ha^{-1} (EC3 2017/18) of aboveground DM. As seeding of cover crops generally took place before 1 September to meet the requirements of the EU Common Agricultural Policy, GDD before the end of the vegetation period should have been sufficient for high biomass accumulation (Komainda et al., 2016). Thus, the high variability in cover crop development was most likely controlled by seeded species and growing conditions in late summer and autumn.

On average, cover crop growth strongly reduced C losses after harvest of the main crops from our study sites. In KR, the mean daily fluxes for the period September-October were 13.9 kg CO_2-C ha^{-1} d^{-1} without cover crops (bare soil/stubbles/voluntary emerged weeds or rapeseed) versus 4.8 kg CO_2-C ha^{-1} d^{-1} when cover crops were seeded. The difference was even larger in SJ: 18.7 versus 2.9 kg CO_2-C ha^{-1} d^{-1}, respectively. Cover crops can only be grown before summer crops. Due to the chosen budgeting for

calendar years, C fixation by cover crops in autumn reduces C losses attributed to the previous main crop. The potentially enhanced soil CO_2 efflux after cover crop incorporation in the following year might, however, increase C losses attributed to the subsequent summer crop. The picture of substantial C losses in silage maize years (Table 4.3 and Fig. 4.9), however, would not change essentially by accounting for this effect.

Management related C fluxes were the most important factor affecting the annual NBP of the study sites. As the application of organic fertilizers is known to increase SOC stocks (Tian et al., 2017), historical manure and slurry application on SJ sites might partly explain the higher SOC stocks compared to KR with a traditional rotation of cash crops and low or missing organic fertilizer inputs. Among the SJ sites, EC4 received much lower inputs of organic fertilizers and had the lowest SOC stock in the top soil although only slightly lower compared to EC5. In addition to organic fertilization, residue management represents a main factor for SOC conservation with residue addition generally related to positive effects on C sequestration. Consequently, frequent silage maize cropping (very high C removal) was the main reason for net C losses from the study sites. At EC4, where silage maize was grown only in the last year, the equally high mean NBP was additionally caused by the low net CO_2 uptake of spring barley.

C losses induced by land use changes are expected to attenuate in the long-term until a new equilibrium is reached (Poeplau et al., 2011). As our sites have been utilized as croplands since several decades, one interpretation of the observed C losses is that they might have been initiated by a considerable shift in crop rotations and management (Capriel, 2013). The German Renewable Energy Directive was legislated in 2000 and reimburses power generation from biomass. This led to a great expansion of the area cropped with silage maize for biogas production. According to the farmer managing the KR sites, silage maize has been grown since 2008 due to the installation of a nearby biogas plant. It has replaced grain maize and legumes in crop rotations. In contrast to silage maize, grain maize produces high inputs of aboveground harvest residues. In SJ, silage maize is used for both biogas production and as a forage crop. Therefore, its introduction to crop rotations occurred earlier than in KR. Nonetheless, growing maize for ruminant nutrition is still a rather recent development: due to the larger C stocks in SJ, even there, the time may have been insufficient to reach a new SOC equilibrium.

Maize, as a C4 crop, has a high resource use efficiency in terms of water and N (Wienforth et al., 2018). Our results, however, challenge the expansion of annual bioenergy cropping with the intention of mitigating CO_2 emissions. This strategy needs rejection not only when permanent grassland or natural vegetation is converted to cropland (Don et al., 2012; Abraha et al., 2018), but also when bioenergy

maize is grown on historical croplands. In line with our observations, Capriel (2013) reported decreasing SOC contents in top soils of Bavarian croplands (south Germany) during the period 1986-2007. The author attributed these C losses to decreasing amounts of applied farmyard manure and incorporated harvest residues. Higher SOC losses were found on croplands with higher proportions of silage maize, sugar beet and potato in crop rotations. For the northeastern United States, Dell et al. (2018) demonstrated that dairy forage or bioenergy crop rotations that combine silage maize with a multi-year perennial phase of alfalfa are able to sequester SOC. These findings indicate a promising alternative to the conventional rotations with annual crops and raises the need for more research on such kind of land use systems under Central European conditions.

4.5. Conclusions

Our multi-site approach demonstrated that the inter-annual on-site variability of net ecosystem exchange (NEE) and net biome productivity (NBP) was as large as the inter-site and even inter-region variability. Importantly, we identified the amount of harvested biomass as the major trigger controlling NBP and thus C losses. On the one hand, the high carbon use efficiency of maize compared to C3 crops makes it a valuable crop due to the high amounts of produced shoot biomass. Silage maize cropping with harvest of the whole aboveground biomass, on the other hand, has the potential to decrease soil organic carbon (SOC) stocks and thus deteriorate soil quality. Our results indicate that the recent increase in silage maize cropping for ruminant nutrition and biogas production has disturbed SOC stocks and induced the observed depletion. Particularly in Swabian Jura, high SOC stocks – combined with changing climatic conditions that potentially favor microbial decomposition – indicate that CO_2 emissions from soil C losses might be a long-lasting phenomenon. The recorded mean annual CO_2 emissions in silage maize years (15700 kg CO_2 ha^{-1} yr^{-1}) were substantially higher than what is generally considered as the mitigation potential of bioenergy maize compared to fossil fuels (roughly 10000 kg CO_2-equivalents ha^{-1} yr^{-1}). This makes it highly questionable whether growing silage maize for biogas production is actually a mitigation measure for CO_2 emissions from fossil fuels. The share of silage maize in crop rotations should therefore be low, underlining the need to diversify agroecosystems. Evaluating C sequestration potential therefore calls for more information on the C budgets of alternative crops such as grain legumes or temporary grass-clover mixtures and on full, more diverse crop rotations.

Acknowledgements

The authors gratefully acknowledge the financial support by the German Research Foundation (DFG) in the framework of the integrated research project PAK 346 'Structure and Function of Agricultural Landscapes under Global Climate Change', which was continued by the Research Unit FOR 1695 'Agricultural Landscapes under Global Climate Change – Processes and Feedbacks on a Regional Scale'. We thank the farmers Mr. Bosch senior† and Mr. Bosch junior (EC1-EC3), Mr. Fink (EC4), Mr. Hermann (EC5) and Mr. Reichart (EC6) for their committed cooperation. We also acknowledge the technical assistance with the eddy covariance measurements by Mr. Prechter, Mr. Baur, Mr. Schade and Mr. Schreiber.

References

Abraha, M., Hamilton, S.K., Chen, J., Robertson, G.P. (2018): Ecosystem carbon exchange on conversion of Conservation Reserve Program grasslands to annual and perennial cropping systems. Agr. Forest Meteorol., 253-254, 151-160, doi: 10.1016/j.agrformet.2018.02.016.

Ali, R.S., Ingwersen, J., Demyan, M.S., Funkuin, Y.N., Wizemann, H.-D., Kandeler, E., Poll, C. (2015): Modelling *in situ* activities of enzymes as a tool to explain seasonal variation of soil respiration from agro-ecosystems. Soil Biol. Biochem., 81, 291-303, doi: 10.1016/j.soilbio.2014.12.001.

Ali, R.S., Kandeler, E., Marhan, S., Demyan, M.S., Ingwersen, J., Mirzaeitalarposhti, R., Rasche, F., Cadisch, G., Poll, C. (2018): Controls on microbially regulated soil organic carbon decomposition at the regional scale. Soil Biol. Biochem., 118, 59-68, doi: 10.1016/j.soilbio.2017.12.007.

Béziat, P., Ceschia, E., Dedieu, G. (2009): Carbon balance of a three crop succession over two cropland sites in South West France. Agr. Forest Meteorol., 149, 1628-1645, doi: 10.1016/j.agrformet.2009.05.004.

Buysse, P., Bodson, B., Debacq, A., De Ligne, A., Heinesch, B., Manise, T., Moureaux, C., Aubinet, M. (2017): Carbon budget measurement over 12 years at a crop production site in the silty-loam region in Belgium. Agr. Forest Meteorol., 246, 241-255, doi: 10.1016/j.agrformet.2017.07.004.

Bretz, F., Hothorn, T., Westfall, P. (2011): Multiple comparisons using R, Chapman and Hall, CRC Press, London.

Capriel, P. (2013): Trends in organic carbon and nitrogen contents in agricultural soils in Bavaria (south Germany) between 1986 and 2007. Eur. J. Soil Sci., 64, 445-454, doi: 10.1111/ejss.12054.

Ceschia, E., Béziat, P., Dejoux, J.F., Aubinet, M., Bernhofer, Ch., Bodson, B., Buchmann, N., Carrara, A., Cellier, P., Di Tommasi, P., Elbers, J.A., Eugster, W., Grünwald, T., Jacobs, C.M.J., Jans, W.W.P., Jones, M., Kutsch, W., Lanigan, G., Magliulo, E., Marloie, O., Moors, E.J., Moureaux, C., Olioso, A., Osborne, B., Sanz, M.J., Saunders, M., Smith, P., Soegaard, H., Wattenbach, M. (2010): Management effects on net ecosystem carbon and GHG budgets at European crop sites. Agr. Ecosyst. Environ., 139, 363-383, doi: 10.1016/j.agee.2010.09.020.

Choudhury, B.J. (2001): Modeling radiation- and carbon-use efficiencies of maize, sorghum, and rice. Agr. Forest Meteorol., 106, 317-330, doi: 10.1016/S0168-1923(00)00217-3.

Dell, C.J., Gollany, H.T., Adler, P.R., Skinner, R.H., Polumsky, R.W. (2018): Implications of observed and simulated soil carbon sequestration for management options in corn-based rotations. J. Environ. Qual., 47, 617-624, doi: 10.2134/jeq2017.07.0298.

Demyan, M.S., Ingwersen, J., Funkuin, Y.N., Ali, R.S., Mirzaeitalarposhti, R., Rasche, F., Poll, C., Müller, T., Streck, T., Kandeler, E., Cadisch, G. (2016): Partitioning of ecosystem respiration in winter wheat and silage maize – modeling seasonal temperature effects. Agr. Ecosyst. Environ., 224, 131-144, doi: 10.1016/j.agee.2016.03.039.

Destatis (2017): Statistisches Bundesamt. https://www.destatis.de/DE/Startseite.html

Dietiker, D., Buchmann, N., Eugster, W. (2010): Testing the ability of the DNDC model to predict CO_2 and water vapor fluxes of a Swiss cropland site. Agr. Ecosyst. Environ., 139, 396-401, doi: 10.1016/j.agee.2010.09.002.

Don, A., Osborne, B., Hastings, A., Skiba, U., Carter, M.S., Drewer, J., Flessa, H., Freibauer, A., Hyvönen, N., Jones, M.B., Lanigan, G.J., Mander, Ü., Monti, A., Djomo, S.N., Valentine, J., Walter, K., Zegada-Lizarazu, W., Zenone, T. (2012): Land-use change to bioenergy production in Europe: implications for the greenhouse gas balance and soil carbon. GCB Bioenergy, 4, 372-391, doi: 10.1111/j.1757-1707.2011.01116.x.

Eugster, W., Moffat, A.M., Ceschia, E., Aubinet, M., Ammann, C., Osborne, B., Davis, P.A., Smith, P., Jacobs, C., Moors, E., Jans, W., Le Dantec, V., Béziat, P., Saunders, M., Jans, W., Grünwald, T., Rebmann, C., Kutsch, W.L., Czerný, R., Janouš, D., Moureaux, C., Dufranne, D., Carrara, A., Magliulo, V., Di Tommasi, P., Olesen, J.E., Schelde, K., Olioso, A., Bernhofer, C., Cellier, P., Larmanou, E., Loubet, B., Wattenbach, M., Marloie, O., Sanz, M.-J., Søgaard, H., Buchmann, N. (2010): Management effects on European cropland respiration. Agr. Ecosyst. Environ., 139, 236-362, doi: 10.1016/j.agee.2010.09.001.

Falge, E., Baldocchi, D., Olson, R., Anthoni, P., Aubinet, M., Bernhofer, C., Burba, G., Ceulemans, R., Clement, R., Dolmani, H., Granier, A., Gross, P., Grünwald, T., Hollinger, D., Jensen, N.O., Katulm, G., Keronen, P., Kowalski, A., Lai, C.T., Law, B.E., Meyers, T., Moncrieff, J., Moors, E., Munger, J.W., Pilegaard, K., Rannik, Ü., Rebmann, C., Suyker, A., Tenhunen, J., Tu, K., Verma, S., Vesala, T., Wilson, K., Wofsy, S. (2001): Gap filling strategies for defensible annual sums of net ecosystem exchange., Agr. Forest Meteorol., 107, 43-69, doi: 10.1016/S0168-1923(00)00225-2.

Foken, T., Göckede, M., Mauder, M., Mahrt, L., Amiro, B., Munger, W. (2004): Post-field data quality control. In: Lee, X., Massmann, W., Law, B. (Eds.): Handbook of micrometeorology. Atmospheric and oceanographic sciences library, vol. 29. Springer, Dordrecht, 181-208.

Foken, T., Wichura, B. (1996): Tools for quality assessment of surface-based flux measurements. Agric. For. Meteorol., 78, 83-105, doi: 10.1016/0168-1923(95)02248-1.

Foken, T. (2008): The energy balance closure problem: an overview. Ecol. Appl., 18, 1351-1367, doi: 10.1890/06-0922.1.

Gilmanov, T. G., Baker, J.M., Bernacchi, C.J., Billesbach, D.P., Burba, G.G., Castro, S., Chen, J., Eugster, W., Fischer, M.L., Gamon, J.A., Gebremedhin, M.T., Glenn, A.J., Griffis, T.J., Hatfield, J.L., Heuer, M.W., Howard, D.M., Leclerc, M.Y., Loescher, H.W., Marloie, O., Meyers, T.P., Olioso, A., Phillips, R.L., Prueger, J.H., Skinner, R.H., Suyker, A.E., Tenuta, M., Wylie, B.K.

(2014): Productivity and carbon dioxide exchange of leguminous crops: estimates from flux tower measurements. Agron. J., 106, 545-559, doi: 10.2134/agronj2013.0270.

Högy, P., Wieser, H., Köhler, P., Schwadorf, K., Breuer, J., Franzaring, J., Muntifering, R., Fangmeier, A. (2009): Effects of elevated CO_2 on grain yield and quality of wheat: results from a 3-year free-air CO_2 enrichment experiment. Plant Biol., 11 (Suppl. 1), 60-69, doi: 10.1111/j.1438-8677.2009.00230.x.

Högy, P., Franzaring, J., Schwadorf, K., Breuer, J., Schütze, W., Fangmeier, A. (2010): Effects of free-air CO_2 enrichment on energy traits and seed quality of oilseed rape. Agr. Ecosyst. Environ., 139, 239-244, doi: 10.1016/j.agee.2010.08.009.

Imukova, K., Ingwersen, J., Streck, T. (2015): Determining the spatial and temporal dynamics of the green vegetation fraction of croplands using high-resolution RapidEye satellite images. Agr. Forest Metorol., 206, 113-123, doi: 10.1016/j.agrformet.2015.03.003.

Ingwersen, J., Steffens, K., Högy, P., Warrach-Sagi, K., Zhunusbayeva, D., Poltoradnev, M., Gäbler, R., Wizemann, H.-D., Fangmeier, A., Wulfmeyer, V., Streck, T. (2011): Comparison of Noah simulations with eddy covariance and soil water measurements at a winter wheat stand. Agr. Forest Meteorol., 151, 345-355, doi: 10.1016/j.agrformet.2010.11.010.

Kidston, J., Brümmer, C., Black, T.A., Morgenstern, K., Nesic, Z., McCaughey, J.H., Barr, A.G. (2010): Energy balance closure using eddy covariance above two different land surfaces and implications for CO_2 flux measurements. Boundary-Layer Meteorol., 136, 193-218, doi: 10.1007/s10546-010-9507-y.

Klosterhalfen, A., Herbst, M., Weihermüller, L., Graf, A., Schmidt, M., Stadler, A., Schneider, K., Subke, J.-A., Huisman, J.A., Vereecken, H. (2017): Multi-site calibration and validation of a net ecosystem carbon exchange model for croplands. Ecol. Model., 363, 137-156, doi: 10.1016/j.ecolmodel.2017.07.028.

Komainda, M., Taube, F., Kluß, C., Herrmann, A. (2016): Above- and belowground nitrogen uptake of winter catch crops sown after silage maize as affected by sowing date. Eur. J. Agron., 79, 31-42, doi: 10.1016/j.eja.2016.05.007.

Komainda, M., Taube, F., Kluß, C., Herrmann, A. (2017): Effects of catch crops on silage maize (*Zea mays* L.): yield, nitrogen uptake efficiency and losses. Nutr. Cycl. Agroecosyst., doi: 10.1007/s10705-017-9839-9.

Kowalski, A.S. (2006): Comment on "An alternative approach for CO_2 flux correction caused by heat and water vapour transfer" by Liu. Bound.-Lay. Meteorol., 120, 353-355, doi: 10.1007/s10546-005-9044-2.

Körschens, M., Albert, E., Baumecker, M., Ellmer, F., Grunert, M., Hoffmann, S., Kismanyoky, T., Kubat, J., Kunzova, E., Marx, M., Rogasik, J., Rinklebe, J., Rühlmann, J., Schilli, C., Schröter, H., Schroetter, S., Schweizer, K., Toth, Z., Zimmer, J., Zorn, W. (2014): Humus and climate change – results of 15 long-term experiments. Arch. Agron. Soil Sci., 60:11, 1485-1517, doi: 10.1080/03650340.2014.892204.

Kutsch, W.L., Aubinet, M., Buchmann, N., Smith, P., Osborne, B., Eugster, W., Wattenbach, M., Schrumpf, M., Schulze, E.D., Tomelleri, E., Ceschia, E., Bernhofer, C., Béziat, P., Carrara, A., Di Tommasi, P., Grünwald, T., Jones, M., Magliulo, V., Marloie, O., Moureaux, C., Olioso, A., Sanz, M.J., Saunders, M., Søgaard, H., Ziegler, W. (2010): The net biome production of full crop rotations in Europe. Agr. Ecosyst. Environ., 139, 336-345, doi: 10.1016/j.agee.2010.07.016.

Laird, N. M., Ware, J. H. (1982): Random-effects models for longitudinal data, Biometrics, 38, 963-974, doi: 10.2307/2529876.

Lal, R. (2004): Soil carbon sequestration to mitigate climate change. Geoderma, 123, 1-22, doi: 10.1016/j.geoderma.2004.01.032.

Lasslop, G., Reichstein, M., Papale, D., Richardson, A.D., Arneth, A., Barr, A., Stoy, P., Wohlfahrt, G. (2010): Separation of net ecosystem exchange into assimilation and respiration using a light response curve approach: critical issues and global evaluation. Global Change Biol., 16, 187-208, doi: 10.1111/j.1365-2486.2009.02041.x.

Liu, H. (2005): An alternative approach for CO_2 flux correction caused by heat and water vapour transfer. Bound.-Lay. Meteorol., 115, 151-168, doi: 10.1007/s10546-004-2420-5.

Liu, H. (2006): Reply to the comment by Kowalski on "An alternative approach for CO_2 flux correction caused by heat and water vapour transfer". Bound.-Lay. Meteorol., 120, 357-363, doi: 10.1007/s10546-005-9042-4.

Loges, R., Bunne, I., Reinsch, T., Malisch, C., Kluß, C., Herrmann, A., Taube, F. (2018): Forage production on rotational systems generates similar yields compared to maize monocultures but improves soil carbon stocks. Eur. J. Agron., 97, 11-19, doi: 10.1016/j.eja.2018.04.010.

Loubet, B., Laville, P., Lehuger, S., Larmanou, E., Fléchard, C., Mascher, N., Genermont, S., Roche, R., Ferrara, R.M., Stella, P., Personne, E., Durand, B., Decuq, C., Flura, D., Masson, S., Fanucci, O., Rampon, J.-N., Siemens, J., Kindler, R., Gabrielle, B., Schrumpf, M., Cellier, P. (2011): Carbon, nitrogen and greenhouse gases budgets over a four years crop rotation in northern France. Plant Soil, 343, 109-137, doi: 10.1007/s11104-011-0751-9.

Loveland, P., Webb, J. (2003): Is there a critical level of organic matter in the agricultural soils of temperate regions: a review. Soil Tillage Res., 70, 1-18, doi: 10.1016/S0167-1987(02)00139-3.

LWKSH/Landwirtschaftskammer Schleswig-Holstein (2013): Richtwerte für die Düngung. 22. Auflage, LWKSH, Rendsburg, Germany.

Mauder, M., Foken, T., (2006): Impact of post-field data processing on eddy covariance flux estimates and energy balance closure. Meteorol. Zeitschrift, 15, 597–609, doi: 10.1127/0941-2948/2006/0167.

Mauder, M., Cuntz, M., Drüe, C., Graf, A., Rebmann, C., Schmid, H.P., Schmidt, M., Steinbrecher, R. (2013): A strategy for quality and uncertainty assessment of long-term eddy-covariance measurements. Agr. Forest Meteorol., 169, 122-135, doi: 10.1016/j.agrformet.2012.09.006.

McMaster, G.S., Wilhelm, W.W. (1997): Growing degree-days: one equation, two interpretations. Agr. Forest Meteorol., 87, 291–300, doi: 10.1016/S0168-1923(97)00027-0.

Mcmillen, R.T. (1988): An eddy-correlation technique with extended applicability to non-simple terrain, Bound.-Lay. Meteorol., 43, 231–245, doi: 10.1007/Bf00128405.

Minasny, B., Malone, B.P., McBratney, A.B., Angers, D.A., Arrouays, D., Chambers, A., Chaplot, V., Chen, Z.-S., Cheng, K., Das, B.S., Field, D.J., Gimona, A., Hedley, C.B., Hong, S.Y., Mandal, B., Marchant, B.P., Martin, M., McConkey, B.G., Mulder, V.L., O'Rourke, S., Richer-de-Forges, A.C., Odeh, I., Padarian, J., Paustian, K., Pan, G., Poggio, L., Savin, I., Stolbovoy, V., Stockmann, U., Sulaeman, Y., Tsui, C.-C., Vågen, T.-G., van Wesemael, B., Winowiecki, L. (2017): Soil carbon 4 per mille. Geoderma, 292, 59-86, doi: 10.1016/j.geoderma.2017.01.002.

Moore, C.J. (1986): Frequency response corrections for eddy correlation systems. Bound. Layer Meteor., 37, 17-35, doi: 10.1007/BF00122754.

Moors, E.J., Jacobs, C., Jans, W., Supit, I., Kutsch, W.L., Bernhofer, C., Béziat, P., Buchmann, N., Carrara, A., Ceschia, E., Elbers, J., Eugster, W., Kruijt, B., Loubet, B., Magliulo, E., Moureaux, C., Olioso, A., Saunders, M., Soegaard, H. (2010): Variability in carbon exchange of European croplands. Agr. Ecosyst. Environ., 139, 325-335, doi: 10.1016/j.agee.2010.04.013.

Ogle, S.M., Swan, A., Paustian, K. (2012): No-till management impacts on crop productivity, carbon input and soil carbon sequestration. Agr. Ecosyst. Environ., 149, 37-49, doi: 10.1016/j.agee.2011.12.010.

Osborne, B., Saunders, M., Walmsley, D., Jones, M., Smith, P. (2010): Key questions and uncertainties associated with the assessment of the cropland greenhouse gas balance. Agr. Ecosyst. Environ., 139, 293-301, doi: 10.1016/j.agee.2010.05.009.

Papale, D., Reichstein, M., Aubinet, M., Canfora, E., Bernhofer, C., Kutsch, W., Longdoz, B., Rambal, S., Valentini, R., Vesala, T., Yakir, D. (2006): Towards a standardized processing of net ecosystem Exchange measured with eddy covariance technique: algorithms and uncertainty estimation. Biogeosciences, 3, 571-583, doi: 10.5194/bg-3-571-2006.

Pausch, J., Kuzyakov, Y. (2018): Carbon input by roots into the soil: Quantification of rhizodeposition from root to ecosystem scale. Glob. Change Biol., 24, 1-12, doi: 10.1111/gcb.13850.

Poeplau, C., Don, A., Vesterdal, L., Leifeld, J., Van Wesemael, B., Schumacher, J., Gensior, A. (2011): Temporal dynamics of soil organic carbon after land-use change in the temperate zone - carbon response functions as a model approach. Global Change Biol., 17, 2415-2427, doi: 10.1111/j.1365-2486.2011.02408.x.

Poeplau, C., Don, A. (2015): Carbon sequestration in agricultural soils via cultivation of cover crops – A meta-analysis. Agr. Ecosyst. Environ., 200, 33-41, doi: 10.1016/j.agee.2014.10.024.

Poyda, A., Reinsch, T., Skinner, R.H., Kluß, C., Loges, R., Taube, F. (2017): Comparing chamber and eddy covariance based net ecosystem CO_2 exchange of fen soils. J. Plant Nutr. Soil Sc., 180, 252-266, doi: 10.1002/jpln.201600447.

Powlson, D.S., Stirling, C.M., Jat, M.L., Gerard, B.G., Palm, C.A., Sanchez, P.A., Cassman, K.G. (2014): Limited potential of no-till agriculture for climate change mitigation. Nat. Clim. Change, 4, 678-683, doi: 10.1038/NCLIMATE2292.

Premke, K., Attermeyer, K., Augustin, J., Cabezas, A., Casper, P., Deumlich, D., Gelbrecht, J., Gerke, H.H., Gessler, A., Grossart, H.-P., Hilt, S., Hupfer, M., Kalettka, T., Kayler, Z., Lischeid, G., Sommer, M., Zak, D. (2016): The importance of landscape diversity for carbon fluxes at the landscape level: small-scale heterogeneity matters. WIREs Water, doi: 10.1002/wat2.1147.

Prescher, A.-K., Grünwald, T., Bernhofer, C. (2010): Land use regulates carbon budgets in eastern Germany: From NEE to NBP. Agr. Forest Meteorol., 150, 1016-1025, doi: 10.1016/j.agrformet.2010.03.008.

Reichstein, M., Falge, E., Baldocchi, D., Papale, D., Aubinet, M., Berbigier, P., Bernhofer, C., Buchmann, N., Gilmanov, T., Granier, A., Grünwald, T., Havránková, K., Ilvesniemi, H., Janous, D., Knohl, A., Laurila, T., Lohila, A., Loustau, D., Matteucci, G., Meyers, T., Miglietta, F., Ourcival, J.-M., Pumpanen, J., Rambal, S., Rotenberg, E., Sanz, M., Tenhunen, J., Seufert, G., Vaccari, F., Vesala, T., Yakir, D., Valentini, R. (2005): On the separation of net ecosystem

exchange into assimilation and ecosystem respiration: review and improved algorithm. Global Change Biol., 11, 1424–1439. doi: 10.1111/j.1365-2486.2005.001002.x.

Riederer, M., Pausch, J., Kuzyakov, Y., Foken, T. (2015): Partitioning NEE for absolute C input into various ecosystem pools by combining results from eddy-covariance, atmospheric flux partitioning and $^{13}CO_2$ pulse labelling. Plant Soil, 390, 61-76, doi: 10.1007/s11104-014-2371-7.

Sakai, R.K., Fitzjarrald, D.R., Moore, K.E. (2001): Importance of low-frequency contributions to eddy fluxes observed over rough surfaces. J. Appl. Meteorol., 40, 2178–2192, doi: 10.1175/1520-0450(2001)040<2178:Iolfct>2.0.Co;2.

Schmidt, M., Reichenau, T.G., Fiener, P., Schneider, K. (2012): The carbon budget of a winter wheat field: An eddy covariance analysis of seasonal and inter-annual variability. Agr. Forest Meteorol., 165, 114-126, doi: 10.1016/j.agrformet.2012.05.012.

Schotanus, P., Nieuwstadt, F.T.M., De Bruin, H.A.R. (1983): Temperature measurement with a sonic anemometer and its application to heat and moisture fluxes. Bound. Layer Meteor., 26, 81-93, doi: 10.1007/BF00164332.

Sievers, J., Papakyriakou, T., Larsen, S.E., Jammet, M.M., Rysgaard, S., Sejr, M.K., Sørensen, L.L. (2015): Estimating surface fluxes using eddy covariance and numerical ogive optimization. Atmos. Chem. Phys., 15, 2081-2103, doi: 10.5194/acp-15-2081-2015.

Six, J., Paustian, K. (2014): Aggregate-associated soil organic matter as an ecosystem property and a measurement tool. Soil Biol. Biochem., 68, A4-A9, doi: 10.1016/j.soilbio.2013.06.014.

Skinner, R.H., Dell, C.J. (2014): Comparing pasture C sequestration estimates from eddy covariance and soil cores. Agr. Ecosyst. Environ., 199, 52-57, doi: 10.1016/j.agee.2014.08.020.

Smith, J., Smith, P., Wattenbach, M., Zaehle, S., Hiederer, R., Jones, R.J.A., Montanarella, L., Rounsevell, M.D.A., Reginster, I., Ewert, F. (2005): Projected changes in mineral soil carbon of European croplands and grasslands, 1990 – 2080. Global Change Biol., 11, 2141-2152, doi: 10.1111/j.1365-2486.2005.01075.x.

Smith, P., Powlson, D.S., Glendining, M.J., Smith, J.U. (1997): Potential for carbon sequestration in European soils: preliminary estimates for five scenarios using results from long-term experiments. Global Change Biol., 3, 67-79, doi: 10.1046/j.1365-2486.1997.00055.x.

Smith, P., Falloon, P.D., Körschens, M., Shevtsova, L.K., Franko, U., Romanenkov, V., Coleman, K., Rodionova, V., Smith, J.U., Schramm, G. (2002). EuroSOMNET – a European database of long-term experiments on soil organic matter: the WWW metadatabase. J. Agr. Sci., 138, 123-134, doi: 10.1017_S0021859601001800.

Smith, P., Martino, D., Cai, Z., Gwary, D., Janzen, H., Kumar, P., McCarl, B., Ogle, S., O'Mara, F., Rice, C., Scholes, B., Sirotenko, O., Howden, M., McAllister, T., Pan, G., Romanenkov, V., Schneider, U., Towprayoon, S., Wattenbach, M., Smith, J. (2008): Greenhouse gas mitigation in agriculture. Philos. Trans. R. Soc. B, 363, 789-813, doi:10.1098/rstb.2007.2184.

Smith, P., Lanigan, G., Kutsch, W.L., Buchmann, N., Eugster, W., Aubinet, M., Ceschia, E., Béziat, P., Yeluripati, J.B., Osborne, B., Moors, E.J., Brut, A., Wattenbach, M., Saunders, M., Jones M. (2010): Measurements necessary for assessing the net ecosystem carbon budget of croplands. Agr. Ecosyst. Environ., 139, 302-315, doi: 10.1016/j.agee.2010.04.004.

Stockmann, U., Adams, M.A., Crawford, J.W., Field, D.J., Henakaarchchi, N., jenkins, M., Minasny, B., McBratney, A.B., de Remy de Courcelles, V., Singh, K., Wheeler, I., Abbott, L., Angers, D.A.,

Baldock, J., Bird, M., Brookes, P.C., Chenu, C., Jastrow, J.D., Lal, R., Lehmann, J., O'Donnell, A.G., Parton, W.J., Whitehead, D., Zimmermann, M. (2013): The knowns, known unknowns and unknowns of sequestration of soil organic carbon. Agr. Ecosyst. Environ., 164, 80-99, doi: 10.1016/j.agee.2012.10.001.

Tian, J., Lou, Y., Gao, Y., Fang, H., Liu, S., Xu, M., Blagodatskaya, E., Kuzyakov, Y. (2017): Response of soil organic matter fractions and composition of microbial community to long-term organic and mineral fertilization. Biol. Fertil. Soils, doi: 10.1007/s00374-017-1189-x.

TLL/Thüringer Landesanstalt für Landwirtschaft (2012): Inhaltsstoffe von Biogassubstraten und Gärresten (Datenblätter). TLL, Jena, Germany.

UBA/Umweltbundesamt (2018): National Inventory Report for the German Greenhouse Gas Inventory 1990 – 2016, Submission under the United Nations Framework Convention on Climate Change and the Kyoto-Protocol 2018, UBA, Dessau-Roßlau, Germany.

Valkama, E., Lemola, R., Känkänen, H., Turtola, E. (2015): Meta-analysis of the effects of undersown catch crops on nitrogen leaching loss and grain yields in the Nordic countries. Agr. Ecosyst. Environ., 203, 93-101, doi: 10.1016/j.agee.2015.01.023.

VandenBygaart, A.J. (2015): The myth that no-till can mitigate global climate change. Agr. Ecosyst. Environ., 216, 98-99, doi: 10.1016/j.agee.2015.09.013.

Verbeke, G., Molenberghs, G. (2000): Linear mixed models for longitudinal data, Springer, New York.

Vickers, D., Mahrt, L. (1997): Quality control and flux sampling problems for tower and aircraft data. J. Atmos. Ocean. Technol., 14, 512-526, doi: 10.1175/1520-0426(1997)014<0512:QCAFSP>2.0.CO;2.

Webb, E.K., Pearman, G.I., Leuning, R. (1980): Correction of flux measurements for density effects due to heat and water vapour transfer. Quart. J. R. Met. Soc., 106, 85-100, doi: 10.1002/qj.49710644707.

Wienforth, B., Knieß, A., Böttcher, U., Herrmann, A., Sieling, K., Taube, F., Kage, H. (2018): Evaluating bioenergy cropping systems towards productivity and resource use efficiencies: an analysis based on field experiments and simulation modelling. Agronomy, 8, 117, doi: 10.3390/agronomy8070117.

Wilczak, J.M., Oncley, S.P., Stage S.A. (2001): Sonic anemometer tilt correction algorithms. Bound. Layer Meteor., 99, 127-150, doi: 10.1023/A:1018966204465.

Wizemann, H.-D., Ingwersen, J., Högy, P., Warrach-Sagi, K., Streck, T., Wulfmeyer, V. (2015): Three year observations of water vapor and energy fluxes over agricultural crops in two regional climates of Southwest Germany. Meteorol. Z., 29, 39-59, doi: 10.1127/metz/2014/0618.

WRB (2015): World reference base for soil resources 2014, update 2015. International soil classification system for naming soils and creating legends for soil maps. World soil resources reports no. 106. FAO, Rome, Italy.

Wutzler, T., Reichstein, M., Moffat, A.M., Menzer, O., Migliavacca, M., Sickel, K., Šigut, L. (2018): REddyProc: Post processing of (half-)hourly eddy-covariance measurements. R package version 1.1.3. Available at: https://cran.r-project.org/web/packages/REddyProc/index.html.

Chapter 5

5. General discussions

The present study was designed to clarify the contribution of minor storage and flux terms to improving energy balance closure, to determine potential reasons for energy imbalance, and to investigate the effects of different regions, sites, years and crops on the carbon balance and budgets in agricultural croplands. This thesis is based on the analyses of data obtained from fully equipped EC stations at six fields in two climatically contrasting regions over 8 years (2010-2017). The chapters provide the following findings.

Chapter 2 demonstrates that accounting for and considering minor storage and flux terms was important to obtain an improved energy balance closure (EBC). First and foremost, the role of minor storage and flux terms was evaluated over winter wheat in two consecutive seasons in the Kraichgau region in southwest Germany. The results showed that the energy stored or released by CO_2 exchange contributed more to the EBC compared to other minor storage terms such as the enthalpy change in the plant canopy, the air enthalpy change or the atmospheric moisture change. Moreover, and its contribution depended mainly on crop type and growing stage in the fields. Considering the energy stored or released by CO_2 exchange in evaluating EBC yielded a mean improvement from 74 to 79 % and from 80 to 87 % in 2015 and 2016, respectively. The maximum improvement of EBC by considering this stored or released energy was observed in May, namely a 7.4 and 8.4 % contribution in 2015 and 2016, respectively. The second most important minor storage term was the enthalpy change in the plant canopy. The contribution of that enthalpy change to the EBC ranged between 1.2 and 1.7 % in the growing periods of 2015 and 2016. We therefore concluded that it is important to consistently estimate minor storage terms in order to achieve a better energy balance in agricultural croplands. The minimum requirement would be the energy consumption and release by photosynthesis and respiration. Moreover, the enthalpy change in the plant canopy is significant and needs to be considered in estimating EBC. Our analysis revealed the significant contribution of minor energy terms to EBC, indicating that turbulent energy fluxes are most likely overestimated when all the missing energy is assumed to be turbulent − the typical approach when fluxes are corrected by the Bowen ratio post-closure method, for instance. Improving EBC requires accurately determining the energy balance components, soil heat storage and ground heat flux (G). The spatial variability of the soil heat storage between single point measurements (close to the EC station) and within the field footprint differed considerably. The spatial variability of soil moisture and plant cover over the

field footprint was assumed to be responsible for this large difference. Accordingly, single-site measurements of the ground flux might not be representative for the entire footprint. We also compared ground heat flux calculation methods and their different results. The ground heat flux calculated by the harmonic method showed the highest positive effect, improving EBC by 2-3 %. This influence is corroborated by Jacobs et al. (2008) in a mid-latitude grassland, where EBC was improved even by 9 %. Heusinkveld et al. (2004) also obtained better results of *G* using the harmonic analysis versus the calorimetric method. Chapter 2 also determined that it is possible to approximate the ground heat flux based on soil temperature measurements; the latter are easier to obtain at several points throughout the footprint, compared to the more expensive soil heat flux plate.

Chapter 3 investigates the influence of meteorological conditions and surface-layer turbulent parameters on the energy imbalance. The investigation of the significance of different factors on EBC showed that region (a surrogate for different climates) played an insignificant role. In contrast, the measurement sites within a region showed significant effects on EBC ($p < 0.001$). For the investigated setting and position, this demonstrated that EBC was mainly controlled by site conditions, a finding confirming other studies (Masseroni et al., 2014; Mauder et al., 2013; Stoy et al., 2013; Varmaghani et al., 2016). Finally, we were able to show that the EBC was not controlled by crop, contradicting what Wilson et al. (2002) reported. This was confirmed by analyzing the effect of u* on the energy balance ratio (EBR): under high u* ($u^* > 0.5$ m s^{-1}) the EBR distinctly narrowed at all EC stations. These site-specific characteristics include elevation, meteorological conditions, soil type and soil physical properties, as well as the homogeneity/heterogeneity of the field footprint – all considerably influenced EBC. Our results showed that flux footprint area was negatively correlated with EBC and that an increased footprint area reduced the EBC, for example at EC3 and EC5 in 2015. Our explanation is that, as the footprint becomes smaller, it becomes more homogeneous. Thus, the energy fluxes originated from a more homogeneous area. Overall, our results showed that field homogeneity/heterogeneity is partly responsible for the energy imbalances, an interpretation confirmed by Stoy et al. (2013) and Xu et al. (2017). A shadow effect of the sonic anemometer became apparent and contributed to EBC. At EC4, discarding the fluxes between 0° and 90°, which is behind the anemometer, increased EBC from 80 to 84 %. These findings agree with Friebel et al. (2009).

Chapter 4 examines the effects of site, year and region on the CO_2 fluxes and budgets in croplands based on measured data (from 2010 to 2017) from six research sites in two climatically contrasting regions. The results showed that the mean annual net biome production (NBP) from 46 site-years was 1190 kg C

ha^{-1} yr^{-1}, which was slightly higher than the average 950 kg C ha^{-1} yr^{-1} observed by Kutsch et al. (2010) at seven European cropland sites. The inter-annual variability of net ecosystem exchange (NEE) and NBP was large between research sites and even between regions. The crop exerted a statistically significant effect on the variability of CO_2 and C budgets, but sites or region did not. In comparing crops with regard to CO_2 uptake and annual NEE, the winter rapeseed showed significantly lower values. Harvesting whole silage maize biomass tended to deplete soil organic carbon (SOC) stocks.

We then analyzed the effect of low frequency contributions to the determined CO_2 fluxes using a recently proposed ogive optimization method (Sievers et al, 2015) and compared the results to the standard 30-min flux averaging. Net CO_2 uptake was crop-type dependent during June 2015 and, in most cases, the ogive-optimized daytime fluxes showed slightly higher values than the standard 30-min averaging interval. The lowest relative change of mean monthly NEE in calculated fluxes between ogive optimization and standard computation occurred at EC3 and EC5 (-3 %), and the highest at EC4 (13 %, June 2015). The difference between the two methods indicates that the contribution of CO_2 fluxes at low frequencies is not identical. Hence, each EC station has its own site-specific characteristics such as meteorology, footprint and surrounding area, crop type and soil physical properties (Kidston et al., 2010; Sievers et al., 2015). Accordingly, the difference between the two above methods, based on the analyses of CO_2 fluxes with respect to low frequency contributions, is in the acceptable range of previously reported deviations. One limitation, however, is the long data processing time with the ogive optimization method, which did not allow analyzing all measured 8-year fluxes. This prevents comparing the NEE of CO_2 results between the ogive optimization and standard 30-min outputs because of the requirements for long-term data analyses (Moors et al., 2010; Schmidt et al., 2012; Zeri and Sá, 2010). Clarifying this question would help to investigate the consequence of the energy balance gap in underestimating/overestimating CO_2 fluxes.

Several studies examined and discussed the relationship between the lack of EBC and CO_2 flux estimation (Kidston et al., 2010; Liu et al., 2006; Twine et al., 2000; Wilson et al., 2002). The FLUXNET community provided several implications of the energy balance gap for CO_2 flux (Wilson et al., 2002). According to them, the instrument bias (sonic anemometer and gas analyzer), the flux loss in high/low frequencies and the advection of fluxes to some extent affect CO_2 measurements. Moreover, they highlighted that the poor EBC and lower CO_2 fluxes usually occur during the night, when sufficiently high turbulent intensities are lacking (Anthoni et al., 2004). Therefore, CO_2 fluxes measured by the EC method have been compared with closed chamber methods (Poyda et al., 2017; Twine et al., 2000). These

studies revealed great differences due to transition periods such as starting growing season and different spatial scales. The NEE of CO_2 measurements based on EC were systematically lower than the chamber-based method (Poyda et al., 2017). In order to reduce the disadvantages of these methods, new approaches were recommended to combine chamber measurements with EC data (Reth et al., 2005). Kidston et al. (2010) reported that using the Bowen ratio post-closure method biases NEE according to different diurnal variations. In contrast, Liu et al. (2006) suggested that the lack of EBC does not directly propagate to the measured CO_2 fluxes. They concluded that the inaccuracy of CO_2 measurements was probably associated with local atmospheric conditions and measurement errors in turbulent fluxes.

Conclusion and outlook

This study has considerably furthered our knowledge about the energy balance closure problem and the effects of different years, regions and crops on C fluxes and budgets in intensively managed cropland. The conclusions are based on analyzing multi-year and multi-site EC data from two climatically contrasting regions. The EBC problem of EC measurements is the main challenge in micrometeorology and directly affects the validation of land surface models. Taking into account all minor storage terms and paying careful attention to all energy components helps solve the energy balance gap problem. This approach corresponds to standpoints postulated by Leuning et al. (2012). The maximum contribution of minor storage terms reached 8.4 % over winter wheat in 2016 (Chapter 2). Discarding the negative influences of the sonic anemometer from energy fluxes increased the EBC by 4 % (Chapter 3). Finally, separating the low-frequency influences from vertical turbulent fluxes in order to isolate local exchange processes improved the CO_2 measurements (Chapter 4). Accordingly, my dissertation confirms that Leuning et al.'s (2012) hypothesis – to achieve better EBC by considering data process errors and minor energy storage terms – is feasible. The results presented here contribute to tackling the challenges of interpreting EC measurement data from cropland sites. Future research will no doubt help to further improve the representation of EC measurements in croplands by explicitly considering all available energy storages and possible measurement errors.

This dissertation highlights that the EC method cannot accurately capture the turbulent exchange of energy, water and carbon fluxes between crop canopies and the atmosphere. I demonstrated the benefit of carefully considering and accounting neglected storage terms in order to achieve better EBC. The results also confirmed that a better EBC could be achieved when the conditions are close to ideal, which is defined as an unstable atmospheric conditions, strong buoyancy, high friction velocity and horizontally

homogeneous land cover. Determining the contribution of cropland for mitigating global change consequences required conducting long-term EC measurements. The analysis showed that croplands, under the given management, are a significant CO_2 sources.

Importantly, although much has been done to understand the complex processes and feedbacks in the land system over the last 35-40 years by applying the EC method, we are still struggling to find solutions for the EBC problem. This dissertation is a step forward in more profoundly understanding and evaluating the energy, water and carbon exchange between crop canopies and the atmosphere.

References

Anthoni, P.M., Freibauer, A., Kolle, O., Schulze, E.D., 2004. Winter wheat carbon exchange in Thuringia, Germany. Agric. For. Meteorol. 121, 55–67. https://doi.org/10.1016/S0168-1923(03)00162-X

Friebel, H.C., Herrington, T.O., Benilov, A.Y., 2009. Evaluation of the flow distortion around the Campbell Scientific CSAT3 sonic anemometer relative to incident wind direction. J. Atmos. Ocean. Technol. 26, 582–592. https://doi.org/10.1175/2008JTECHO550.1

Heusinkveld, B.G., Jacobs, A.F.G., Holtslag, A.A.M., Berkowicz, S.M., 2004. Surface energy balance closure in an arid region: Role of soil heat flux. Agric. For. Meteorol. 122, 21–37. https://doi.org/10.1016/j.agrformet.2003.09.005

Jacobs, A.F.G., Heusinkveld, B.G., Holtslag, A.A.M., 2008. Towards closing the surface energy budget of a mid-latitude grassland. Boundary-Layer Meteorol. 126, 125–136. https://doi.org/10.1007/s10546-007-9209-2

Kidston, J., Brümmer, C., Black, T.A., Morgenstern, K., Nesic, Z., McCaughey, J.H., Barr, A.G., 2010. Energy balance closure using eddy covariance above two different land surfaces and Implications for CO_2 flux measurements. Boundary-Layer Meteorol. 136, 193–218. https://doi.org/10.1007/s10546-010-9507-y

Leuning, R., van Gorsel, E., Massman, W.J., Isaac, P.R., 2012. Reflections on the surface energy imbalance problem. Agric. For. Meteorol. 156, 65–74. https://doi.org/10.1016/j.agrformet.2011.12.002

Liu, H., Randerson, J.T., Lindfors, J., Massman, W.J., Foken, T., 2006. Consequences of incomplete surface energy balance closure for CO_2 fluxes from open-path CO_2/H_2O infrared gas analysers. Boundary-Layer Meteorol. 120, 65–85. https://doi.org/10.1007/s10546-005-9047-z

Masseroni, D., Corbari, C., Mancini, M., 2014. Limitations and improvements of the energy balance closure with reference to experimental data measured over a maize field. Atmosfera 27, 335–352. https://doi.org/10.1016/S0187-6236(14)70033-5

Mauder, M., Cuntz, M., Drüe, C., Graf, A., Rebmann, C., Schmid, H.P., Schmidt, M., Steinbrecher, R., 2013. A strategy for quality and uncertainty assessment of long-term eddy-covariance measurements. Agric. For. Meteorol. 169, 122–135. https://doi.org/10.1016/j.agrformet.2012.09.006

Meyers, T.P., Hollinger, S.E., 2004. An assessment of storage terms in the surface energy balance of maize and soybean. Agric. For. Meteorol. 125, 105–115. https://doi.org/10.1016/j.agrformet.2004.03.001

Moors, E.J., Jacobs, C., Jans, W., Supit, I., Kutsch, W.L., Bernhofer, C., Béziat, P., Buchmann, N., Carrara, A., Ceschia, E., Elbers, J., Eugster, W., Kruijt, B., Loubet, B., Magliulo, E., Moureaux, C., Olioso, A., Saunders, M., Soegaard, H., 2010. Variability in carbon exchange of European croplands. Agric. Ecosyst. Environ. 139, 325–335. https://doi.org/10.1016/J.AGEE.2010.04.013

Poyda, A., Reinsch, T., Skinner, R.H., Kluß, C., Loges, R., Taube, F., 2017. Comparing chamber and eddy covariance based net ecosystem CO_2 exchange of fen soils. J. Plant Nutr. Soil Sci. 1–15. https://doi.org/10.1002/jpln.201600447

Reth, S., Göckede, M., Falge, E., 2005. CO_2 efflux from agricultural soils in Eastern Germany – comparison of a closed chamber system with eddy covariance measurements. Theor. Appl. Climatol. 80, 105–120. https://doi.org/10.1007/s00704-004-0094-z

Schmidt, M., Reichenau, T.G., Fiener, P., Schneider, K., 2012. The carbon budget of a winter wheat field: An eddy covariance analysis of seasonal and inter-annual variability. Agric. For. Meteorol. 165, 114–126. https://doi.org/10.1016/j.agrformet.2012.05.012

Sievers, J., Papakyriakou, T., Larsen, S.E., Jammet, M.M., Rysgaard, S., Sejr, M.K., Sørensen, L.L., 2015. Estimating surface fluxes using eddy covariance and numerical ogive optimization. Atmos. Chem. Phys. 15, 2081–2103. https://doi.org/10.5194/acp-15-2081-2015

Stoy, P.C., Mauder, M., Foken, T., Marcolla, B., Boegh, E., Ibrom, A., Arain, M.A., Arneth, A., Aurela, M., Bernhofer, C., Cescatti, A., Dellwik, E., Duce, P., Gianelle, D., van Gorsel, E., Kiely, G., Knohl, A., Margolis, H., Mccaughey, H., Merbold, L., Montagnani, L., Papale, D., Reichstein, M., Saunders, M., Serrano-Ortiz, P., Sottocornola, M., Spano, D., Vaccari, F., Varlagin, A., 2013. A data-driven analysis of energy balance closure across FLUXNET research sites: The role of landscape scale heterogeneity. Agric. For. Meteorol. 171–172, 137–152. https://doi.org/10.1016/j.agrformet.2012.11.004

Twine, T.E., Kustas, W.P., Norman, J.M., Cook, D.R., Houser, P.R., Meyers, T.P., Prueger, J.H., Starks, P.J., Wesely, M.L., 2000. Correcting eddy-covariance flux underestimates over a grassland. Agric. For. Meteorol. 103, 279–300. https://doi.org/10.1016/S0168-1923(00)00123-4

Varmaghani, A., Eichinger, W.E., Prueger, J.H., 2016. A diagnostic approach towards the causes of energy balance closure problem. Open J. Mod. Hydrol. 101–114.

Wilson, K., Goldstein, A., Falge, E., Aubinet, M., Baldocchi, D., Berbigier, P., Bernhofer, C., Ceulemans, R., Dolman, H., Field, C., Grelle, A., Ibrom, A., Law, B.., Kowalski, A., Meyers, T., Moncrieff, J., Monson, R., Oechel, W., Tenhunen, J., Valentini, R., Verma, S., 2002. Energy balance closure at FLUXNET sites. Agric. For. Meteorol. 113, 223–243. https://doi.org/10.1016/S0168-1923(02)00109-0

Xu, Z., Liu, S., Shi, W., Wang, J., 2017. Assessment of the energy balance closure under advective conditions and Its impact using remote sensing data. Am. Meteorol. Soc. 127–140. https://doi.org/10.1175/JAMC-D-16-0096.1

Zeri, M., Sá, L.D.A., 2010. The impact of data gaps and quality control filtering on the balances of energy and carbon for a southwest Amazon forest. Agric. For. Meteorol. 150, 1543–1552. https://doi.org/10.1016/j.agrformet.2010.08.004

Acknowledgements

It is very important to acknowledge the people who have immeasurable contribution until and in the completion of this dissertation. First and foremost, I would like to express my deepest appreciation and thanks to Prof. Dr. Thilo Streck for supervising my thesis at the University of Hohenheim. In particular, I am grateful to him for giving me the great opportunity to join his team and conducting my research in Biogeophysics. I could not have imagined having a better advisor and mentor at the University of Hohenheim.

My special thanks to Dr. Joachim Ingwersen for his valuable support, supervision, and his rigid critics on my progress which helped me to develop my scientific skills. I would also like to extend my deep gratitude to Dr. Arne Poyda who joined our group in 2015 and contributed significantly to my research work. His immense experience was very beneficial in subject related fieldworks and in the writing process of manuscripts. Moreover, my additional thanks again to both of Dr. Joachim Ingwersen and Dr. Arne Poyda for their patience, prompt feedbacks and inputs at the final stage of reading and editing this thesis for publication.

I am grateful to Dr. Hans-Dieter Wizemann for providing me with R script to calculate ground heat flux with harmonic analysis and for sharing with me his knowledge in the basics of using harmonic analysis.

I am also grateful to Dr. Tobias Weber for giving valuable instructions and motivation to finalize this dissertation. Many thanks to all friends, my current and former colleagues in Hohenheim who worked together during my PhD life. I appreciate their continuous encouragement to finalize my PhD work (Rana Shakhbaz Ali, Lona van Delden, Hossein Zare, Sina Kukowski, Luciana Chaves…).

I am sincerely thankful to Dr. Alim Pulatov, who recommended and gave the opportunity to accomplish my doctoral thesis at Hohenheim University. I greatly appreciate his support and inputs during my study.

Many thanks to Galibjon Sharipov, Lobarkhon Allayeva, Muzaffar Yunusov and Odilbek Matmusayev who were students at Hohenheim University for sharing with me their study experiences which gave me the strength and motivation that was crucial during my study period.

I gratefully acknowledge the funding sources that made my PhD work feasible. I was funded by the Erasmus Mundus grant “TIMUR − Training of Individuals through Mobility from Uzbek Republic to EU (referenced as GA NO 213−2723/001−001−EM Action 2)” between July 2014 and July 2017. I am thankful to the coordinators of the project, Alim Pulatov, Ewa Wietsma and Anna Voitenko for their

support and good collaborations. This study was also accomplished within the framework of project FOR 1695 “Agricultural Landscapes under Global Climate Change-Processes and Feedbacks on a regional Scale” within subproject P2.

Ultimately, I would like to thank and dedicate this work to my family, my beloved parents, lovely wife, dearest sisters and precious grandparents who supported me through the ups and downs of the research process. Especially, I would like to thank my father for his constant support and time on houseworks despite the restrictions on distance and my long absence from home. Last but not least, I would like to thank Marguba Bozorova, my wife, for her love and -massive cares, patience, and being a constant source of inspiration. Without her endless support, this work would not have ended. Cheerful smiles and unconditional love of my children Zafar, Jasmina, and my newborn son Shukhrat motivated me to complete my PhD work despite the challenges.

Ravshan Abdurazakovich Eshonkulov
Stuttgart-Hohenheim, March 2019

Curriculum vitae

Personal information

Last name:	Eshonkulov
First name:	Ravshan
Middle name:	Abdurazakovich
Current address:	Aixheimer Str. 20, 70619, Stuttgart, Germany
Permanent address:	Yozyovon Str. 42, 180100, Karshi, Uzbekistan
E-mail(s):	ravshan.eshonkulov@uni-hohenheim.de, ravshan_ecogis@yahoo.com
Nationality:	Uzbek
Date of Birth:	16 June 1980
Place of Birth:	Karshi, Uzbekistan
Marital status:	married, 3 children

Education

2014−now	PhD student, Institute of Soil Science and Land Evaluation, Biogeophysics, University of Hohenheim, Stuttgart, Germany
2010−2011	Senior Scholar, China University of Geosciences (Wuhan), Wuhan, China
2002−2004	Master (MSc) in Environmental Protection, Tashkent Institute of Irrigation and Melioration, Tashkent, Uzbekistan (graduated with honors)
1998−2002	Bachelor (BSc) in Environmental Protection, Karshi Engineering Economic Institute, Karshi, Uzbekistan

Professional experience

2011−2014	Senior teacher, department of Environmental protection and ecology, Karshi Engineering Economic Institute, Karshi, Uzbekistan
2008−2010	Assistant teacher, department of Environmental protection and ecology, Karshi Engineering Economic Institute, Karshi, Uzbekistan
2006−2008	Assistant teacher, department of Environmental protection and ecology, Karshi Engineering Economic Institute, Karshi, Uzbekistan
2004−2006	Senior laboratory assistant, department of Ecology, Karshi State University, Karshi, Uzbekistan

Publications

Eshonkulov, R., Poyda, A., Ingwersen, J., Pulatov, A., Streck, T., 2019. Improving the energy balance closure over a winter wheat field by accounting for minor storage terms. Agric. For. Meteorol. 264, 283–296. https://doi.org/10.1016/J.AGRFORMET.2018.10.012.

Eshonkulov, R., Poyda, A., Ingwersen, J., Wizemann, H., KD, T., Kremer, P., Högy, P., Pulatov, A., Streck, T., 2019b. Evaluating multi-year , multi-site data on the energy balance closure of eddy-covariance flux measurements at cropland sites in southwestern Germany. Biogeosciences 521–540. https://doi.org/10.5194/bg-16-521-2019.

Poyda, A., Wizemann, H., Ingwersen, J., Eshonkulov, R., Högy, P., Demyan, M.S., Kremer, P., Wulfmeyer, V., Streck, T., 2019. Carbon fluxes and budgets of intensive crop rotations in two regional climates of southwest Germany. Agric. Ecosyst. Environ. 276, 31–46. https://doi.org/10.1016/j.agee.2019.02.011

Poster presentations

Eshonkulov, R, Poyda, A**.,** Wizemann, HD, Ingwersen, J., Streck, T. 2018. Long-term observations of energy balance closure of eddy covariance flux data over agricultural crops in two regional climates of Southwest Germany. *EGU General Assembly EGU2018*

Eshonkulov, R., Poyda, A**.,** Ingwersen, J., Streck, T. 2017. Determining the spatial variability of crop yields of two different climatic regions in Southwest Germany. *EGU General Assembly EGU2017*

Eshonkulov, R., Poyda, A**.**, Ingwersen, J., Streck, T. 2016. Accounting for minor storage terms in an attempt to close the measured surface energy balance over a winter wheat field in Southwest Germany. *EGU General Assembly EGU2016*

Author’s declaration

I hereby declare that this doctoral dissertation is a result of my own work, and that no other than the indicated aids have been used for its completion. All sources of information I exploited have been cited appropriately.

Furthermore, I assure that the work has not been used, neither completely nor in parts, for achieving any other academic degree.

Ravshan Abdurazakovich Eshonkulov

Stuttgart-Hohenheim, March 2019